

Benzisoxazoles: New Routes to Coleophomone Analogues

by

Alexander Chatterley

A doctoral thesis submitted in partial fulfilment of the
requirements for the award of:

Doctor of Philosophy

Loughborough University

November 2014

Abstract

This project has been part of an ongoing interest in metabolites with a *cyclic tricarbonyl* motif **1**, usually enolised. Coleophomones A–C have a unique architecture with the cyclic tricarbonyl motif embedded in an 11-membered ring: A & B exist in ‘aldol’ equilibrium, B & C are geometric isomers, and D lacks the macrocycle.^{1,2} Antifungal & antibiotic activity, and inhibition of human heart chymase & bacterial cell-wall transglycosylase, has generated synthetic interest.

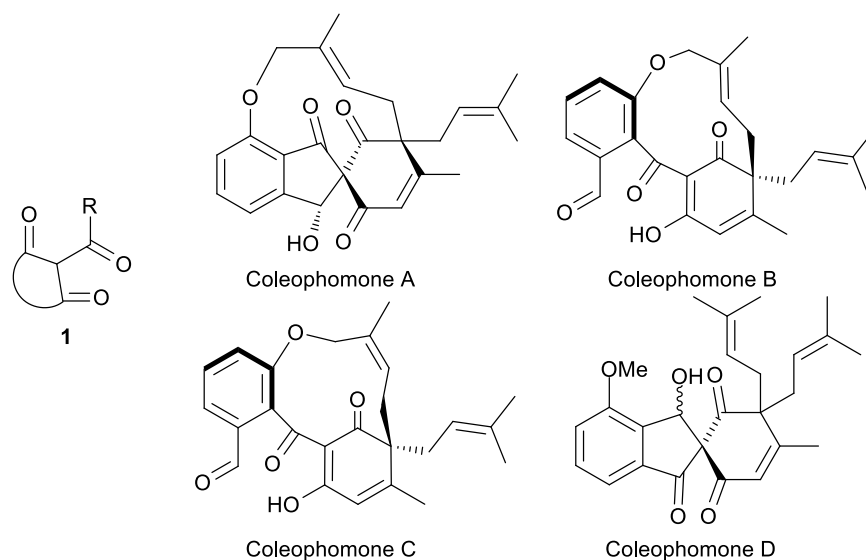
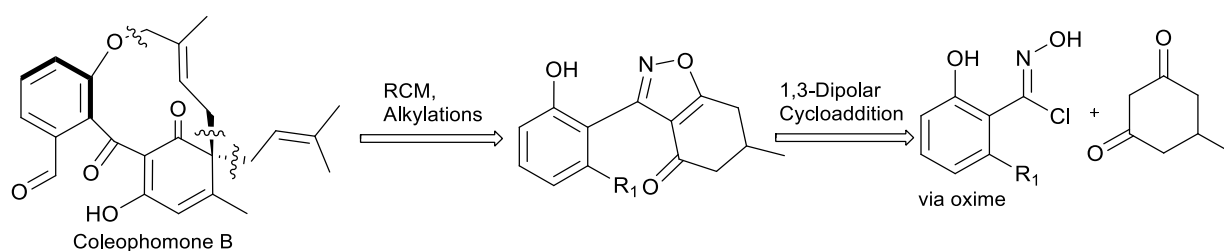


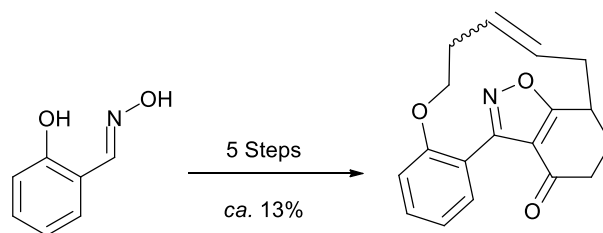
Figure 1

In an approach distinct from reported studies,³ we propose 4-carbonyl-substituted isoxazoles, from dipolar cycloaddition of nitrile oxides, as building blocks for the tricarbonyl framework. Our strategic disconnection to benzisoxazoles is exemplified in the Scheme 1.



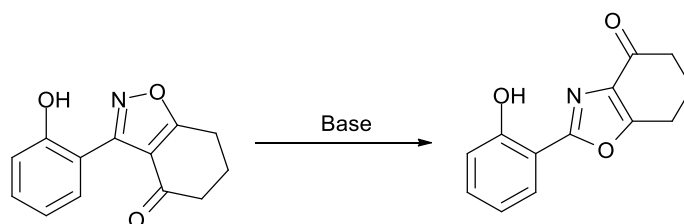
Scheme 1

During this investigation precursors to the macrocycles of coleophomones A, B, C and analogues were developed. (Scheme 2).



Scheme 2

En route to these precursors we have uncovered and probed a facile and highly unusual benzisoxazole to oxazole rearrangement (Scheme 3).



Scheme 3

Acknowledgements

Wow where to begin? So many people have helped me get this far. I hope this doesn't sound too much like an Oscar speech!

Firstly I'd like to thank Ray and Martin for not only giving me the opportunity to do this, but also for their constant support and taking the time to listen. Ray especially who has had to endure reading not only countless reports, but also this thesis, multiple times!

I'd then like to thank everyone I've met in the labs at Loughborough. You've all made my time there memorable to say the least. Especially Maria who has been a constant; as well as, Sam, Trish, Rossi, James and everyone else, you know who you are!

Following that I'd like to thank all of my friends who have been with me in Nott's and beyond! Especially Harriet, James, Tom, Martyn but also Chris, Harry, Paul and Matt to name a scant few.

Next I want to thank all of the staff at Loughborough for taking the time to answer all of my questions and provide support, especially those in the analytical services department.

Also all the people at Lilly who made me feel so welcome there during my placement and again upon my return. Chemistry and the pub, who would have thought the two, would go together so well?

Almost there, only a few more people left now!

A special thanks to Dr Ray Leslie of Nottingham Trent, without your inspiration I'd never have pursued a career in organic/medicinal chemistry. I think it was the fear during lectures that did it!

Finally I'd like to thank my family, especially my grandmother and late grandfather for not only constantly supporting me, but pushing me to be the best I can be.

Contents

| | |
|--|-----|
| Abstract..... | i |
| Acknowledgements..... | iii |
| Table of Abbreviations..... | vi |
| 1.0 Introduction..... | 1 |
| History of the Coleophomone Natural Products..... | 1 |
| Structure of the Coleophomones..... | 2 |
| Retrosynthesis..... | 3 |
| 1.1 The Isoxazole Functionality..... | 8 |
| Chemistry of Isoxazoles..... | 8 |
| Preparation..... | 11 |
| Nitrile Oxides..... | 12 |
| Formation..... | 12 |
| 1.2 1,3- Dipolar Cycloadditions..... | 14 |
| The 1,3-Dipole..... | 15 |
| The Dipolarophile..... | 18 |
| Mechanism of 1,3-Dipolar Cycloaddition..... | 18 |
| 1.3 Alkene Metathesis..... | 21 |
| Origins of Metathesis..... | 21 |
| Ring Closing Metathesis..... | 25 |
| 1.4 Previous Synthesis..... | 27 |
| Nicolaou's Total Synthesis..... | 27 |
| Suzuki's Comparison..... | 32 |
| Goldring's Investigation..... | 36 |
| 2.0 Progression towards the Coleophomone Natural Products..... | 38 |
| 2.1 Functionalized Imidoyl Chlorides..... | 39 |
| <i>Mono-Ortho</i> Imidoyl Chlorides..... | 39 |
| <i>Bis-Ortho</i> Substituted Imidoyl Chlorides..... | 40 |
| <i>Ortho,meta</i> -Imidoyl Chlorides..... | 43 |
| Additional examples..... | 44 |
| 2.2 Benzisoxazole Formation..... | 45 |
| 2.3 Aromatic O and C-Alkylation..... | 48 |
| O-Alkylation..... | 48 |
| Alternative Method for O-Alkylation..... | 56 |

| | |
|---|-----|
| Aryl Ring C-Alkylation..... | 57 |
| 2.4 Cyclohexanone Alkylation..... | 59 |
| α -Carbonyl Alkylation..... | 59 |
| Carbonyl Addition..... | 82 |
| 2.5 Isoxazole Ring Cleavage..... | 84 |
| 2.6 Ring Closing Metathesis..... | 88 |
| 2.7 Benzisoxazole to Oxazole Rearrangement..... | 95 |
| Benzoxazole Chemistry..... | 113 |
| Carbonyl Addition..... | 113 |
| Ring Closing Metathesis..... | 115 |
| Synthetic Utility..... | 116 |
| 2.8 Progress towards Coleophomone D..... | 118 |
| 3.0 Conclusions and Future Research..... | 124 |
| Coleophomones A, B and C..... | 124 |
| Coleophomone D..... | 125 |
| Benzisoxazole to Oxazole Rearrangement..... | 127 |
| 4.0 Experimental..... | 129 |
| 5.0 References..... | 189 |
| Appendix i – Crystal Structures..... | i |

Table of Abbreviations

| | |
|------------------------|---|
| Ac₂O | Acetic Anhydride |
| AcOH | Acetic Acid |
| BnBr | Benzyl Bromide |
| Bn | Benzyl |
| BTAF | Tetra-N-butylammonium fluoride |
| Bz | Benzoyl |
| CSA | Camphorsulfonic acid |
| Cy | Cyclohexyl |
| DBU | 1,8-Diazabicyclo[5.4.0]undec-7-ene |
| DCM | Dichloromethane |
| DIAD | Diisopropyl azodicarboxylate |
| DMA | Dimethylacetamide |
| DMAP | 4-(Dimethylamino)pyridine |
| DMDC | Dimorpholine azodicarboxamide |
| DME | Dimethoxyethane |
| HRMS | High resolution mass spectra |
| iPrOH | Propan-2-ol |
| LC-MS | Liquid chromatography mass spectrometry |
| LDA | Lithium diisopropylamide |
| LiHMDS | Lithium hexamethyldisilazide |
| Me | Methyl |
| Mes | Mesitylene |
| NaHMDS | Sodium hexamethyldisilazide |
| NBS | N-Bromosuccinimide |
| n-BuLi | N-Butyllithium |
| NCS | N-Chlorosuccinimide |
| NMR | Nuclear magnetic resonance spectroscopy |
| nOe | Nuclear Overhauser effect |
| NOESY | Nuclear Overhauser effect spectroscopy |
| Ph | Phenyl |
| p-TSA | p-Toluenesulfonic acid |
| RCM | Ring closing metathesis |
| ROMP | Ring opening metathesis polymerisation |
| TBAI | Tetrabutylammonium iodide |

| | |
|----------------|---|
| t-BuLi | Tertiary-Butyllithium |
| Tert | Tertiary |
| TFA | Trifluoroacetic acid |
| THF | Tetrahydrofuran |
| TIPSOTf | Triisopropylsilyl trifluoromethanesulfonate |

1.0 Introduction

The initial aim of the work described herein was the synthesis of the coleophomone family of natural products and related compounds *via* an isoxazole route.

This family of natural products is of interest as its member's exhibit antibacterial, antifungal activity, and enzyme inhibition; as well as a synthetic challenge. There are four members of the coleophomone family: coleophomones A, B, C and D.

History of the Coleophomone Natural Products

The coleophomone family (Figure 1) of compounds was first reported in a Japanese patent made on behalf of the Shionogi Pharmaceutical Company.² Coleophomones A **1**, B **2** and C **3** were isolated from a fungal broth of *Stachybotrys cylindrospora*; Coleophomone D **4** was isolated one year later by the same company from a *Stachybotrys parvispora* Hughes broth as a mixture of isomers.¹ The following year, a research group based at Merck published a paper describing the isolation of coleophomones A and B from a broth of *Coleophoma* sp.⁴

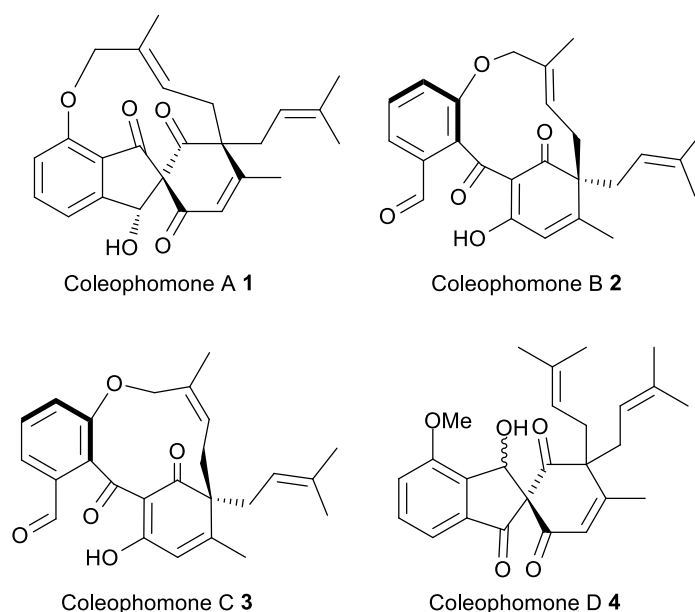


Figure 1

The coleophomones have been shown to inhibit bacterial cell wall transglycosylase and human heart chymase; transglycosylase catalyses the polymerisation of disaccharide-pentapeptide units to form uncrosslinked peptidoglycan, also known as murein.⁵ Murein is a building block for bacterial cell walls and so is necessary for survival and reproduction, and therefore if production is inhibited, cell death will occur.

Human heart chymase is responsible for the conversion of Angiotensin I to Angiotensin II, with the latter being linked to hypertension, which is considered to be a major risk factor for death and organ damage.^{6,7} It can be envisaged that the coleophomone family and their analogues could be used as a treatment for both bacterial infection and hypertension.

Structure of the Coleophomones

The coleophomones are a structurally intriguing group of compounds; every member of the group contains a highly reactive cyclic tri-carbonyl unit, multiple alkenes, as well as complex inter-connected ring systems; also A, B and C possess an 11 member macrocycle containing an ether oxygen.

Coleophomones A and B are isomeric to each other and exist in equilibrium, rapidly interconverting through an aldol type reaction; B and C are geometric isomers with E and Z macrocycles respectively (Figure 2).

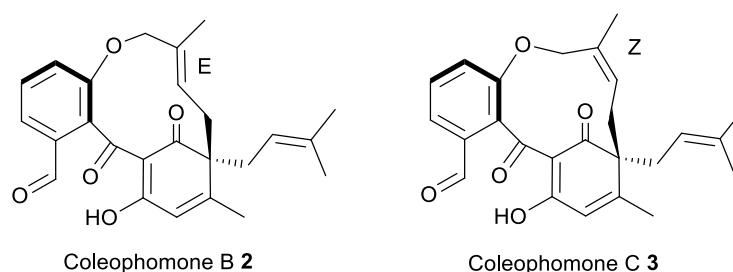
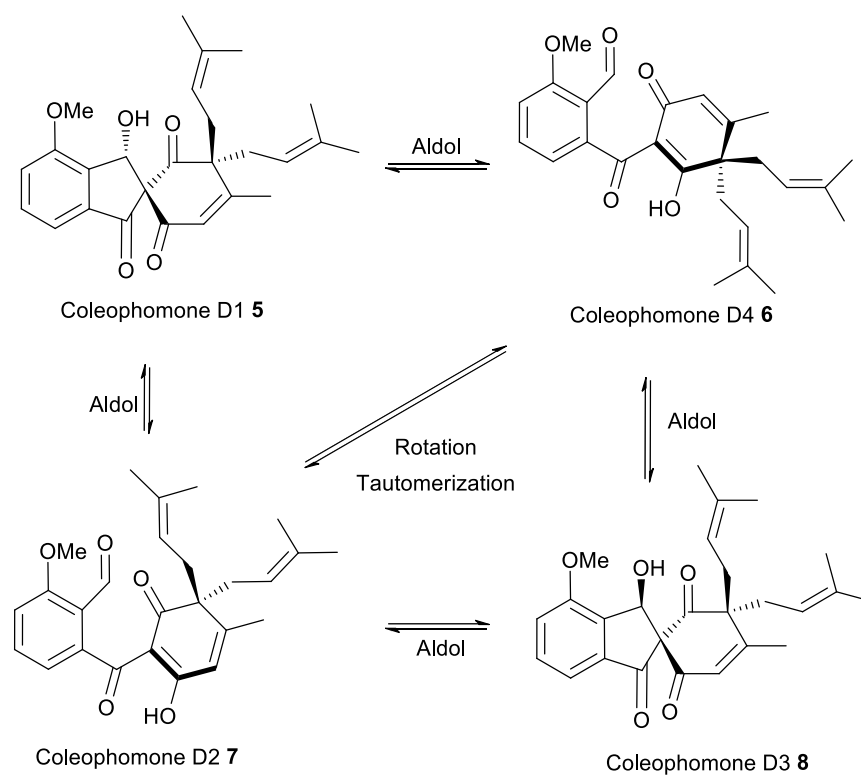


Figure 2

Coleophomone D does not exhibit the macrocycle, instead a methoxy group is present on the aromatic ring, which also possesses opposite regiochemistry when compared to A, B and C. As it does not contain the macrocycle, D has more rotational freedom than the other members of the family, existing as a mixture of isomers (Scheme 1).²

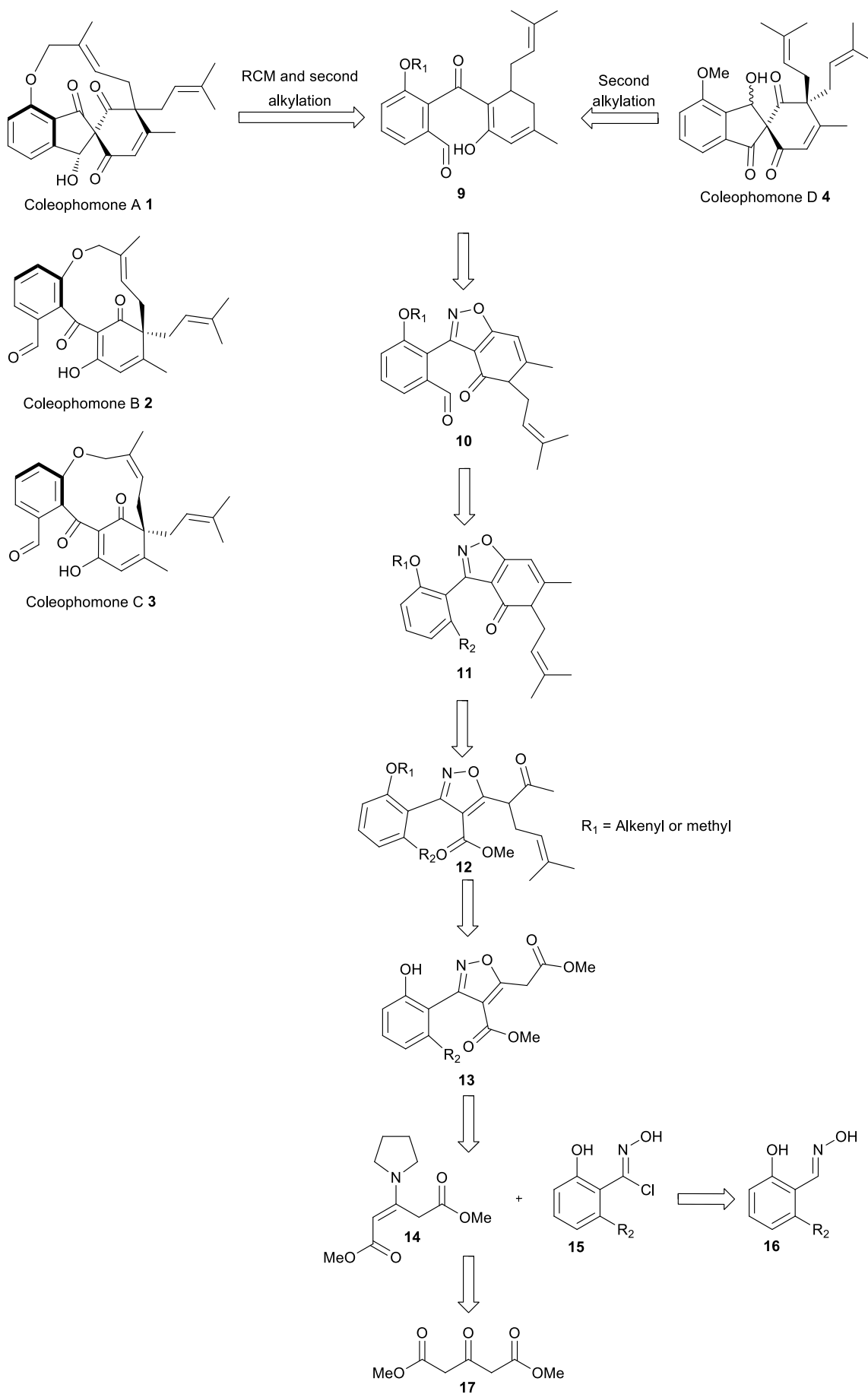


Scheme 1. Coleophomone D as a mixture of isomers.

Coleophomone D1 interconverts into D2 and D4 *via* a reversible aldol process, D4 and D2 can then convert into D3 or back into D1 *via* the same processes. D4 and D2 can also interconvert into the other *via* rotation.

Retrosynthesis

The aim of this project is to attempt the synthesis of the Coleophomone natural products and their analogues by masking the cyclic-tricarbonyl system as an isoxazole. Previous work on this project identified two separate approaches to accomplish this and the first is shown below (Scheme 2).⁸

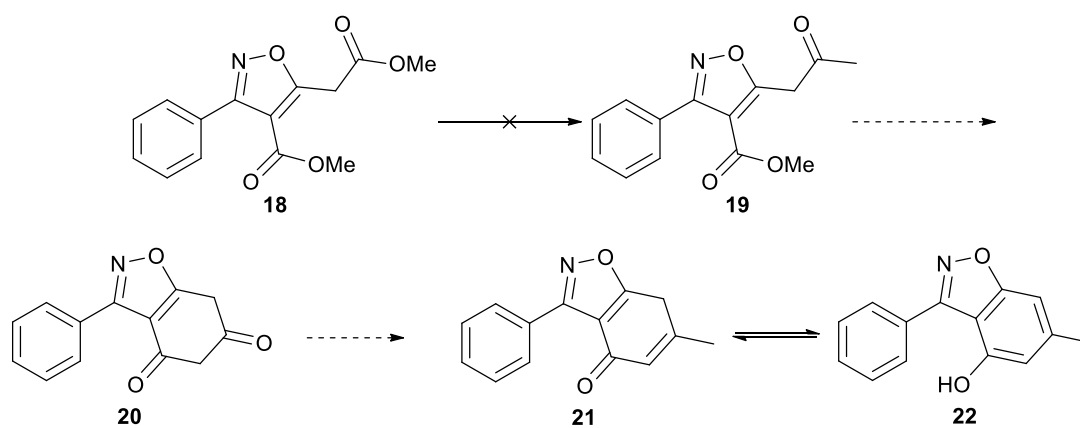


Scheme 2

This approach proposed the cycloaddition of a nitrile oxide, prepared from aromatic oxime **16** where R_2 represents a handle for forming the aldehyde at a later step, with enamine **14**, derived from acetonedicarboxylate **17**. Alkylations were to be carried out alpha to the isoxazole and at the phenolic position, installing the alkyl groups present in the desired natural product.

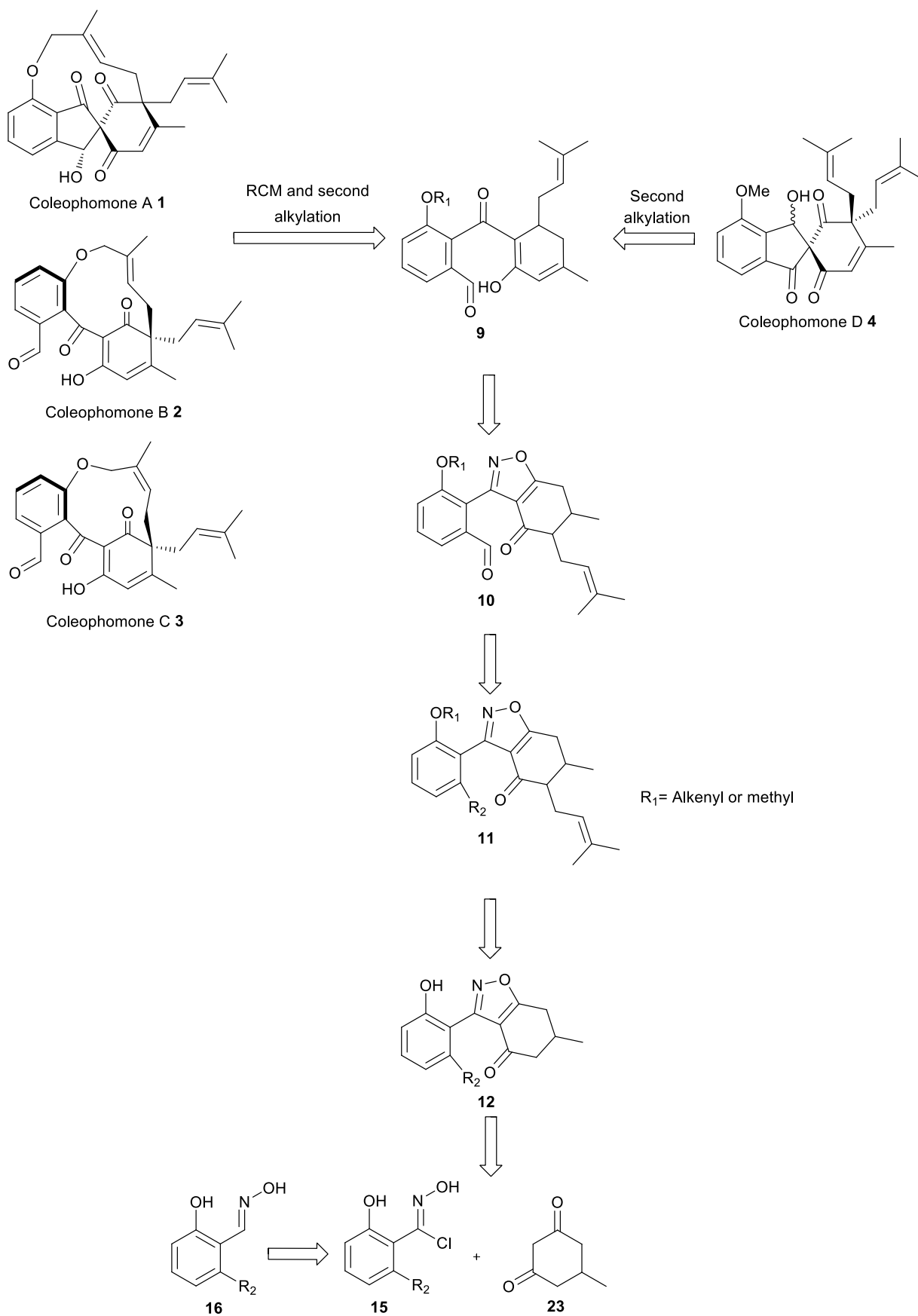
Following this, the esters were to be converted into ketones and undergo aldol closure to generate the six-membered ring, thereby forming the tricyclic system found in the natural products. At this stage further elaborations were to be undertaken to furnish this core structure, yielding the required aldehyde. Finally the isoxazole would be cleaved and hydrolysed yielding either coleophomone D or a precursor, which would be closed using ring closing metathesis (RCM) or Wittig type chemistry to yield coleophomones A, B and C.

However, using this approach, it was not possible to synthesise the desired methyl ketone required for aldol closure from test compound **18**, and consequently, this approach was deemed ineffective (Scheme 3).



Scheme 3

At this juncture a second approach based on the work by Suzuki *et. al.* was identified (Scheme 4).⁹



Scheme 4

Similar to the last, this approach proposed the cycloaddition of aromatic precursor **15** to cyclic diketone **23** to yield fused benzisoxazole **12**, albeit in fewer steps. Once this had been accomplished, this system would be further elaborated to yield the desired natural product.

Using this approach, a previous researcher was able to successfully form fused benzisoxazole **24** (Figure 3).⁸

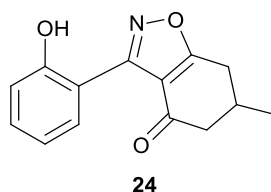
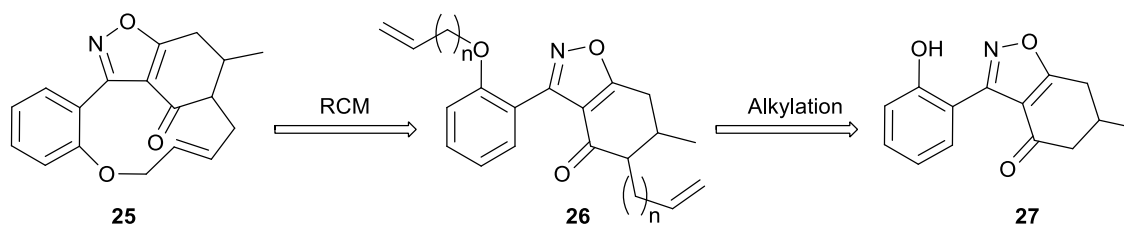


Figure 3

At this point in the project, we wanted to determine whether it would be possible to form the 11-membered macrocycle with the isoxazole present. It would be synthetically advantageous if this were possible, however, fused *bis*-alkyl benzisoxazole **25** might be too strained to permit this (Scheme 5).



Scheme 5

As such, *bis*-alkyl benzisoxazole **26** represents the first synthetic target of this program, as we wished to use it as a test compound for RCM. Once we had determined whether it possible to form the macrocycle, we planned to then proceed to implement the rest of the functionality found in the coleophomones.

1.1 The Isoxazole Functionality

One of the key points of our methodology is to mask the highly reactive tri-carbonyl system present in the coleophomones as an isoxazole (Figure 4). This will allow the introduction of additional functionality without being constrained by the reactivity of the tri-carbonyl group.

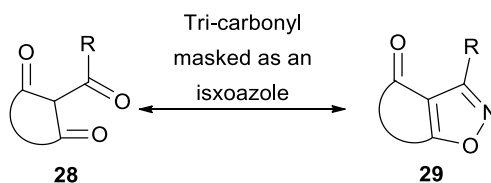


Figure 4

Therefore an understanding of isoxazole chemistry is required, as will now be described.

Chemistry of Isoxazoles

The isoxazole functionality was first proposed in 1888 by Claisen who suggested the name monoazole.¹⁰ They were first named isoxazole after a publication by Hantzsch, even though the isoxazole structure was not determined until 1946.¹¹⁻¹³ The standard ways of labelling positions on an isoxazole ring is illustrated below (Figure 5).

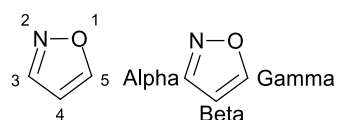
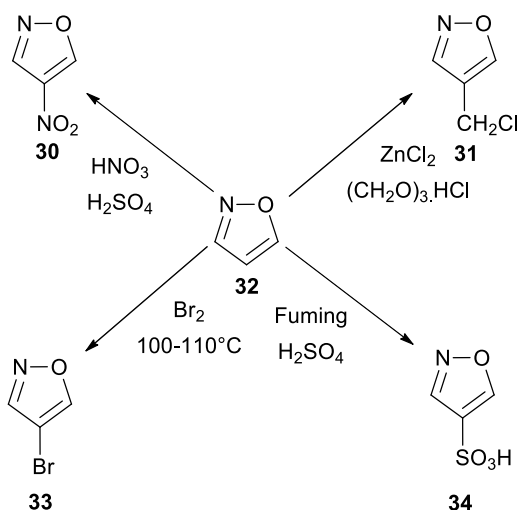


Figure 5

Isoxazoles can undergo a variety of reactions as the ring contains a range of chemical properties. The ring itself shows some aromatic character with the nitrogen atom acting as an electron withdrawing group and the oxygen as electron donating.

Electrophilic Reactions

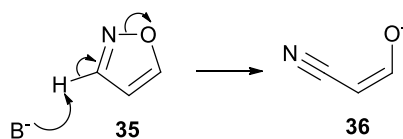
C4 is the most reactive position towards electrophilic substitution. Its reactivity is determined by the substituents at the adjacent positions, electron donating groups activate and conversely electron donating groups will deactivate position C4. Isoxazole will undergo a range of electrophilic substitution reactions (Scheme 6).¹⁴



Scheme 6

Nucleophilic Reactions

Nucleophilic substitution reactions typically occur at positions C3 and C5. However, if the nucleophile is a strong base, for example butyllithium and C3 is unsubstituted, then isoxazole ring opening will take place as the proton at C3 is acidic (Scheme 7).



Scheme 7

Side chains at C3 and C5 can be deprotonated with a strong base such as lithium diisopropyl amine (LDA) or butyllithium, with C5 substituents being considerably more reactive than those at C3 due to extended conjugation (Figure 6).¹⁵⁻¹⁷

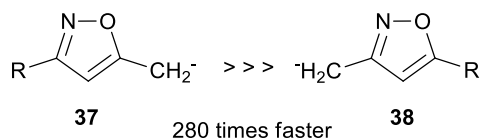
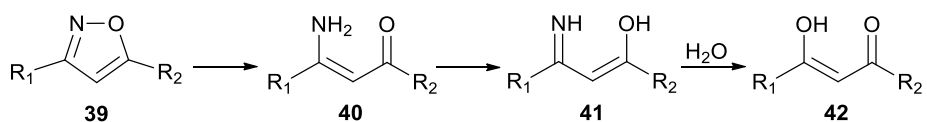


Figure 6

Ring Cleavage

The N-O bond of the isoxazole ring is relatively weak and can be cleaved to expose the corresponding enamino ketone and hydrolysis or diazotization can then be employed to reveal the 1,3-dicarbonyl functionality (Scheme 8).^{18,19}

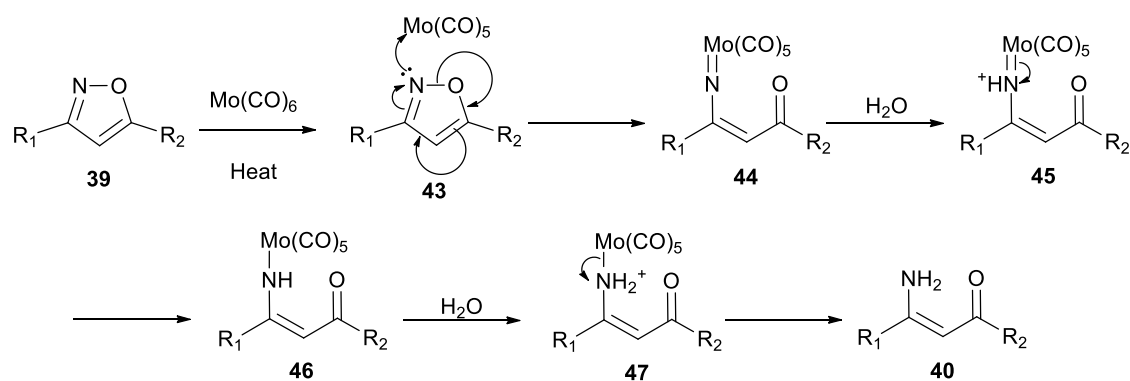


Scheme 8

Ring cleavage is typically achieved *via* hydrogenation over a range of catalysts such as: palladium on charcoal, palladium oxide and Raney nickel.^{20–23}

Although these methods are reliable, one of the main disadvantages is that they will also reduce other sensitive functionality, such as olefins and some heterocycles. Consequently other cleavage methods have been developed; these include titanium trichloride and sodium in ethanol, samarium diiodide, molybdenum hexacarbonyl and as mentioned, de-protonation at the C3 position.^{24–26}

Ring cleavage *via* molybdenum hexacarbonyl is of interest to us as other reductive methods may affect the functionality present in the colephomones. Below is the mechanism of this cleavage as proposed by *Nitta et al.* (Scheme 9).²⁴



Scheme 9

Cleavage is initiated when the nitrogen lone pair coordinates to the metal atom. This prompts N-O bond cleavage to yield (β-oxo alkenyl)nitrene complex **44** and upon heating in the presence of water this decomposes to yield enamino ketone **40**.

Preparation

Isoxazole preparation is classified in five main categories, which are defined by their ring closure pattern (Figure 7).

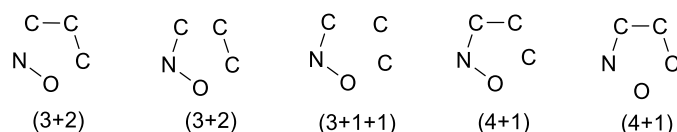
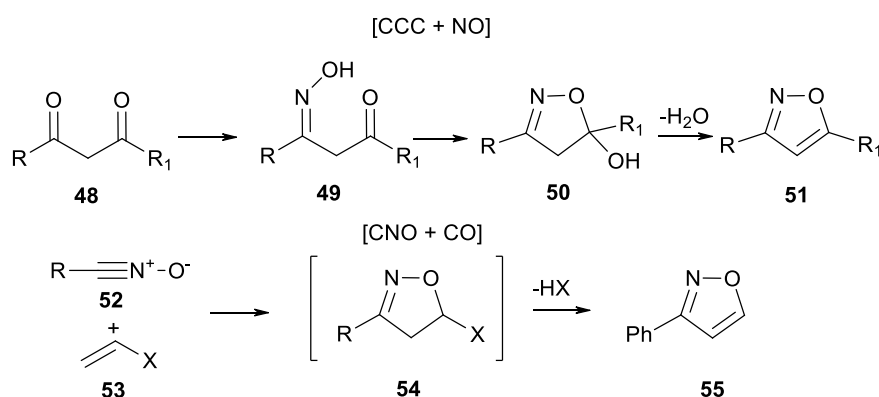


Figure 7

These are: two (3+2), one (3+1+1) and two (4+1) processes, with the numbers in the brackets referring to the number of atoms in each component involved in the formation reaction.²⁷

The two (3+2) reactions can be further subdivided into two different types, the [CCC + NO] and the [CNO + CC] processes. The first process involves the oximation of 1,3-dicarbonyl compounds, whilst the second, is the 1,3-dipolar cycloaddition of a nitrile oxide to an alkene (Scheme 10).^{28,29}



Scheme 10

The [CNO + CC] is the process relevant to this project. The CC portion is an enolate derived from the corresponding ketone and the CNO portion is a nitrile oxide, the formation of which will be discussed at length in the following section.³⁰

Nitrile Oxides

The use of nitrile oxides has been catalogued for a long time and their applications are still being studied today.^{31,32} Nitrile oxides are made up of three atoms and they adopt a linear shape due to the two formal π bonds between carbon and nitrogen (Figure 8).

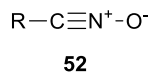


Figure 8

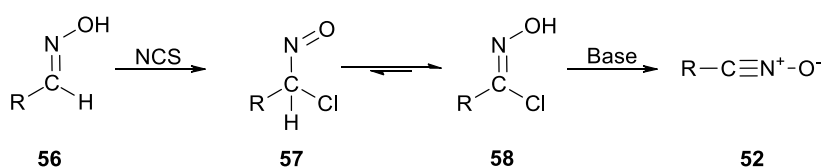
Nitrile oxides are also sensitive to moisture and are therefore formed *in situ* in the majority of reactions.

Formation

There are several approaches to generating nitrile oxides, some examples being: dehydrohalogenation of C-halogenated oximes, dehydration of nitroalkenes, thermolysis of furoxans and oxidation of aldoximes.

Dehydrohalogenation of C-halogenated Oximes

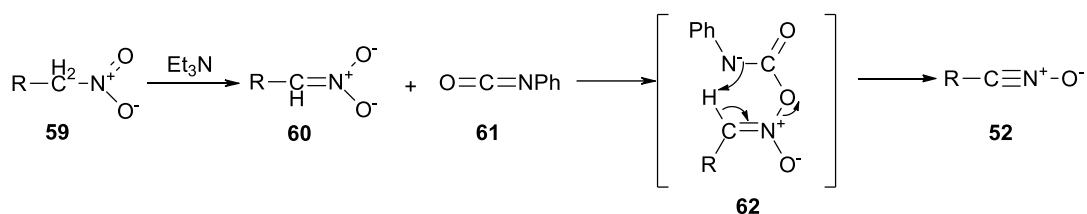
This method was first introduced in 1894 by Werner and Buss.³³ It comprises two steps, starting with an aldoxime. Aldoxime **56** can be C-halogenated with a variety of different halogenating agents to supply a 'positive halogen', examples being N-iodosuccinimide, N-chlorosuccinimide, *t*-butyl hypochlorite or chlorine which yields an α -halonitroso compound, that will tautomerise (as illustrated in scheme 5) to a hydroxyimoyl chloride **57** which will slowly decompose in air. The hydroxyimoyl chloride then undergoes dehydrohalogenation *in situ* to yield nitrile oxide **51**, usually in the presence of a base such as pyridine, which acts as a dehydrohalogenating agent (Scheme 11).



Scheme 11

Dehydration of Nitroalkanes

Hoshino and Mukaiyama introduced an effective one-step reaction for the formation of aromatic and aliphatic nitrile oxides from primary nitroalkanes.³⁴ This protocol commonly utilises phenyl isocyanate **60** and triethylamine as the dehydrating mixture, although, other reagent combinations have also been reported (Scheme 12).³⁵

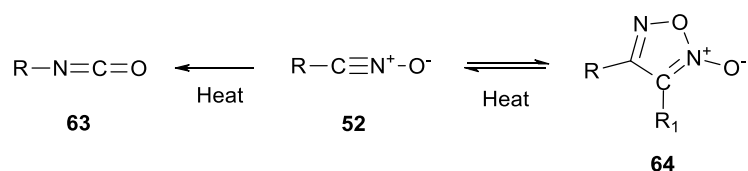


Scheme 12

It is also possible to employ di-tert-butyl dicarbonate (Boc_2O) instead of phenyl isocyanate, which yields the respective *N*- or *O*-tert-butoxycarbonyl (Boc) protected products.

Thermolysis of Furoxans

Stable heterocyclic products known as furoxans **63** are formed by the dimerisation of nitrile oxides; this process can be reversed by the addition of heat (Scheme 13).^{36,37}

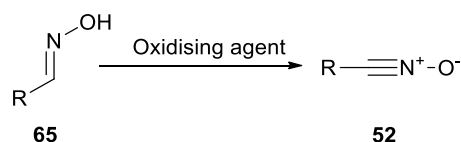


Scheme 13

If the nitrile oxide is generated in the presence of dipolarophiles, cycloaddition will take place avoiding re-dimerisation. However, at high temperatures nitrile oxides will rearrange to form isocyanates **62** which is a drawback of this method.

Oxidation of Aldoximes

Aldoximes can be oxidised to nitrile oxides with a variety of oxidising agents, for example, iodobenzene diacetate, lead tetraacetate, chlorobenzotriazole and metal oxides manganese dioxide or chromium(IV) oxide (Scheme 14).³⁸⁻⁴¹



Scheme 14

1.2 1,3- Dipolar Cycloadditions

A cycloaddition is a pericyclic reaction that is defined as:

“A reaction in which two or more unsaturated molecules (or parts of the same molecule) combine with the formation of a cyclic adduct in which there is a net reduction of the bond multiplicity”⁴²

Pericyclic reactions are often used to assemble four-, five- and six-membered heterocyclic rings. The three simplest types of cycloaddition reaction are as follows: 1) the [2+2] cycloaddition, 2) the Diels-Alder reaction, and 3) the 1,3-dipolar cycloaddition (Figure 9).

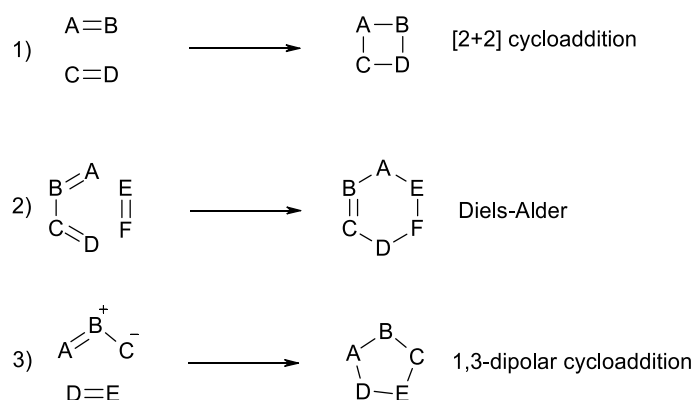


Figure 9

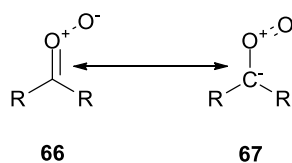
The [2+2] cycloaddition and Diels-Alder reactions are used to form four- and six-membered rings respectively, while the 1,3-dipolar cycloaddition, also known as the Huisgen Cycloaddition, is used to form five-membered rings, for example isoxazoles.⁴³

The 1,3-dipolar cycloaddition is related to the Diels-Alder reaction in that it is a $[4\pi+2\pi]$ process; however, the 4π -electron component is a 1,3-dipole rather than a diene, and the 2π -electron component is a multiply-bonded two-atom section. The relationship of these two components can either be intra or inter-molecular and the mechanism proceeds through a 6π -electron aromatic transition state.

The isoxazoles that will be synthesised in this project will be produced using a 1,3-dipolar cycloaddition, with a nitrile oxide acting as the 1,3-dipole and a cyclohexane 1,3-dione as the dipolarophile.

The 1,3-Dipole

A 1,3-dipole is a molecule that has charge separated over three atoms, an example being carbonyl oxide (Scheme 15).



Scheme 15

There are two main resonance forms for the 1,3-dipole, one in which the carbon atom contains eight electrons in the outer shell **65** and one in which it contains six **66**. As the latter would be unstable the 1,3-dipole is traditionally displayed in the octet form.

There are two primary types of 1,3-dipolar compounds. The first, type-1, has a 1,3-dipolar canonical form in which there is a double bond between atoms A and B in the sextet form and a triple bond in the octet form; the central atom B is in an sp-hybridized state (Figure 10).

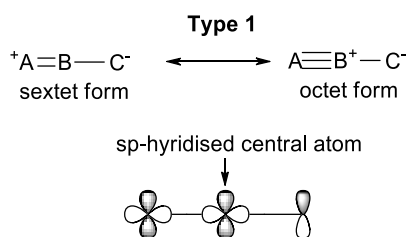


Figure 10

This type of dipole is known as the propargyl-allenyl type and is linear; some examples of this type of dipole are shown below (Figure 11).⁴⁴

Common Type-1 1,3-Dipoles

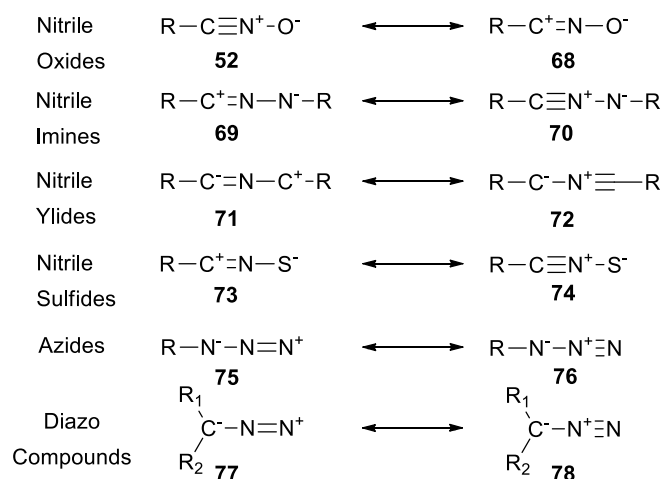


Figure 11

The second type is known as the allyl anion type and has a 1,3-dipolar canonical form which has a single bond between A and B in the sextet form, and a double bond between them in the octet form; the central atom is sp^2 -hybridized (Figure 12).

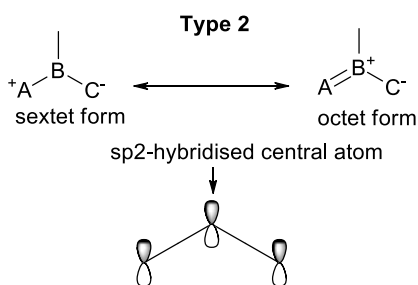


Figure 12

The structure of these dipoles is bent, and again, some examples are shown below (Figure 13).

Common Type-2 1,3-Dipoles

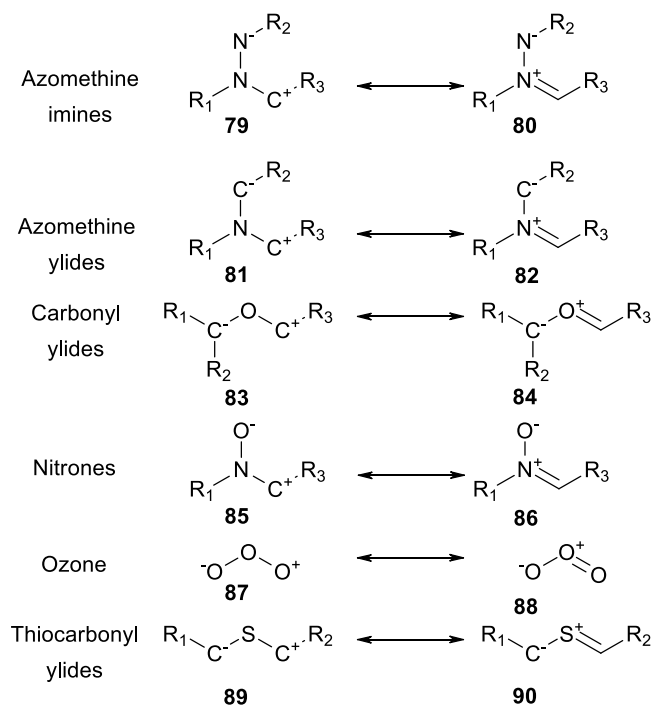


Figure 13

As stated, in this project, the dipole used is a nitrile oxide, which is type-1; this dipole contains both an electrophilic and a nucleophilic portion (Figure 14).

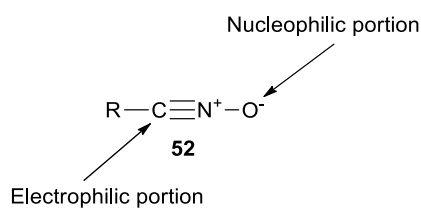


Figure 14

The Dipolarophile

Dipolarophiles are compounds that will react with dipoles, in this case a 1,3-dipole. Traditional examples of dipolarophiles are alkenes such as those used in the Diels-Alder reaction. However, there are many other examples as illustrated below (Figure 15).^{45,46}

Common Dipolarophiles

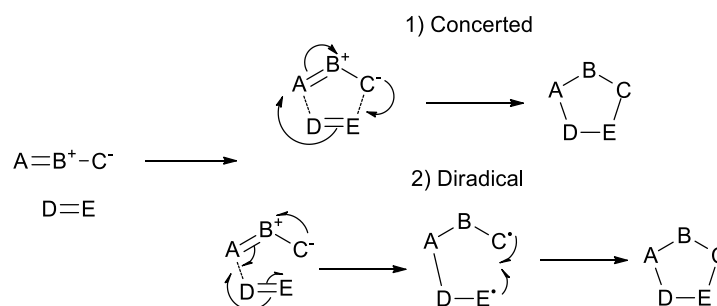
| | |
|--------------|------------------|
| Alkene | C=C |
| | 91 |
| Alkyne | C≡C |
| | 92 |
| Diazo | C=N ₂ |
| | 93 |
| Nitrile | C≡N |
| | 94 |
| Carbonyl | C=O |
| | 95 |
| Thiocarbonyl | C=S |
| | 96 |

Figure 15

In the case of this project, the dipolarophile is an alkene as part of an enolate.⁹

Mechanism of 1,3-Dipolar Cycloaddition

Two different mechanisms have been proposed for 1,3-dipolar cycloaddition. R. Huisgen⁴⁷ proposed the concerted mechanism in 1968 and in the same year R. A. Firestone⁴⁸ proposed a di-radical mechanism (Scheme 16).



Scheme 16

Later evidence was provided to suggest that the reaction follows the concerted mechanism.⁴⁹

The success of the reaction depends on two factors: the reaction must be sterically favourable and a full π -orbital of one reactant must be able to favourably interact with an empty π^* orbital of the other

reactant i.e. they must be of the same phase. The better these interactions, the lower the energy gap between the two orbitals and therefore, the greater the reactivity.

This can be explained using FMO (Frontier Molecular Orbital) theory.⁵⁰ The FMOs involved in this mechanism are the HOMO (Highest Occupied Molecular Orbital) and LUMO (Lowest Unoccupied Molecular Orbital) of the 1,3-dipole interacting with the LUMO and HOMO of the dipolarophile. If these molecular orbitals overlap correctly, then new bonds will be formed, yielding a new ring (Figure 16).⁵¹

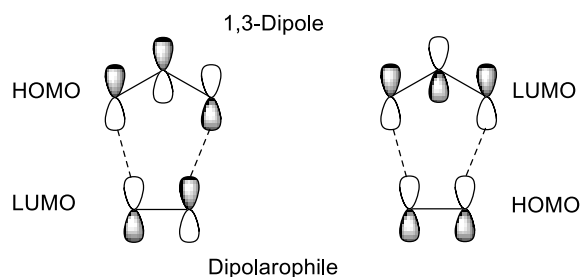
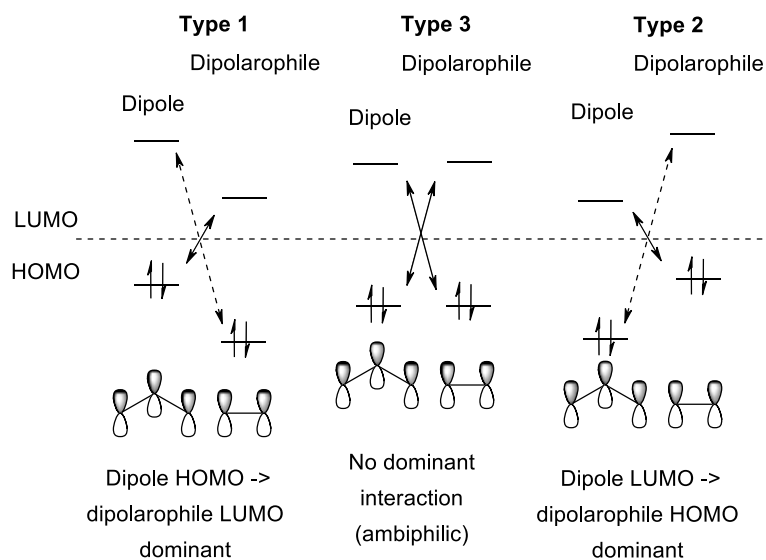


Figure 16

Based on direction of charge transfer in the above interactions it is possible to separate 1,3-dipolar cycloadditions into three distinct types: 1) Dipole-HOMO controlled reactions in which the charge moves from dipole to dipolarophile, 2) Dipole-LUMO controlled reactions where the charge moves from dipolarophile to dipole, or 3) where both control the reaction (Scheme 17).



Scheme 17⁸

Type-1 reactions have the smallest energy gap between the HOMO of the 1,3-dipole and the LUMO of the dipolarophile; examples being reactions of ylides⁵² and other nucleophilic dipoles. Electron

withdrawing substituents on the dipolarophile, which lower the energy of the LUMO, or electron donating substituents on the dipole, which raise the energy of the HOMO, accelerate this type of reaction.

Type-2 reactions are the opposite of type -1, the smallest energy separation being between the HOMO of the dipolarophile and the LUMO of the dipole; examples are reactions of ozone⁵³ and other electrophilic 1,3-dipoles.

Type-3 reactions have neither HOMO nor LUMO dominating the FMO interactions; this type of reaction is known as ambiphilic; an example being azides.⁵⁴

It is possible to form different stereo- and regio-isomers during the 1,3-dipolar cycloaddition (Figure 17); however, the selectivity usually favours one over the other i.e. it is not a 1:1 mixture of isomers.

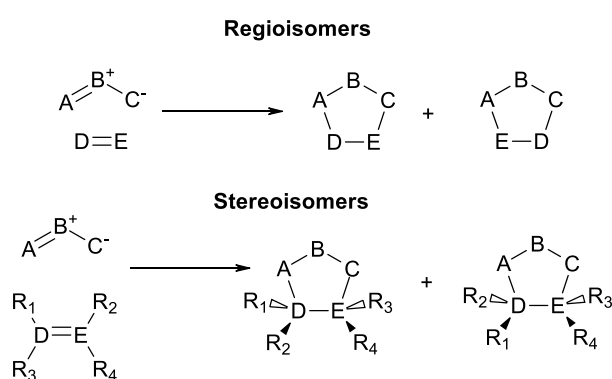


Figure 17

Regioselectivity is determined both by the class of 1,3-dipolar cycloaddition taking place and by which molecules possess the dominant HOMO and LUMO. Stereochemistry is determined by the geometrical approach of the dipole and dipolarophile, with both *exo* and *endo*-transition states being possible. However, the configuration of the dipolarophile is usually retained which is evidence for a concerted mechanism.⁵⁰

Whilst stereochemical or regiochemical issues could have been a concern in this synthesis; they were not, as the dipolarophile is planned to be a symmetrical six-membered ring, forming a fused isoxazole and no other products were observed by Suzuki *et al.*³⁰

1.3 Alkene Metathesis

As one of the key steps in this project will be the investigation of ring closing metathesis using Grubbs II catalyst, this process warrants some discussion.

Olefin metathesis is a well-documented process that has been used in the synthesis of a range of natural products.⁵⁵ It is defined as:

“A bimolecular process formally involving the exchange of a bond (or bonds) between similar interacting chemical species so that the bonding affiliations in the products are identical (or closely similar) to those in the reactants.”⁴²

There are three types of olefin metathesis: 1) ring-closing metathesis (RCM), 2) cross metathesis and 3) ring-opening metathesis polymerisation (ROMP) (Figure 18).

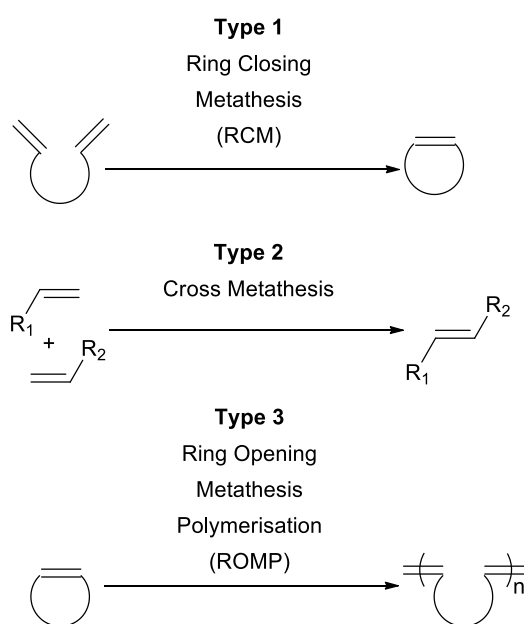
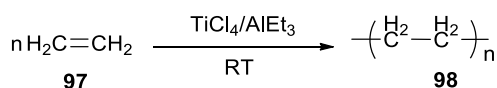


Figure 18

Ring closing metathesis is a reaction in which two acyclic alkenes undergo a reaction that closes a ring and is promoted by a catalyst. Cross metathesis is the reaction between two different alkenes to yield a “dimerised” product connected by an alkene. Ring opening metathesis polymerisation is the opposite of RCM in that it opens a ring; however, the two units are then polymerised with other units.

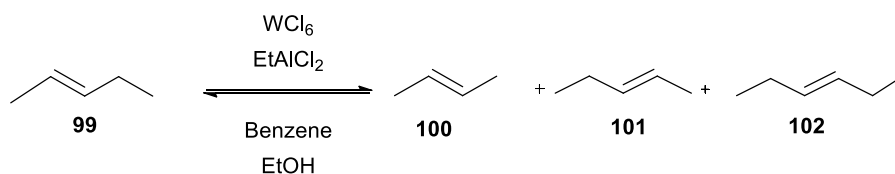
Origins of Metathesis

The roots of metathesis can be traced back to the Nobel Prize winning work by Ziegler and Natta in the middle of the 20th century.^{56,57} This involved the synthesis of α -olefins using titanium tetrachloride and triethylaluminium catalysts (Scheme 18).



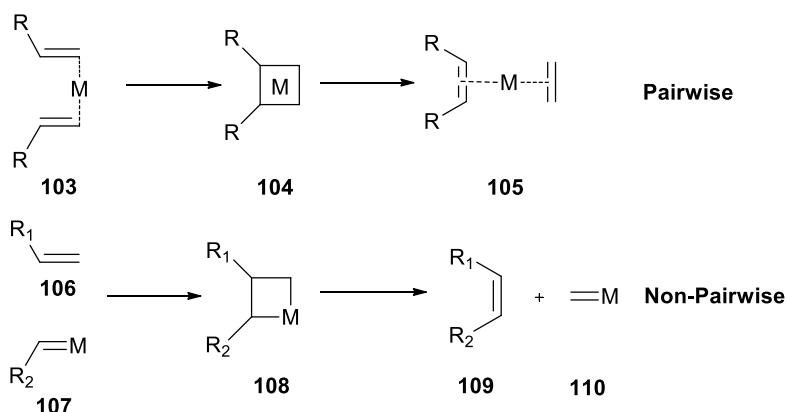
Scheme 18

Calderon *et. al.* who were working at the Goodyear Tyre and Rubber company were the first to coin the term olefin metathesis in 1968. They found that it was possible to carry out the metathesis of 2-pentene using a tungsten catalyst in conjunction with ethylaluminium dichloride (Scheme 19).⁵⁸



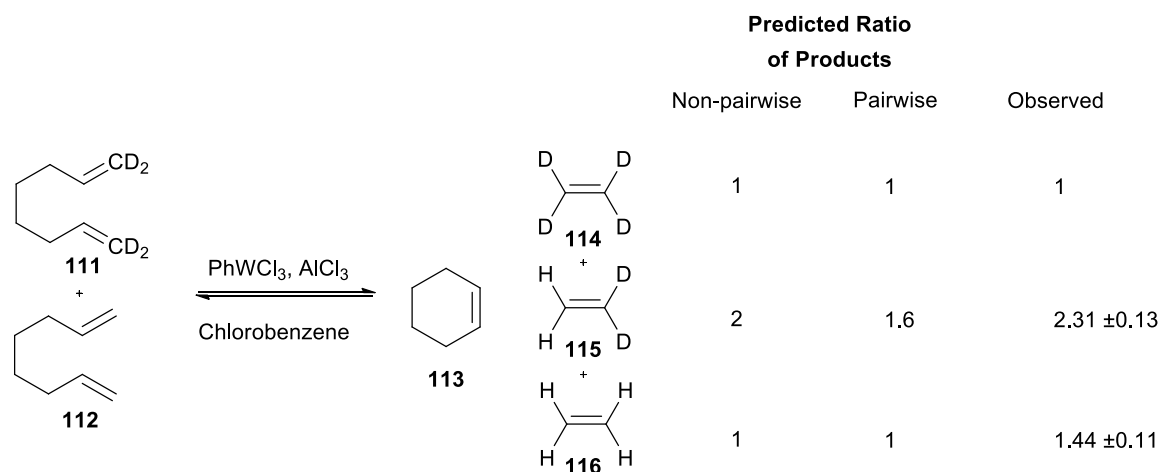
Scheme 19

As the field of metathesis was starting to grow there was some debate as to the mechanism for this reaction. Two potential mechanistic pathways were proposed, the **pairwise** and **non-pairwise** (Chauvin) mechanisms (Scheme 20).^{59,60}



Scheme 20

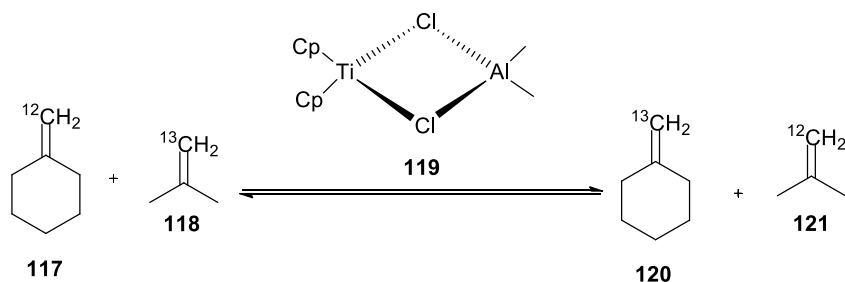
These proposed mechanisms were investigated by Grubbs *et. al.* who made predictions on the ratio of products that should be observed for each pathway (Scheme 21).⁶¹



Scheme 21

The experimentally observed results suggested that the **non-pairwise** mechanism was most likely.

At approximately the same time as Grubbs' initial investigations, the Tebbe reagent **119** was discovered by Tebbe and his group. This organometallic catalyst was able to switch isotopically labelled carbon atoms in methylenecyclohexane and isobutene (Scheme 22).⁶²

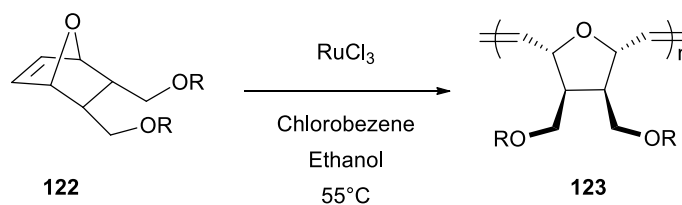


Scheme 22

This laid the foundation for research by Grubbs and his group. Starting in the 1980s Grubbs and Evans began investigating Tebbe's reagent; over the subsequent decades they would carry out research using tungsten, molybdenum and titanium as metathesis catalysts.^{63,64}

This work led to development of one of the most widely used olefin metathesis catalysts: Grubbs Catalyst. Grubbs chose ruthenium for his investigations as when compared to the above metals, it is the most reactive towards olefins but also more tolerant of functional groups and moisture.⁶⁵

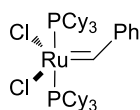
Using this knowledge, Grubbs began the development of a metathesis catalyst that was not only active, but stable under standard atmospheric conditions and protic solvents. One of the first attempts at this was the use of ruthenium trichloride (Scheme 23).⁶⁶



Scheme 23

This catalyst was able to conduct ROMP reactions on 7-oxanorbomene derivatives in both wet and dry conditions; however, this catalyst, whilst stable, was not as active as Grubbs desired. Its reactivity was increased by adding groups that exhibited greater electron donating potential, such as triphenylphosphine.⁶⁷⁻⁶⁹

Eventually this led to the development of Grubbs 1st generation catalyst **124**; this catalyst showed both good reactivity and stability under atmospheric conditions (Figure 19).⁷⁰

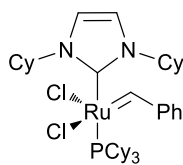


124

Grubbs I catalyst

Figure 19

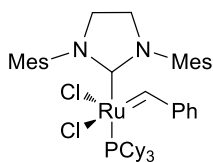
Grubbs continued his work in this field with the aim of designing a catalyst that retained the same stability but exhibited even greater activity. As mentioned in the paragraph above, groups with greater electron donating potential placed at the axial position increased catalyst activity. In 1998 Hermann *et. al.* reported that replacing the tricyclohexyl phosphine (PCy₃) group with an N-heterocyclic carbene displayed an increase in reactivity over the first generation catalyst (Figure 20).⁷¹



125

Figure 20

Grubbs screened a range of ligands of this type and this subsequently led to the synthesis of Grubbs 2nd generation catalyst **126** (Figure 21).⁶⁵



Grubbs II catalyst

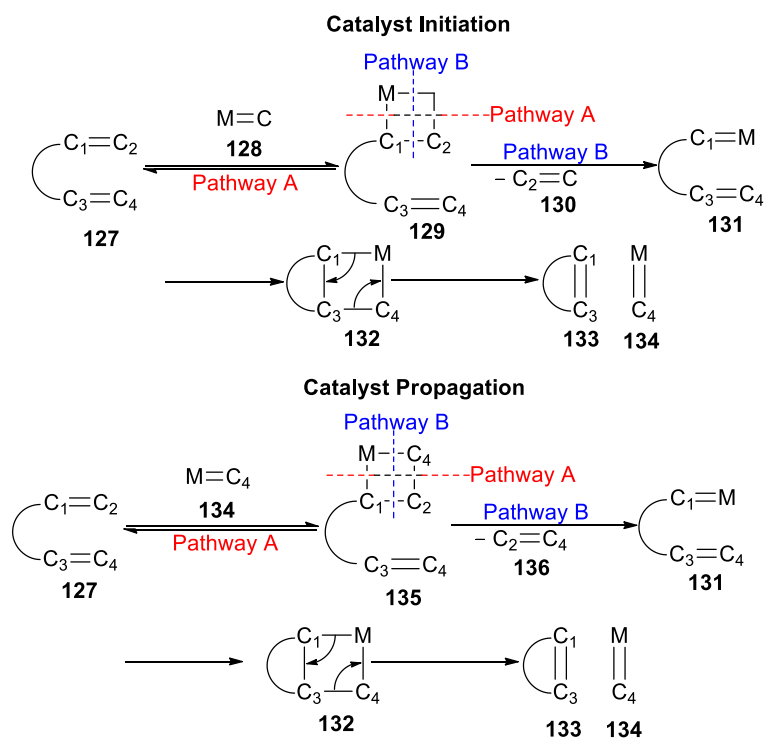
126

Figure 21

Although this section has focused on Grubbs, it is important to note that there have been many other groups who have worked on metathesis and its catalysts, examples being Hoveyda and Schrock.^{72,73} In 2005 Grubbs, Chauvin and Schrock shared the Noble prize for chemistry, for their work on metathesis.

Ring Closing Metathesis

The mechanism of ring closing metathesis comprises two main stages: 1) Catalyst initiation and 2) Catalyst Propagation, where the active complex promotes addition catalytic cycles (Scheme 24).^{74,75}



Scheme 24

The first step is the binding of the catalyst to one of the olefins present in the substrate **127** to form a metallacyclobutane complex **129**. This can either revert to the substrate **127** and catalyst **128** or alternatively an alkene **130** can be ejected and complex **131** is formed. This then goes on to form intermediate **132** before breaking down to yield the ring closed product **133** and metal complex **134**.

Catalyst propagation then continues where the active complex **134** will go on to bind the un-cyclised substrate **127** and carry out the reaction in much the same fashion as in initiation. This cycle continues until all of the available substrate has been consumed.

Regardless of the metal used this mechanism remains the same; however, there are differences, for example in a ruthenium-based catalyst such as Grubbs the olefin acts as a π -Lewis acid; conversely in a molybdenum catalyst the metal acts as the Lewis acid and the olefin as the base.

It is important to note that this mechanism will give rise to both E and Z isomers of the double bond depending on which is the most energetically favourable. In the case of small strained ring systems, the *cis*-isomer is often favoured, as the system may be too strained to form the *trans*-isomer. However, in larger ring systems it is not uncommon to see a mixture of isomers.

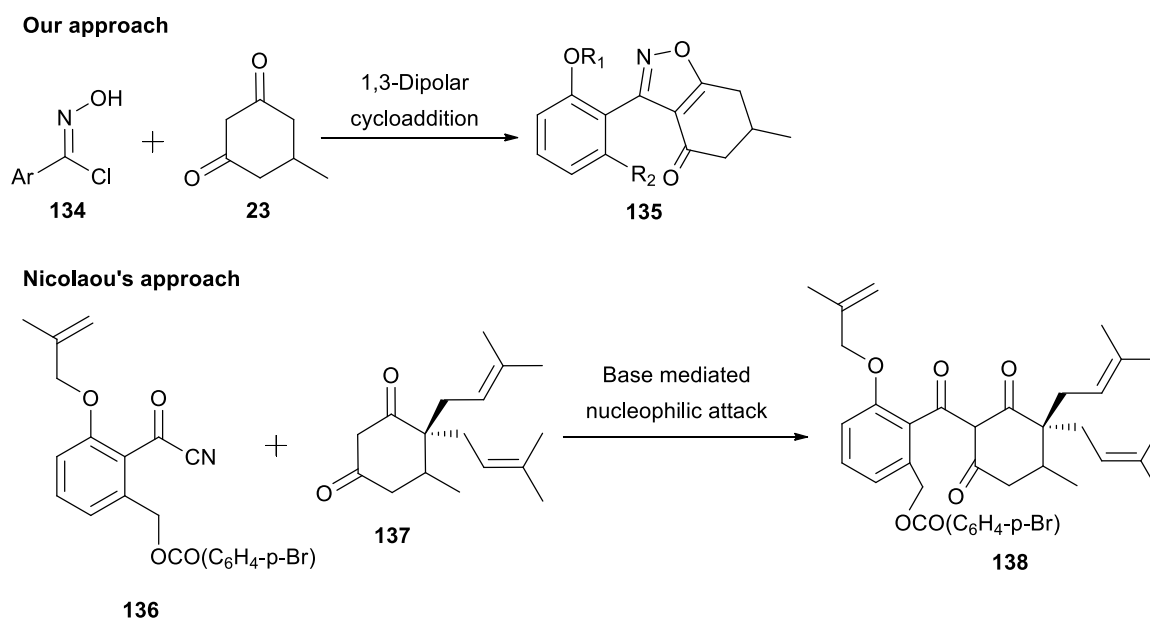
1.4 Previous Synthesis

As has been discussed, the coleophomone group of natural products possess a range of properties that make them attractive to the synthetic chemist. As a result, in the fifteen years since they were isolated they have received some attention from the chemistry community.

The two major contributions have come from K.C. Nicolaou *et al.* in the form of a total synthesis paper for coleophomones B, C and D³ and from Suzuki *et al.* in the form of an investigation into apparent structural anomalies.⁹ There have also been some preliminary investigations carried out by Goldring *et al.*, who have been working towards precursors for coleophomone A.⁷⁶

Nicolaou's Total Synthesis

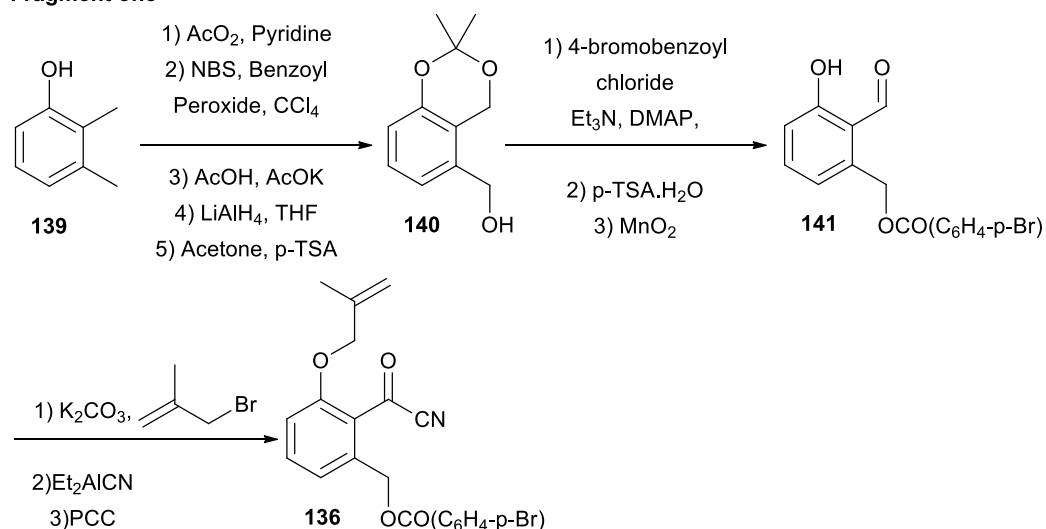
Nicolaou was the first chemist to complete the total synthesis of coleophomones B, C and D. His approach differs from ours in that while we intend to form the aryl cyclohexanedione unit using a 1,3-dipolar cycloaddition of a nitrile oxide to a dipole, he builds both fragments separately and then combines them *via* base-mediated nucleophilic attack (Scheme 25).



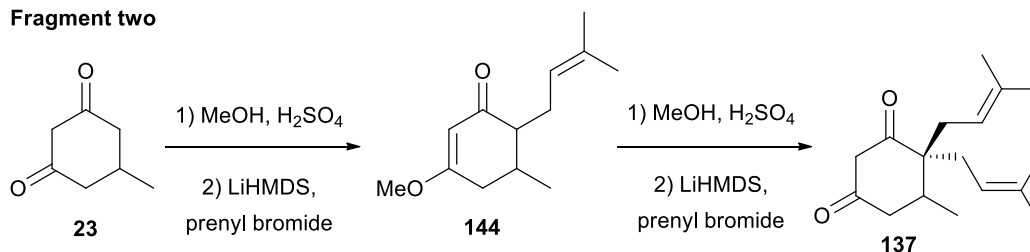
Scheme 25

The Nicolaou group was able to form these fragments from commercially available starting materials (Scheme 26).

Fragment one

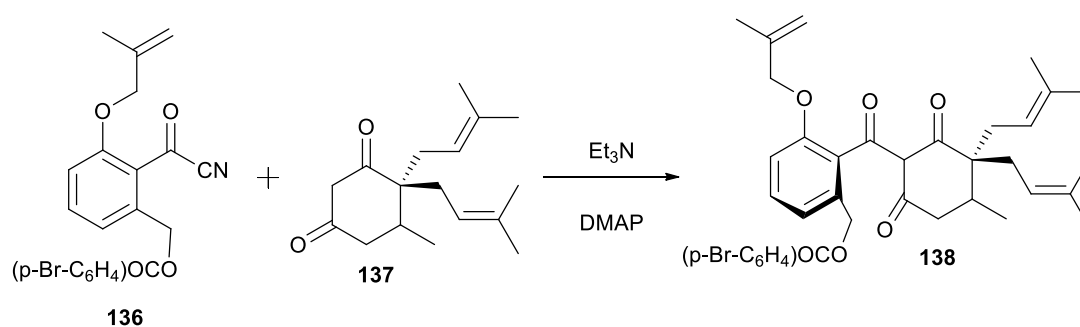


Fragment two



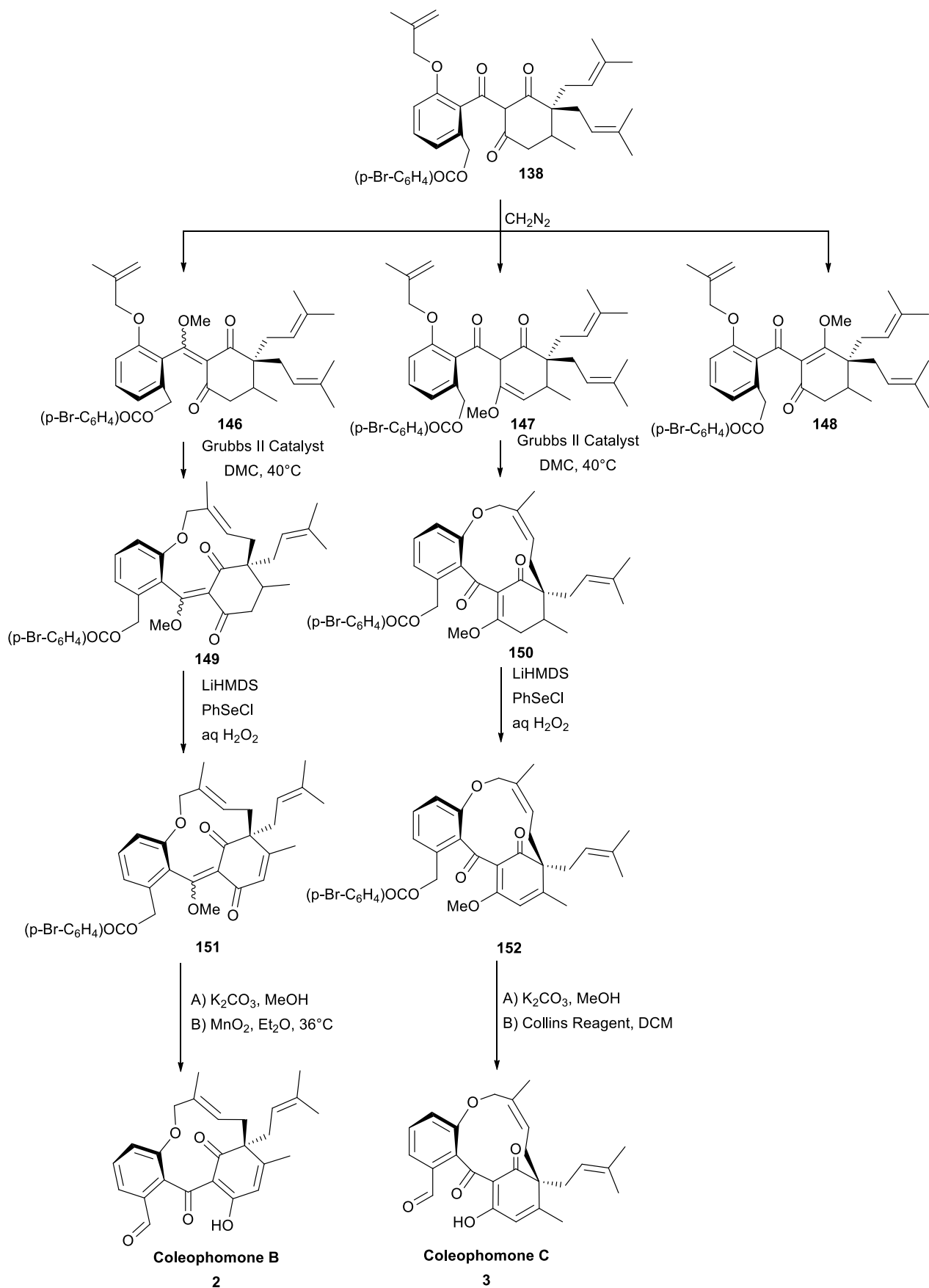
Scheme 26

These fragments were then combined in the step that creates the C-C bond that we plan to form in the 1,3-dipolar cycloaddition we intend to use, this is C-acylation of a 1,3-dicarbonyl compound (Scheme 27).



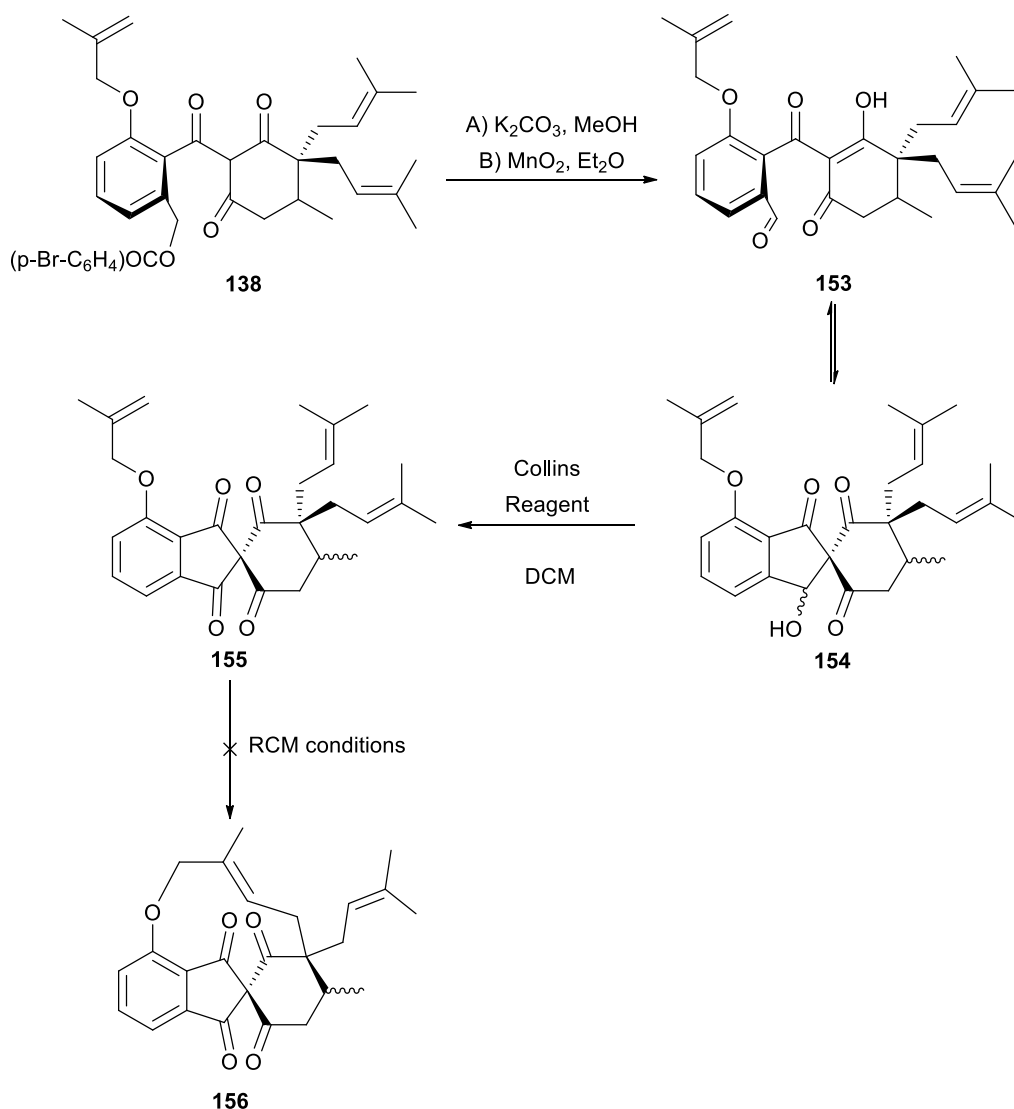
Scheme 27

With the successful formation of this core structure, Nicolaou was then able to proceed and concentrate on the next challenge, forming the 11-membered macrocycle. At this point in the synthesis precursor **138** is able to interconvert between several tautomers, which were isolated *via* protection with diazomethane. Following this the 11-membered macrocycle was formed using RCM and the resulting macrocycles were furnished with the remaining functionality present in the natural products (Scheme 28).



Scheme 28

Using this methodology, Nicolaou *et al.* were able to successfully form coleophomones B and C. However, contrary to the findings by the Merck isolation team, they were unable to convert B to A under a range of conditions. Due to this a *de novo* approach towards forming this member of the coleophomone family was required (Scheme 29).

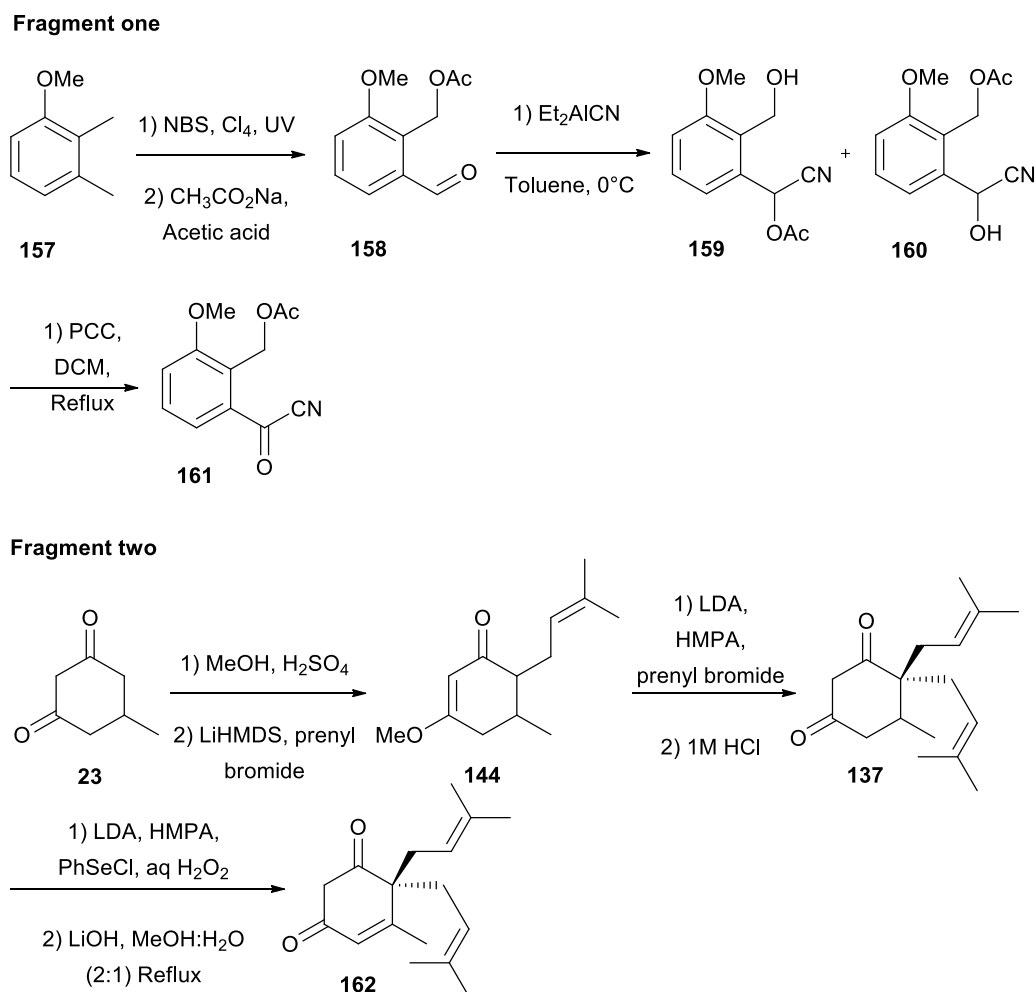


Scheme 29

Whilst it was possible to generate spirocyclic system **155**, it was not possible to close the ring using a wide range of ring closing metathesis conditions. This was believed to be due to the inherent strain of the spirocycle, and unfortunately current metathesis reagents were not powerful enough to overcome this. The synthesis of coleophomone A was therefore unsuccessful.

Nicolaou also attempted the synthesis of coleophomone D. As it lacks the macrocycle found in A, B and C the synthesis of D was more accessible when compared to the others. Once again the initial

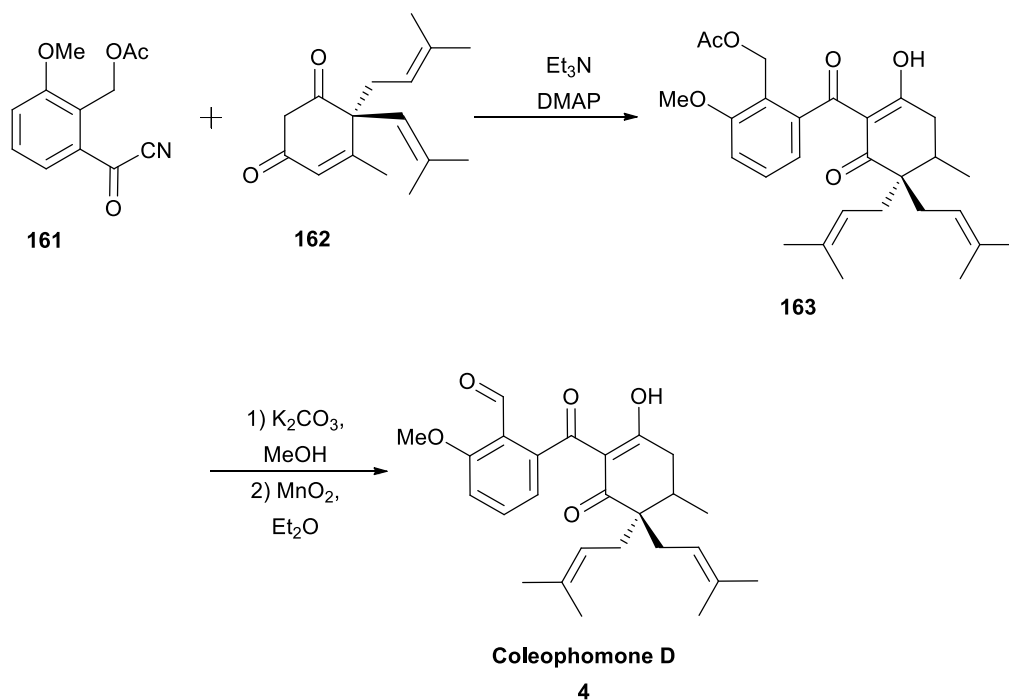
approach is to furnish both cyclic fragments before combining them in base-mediated nucleophilic attack (Scheme 30).



Scheme 30

This approach differs from the previous in that the initial steps in the formation of fragment one were radical bromination followed by acetylation under acidic conditions to yield the corresponding acetylated aldehyde **158**. Following this the desired nitrile group was introduced using diethyl aluminium cyanide, However, this yielded a mixture of de-acetylated products **159** and **160**. The desired product, **160**, was carried through and oxidised to yield the desired acetyl cyanide **161**.

Once again, these two fragments were combined to yield the furnished core of coleophomone D. However, as there is no macrocycle to form, the remaining steps were relatively straightforward (Scheme 31).



Scheme 31

In conclusion, Nicolaou *et al.* were able to complete the total synthesis of coleophomones B, C and D; however, it was not possible for him to form coleophomone A, and to date, this remains a synthetic challenge.

Suzuki's Comparison

Suzuki *et al.* noted that there was an unusual difference between the biosynthetically expected structure **163** and that which was reported in the literature **162** (Figure 22).⁹

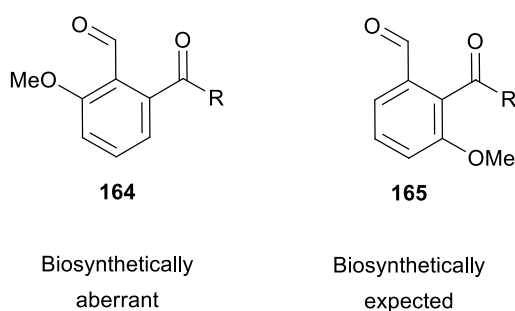
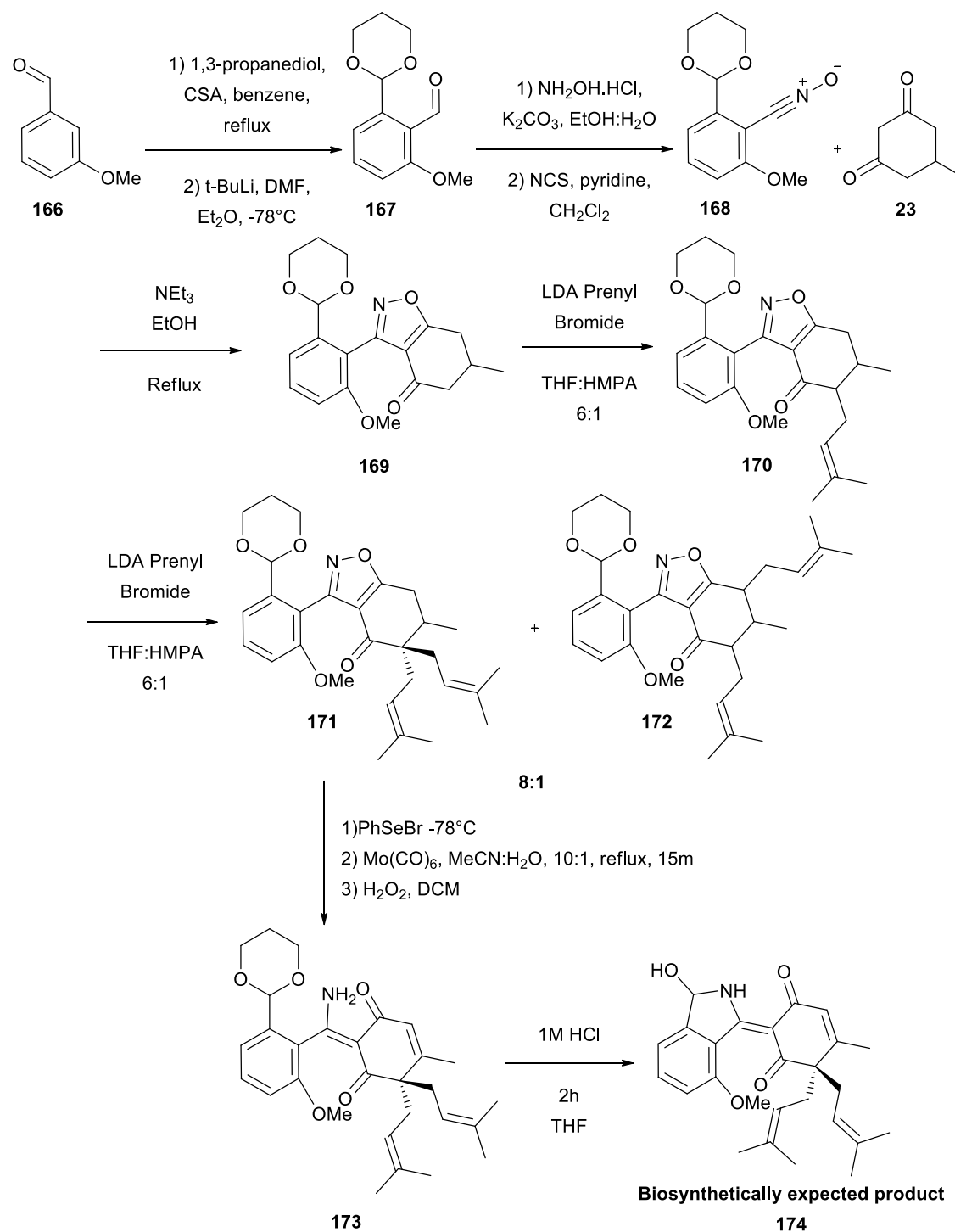


Figure 22

In order to resolve this discrepancy, Suzuki *et al.* conducted the synthesis of both the expected and aberrant isomers of a derivative of the natural product. However, unlike the synthesis Nicolaou performed, this required the tri-carbonyl system to be masked in order to prevent any potential

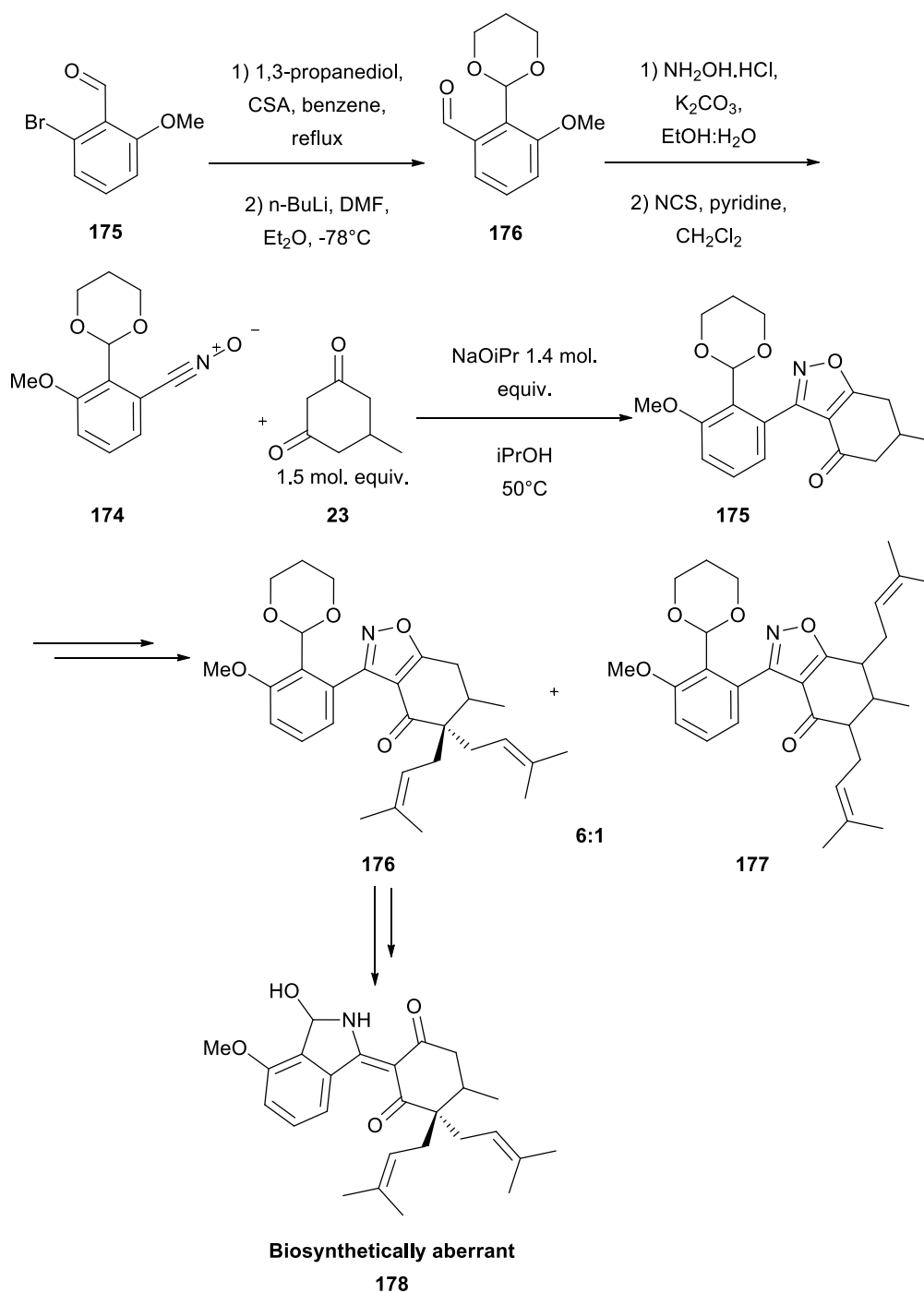
tautomeric inter-conversion. They began with the biosynthetically expected isomers, masking the reactive tricarbonyl system as an isoxazole (Scheme 32).



Scheme 32

One notable point of this synthesis is that hexamethylphosphoramide (HMPA) was required to achieve the desired *bis*-prenyl **171** in good ratios. In the absence of HMPA regioisomer **172** was obtained

almost exclusively. With biosynthetically expected aminal **174** obtained, the next challenge was to repeat this process for the aberrant version, using aryl bromide **175** as a starting point (Scheme 33).⁷⁷



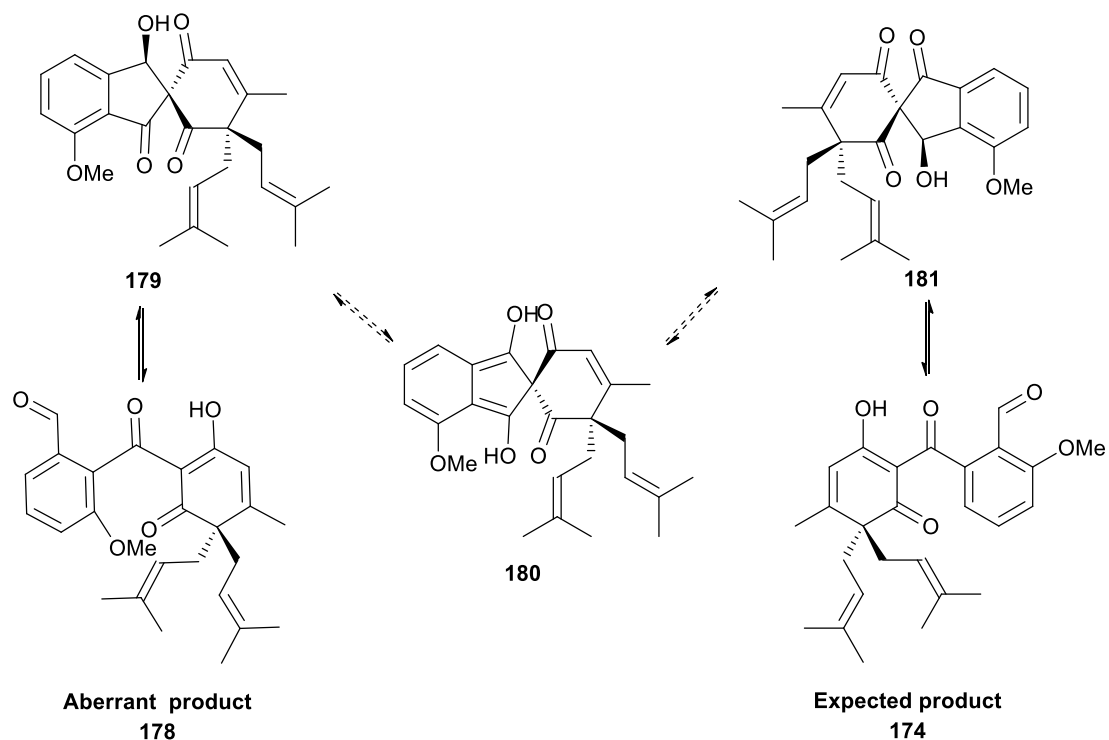
Scheme 33

This sequence was much the same as the previous with only two notable exceptions. Firstly the cycloaddition was carried out under a different set of conditions; illustrating how sensitive this reaction is. Secondly, the ratio of *bis*-prenyl regioisomers is slightly lower in this case.

The ^1H and ^{13}C data for both of these compounds were compared to those which were reported by the Merck isolation group, confirming that this unusual structure is indeed correct.

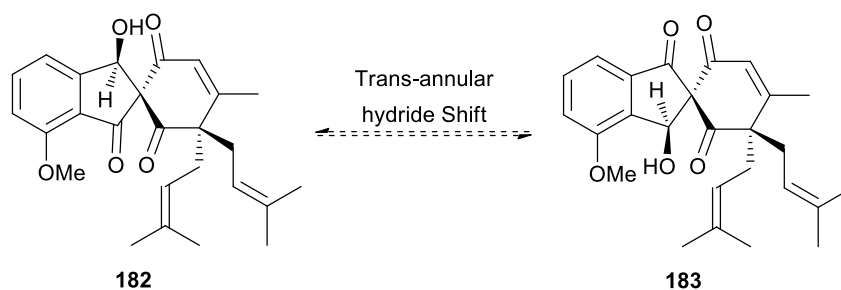
Suzuki *et. al.* postulated several mechanisms by which aberrant structure **178** could have been formed. The first is that specific oxidative enzymes that introduce hydroxyl functionality at that position.

The second is structural inter-conversion *via* a pseudo-symmetrical enol which could form under acidic, basic or photochemical conditions (Scheme 34).^{78,79}



Scheme 34

The third suggested mechanism for inter-conversion is *via* a *trans*-annular C-hydride shift (Scheme 35).⁸⁰

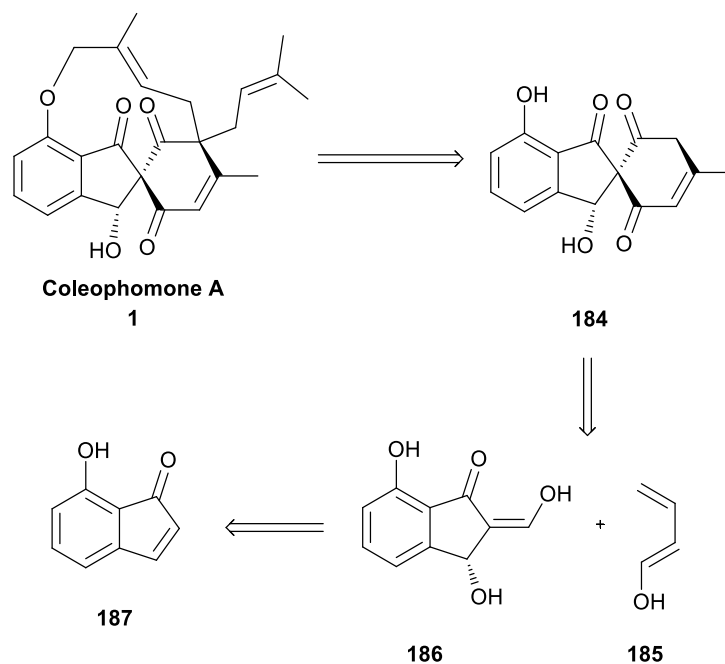


Scheme 35

However, in this case, these processes are only speculative at this point and they do not explain why only one isomer is observed.

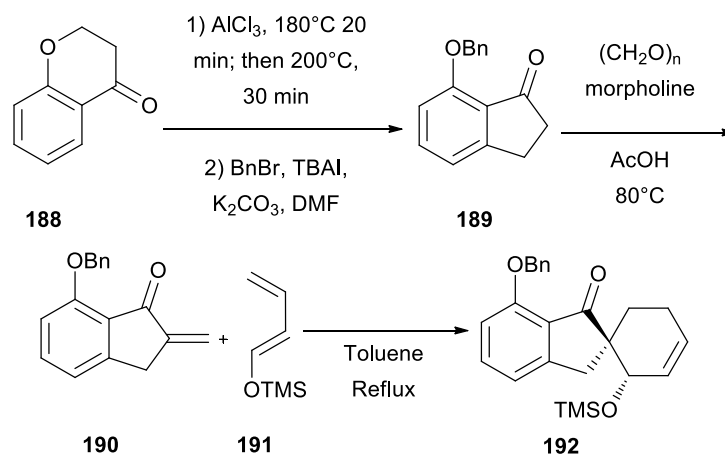
Goldring's Investigation

Goldring *et al.* have begun tentative investigations towards forming Colephomone A *via* a spiro-fused indanone route (Scheme 36).⁸¹



Scheme 36

This approach differs from Nicolaou and Suzuki in that it builds the fused six-five membered ring system first before going on to add the *spiro* ring *via* a [4 + 2] cycloaddition reaction. To date Goldring *et al.* have only been able to demonstrate the synthetic utility of this methodology, they have not synthesised the natural product (Scheme 37).



Scheme 37

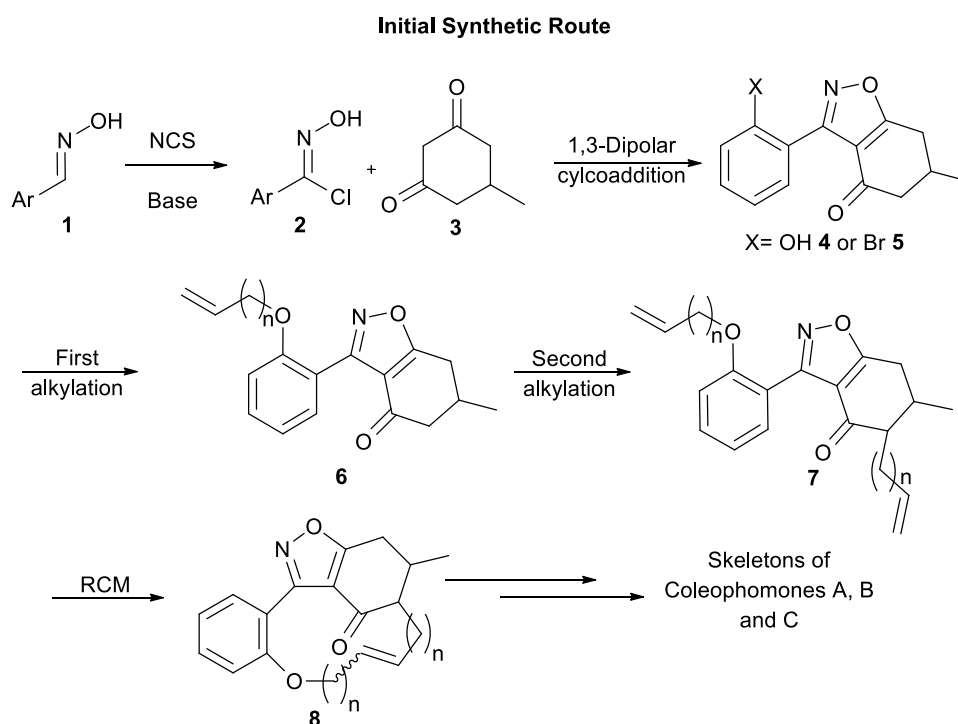
It can be seen how this methodology could be applied to the synthesis of coleophomone A in the future, as this compound still represents an unresolved synthetic challenge.

2.0 Progression towards the Coleophomone Natural Products

Natural Products

The aim of the project was to develop a synthetic route to the coleophomone natural products and their analogues *via* an isoxazole route.

One of the first challenges the natural products present is the formation of the core bi-cyclic tri-carbonyl system. As discussed in chapter one, our synthetic approach intended to accomplish this by performing a 1,3-dipolar cycloaddition to generate a benzisoxazole. Once this had been accomplished the next challenge would be to form the distinctive macrocycle (Scheme 1).³⁰



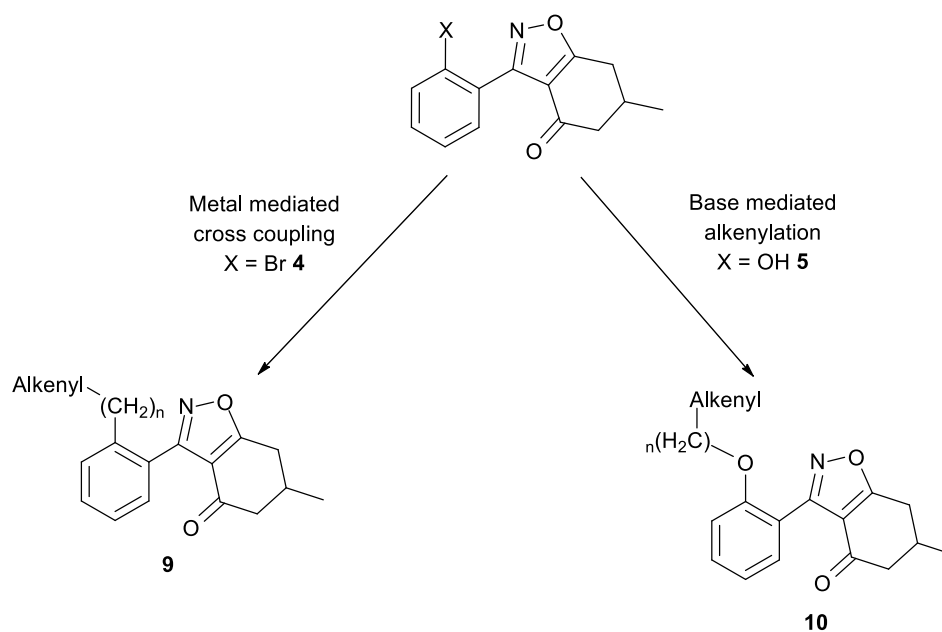
Scheme 1

As discussed earlier, we would aim to alkylate our benzisoxazole twice, once O and once on C before employing RCM to form the macrocycle. However, we were unsure whether it would be possible to generate the 11-membered ring due to the rigidity of the fused isoxazole system and as such *bis*-alkenyl benzisoxazole **7** was the first synthetic objective following isoxazole formation.

2.1 Functionalized Imidoyl Chlorides

Mono-Ortho Imidoyl Chlorides

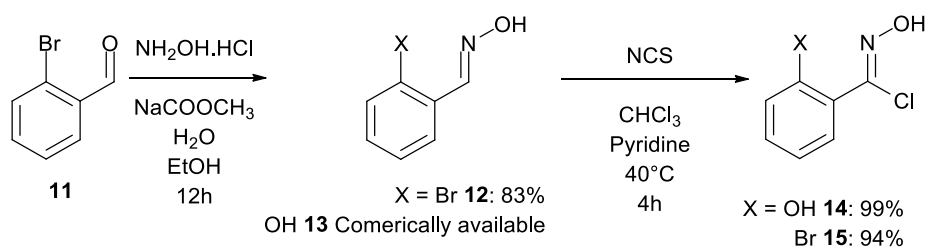
The first step in the synthetic plan is the formation of an aryl imidoyl chloride from which we could generate the nitrile oxide dipole. Although we believed that we would be able to successfully O-alkylate a phenolic aryl ring; we also pursued the precursors for metal mediated cross coupling, as this represented an alternative approach to analogues (Scheme 2)



Scheme 2

While bromo-substituted benzisoxazole **4** in C-C cross-coupling would not give the desired C-O linkage present in the natural product, it would still present a *viable* route to analogues of coleophomones, furthermore C-O coupling can be envisaged.

With the initial targets identified; we proceeded to synthesise the chosen imidoyl chlorides from their corresponding oximes (Scheme 3). The oximes were available commercially for salicaldehyde and prepared by standard methods for 2-bromobenzaldehyde (hydroxylamine hydrochloride and sodium acetate). C-Chlorination was achieved in good yield using N-chlorosuccinimide and pyridine in chloroform at 40°C.

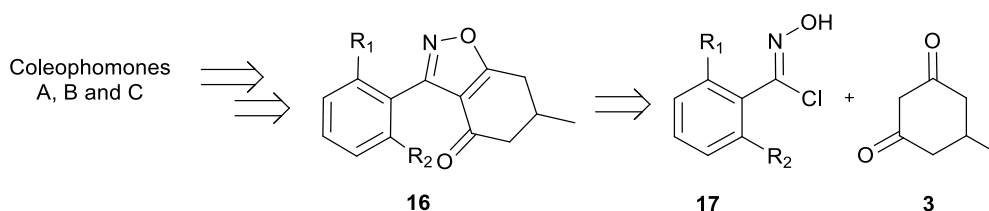


Scheme 3

This demonstrates the ability of this methodology to synthesise the known *ortho*-functionalized benzimidoyl chlorides in excellent yields.³⁰

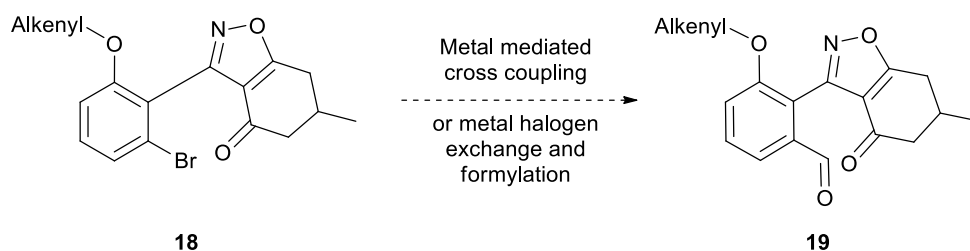
***Bis-Ortho* Substituted Imidoyl Chlorides**

While initially the focus was to be building the macrocycle using mono-functionalized imidoyl chlorides; the coleophomones A, B and C will require *bis-ortho* substituted aryl imidoyl chlorides (Scheme 4).



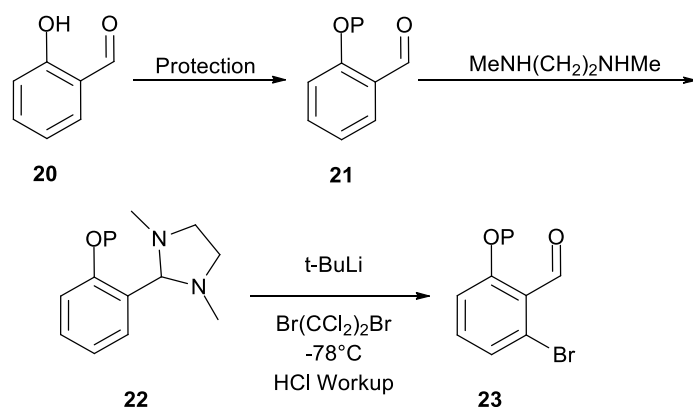
Scheme 4

Bis-ortho substituted benzisoxazole **16** was chosen as the building block, as its functionality should prove versatile enough to allow the introduction of the desired aldehyde in a number of ways (Scheme 5).



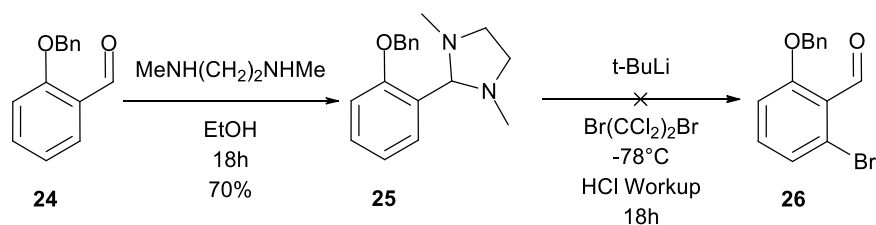
Scheme 5

Initially the following route was planned, deprotonation of an aminal followed by substitution from an electrophilic source of bromine (Scheme 6).⁷⁷



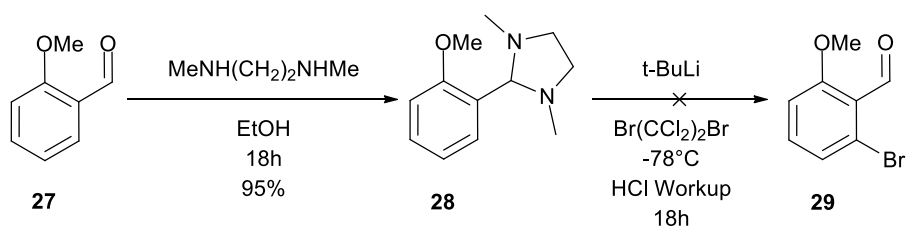
Scheme 6

As 2-benzyloxybenzaldehyde **24** was commercially available it was chosen as the starting point in this synthesis (Scheme 7). The aminal **25** was easily prepared in good yield.



Scheme 7

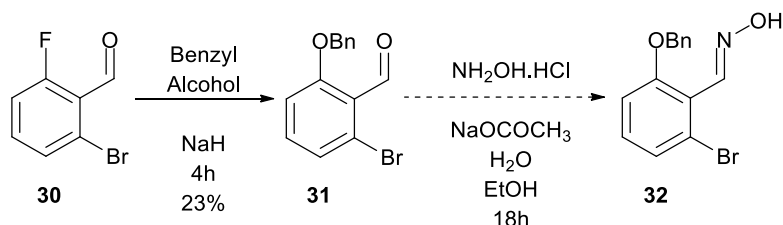
Although it had been reported as possible to deprotonate at the desired *ortho*-position with two or more molar equivalents of base, no bromination was observed.⁷⁷ To determine if the benzyl protecting group was being deprotonated the reaction was repeated with a methoxy substituent *ortho* to the imidazolidine ring **28** (Scheme 8).



Scheme 8

Again no bromination was observed; it is believed that this reaction may have failed due to deprotonation occurring at the tertiary carbon on the imidazolidine ring or anion quench occurring *via* a benzyne intermediate.

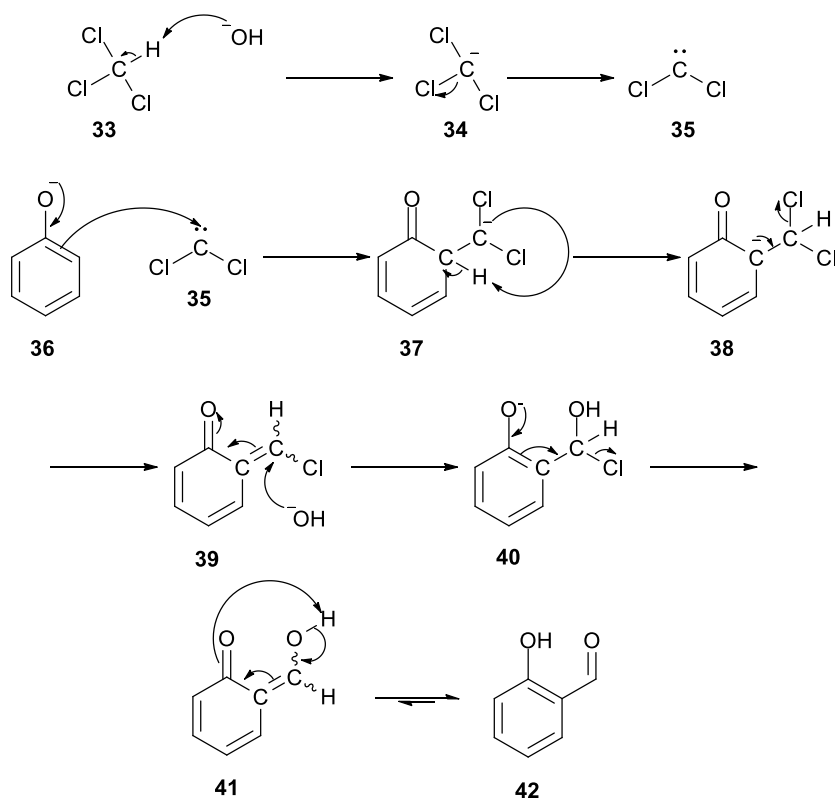
With this failure a new approach was required. It was possible to find a commercially available compound with the required bromine substituent in place, namely 2-bromo-6-fluorobenzaldehyde; however, the required protected phenolic group would have to be introduced *via* nucleophilic aromatic substitution (Scheme 9). This reaction proceeded, but only in low yield (23%).



Scheme 9

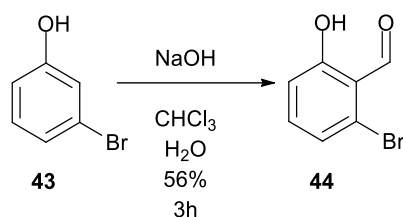
Although oxime formation was attempted, the ^1H NMR spectra indicated what was believed to be complex mixture of starting material and product, which we were unable to assign completely. This avenue of investigation was not explored further, as it was not possible to increase the yield of the first $\text{S}_{\text{N}}\text{Ar}$ step.

As the previous attempts were not acceptable a new tactic was required; this came in the form of the Reimer-Tiemann reaction. Using this reaction it should be possible to achieve formylation *via* electrophilic substitution with dichlorocarbene. Scheme 10 illustrates the prototype reaction.⁸²



Scheme 10

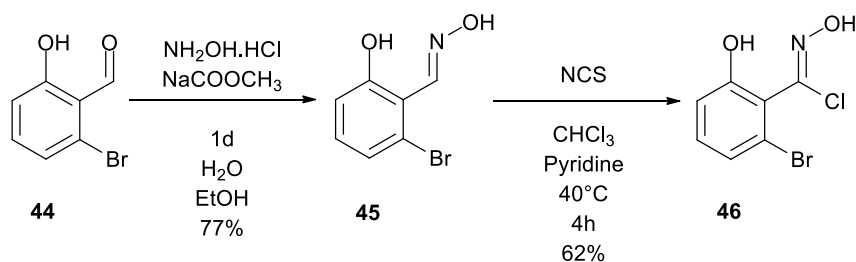
We applied this approach to commercial 3-bromophenol. A benefit of this approach is that protection of the hydroxyl group was not required (Scheme 11). The Reimer-Tiemann protocol afforded 2-bromo-6-hydroxybenzaldehyde in moderate yield.



Scheme 11

Although other isomers are observed in the crude mixture, the desired phenol **44** was the major component.

With the successful formation of phenol **44** in reasonable yields it was possible to progress with the synthetic strategy (Scheme 12).

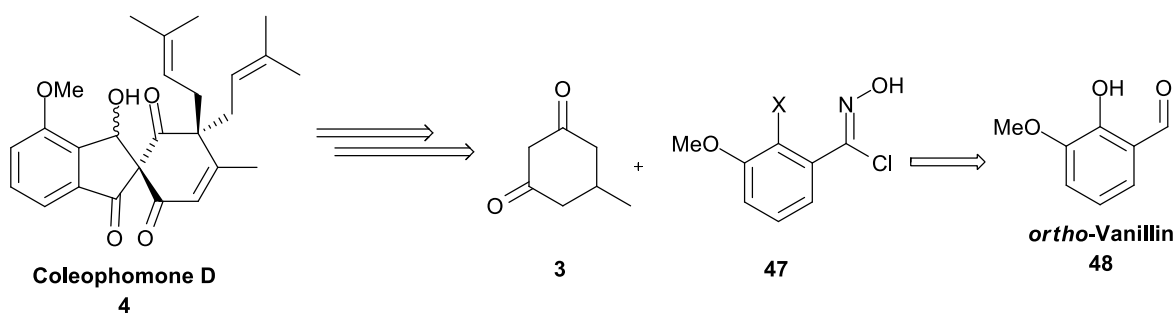


Scheme 12

The synthesis of oxime **45** and imidoyl chloride **46** proceeded well by our established procedures, with good yields being obtained at both stages. The success of this methodology put us in a position to synthesise precursors to coleophomones A, B and C as required.

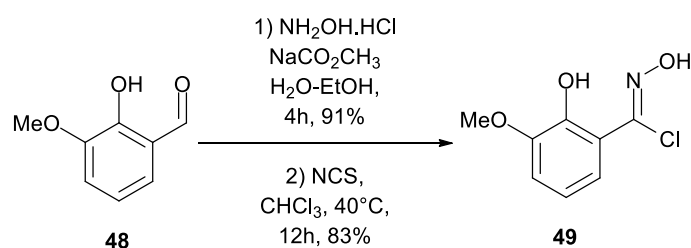
***Ortho,meta*-Imidoyl Chlorides**

As mentioned, coleophomone D has a different substitution pattern to A, B and C and as such, it requires a different imidoyl chloride precursor. Fortunately the desired substitution pattern was available in the form of *ortho*-vanillin (Scheme 13).



Scheme 13

It was hoped that the phenol functionality would provide a synthetic handle to install the desired aldehyde at a later date. As *ortho*-vanillin is commercially available in large quantities it made an appropriate starting point (Scheme 14).



Scheme 14

It was possible to synthesise the corresponding oxime and imidoyl chloride in excellent yields from *o*-vanillin and as such, a precursor for coleophomone D was readily available.

Additional examples

Over the course of this project it has been necessary to synthesize several imidoyl chlorides to provide additional examples for a publication (Figure 1) as will be reported later in this thesis. This was completed from commercial aldehydes *via* the oxime, or from commercial oxime in one case.

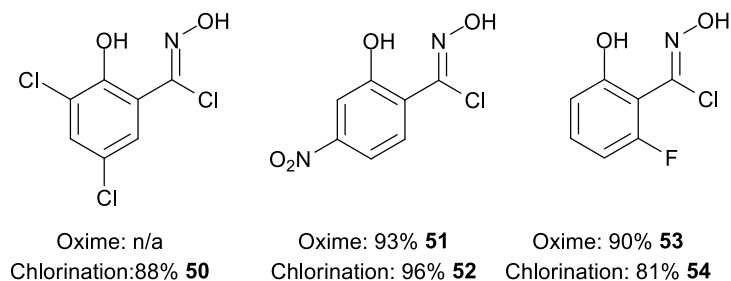
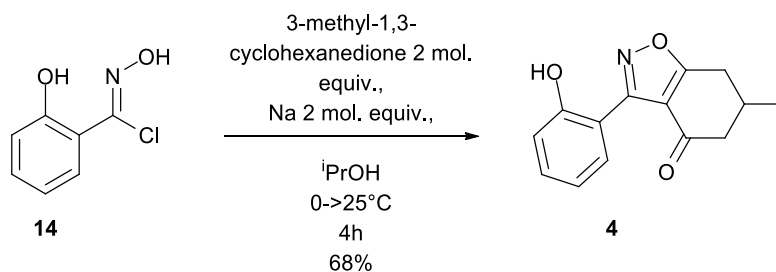


Figure 1

Although they are not related exactly to the coleophomones, they could be used to provide analogues if required.

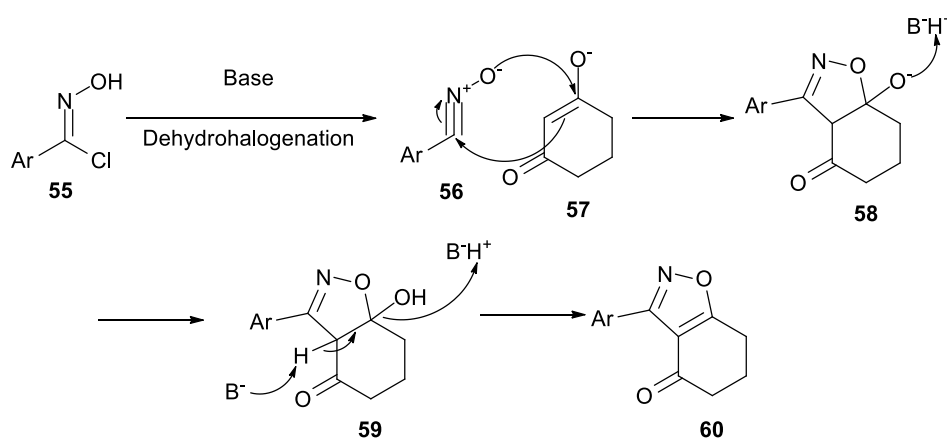
2.2 Benzisoxazole Formation

The next stage in the synthetic route was the formation of the core masked tricarbonyl system present in the coleophomones. This was accomplished as discussed earlier in this thesis (Scheme 32, Chapter 1), using a dipolar cycloaddition onto the enolate of a cyclohexane-1,3-dione (Scheme 15).



Scheme 15

Two equivalents of sodium were dissolved in propan-2-ol to form isopropoxide, this was added slowly to a mixture of dione and imidoyl chloride in propan-2-ol. It was necessary to conduct this at a lower temperature otherwise significantly lower yields were observed, we postulate this could be due to degradation of the nitrile oxide formed in situ. A reasonable mechanism for this reaction is outlined in (Scheme 16).³⁰



Scheme 16

A series of functionalized benzisoxazoles were synthesised from the corresponding imidoyl chlorides using a range of commercially available cyclohexane-1,3-diones (Figure 2); unsubstituted, 5-methyl (corresponding to the coleophomone substitution pattern) and 5,5-dimethyl.

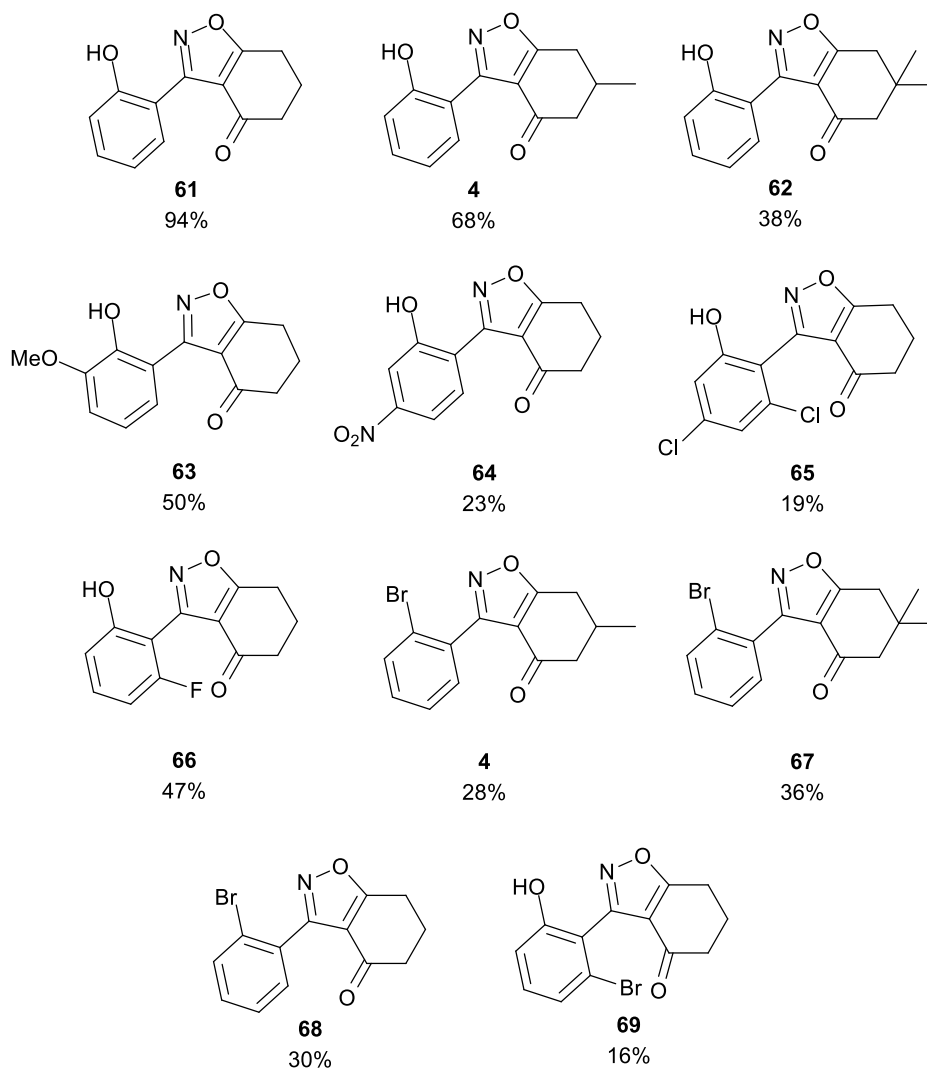


Figure 2

Figure 2: Note that benzisoxazole **61** was formed using an optimised procedure, the other examples remain to be optimised. It should be noted that compounds **61** and **68** have been described in existing literature.³⁰

There are some notable examples in this series, non-methylated- and dimethyl-benzisoxazoles **61** and **62** represent possible analogues of the coleophomones. Bromobenzisoxazole **69** is of interest as it represents the 1,2,3-substitution pattern found in coleophomones A,B and C. Other important examples are fluoro- and bromo-benzisoxazoles **66**, **67**, **68** and **69**, as these open up the possibility of nucleophilic aromatic substitution (S_NAr) and metal-mediated cross coupling studies, respectively. Finally methoxy-phenol **63** is significant as it represents the necessary precursor for coleophomone D.

The exact constitution of phenolic benzisoxazole **61** was established *via* single crystal X-ray crystallography (Figure 3).

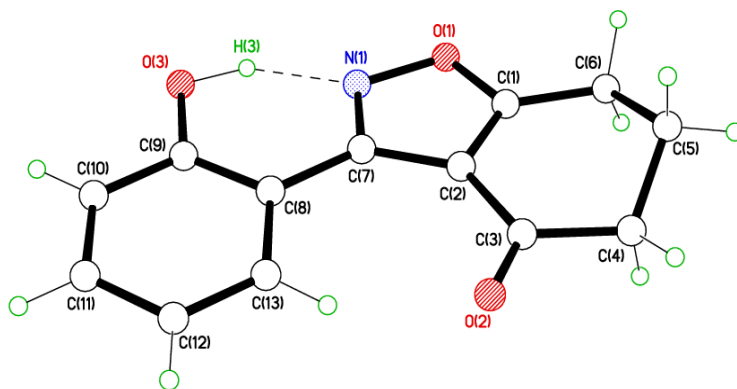


Figure 3. X-Ray crystal structure of 3-(2-Hydroxyphenyl)-6,7-dihydrobenzo[d]isoxazol-4(5H)-one **61**.

This crystal structure was solved by Dr Mark Elsegood of Loughborough University.

This ensured we had the desired product following this reaction, an issue which will become apparent later in this thesis. It is also worth noting the intramolecular hydrogen-bond from the phenol to the isoxazole N-atom, it could be hypothesised that this decreases the acidity of the phenol.

2.3 Aromatic O and C-Alkylation

O-Alkylation

Following the success of the benzisoxazole formation, the next objective was O-alkylation of the phenolic ring. Benzisoxazole **61** was chosen as a test compound as the corresponding unsubstituted cyclohexane-1,3-dione (£34.00/100g Sigma-Aldrich as of 28/10/14) is considerably cheaper than the mono-methyl version (£83.60/5g Sigma-Aldrich as of 28/10/14) present in the natural products (Figure 4).

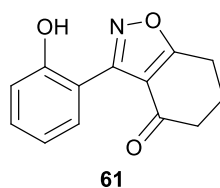
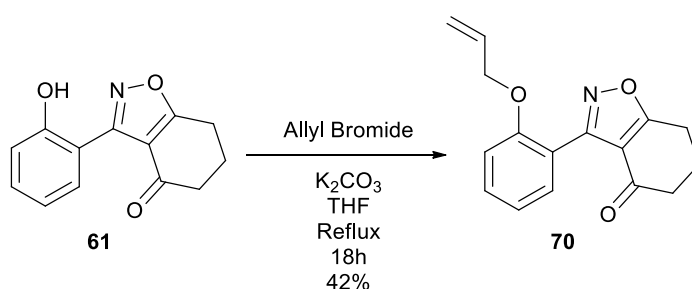


Figure 4

As mentioned previously, several routes for alkylation had been identified. The most direct, base mediated alkylation was attempted first (Scheme 17).



Scheme 17

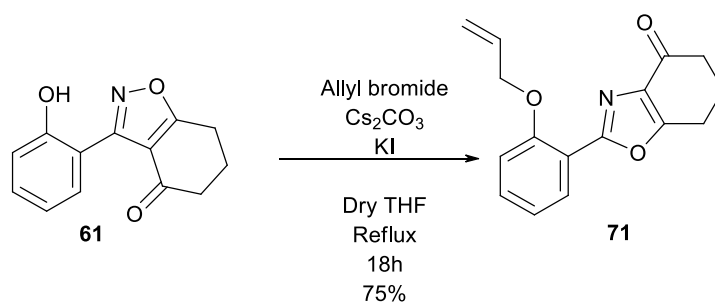
Initially it was believed that this had been successful and yield optimization investigations were carried out (Table 1).

| Electrophile | Base | Additive | Yield |
|------------------------------|---------------------------|-------------------|-------|
| 1.1 mol equiv. allyl bromide | 1.1 mol equiv. K_2CO_3 | None | 42% |
| 1.1 mol equiv. allyl bromide | 1.1 mol equiv. K_2CO_3 | 0.2 mol equiv. KI | 52% |
| 1.1 mol equiv. allyl bromide | 1.1 mol equiv. CS_2CO_3 | 0.2 mol equiv. KI | 75% |

Table 1. *n.b.* All reactions were carried out in refluxing THF with 1 mMol of substrate.

It is believed that the yield increase between potassium and caesium carbonate can be attributed to the improved solubility of the latter in organic solvents.^{83,84}

However, whilst optimisation was successful, we later discovered that allyl benzisoxazole **70** was not the product of this reaction. In fact a very interesting rearrangement had taken place, yielding O-allyl benzoxazole **72** (Scheme 18).

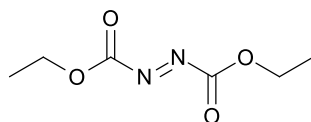
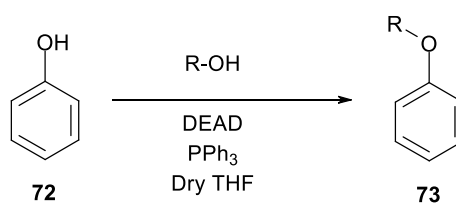


Scheme 18

This rearrangement is extremely interesting as it represented something unreported which could potentially be explored. In the interests of continuity this rearrangement will be discussed at length towards the end of this thesis. In summary, the rearrangement was observed under a range of basic conditions.

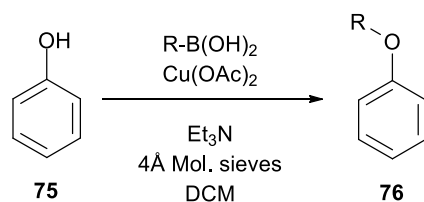
As a method was still required for O-alkylation research into this area continued in a search for a non-basic protocol. We felt Mitsunobu chemistry was more appropriate when compared to a Chan-Lam-Evans style coupling, as we had been developing it in parallel to the base mediated method (Scheme 19).^{85,86}

Mitsunobu coupling



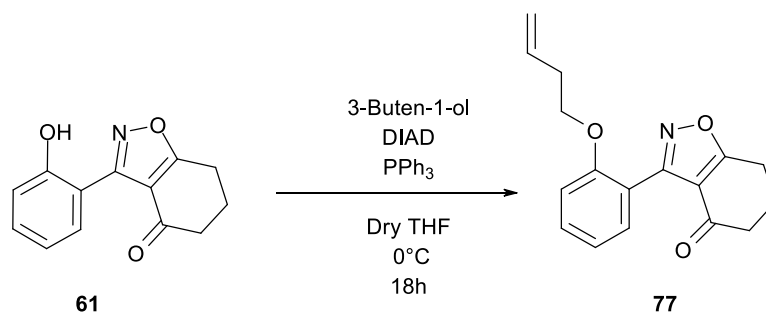
DEAD = Diethylazodicarboxylate
74

Chan-Lam-Evans coupling



Scheme 19

Initially attempts were made using 3-buten-1-ol, as the original aim of the Mitsunobu method was to introduce chains longer than allyl, and using diisopropyl azodicarboxylate (Scheme 20).



Scheme 20

However, following purification *via* column chromatography, it was found that what was believed to be the isolated fraction for O-alkyl benzisoxazole **77** contained both the desired product and di-acyl hydrazine by product **78** (Figure 5).

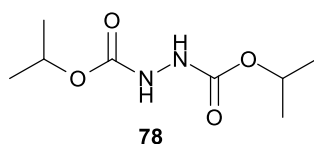


Figure 5

Further attempts were made to isolate the desired product from the mixture; however, it was not possible to achieve this *via* column chromatography on silica.

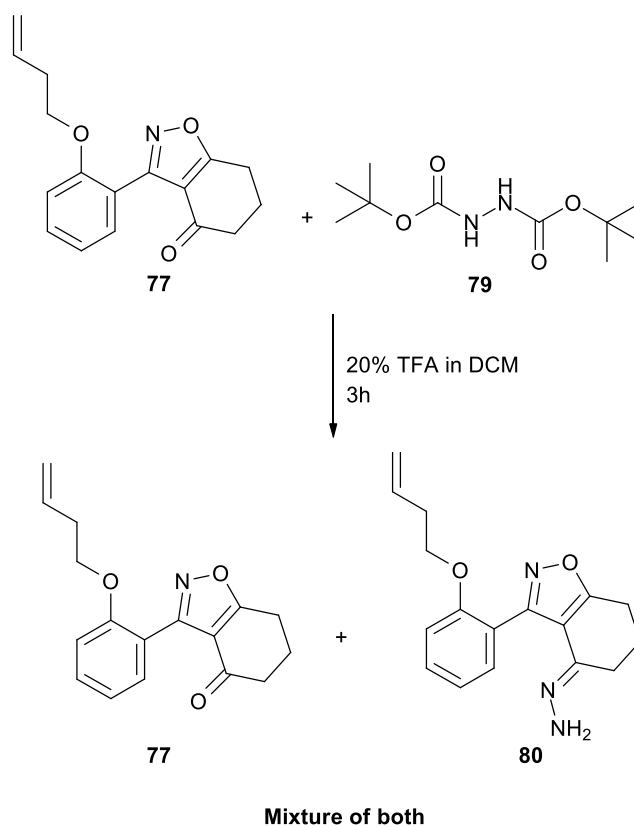
Initially it was hoped that separation would be possible using a different azodicarboxylate (Table 2).

| Reagent | Outcome |
|--------------------------------|--|
| Diisopropyl azodicarboxylate | Reaction successful. Di-acylhydrazine present. |
| Diethyl azodicarboxylate | Reaction successful. Di-acylhydrazine present. |
| Di-tert-butyl azodicarboxylate | Reaction successful. Di-acylhydrazine present. |
| Dibenzyl azodicarboxylate | Reaction successful. Di-acylhydrazine present. |

Table 2. *n.b.* All reactions were carried out in THF with 2.5 mMol of substrate.

Unfortunately these attempts were also unsuccessful, and we suggest the co-elution might be due to hydrogen bonding between O-butenyl benzisoxazole **77** and the acyl-hydrazine by-product.

Evidence suggested that it should be possible to cleave di-tert-butoxycarbonyl hydrazine **79** using trifluoroacetic acid, yielding CO₂, hydrazine as a salt and 2-methylpropene.⁸⁷ Although this was successful, a further, unexpected reaction took place to afford a mixture of the desired O-butenyl ketone and its hydrazone (Scheme 21).



Scheme 21

This was unexpected as hydrazine should be relatively unreactive as a salt. While it should be possible to convert hydrazone **80** back to benzisoxazole ketone **77**, this was undesirable as it would add an unnecessary step to the synthetic route.

Finally dimorpholine azodicarboxamide (DMDC) **81** was used as a coupling agent, in the hope that the hydrazine by-product would be separable, as its functionality is significantly different to the oxycarbonyl coupling agents that had been employed previously (Figure 6).⁸⁸

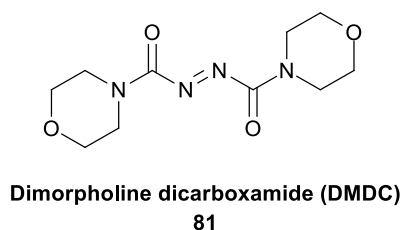
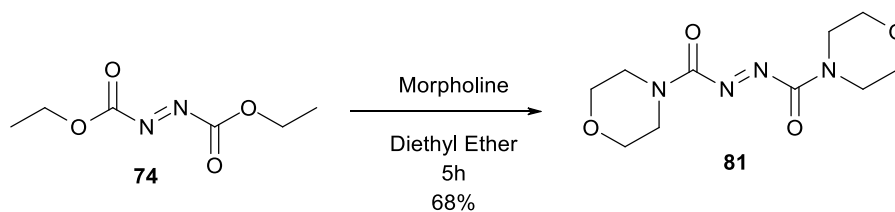


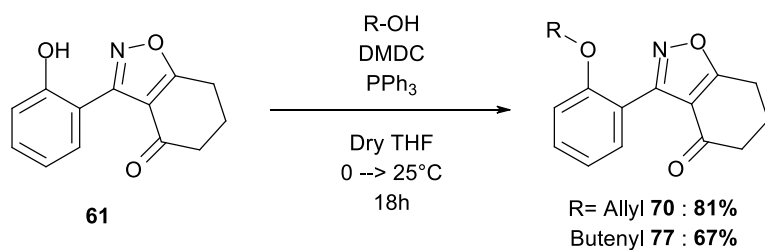
Figure 6

Whilst DMDC is commercially available, it is not cheap (£72.80/5g Sigma-Aldrich as of 19/07/14) and as we would be using it on a relatively large scale this presented a problem. Fortunately it proved to be readily synthesised on multi-gram scale *via* condensation reaction between DEAD and morpholine at room temperature (Scheme 22).⁸⁹



Scheme 22

With the successful synthesis of the coupling agent, it was possible to attempt the coupling itself (Scheme 23).

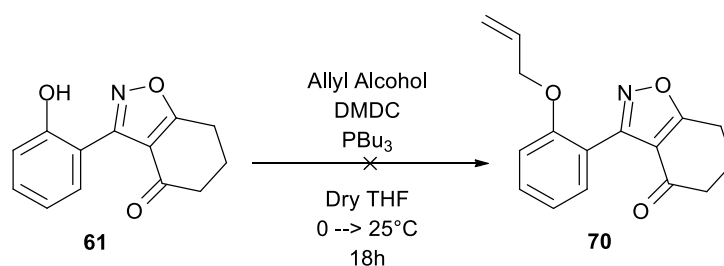


Scheme 23

This new method proved to be very successful for O-allylation and but-3-enylation, as the corresponding carbohydrazide crystallized out from THF at room temperature.

Subsequently investigations of different conditions were carried out in an effort to obtain optimal yields, using O-allylation as test reaction.

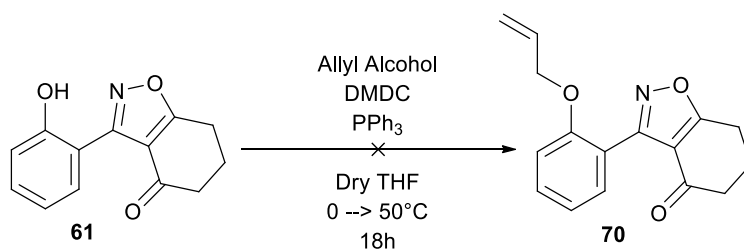
The first of these was testing an alternative tributylphosphine to triphenylphosphine, as it may be more reactive and easier to separate the oxide by-product (Scheme 24).



Scheme 24

However, after 18 hours the reaction showed no signs of reaching completion and was discarded.

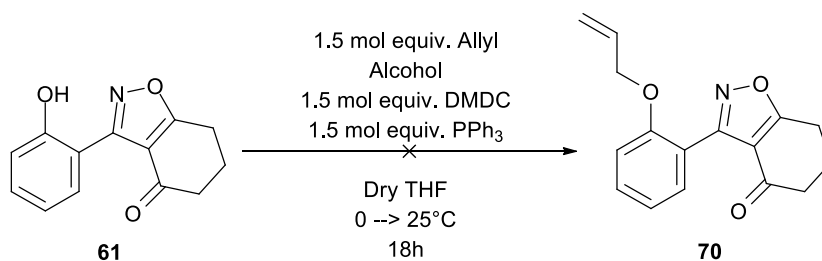
To determine the effect of temperature, the coupling was repeated at a higher temperature (Scheme 25).



Scheme 25

Formation of allyl benzisoxazole **70** was not observed, this suggests at higher temperatures DMDC or a related intermediate degrades before the coupling can take place.

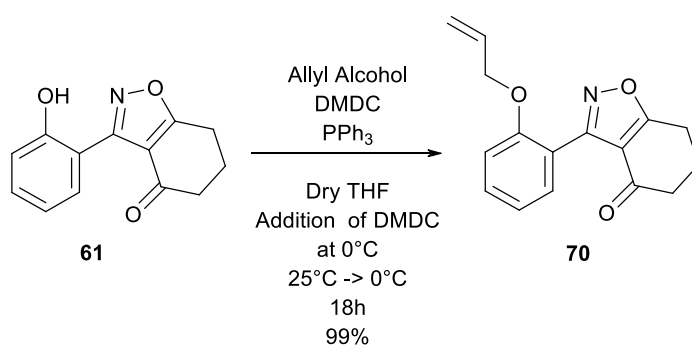
The next attempt at optimization involved using 1.5 molar equivalents of alcohol/DMDC/triphenyl phosphine, compared to the 2.5 molar equivalents that had been used in previous attempts (Scheme 26).



Scheme 26

Once again, the reaction showed no sign of going to completion after 18 hours and was discarded.

Finally the reaction was reattempted using the same conditions, but with an hour at 0°C pre-workup; the aim of this was to freeze out any excess carbohydrazide or DMDC (Scheme 27).



Scheme 27

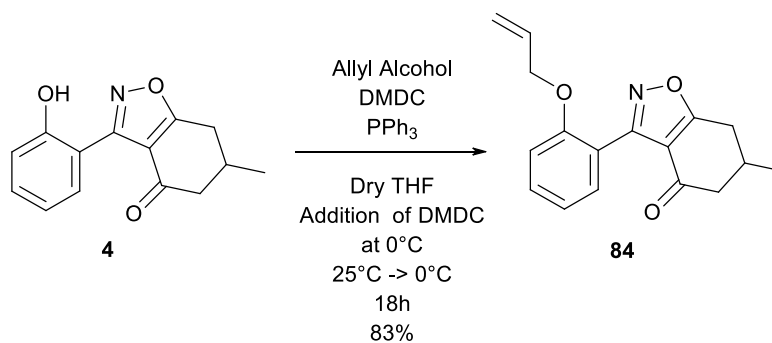
An increase in yield was observed, although it is unknown if this increase in yield was due to increased familiarity with the reaction or to product being retained upon the stationary phase.

With optimal conditions for coupling established, a range of O-alkenyl benzisoxazoles were prepared (Table 3).

| Compound | Alkenyl Chain Length | Yield (%) |
|-----------|----------------------|-----------|
| 70 | Allyl | 99 |
| 77 | But-3-enyl | 83 |
| 82 | Pent-4-enyl | 74 |
| 83 | Hex-5-enyl | 94 |

Table 3. *n.b.* These yields refer to reactions done on varying scales, however, the molar ratio of reactants remained the same, as did the solvent.

We were also able to successfully apply this methodology to O-allylation of the *mono*-methyl substituted isoxazole **4** as this yielded O-allyl precursor **84** which is closer to the natural products (Scheme 28).



Scheme 28

In order to confirm no rearrangement had taken place, the exact constitution of O-butenyl benzisoxazole **77** was confirmed *via* single crystal X-ray crystallography (Figure 7).

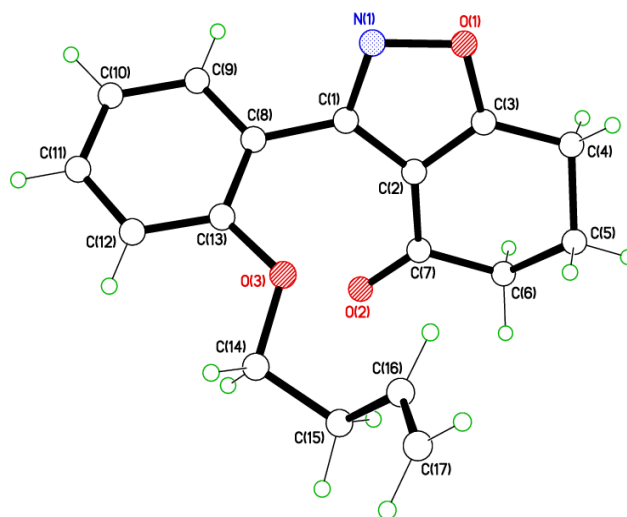
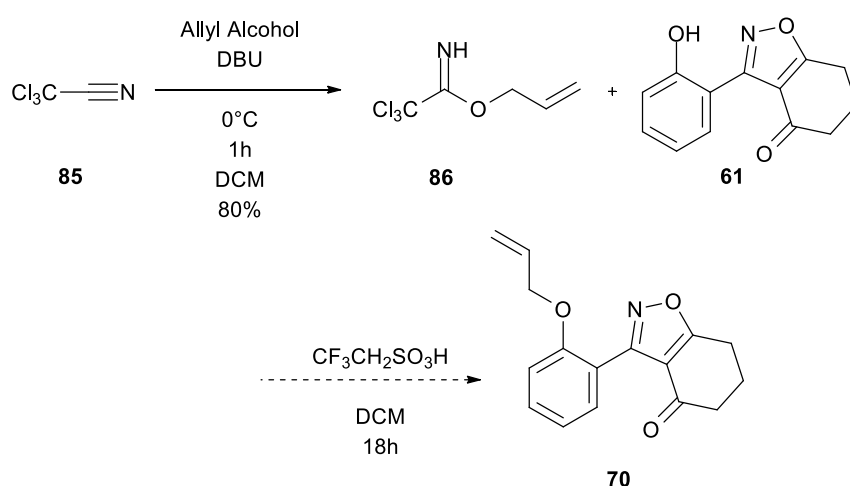


Figure 7. X-Ray crystal structure of 3-(2-(But-3-en-1-yloxy)phenyl)-6,7-dihydrobenzo[d]isoxazol-4(5H)-one **77**. This crystal structure was solved by Dr Mark Elsegood of Loughborough University.

These results indicate that the methodology developed for O-alkylation is a success and it should be possible to introduce any chain length desired, within reason.

Alternative Method for O-Alkylation

While a highly successful method for O-alkylation was developed; it is worth noting another method was attempted. This method involved the use of an alkenyl trichloroacetimidate, as it was believed an acid based method would avoid rearrangement taking place (Scheme 29).⁹⁰ Thus O-allyl trichloroacetimidate **86** was prepared from trichloroacetonitrile and allyl alcohol using a known procedure.⁹⁰



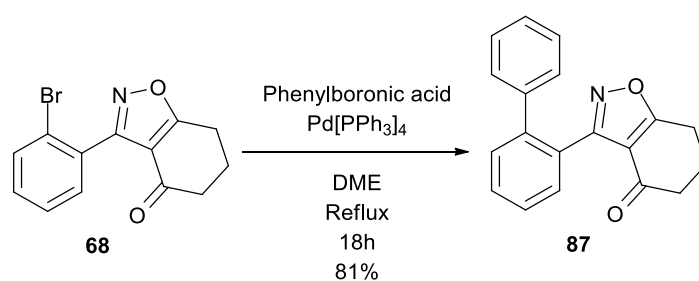
Scheme 29

The ^1H NMR spectrum for the formation of allyl benzisoxazole **70** using this approach suggested that some allylation had taken place; however, it was not possible to be certain. Although interesting, with the success of other methods, this investigation was discontinued.

Aryl Ring C-Alkylation

As mentioned previously, one of the original methods proposed for benzisoxazole alkylation was *via* metal-mediated cross coupling to a 2-bromophenyl derivative.⁹¹ Whilst this would not result in the desired O-C linkage, it would still allow for analogues of the coleophomones to be synthesised. Some success was achieved before the development of an O-alkylation method was completed.

The initial investigation took place using phenylboronic acid, as this is cheaper than the alkyl alternatives and it is still easy to recognise coupling product by ^1H NMR spectroscopy (Scheme 30). This was successful using tetrakis(triphenylphosphine)palladium as catalyst.



Scheme 30

With this success, further coupling attempts were made using alkyl substituents (Table 4) with the same catalyst.

| Boronic Acid | Catalyst | Base | Outcome |
|---------------------------------|-----------------------------|--------------------------|-------------|
| Allylboronic acid pinacol ester | $\text{Pd}[\text{PPh}_3]_4$ | Na_2CO_3 | No reaction |
| Allylboronic acid pinacol ester | $\text{Pd}[\text{PPh}_3]_4$ | CsF | No reaction |
| Vinylboronic acid pinacol ester | $\text{Pd}[\text{PPh}_3]_4$ | Na_2CO_3 | No reaction |
| Vinylboronic acid pinacol ester | $\text{Pd}[\text{PPh}_3]_4$ | CsF | No reaction |

Table 4. *n.b.* All reactions were carried out with 1 mMol of substrate, 0.1 mMol of catalyst, 3 mMol of boronic acid and 2 mMol at reflux in DME.

It is unknown why couplings with allyl or vinylboronic acid failed while the phenyl version was successful. Once again, with the success of O-alkylation, our research focus was shifted away from this area.

2.4 Cyclohexanone Alkylation

Having put one alkyl chain in place, the next objective was to introduce a second alkyl chain, this time on the cyclohexanone ring, either alpha to the carbonyl or to the isoxazole for the natural products; or directly attached at the carbonyl carbon for analogues (Figure 8).

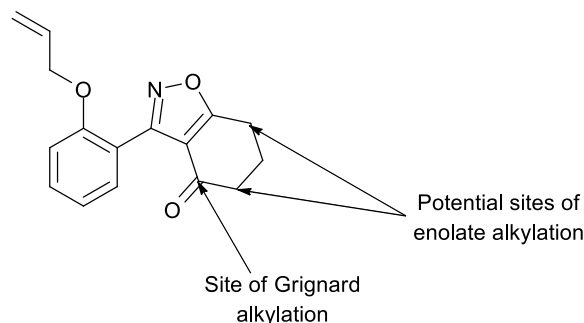
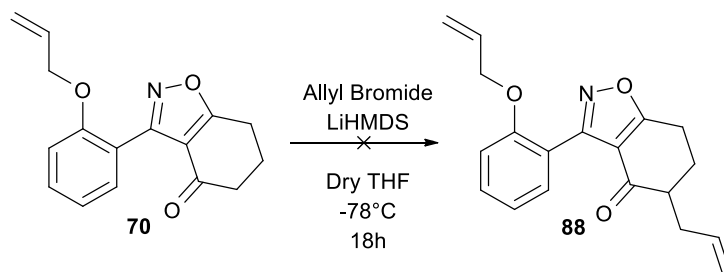


Figure 8

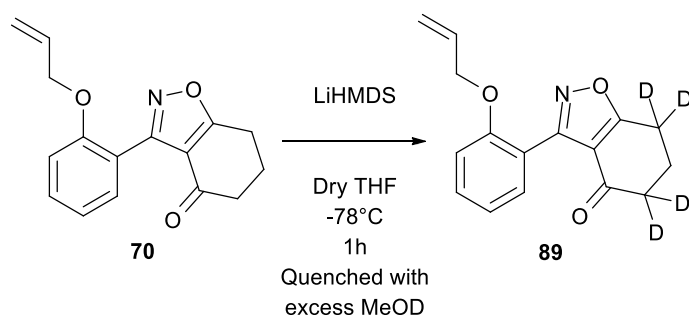
α -Carbonyl Alkylation

Traditional alkylation methods for this position involve forming the corresponding enolate using a non-nucleophilic base such as lithium bis(trimethylsilyl)amide (LiHMDS) or lithium diisopropylamide (LDA) and quenching the anion with an electrophile, in this case allyl bromide. When this reaction was attempted using lithium bis(trimethylsilyl)amide (LiHMDS) and allyl bromide at low temperature it did not provide any C-allyl isoxazole **88** (Scheme31).⁹²



Scheme 31

As this reaction was unsuccessful, we initiated studies to determine why. One possibility is that the cyclohexanone ring was less acidic than expected. To determine if this was the case, the deprotonation was carried out as before, however, this time the anion was quenched with a source of deuterons (Scheme 32).

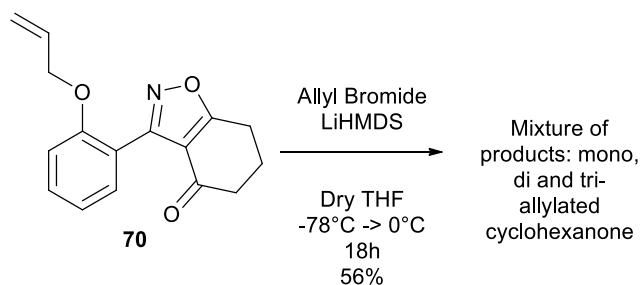


Scheme 32

The recovered ketone proved to be tetra-deuterated, at both positions alpha to the carbonyl and at both positions alpha to the isoxazole. This result suggested that the cyclohexanone ring is acidic enough to readily undergo deprotonation. As only one mole equivalent of LiHMDS was used, further deuteration was either due to keto-enol tautomerism on quenching or as a result of methoxide formation, which is significantly less basic than LiHMDS (pKa of 15.54 and 30.00 \approx respectively).^{93,94}

The previous reaction also indicated that there are two sites of deprotonation on the ring. As each site is different, the initial, kinetic deprotonation in Scheme 39 may have formed an anion that was non-nucleophilic. However, if the anion of benzisoxazole **70** was allowed to warm to room temperature, equilibrium between the two regioisomers may occur, and the thermodynamic anion might be more nucleophilic.

To test this hypothesis, deprotonation was attempted again, but this time the reaction mixture was warmed to 0°C. This was maintained for an hour and then electrophile was added, the mixture was allowed to slowly warm to room temperature (Scheme 33), when evidence for C-allyl product was observed in the ¹H NMR spectra.



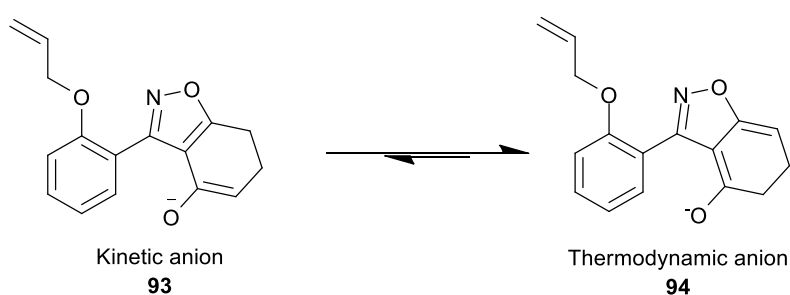
Scheme 33

Initially we believed that we had been successful in achieving mono-alkylation and as such applied this methodology to the longer chain analogues (Table 5).

| Compound Number | O-Alkenyl Chain Length | Yield (%) |
|-----------------|------------------------|-----------|
| 88 | Allyl | 56 |
| 90 | Butenyl | 28 |
| 91 | Pentenyl | 42 |
| 92 | Hexenyl | 24 |

Table 5. *n.b.* All yields are based on what was assumed to be mono-alkylation alpha to the carbonyl.

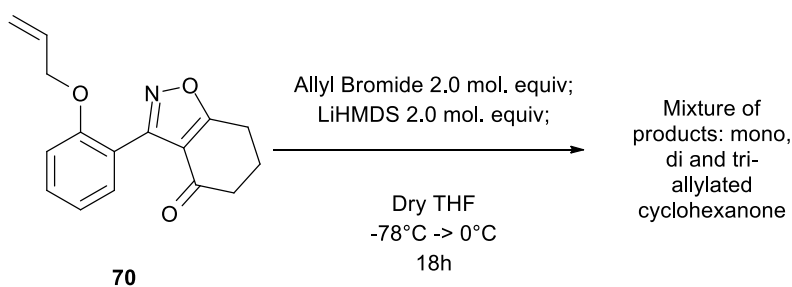
However on scale up the mass spectra suggested the presence of di- and tri-alkylated products, it was not possible at this juncture to determine the ratio of alkylated products. This suggests that at -78°C the kinetic anion is unreactive, but that at 0°C both the kinetic and the thermodynamic anion were reactive (Scheme 34).



Scheme 34

We postulated that the “benzylic” isoxazole alpha-anion may be the thermodynamic product as the negative charge is delocalised over a greater number of atoms when compared to the ketone enolate.

Our suspicions of over-alkylation were confirmed when we repeated the experiment with excess base and halide (Scheme 35).

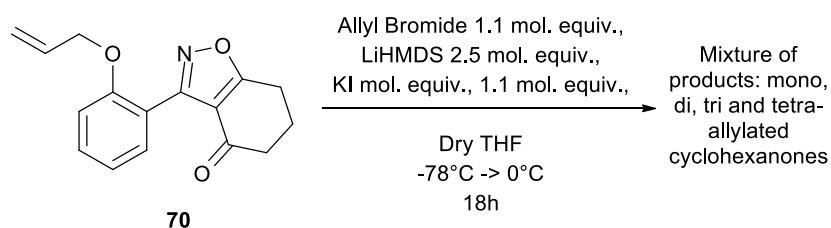


Scheme 35

A controlled temperature study would have been ideal in this situation to try and pinpoint the boundary between reactivity and over-alkylation; unfortunately we lacked the appropriate cooling bath equipment to perform this, and an alternative was required.

Initially we attempted inverse addition (adding the anion to the electrophile) in the hope that this would help control alkylation, but unfortunately it did not.

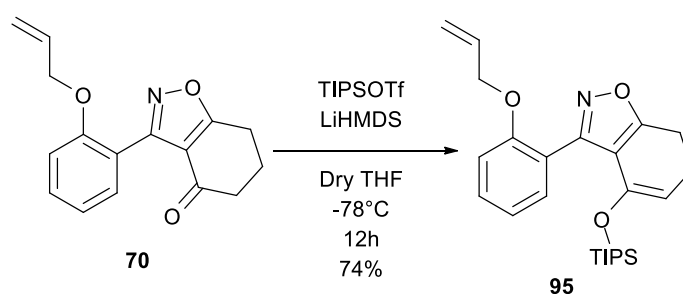
We then attempted form the di-anion in the hope that a second, presumably more reactive anion would react selectively (Scheme 36).



Scheme 36

Over-alkylation was once again observed, and this time an [M+H] peak for what may be a tetra-allylated benzisoxazole was identified in the mass spectrum.

Our next attempt aimed at alkylating under conditions where only the desired mono-alkyl isomer could form; the first step in this was the synthesis of triisopropylsilyl (TIPS) enol ether **95**, which proceeded in good yield (Scheme 37).

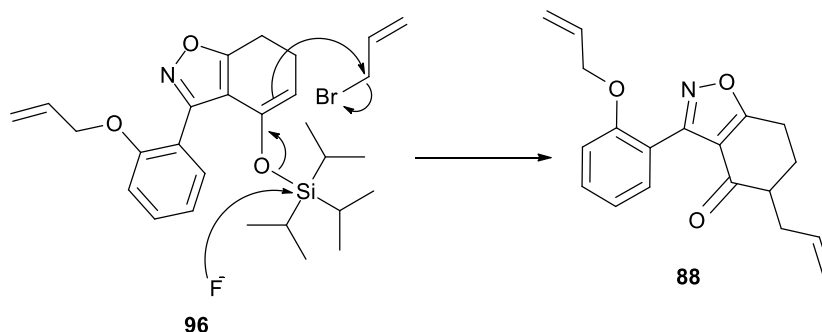


Scheme 37

This reaction is interesting because it suggests that at -78°C some amount of the desired enolate must be formed otherwise no reaction would occur. As to why alkylation does not occur at this temperature, either the temperature is too low for the enolate to be reactive or only trace amounts of it are being formed. Silyl enol ether formation can be explained under these conditions as firstly a silicon oxygen bond is highly favoured, with bond energies of 452 kJ/mol, and secondly if the ketone

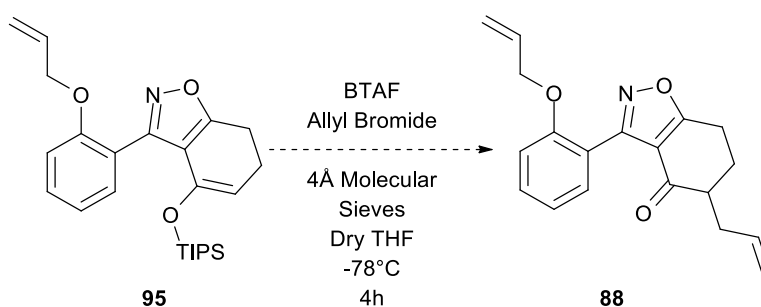
and enolate are equilibrating, then trapping the enolate drives the equilibrium towards the desired anion.^{95,96}

With the successful formation of enol ether **95** in good yields, the next stage was to reform the carbonyl group in the presence of an electrophile (Scheme 38) by the use of fluoride anion.⁹⁷



Scheme 38

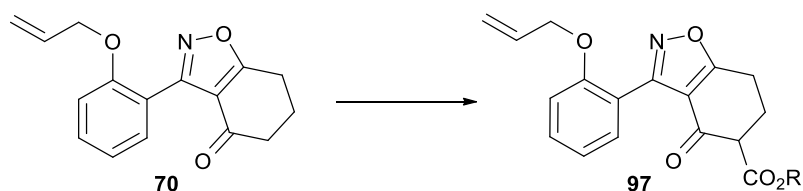
One driving force of this reaction is the formation of an Si-F bond which has a bond energy of 565 kJ/mol.⁹⁵ This also reforms the enolate of the carbonyl group, which drives nucleophilic attack from the enolate double bond towards the electrophile (Scheme 39).



Scheme 39

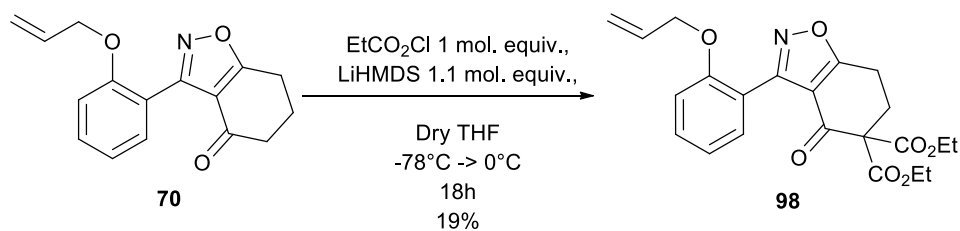
The results from this reaction were inconclusive. Trace amounts of *bis*-allyl benzisoxazole **88** were identified *via* LC-MS, however, isolation was not possible. The remaining mass balance consisted of allyl benzisoxazole **70**. This suggested that de-protection had taken place; however, the anion had been quenched by an unknown source or was simply unreactive towards the electrophile. The latter theory is supported by our previous observations.

Our next attempts focused on acylating the carbon alpha to the ketone in the hope that this would promote deprotonation at this site by increasing its acidity (Scheme 40).



Scheme 40

We estimated that this would lower the pKa of the position by approximately 12 log units, as cyclohexanone and ethyl acetoacetate have a pKa's of 26.45 and 14.20 respectively (DMSO); and these serve as reasonable model systems (Scheme 41).^{98,99}



Scheme 41

It was hoped that this reaction would yield the mono-acylated product; however, di-acylated O-allyl benzisoxazole **98** was isolated in poor yields (based on starting ketone) with no evidence of the mono-acyl product.

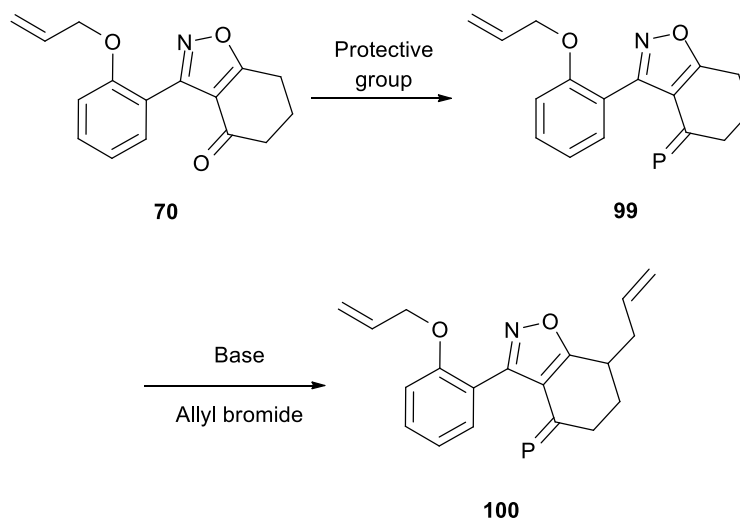
We believe this to be because once a single acylation has occurred, the acidity of the alpha-carbon is increased so much that after proton exchange occurs and it is acylated a second time in preference to starting ketone **70**. Attempts were made to either limit acylation or increase the yield of di-acylation (Table 6).

| Reagents | Addition Method | Temperature | Outcome |
|---|--|-------------|--|
| EtCO ₂ Cl 1 mol. equiv., LiHMDS 1.1 mol. equiv., | Standard | -78->0°C | 19% Diacylated product |
| EtCO ₂ Cl 1 mol. equiv., LiHMDS 1.1 mol. equiv., | Standard | -78°C | 25% Diacylated product |
| EtCO ₂ Cl 1 mol. equiv., LiHMDS 1.1 mol. equiv., | Inverse | -78°C | 20% Diacylated product |
| EtCO ₂ Cl 2 mol. equiv., LiHMDS 2 mol. equiv., | Drop wise addition of base to mixture of benzoxazole and electrophile | 0°C | Inseparable mixture of acylated isomers |

Table 6. *n.b.* All reactions were carried out in refluxing THF with 1 mMol of substrate in THF.

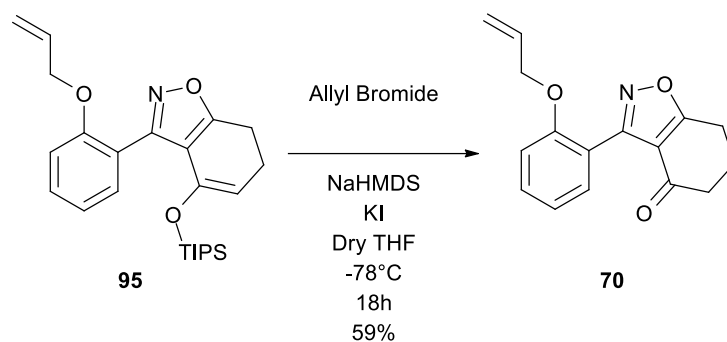
After several attempts we were unable to generate the desired mono-acylation and moved on to alternative methods.

The next tactic focused on converting the ketone to a non-acidic functionality with the intention of limiting the available sites of deprotonation to the “benzylic” position (Scheme 42).



Scheme 42

This first attempts using this approach involved silyl enol ether **95** as the ether greatly reduces the acidity alpha to the ketone (Scheme 43).



Scheme 43

This yielded de-protected O-allyl benzisoxazole **70** and a small quantity of enol ether **95**. This result did not come as a great surprise, as it is possible to cleave silyl enol ethers using sources of small cationic metals, for instance methyl lithium.⁹²

Whilst attempting to synthesise coleophomone D we synthesised and isolated *bis*-triflated enol ether **101** (Figure 9).

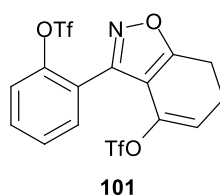
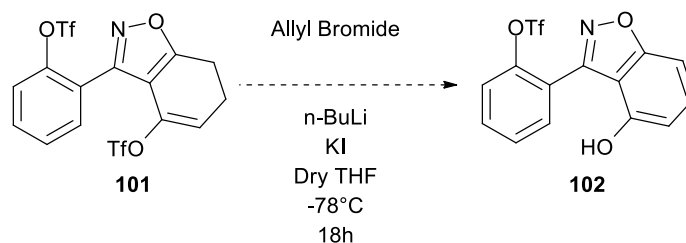


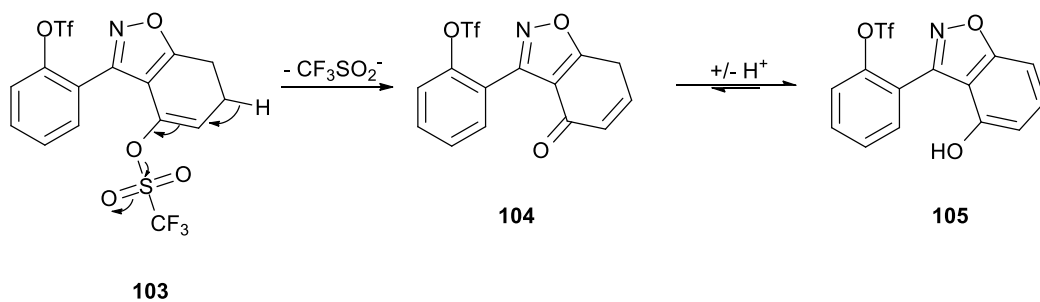
Figure 9

The synthesis of this compound will be discussed in greater detail in the section that relates to coleophomone D. However, as the ketone in this compound is masked we attempted de-protonation and alkylation. The ¹H NMR spectra suggested that the isolated product might be phenol **102**, however, it was not possible to confirm this (Scheme 44).



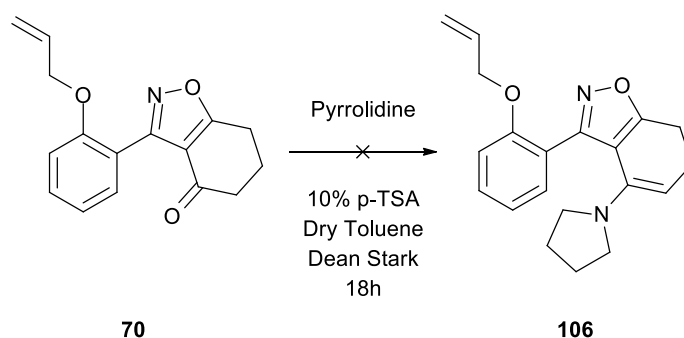
Scheme 44

Elimination of the sulfinate accompanied by loss of H⁺ as the ketone reforms is a pathway that may possibly explain this result.(Scheme 45).



Scheme 45

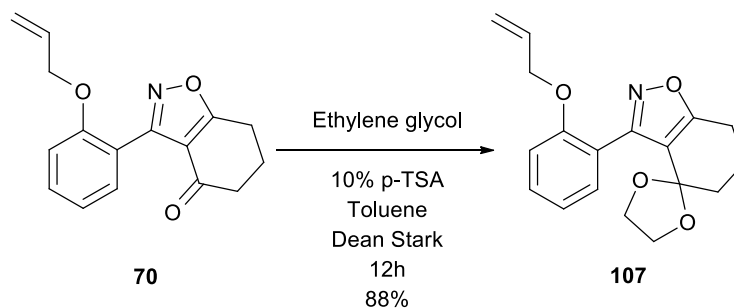
As these functionalities appeared to be incompatible with this approach we attempted to form the enamine of cyclohexanone **106** (Scheme 46).



Scheme 46

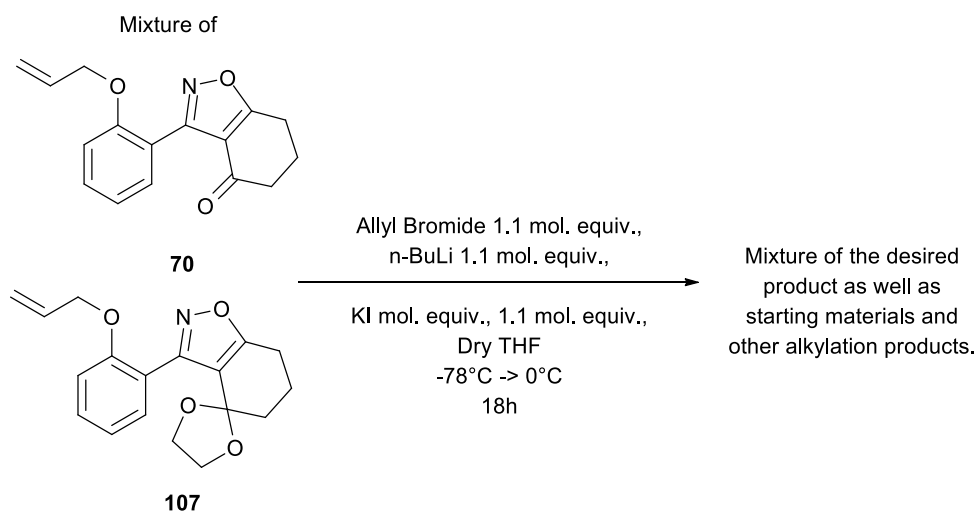
Unfortunately this was unsuccessful; we believe this failed due to steric interactions with the neighbouring aromatic ring. This was unexpected as we were able to successfully form TIPS enol ether **95** in good yields. We believe enol ether formation was successful for two reasons: firstly the longer and less constrained O-Si linkage gives the TIPS group more steric freedom compared to the pyrrolidine ring; and secondly, the bond that is formed between silicon and oxygen is more thermodynamically favoured than that of carbon and nitrogen (452 vs 305 kJ/mol).⁹⁵

Following a related approach we then endeavoured to convert ketone **70** into acetal **107** (Scheme 47).



Scheme 47

Whilst this was successful, it was noted that the ^1H NMR spectra indicated there was approximately 10% of the ketone remaining, and this was not separable *via* column chromatography. However, it was possible to test whether alkylation at the desired location was possible (Scheme 48).



Scheme 48

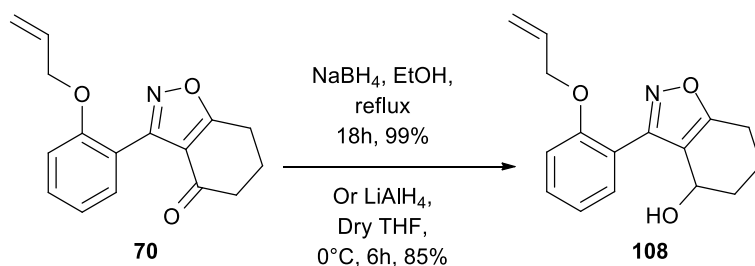
Mass spectra displayed an $[\text{M}+\text{H}]$ ion corresponding to the desired mono-alkyl product. But unfortunately, the mixture of alkylation products and starting materials was again, inseparable *via* column chromatography. It was essential that acetal formation be driven to completion in order for this route to be *viable* so a number of protocol variations were studied.

However, testing this formation with a range of conditions (Table 7) indicated that it was very difficult to drive acetal formation to completion. This could possibly be attributed to the same steric concerns that we encountered with enamine formation.

| Reagents | Drying method | Time | Outcome |
|---|---|--------|---|
| Benzisoxazole 1 mol. equiv., Ethylene glycol 4 mol. equiv., 10 mol. % <i>p</i> -TSA, Toluene. | Dean-Stark conditions | 1 Day | Mixture of ketone and desired acetal, predominantly acetal. |
| Benzisoxazole 1 mol. equiv., Ethylene glycol 4 mol. equiv., 10 mol. % <i>p</i> -TSA, Toluene. | Dean-Stark conditions | 2 Days | Mixture of ketone and desired acetal, predominantly acetal. |
| Benzisoxazole 1 mol. equiv., Ethylene glycol 10 mol. equiv., 10 mol. % <i>p</i> -TSA, Toluene. | Dean-Stark conditions | 1 Day | Mixture of ketone and desired acetal, predominantly acetal. |
| Benzisoxazole 1 mol. equiv., 2,2-dimethylpropane-1,3-diol 10 mol. equiv., 10 mol. % <i>p</i> -TSA, Toluene. | Dean-Stark conditions | 1 Day | No reaction. |
| Benzisoxazole 1 mol. equiv., Ethylene glycol 10 mol. equiv., 10 mol. % <i>p</i> -TSA, Toluene. | 10 mass % molecular sieves | 1 Day | Mixture of ketone and desired acetal, predominantly acetal. |
| Benzisoxazole 1 mol. equiv., Ethylene glycol 10 mol. equiv., 10 mol. % <i>p</i> -TSA, Toluene. | 10 mass % powdered molecular sieves | 1 Day | No reaction. |
| Benzisoxazole 1 mol. equiv., Ethylene glycol 10 mol. equiv., 10 mol. % BF ₃ Etherate, Toluene. | 10 mass % molecular sieves | 1 Day | Mixture of ketone and desired acetal, predominantly ketone. |
| Benzisoxazole 1 mol. equiv., Ethylene glycol 10 mol. equiv., 10 mol. % <i>p</i> -TSA, Toluene. | 1 mass equiv. Ca ₂ SO ₄ | 1 Day | No reaction. |
| Benzisoxazole 1 mol. equiv., methanol 10 mol. equiv., 10 mol. % <i>p</i> -TSA, Toluene. | 1 mass equiv. Ca ₂ SO ₄ | 1 Day | No reaction. |
| Benzisoxazole 1 mol. equiv., Ethylene glycol 10 mol. equiv., 10 mol. % <i>p</i> -TSA, Benzene. | Dean-Stark conditions | 1 Day | Mixture of ketone and desired acetal, predominantly acetal. |

Table 7. *n.b.* All experiments were heated to reflux.

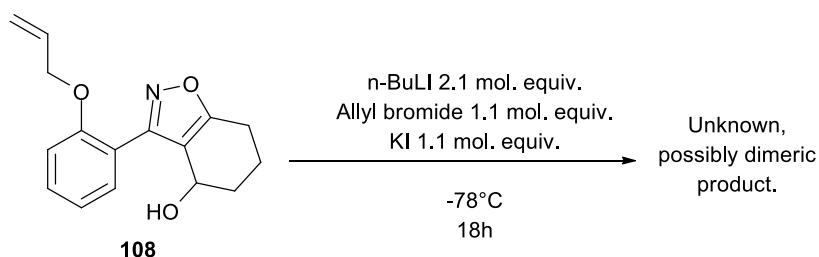
Another approach to masking the ketone as a non-acidic functionality was required; and as such the next logical step was to attempt the reduction of the ketone to the corresponding alcohol (Scheme 49).



Scheme 49

This reduction was attempted with both sodium borohydride and lithium aluminium hydride in parallel, with the former giving almost quantitative conversion.

With this success, the next step was to test to see if it would be possible to form a di-anion (alkoxide and carbanion) and alkylate directly, without the need for a protective group (Scheme 50).



Scheme 50

Following this reaction two products were isolated, the minor (approx. 10% based on starting material mass) showed signs of alkylation, though it was not definitive. The second larger fraction (approx. 50% based on starting material mass) displayed what appeared to be dimeric features *i.e.* what appeared to be a doubling of the integrals in both the ¹H and ¹³C NMR spectra; however, it was not possible to identify this compound.

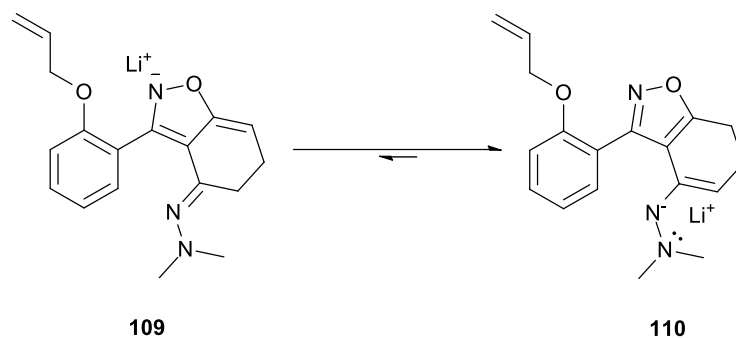
Given this result, the next step was to attempt to protect the alcohol and then re-attempt C-alkylation. We envisaged protection might be problematic due to steric and reactivity issues, so a range of protective groups were screened (Table 8).

| Electrophile | Base/Acid | Temperature (°C) | Outcome |
|--------------------------|--|---------------------|---|
| TES-Cl 1.1 mol. equiv. | Imidazole 2 mol. equiv. | 0 | No Reaction |
| TES-Cl 1.1 mol. equiv. | NaH 1.1 mol. equiv. Imidazole 1 mol. equiv. | 0 | No Reaction |
| TIPS-OTf 1.1 mol. equiv. | NaH 1.1 mol. equiv. | 0 | Trace amounts of protected product |
| TMS-Cl 1.1 mol. Equiv. | NaH 1.1 mol. equiv. Imidazole 1 mol. equiv. | 0 | Some conversion <i>via</i> TLC, however we were unable to isolate product, believed to have hydrolysed on base wash |
| TMSCH2N2 | BF ₄ H | 0 | Trace amounts of protected product |
| MEM-Cl 1.1 mol. equiv. | NaH 1.1 mol. equiv. | 0 | No Reaction |
| MeI 1.1 mol. equiv. | Cs ₂ CO ₃ | 66 | No Reaction |
| MeI 1.1 mol. equiv. | NaH | 66 | Significant amounts of protected product |

Table 8. *n.b.* All reactions were carried out using 1 mMol of substate in either DCM or THF.

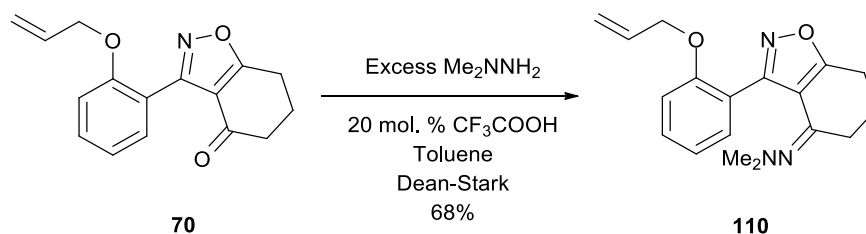
From these results, it can be seen that the alcohol is relatively unreactive towards electrophiles. However, we believe that de-protonation is occurring with sodium hydride, as a colour change is observed upon addition. This supports our initial hypothesis that the anion produced is unreactive due to poor nucleophilicity or steric effects.

Our next approach would involve trying to chelate a lithium cation alpha to the ketone, which should stabilize the anion at this location and therefore reduce or prevent equilibrium (Scheme 51).¹⁰⁰



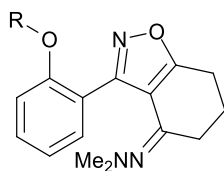
Scheme 51

If it was possible to successfully form hydrazone **109** then having the anion and an additional heteroatom in close proximity should help to chelate the lithium and therefore stabilise the lithio-amine at this location. Attempts were therefore made to convert O-allyl isoxazole **70** into the corresponding hydrazone **110** (Scheme 52).



Scheme 52

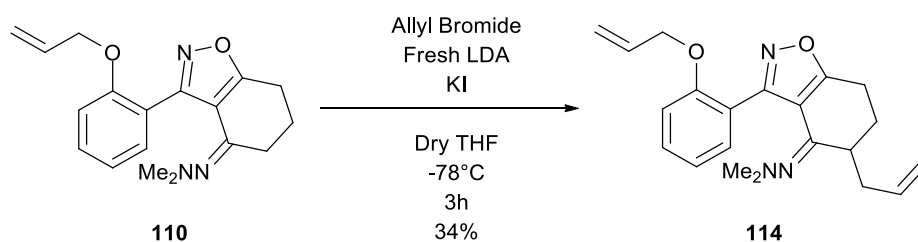
Initially there were some problems obtaining full conversion, as N,N-dimethylhydrazine is volatile and it was presumed that it was being lost from the reaction mixture *via* evaporation, however, this was remedied by improving the cooling efficiency of the reflux condenser. This methodology was then applied to the longer chain O-alkenyl benzisoxazoles (Table 9).



| Compound Number | O-Alkenyl Chain Length (R) | Yield (%) |
|-----------------|----------------------------|-----------|
| 110 | Allyl | 68 |
| 111 | Butenyl | 74 |
| 112 | Pentenyl | 60 |
| 113 | Hexenyl | 69 |

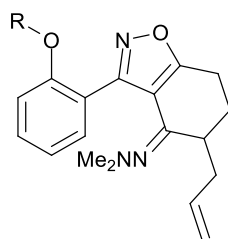
Table 9. *n.b.* Yields refer to reactions done on varying scales, however, the molar ratio of reactants, solvent and temperature remained the same throughout.

We were able to successfully form all of the desired O-alkenyl hydrazones so we progressed to the next stage of this approach, using strong base deprotonation and allyl bromide as electrophile (Scheme 53).



Scheme 53

This reaction was regiochemically extremely successful, as there was no sign of alkylation alpha to the isoxazole or alkylation occurring more than once, however, the yield was moderate. Unfortunately due to time constraints it was not possible to optimise this reaction so it was applied directly to the extended chain O-alkenyl derivatives to achieve mono-C-alkylation in each case (Table 10).



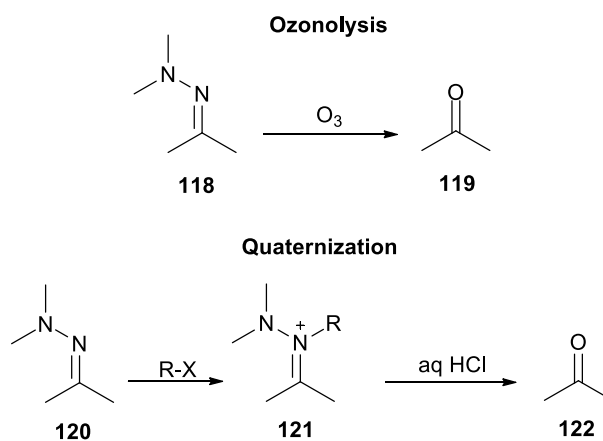
| Compound Number | O-Alkenyl Chain Length (R) | Yield (%) |
|-----------------|----------------------------|-----------|
| 114 | Allyl | 34 |
| 115 | Butenyl | 45 |
| 116 | Pentenyl | 49 |
| 117 | Hexenyl | 63 |

Table 10. *n.b.* Yields refer to reactions done on varying scales, however, the molar ratio of reactants, solvent and temperature remained the same throughout.

In each case the remaining mass balance was starting hydrazone and unidentifiable highly polar material. The increase for yield in the longer chains can be attributed to increased familiarity with the reaction, as the initial C-allyl benzisoxazole was only prepared once.

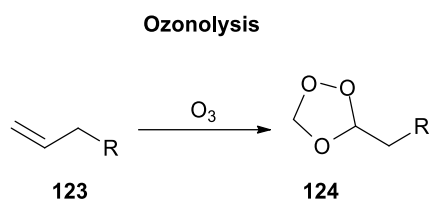
It should also be noted that on scale up, unless the reaction was kept below -65°C then signs of multiple alkylation presented. This suggests that using this methodology we are on the boundary of being able to control alkylation.

Whilst a hydrazone is an isostere of a carbonyl group, and therefore could be considered a cyclic tricarbonyl analogue, we would prefer to be able to unmask it at a later date. The two most well documented approaches to hydrazone to ketone conversion are *via* ozonolysis or quaternization with an alkyl halide followed by hydrolysis (Scheme 54).¹⁰⁰



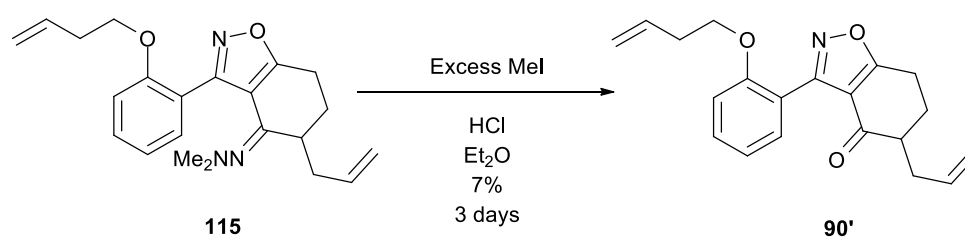
Scheme 54

Unfortunately while ozone is the most straightforward method it is also incompatible with alkenes as it will convert them to the corresponding tri-oxolane (Scheme 55).



Scheme 55

Therefore the quaternization approach, while not as efficient, was the method attempted for hydrazone removal using the O-butenyl derivative (Scheme 56). Only a very low yield of the ketone was recovered.



Scheme 56

It should be noted that due to time constraints this experiment was only conducted once and on a very small scale (*ca.* 20mg). That would suggest this result is not an accurate representation of the potential yield.

Even so we were able to produce a sample of *bis*-alkyl ketone **90'** which we were able to analyse further. When we compared the ^1H NMR spectra of this *bis*-alkylated ketone **90'** with the polyalkyl mixtures produced earlier we noted significant differences. One example is that the CH multiplet of *bis*-alkenyl ketone **90'** comes at 3.23-3.34 ppm, however, the one observed in earlier mixtures appears as part of a larger multiplet at approximately 2.40-2.50 ppm (Figure 10).

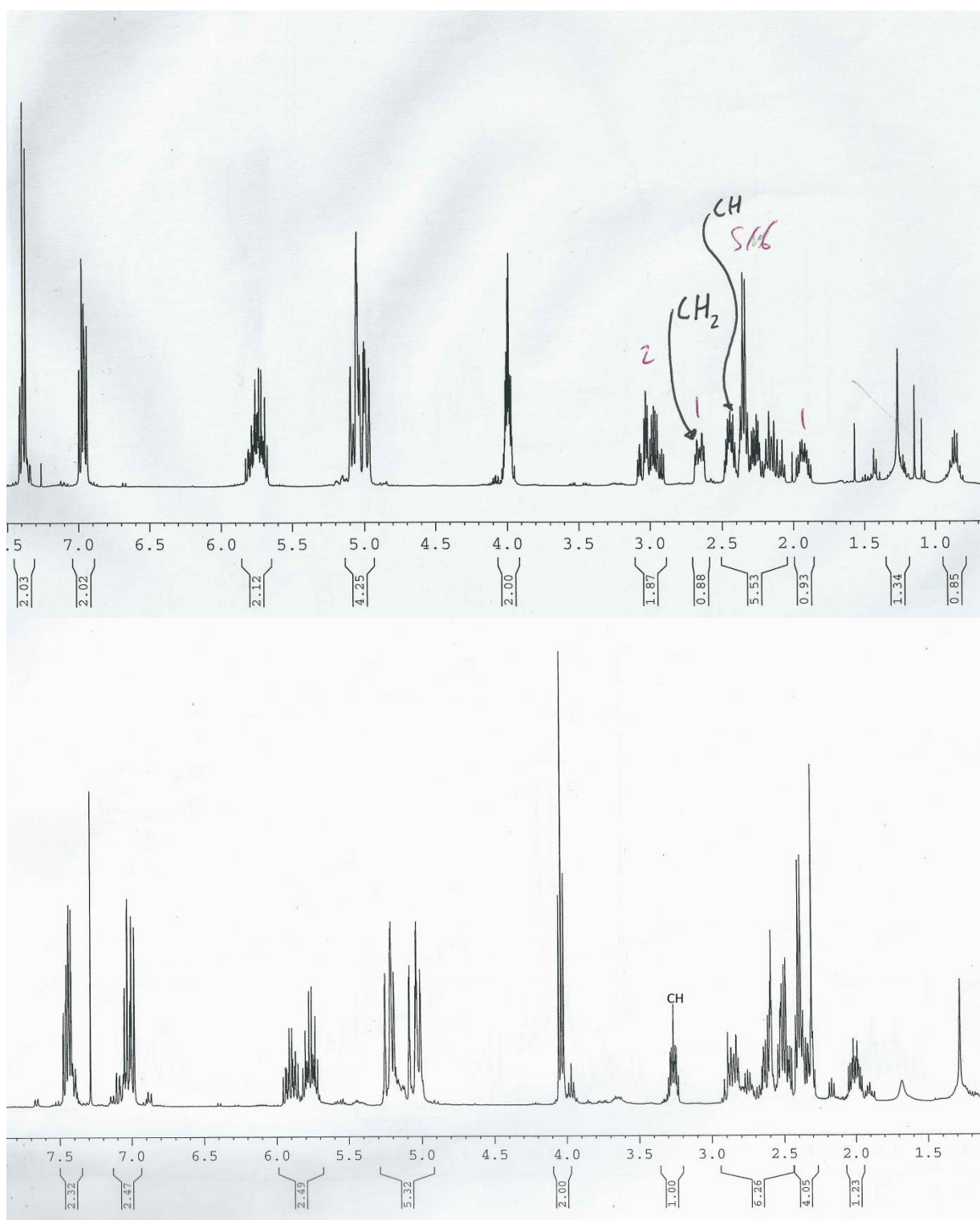
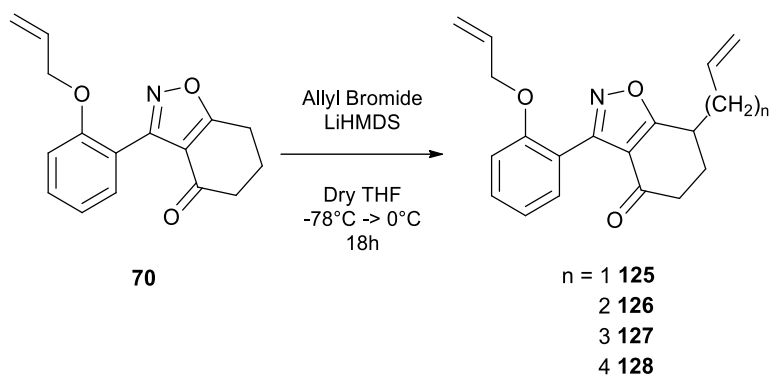


Figure 10. (top) *bis*-alkyl benzisoxazole **90'** derived from hydrazone **115** and (bottom) *bis*-alkyl benzisoxazole **90** derived from ketone **70** (with small amounts of poly-alkyl material present).

These differences suggest that our initial hypothesis about the isoxazole “benzylic” anion being thermodynamically more stable was correct and that any C-allylation that took place was most likely occurring alpha to the isoxazole first (Scheme 57).



Scheme 57

However, alkylation attempts on the hydrazone series of compounds presumably took place alpha to the hydrazone for reasons of chelation as mentioned previously in this chapter.

We attempted to unequivocally prove this by growing a single crystal of *bis*-allyl hydrazone **114** for X-ray crystallography; however, we were met with a surprise, with the isolated crystal revealing an unexpected benzpyrazole **129** (Figure 11).

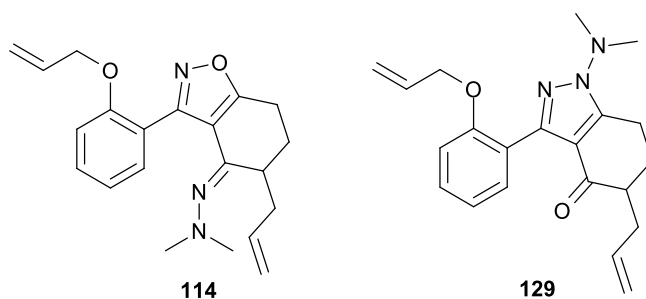
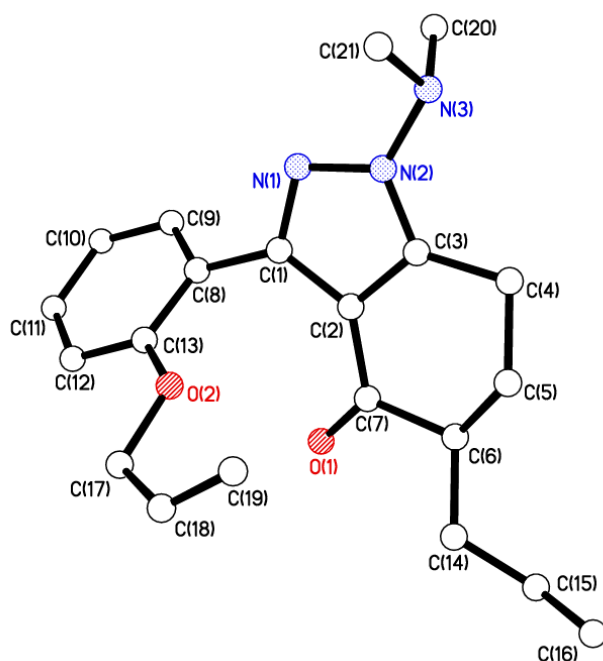


Figure 11. X-Ray crystal structure of 5-Allyl-3-(2-(allyloxy)phenyl)-1-(dimethylamino)-6,7-dihydro-1H-indazol-4(5H)-one **129**. This crystal structure was solved by Dr Mark Elsegood of Loughborough University.

Initially we were worried that we had mis-assigned our previous spectra and this was our major product rather than a ketone hydrazone. However, upon comparison of the ^1H NMR spectra of the single crystal and that of the bulk material, we found they were significantly different (Figure 12).

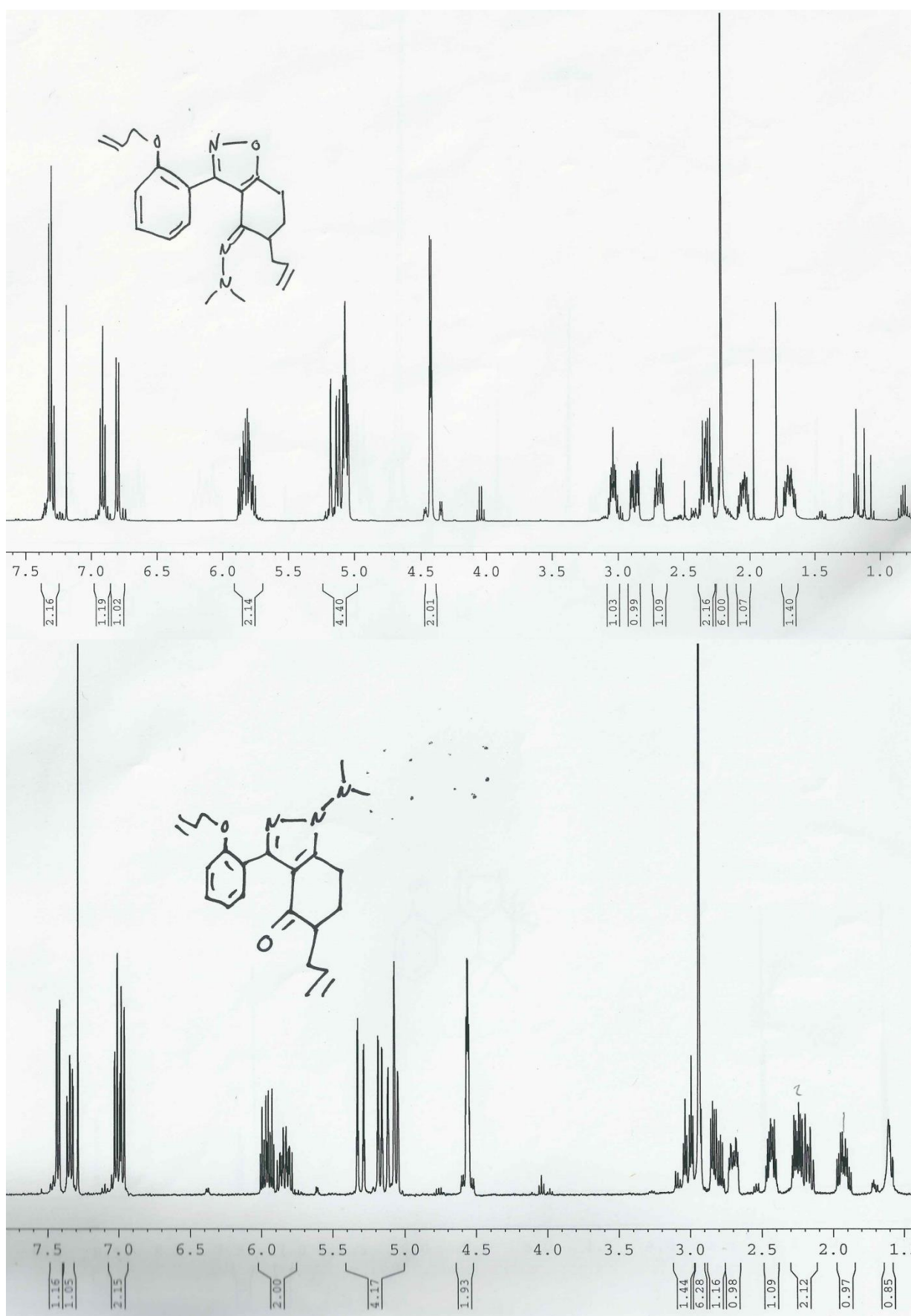
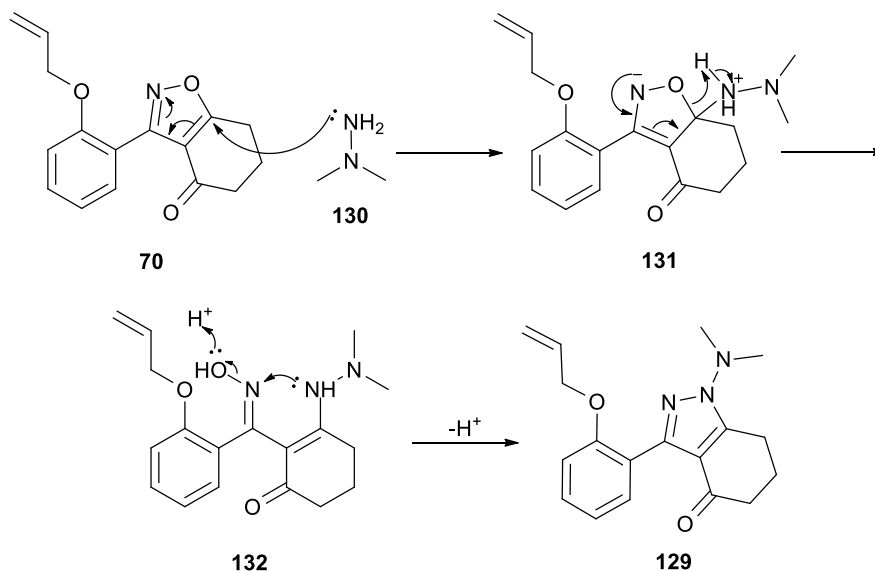


Figure 12. (top) bis-alkyl hydrazone **114** and (bottom) bis-alkyl pyrazole **129**.

Also the crystal of pyrazole **129** exhibits an intense infra-red stretch at 1666 cm^{-1} , however, the bulk of the *bis*-allyl hydrazone material does not. These two pieces of information lead us to believe the sample submitted for X-ray examination is a result of selective crystallization of a by-product that forms at the hydrazone generation stage *via* the following mechanism (Scheme 58).



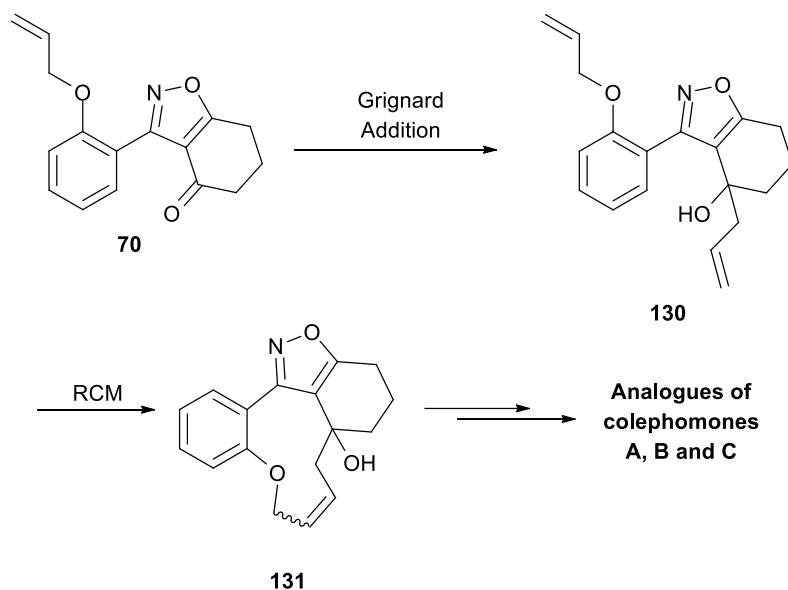
Scheme 58

It can be seen that nucleophilic attack at the isoxazole C-O carbon results in the ring opening of the isoxazole with an oxime acting as the leaving group. Following this the nitrogen lone pair of the hydrazine attacks the neighbouring oxime nitrogen and eliminates water. Aromatization occurs with the loss of a proton, forming the observed pyrazole.

We believe that the bulk of our *bis*-allyl material is hydrazone and not pyrazole based on this information. Unfortunately due to this and time constraints we were not able to grow a crystal of this material and as such, cannot unequivocally determine the regiochemistry of hydrazone allylation.

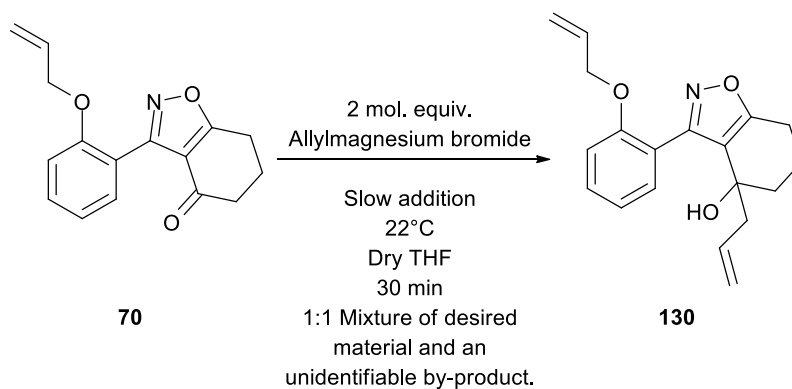
Carbonyl Addition

Whilst direct alkylation of the carbonyl carbon does not result in the natural product, it could still lead to analogues that may exhibit pharmacological activity (Scheme 59).



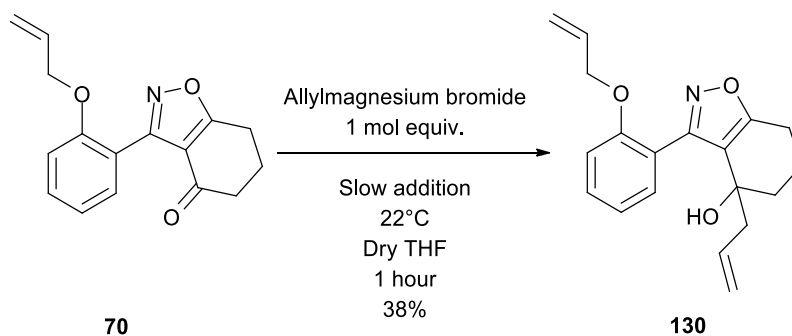
Scheme 59

Initial alkylation attempts were made using allylmagnesium bromide (Scheme 60).



Scheme 60

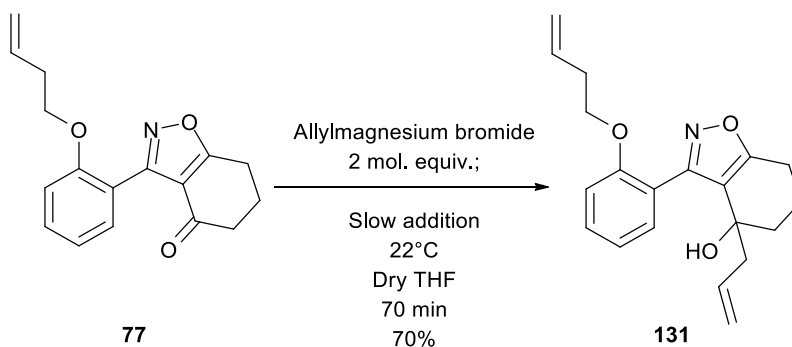
These attempts produced a 1:1 mixture of what appeared to be the desired *bis*-allyl benzisoxazole **130** and an unknown by-product; the ratio of products was calculated from the integration of the ^1H NMR spectra. In an effort to restrict addition to one site, the molar equivalents of Grignard reagent were reduced (Scheme 61).



Scheme 61

Whilst reducing the molar equivalents of Grignard reagent stopped by-product formation, the yield was low and optimization would be required if this route is going to be viable.

Grignard addition was also attempted on butenyl benzisoxazole **77** to determine if by-product formation was a unique feature of allyl benzisoxazole **70** (Scheme 62).



Scheme 62

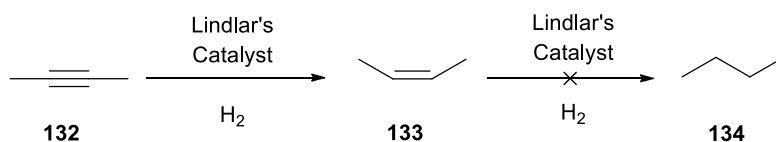
Unexpectedly, by-product formation was not observed in this reaction; currently this cannot be explained. However, as a good yield was obtained, this presents a possible route to analogues of the coleophomones.

2.5 Isoxazole Ring Cleavage

Before investigations into RCM began, it was important to determine if it was possible to cleave the isoxazole ring in the presence of an alkene.

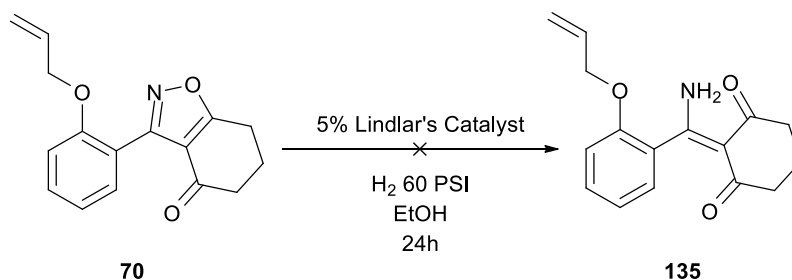
As mentioned previously, there are various methods for isoxazole cleavage, with the cleanest usually being hydrogenation. Unfortunately this was not a possibility using traditional catalysts, as it would reduce both the isoxazole and any alkenes present.

However, it was proposed that the selective cleavage of an isoxazole in the presence of an alkene *via* hydrogenation might be possible with Lindlar's catalyst. The reason for this is that while Lindlar's catalyst will reduce an alkyne to the corresponding *cis*-alkene; it will not reduce an alkene to an alkane (Scheme 63).¹⁰¹



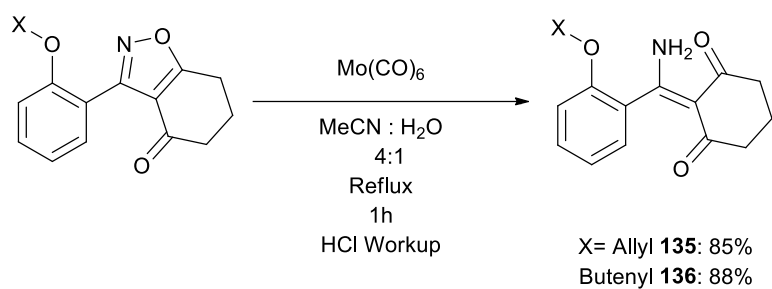
Scheme 63

Allyl benzisoxazole **70** was chosen as a test compound to determine if selective reduction was possible (Scheme 64). After 24 hours there was no evidence to suggest that hydrogenation had taken place and we concluded this was a not a productive approach.



Scheme 64

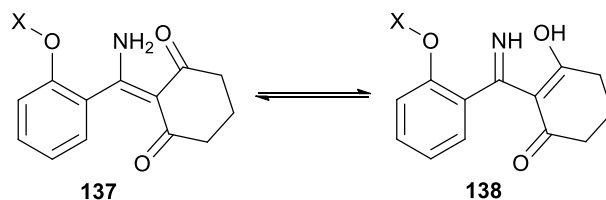
With the unsuccessful attempt at hydrogenation, the next step was to test ring cleavage using molybdenum hexacarbonyl, which has been used previously in the Jones group and which selectively cleaves N-O bonds (Scheme 65).¹⁰²



Scheme 65

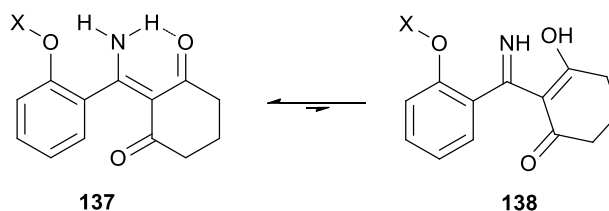
This method proved to be very successful, cleaving both butenyl **77** and allyl benzisoxazoles **70** in excellent yields.

As cleavage was successful, it was important to determine in which tautomeric form these compounds exist, as there is the possibility of both enamino ketone **137** and imino enol **138** being present (Scheme 66).



Scheme 66

¹⁵N HMBC NMR spectroscopy was used to determine which form was predominant. The spectra indicated that the central nitrogen is bonded to two protons, both of which are in separate environments. This suggests that enamino ketone **137** is the exclusive form. It is believed that enamino-ketone **137** is the predominant form due to stabilization from hydrogen bonding between the enamine and ketone (Scheme 67)



Scheme 67

This hydrogen bond forms a six membered ring, which would significantly lower the energy of this conformation; this hypothesis was further reinforced by single crystal X-ray structural determination (Figure 13).

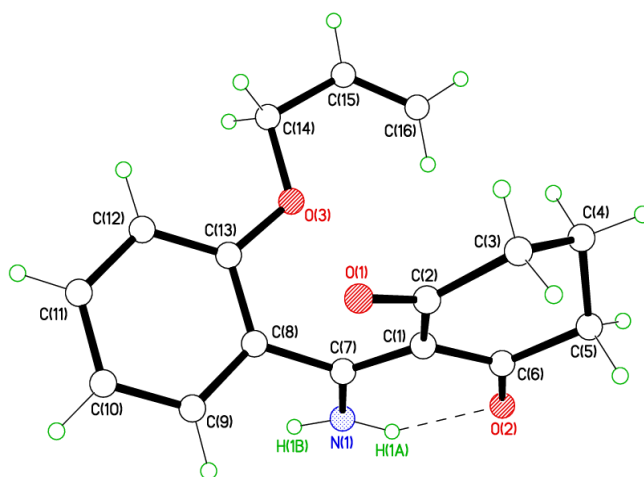
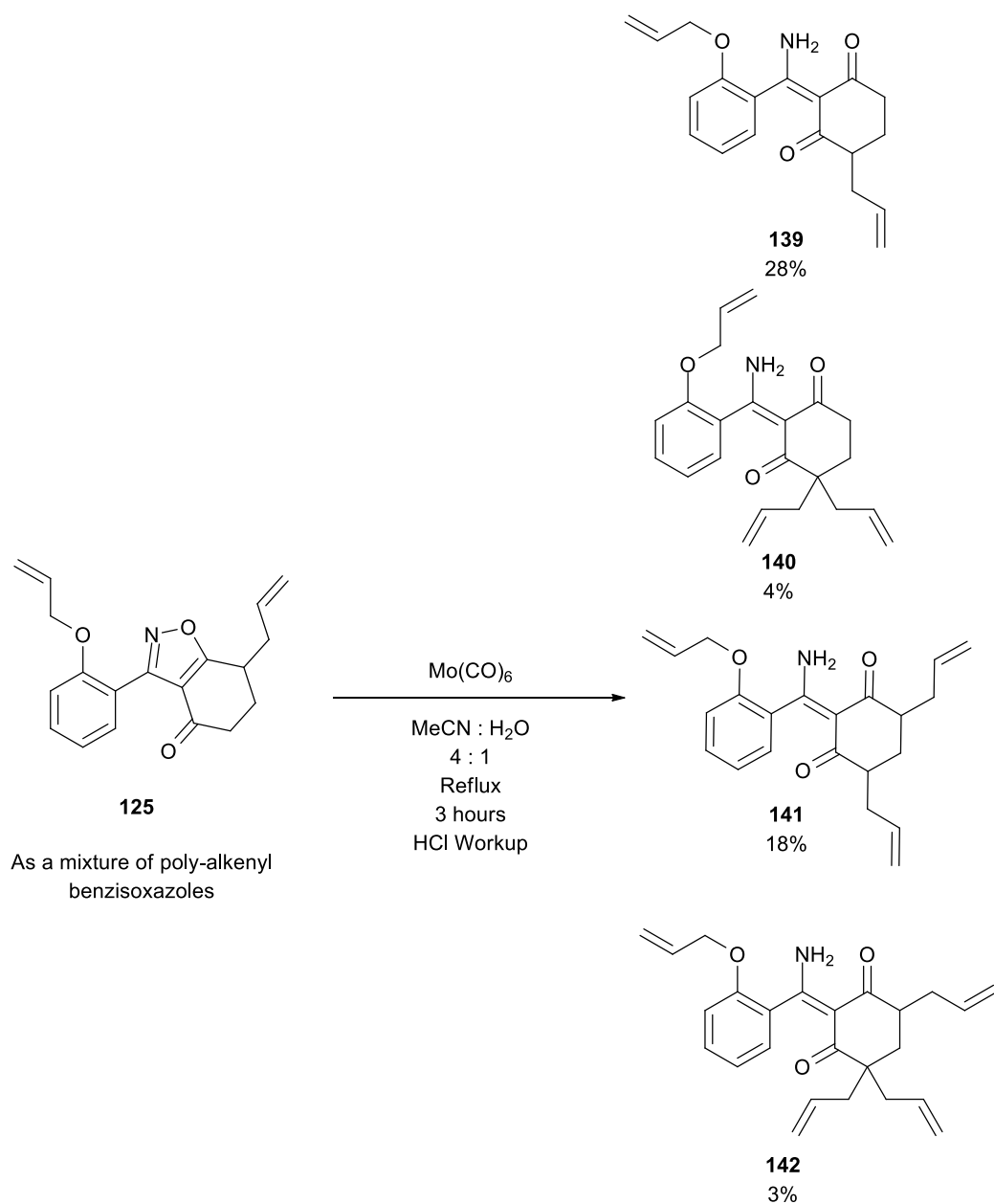


Figure 13. X-Ray crystal structure of 2-((2-(Allyloxy)phenyl)(amino)methylene)cyclohexane-1,3-dione **135**. This crystal structure was solved by Dr Mark Elsegood of Loughborough University.

It is also important to note that only one hydrogen bond is observed, there is no evidence to suggest a second is formed between the ethereal oxygen and the second enamine proton. This is probably due to the energy required to bring the aromatic ring into the plane and that ethereal oxygen is a poor hydrogen bond acceptor.¹⁰³

Following this success, ring cleavage was attempted on a sample of *bis*-allyl benzisoxazole believed to comprise mono-allyl and various over alkylation products (Scheme 68).



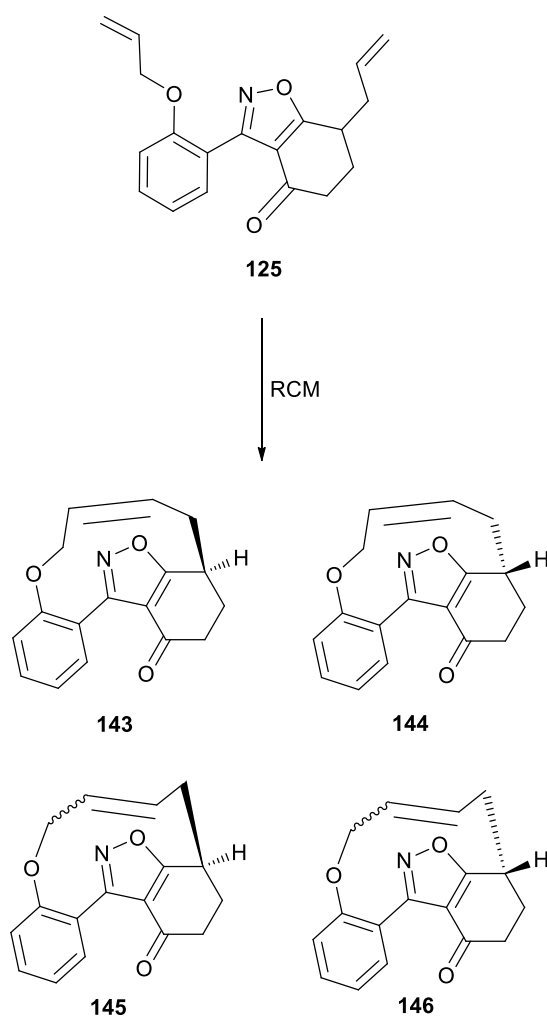
Scheme 68

The yields above were based on isolated material as each derivative has a distinct retention time on silica. Not only did this confirm that it was possible to cleave *bis*-alkyl benzisoxazole **125**, it also confirmed our earlier hypothesis that over-alkylation was occurring in a ratio of approximately 3:2 mono to *bis*-alkylation. The successful formation of *bis*-allyl enaminoketone **139** opened a route towards an 11-membered macrocyclic system.

2.6 Ring Closing Metathesis

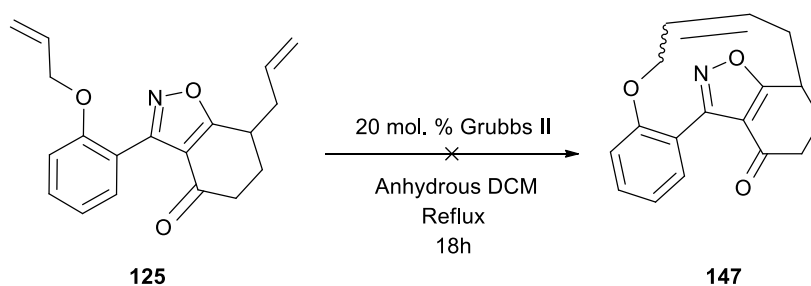
With the successful formation of *bis*-allyl benzisoxazoles we began to test RCM conditions. Although these tests were to be carried out on mixtures of multiple alkylation products, it still allowed us to probe what was possible while we developed methods to control alkylation.

Initial RCM tests were conducted on the mixture contained mostly *bis*-allyl benzisoxazole **125** as this would generate the 11-membered macrocycle present in the natural products. Although performing RCM on this analogue will produce a mixture of chiral *E/Z* diastereoisomers, this was not regarded as a problem at the time as we only wanted to determine if RCM was possible (Scheme 69).



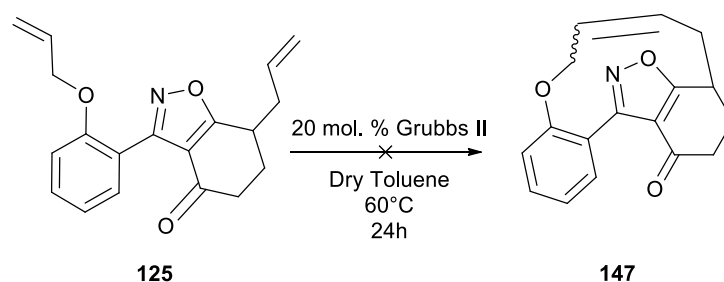
Scheme 69

With this in mind an investigation of RCM conditions was carried out (Scheme 70).



Scheme 70

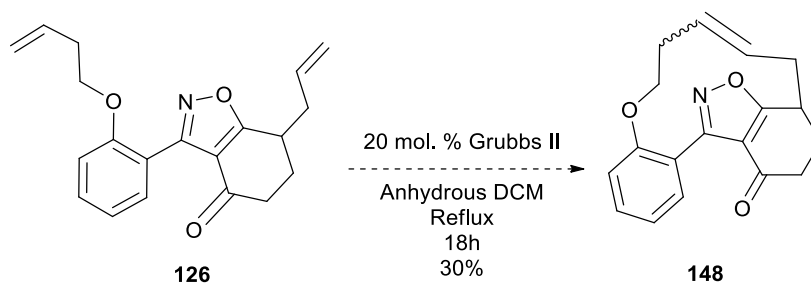
Unfortunately no signs of ring closed benzisoxazole **147** were observed after 24 hour. Ring closure was reattempted at a higher temperature to determine if the reaction required more energy to form the macrocycle (Scheme 71).



Scheme 71

Once again, no evidence was observed to suggest that ring closing had taken place and the reaction was stopped. In both cases, approximately 60% of starting material was recovered, as well as a large amount of unknown baseline material. These are believed to be related to the catalyst and products of cross metathesis.

As it seemed that we would not be able to form the 11-membered ring, we moved and tried to form 12-membered macrocycle **148** (Scheme 72).



Scheme 72

Although it was not possible to fully assign the spectra of macrocycle **148**, we believed we had enough evidence to attempt to optimize the catalyst loading (Table 11).

| Catalyst Loading (Mol. %) | Approximate yield (%) |
|------------------------------|--------------------------|
| 20 | 30 |
| 10 | 60 |
| 5 | 50 |
| 2.5 | 40 |

Table 11. *n.b.* All attempts at optimisation were carried out on the same batch of starting material to ensure that even though it was a mixture, the optimisation results were as accurate as possible.

It can be seen that too much catalyst harms the reaction, possibly due to cross metathesis processes dominating. Ten percent catalyst loading appears to be optimum for ring closing, and as such, this was applied to the longer chain benzisoxazoles (Table 12).

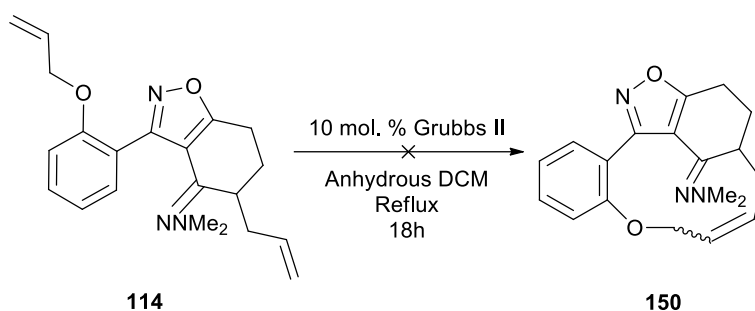
| Ring size | Yield (%) | Compound Number |
|-----------|-----------------|-----------------|
| 11 | No RCM observed | 147 |
| 12 | 60 | 148 |
| 13 | 47 | 149 |
| 14 | Trace | n/a |

Table 12. *n.b.* All attempts were carried out on a mixture.

Twelve and thirteen members appears to be the optimal macrocycle size, at eleven, the ring is too strained to close and at fourteen we believe cross metathesis processes start to dominate, yielding a mixture of oligomers.

Whilst RCM was successful, it was not possible to determine the stereochemistry of the macrocycle formed: we could not determine if it was E or Z, or what the ratio of the two isomers were, nor could it be possible to fully assign the ^1H or ^{13}C NMR spectra obtained.

As mentioned, at the point we were testing the mixtures, we were trying to control alkylation. Once this had been achieved we subjected the newly formed *bis*-alkyl hydrazones to RCM conditions. Initially we tested RCM on *bis*-allyl hydrazone **114** (Scheme 73).



Scheme 73

We were not surprised to find that this attempt at RCM was unsuccessful, as the ketone analogue had also failed. We proceeded to move on to the longer chain analogues using the same conditions as previous RCM attempts. Due to time constraints it was not possible to try with O-hexenyl hydrazone **117** which would yield the fourteen-membered macrocycle (Table 13).

| Ring size | Outcome |
|-----------|-----------------|
| 11 | No RCM observed |
| 12 | No RCM observed |
| 13 | No RCM observed |

Table 13. *n.b.* All reactions were carried out on 1 mMol of substrate.

We were extremely surprised to find that RCM did not take place on these compounds and believe there could be two main factors contributing to this. The first is sterics, the extended length of the N,N-dimethyl group could be blocking the ends of the alkenes coming together in a complex (Figure 14).

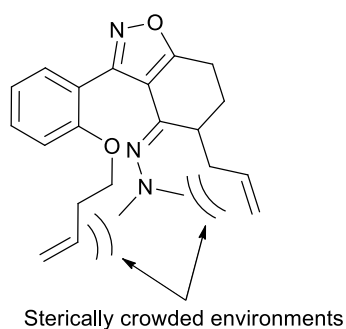


Figure 14

The second cause for the failure of RCM could be attributed to the basic nature of the hydrazone functionality (Figure 15).^{104,105}

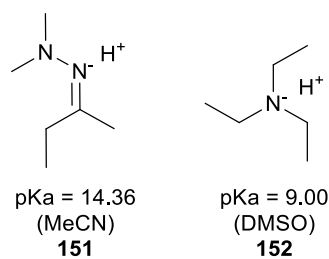


Figure 15

Basic amines are able to coordinate to the ruthenium of Grubbs II forming a stable intermediate which is deactivated towards RCM (Figure 16).^{106,107}

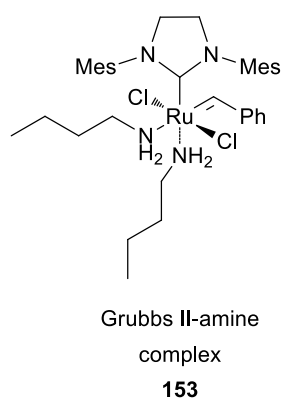
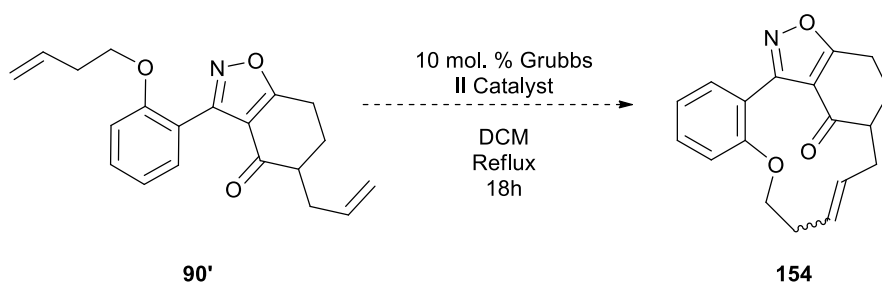


Figure 16

Although currently this has only been reported on primary amines, it is possible a similar mechanism could be taking place in the case of our hydrazone.

We believe it is a combination of these two factors that make the hydrazone series of compounds unreactive under RCM conditions.

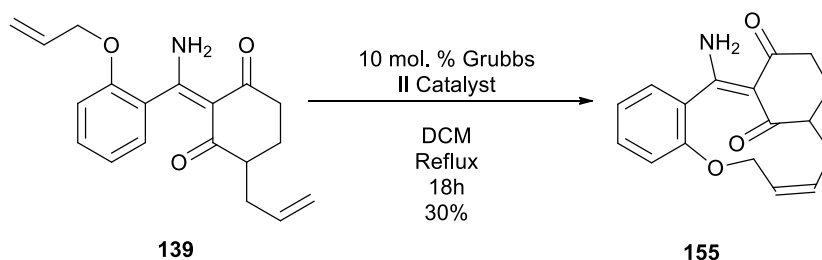
Given the unreactive nature of the hydrazine class of compounds to RCM conditions we went forward and attempted RCM on *bis*-alkyl ketone **90'** derived from the corresponding hydrazone. This attempt was made using the standard conditions we had developed for RCM (10% Grubbs II catalyst at 40°C) (Scheme 74).



Scheme 74

As the reaction was performed on a very small scale, the results were inconclusive. High resolution mass spectrometry (HRMS) did not display an $[M+X]$ ion under 5.00ppm which was consistent with the desired product, however, it did display a peak at 573, which is consistent with a dimer of the desired product plus a proton. ^1H NMR spectroscopy of the purified mixture displayed some features that may be consistent with a macrocycle. Due to time constraints it was not possible to clarify this result further.

As it was not possible to form the eleven-membered macrocycle with the isoxazole in place, we investigated if it were possible on ring opened *bis*-allyl enamino ketone **139** (Scheme 75).



Scheme 75

This attempt at RCM proved to be successful, yielding the desired 11-membered macrocycle. ^1H NMR spectroscopy suggests that the configuration of the macrocycle is *cis*. This is based on the J coupling constant value of the two alkenyl protons (Figure 17)

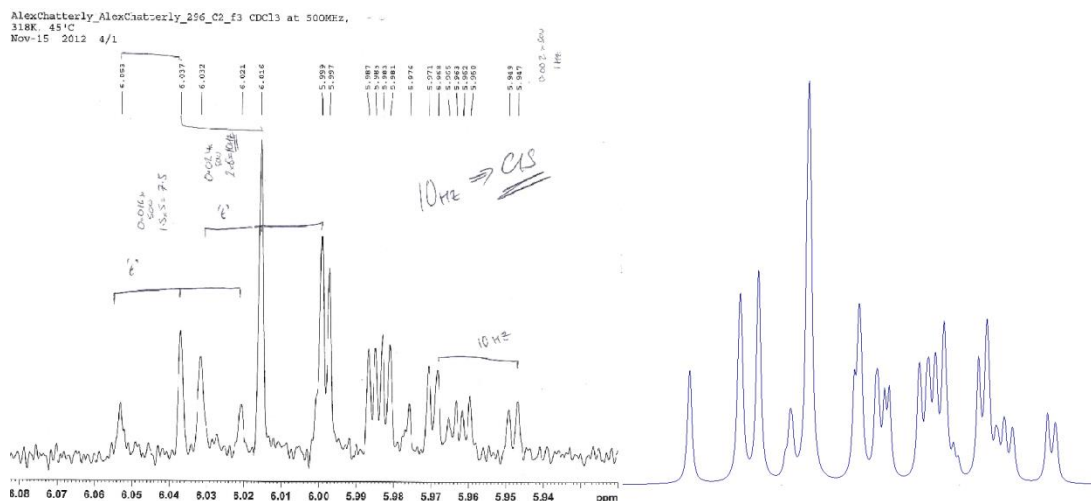


Figure 17. Observed and predicted ^1H NMR 500 MHz spectra of macrocyclic enamine ketone **155** at 40°C . This spectra was generated by Dr Mark Edgar of Loughborough University.

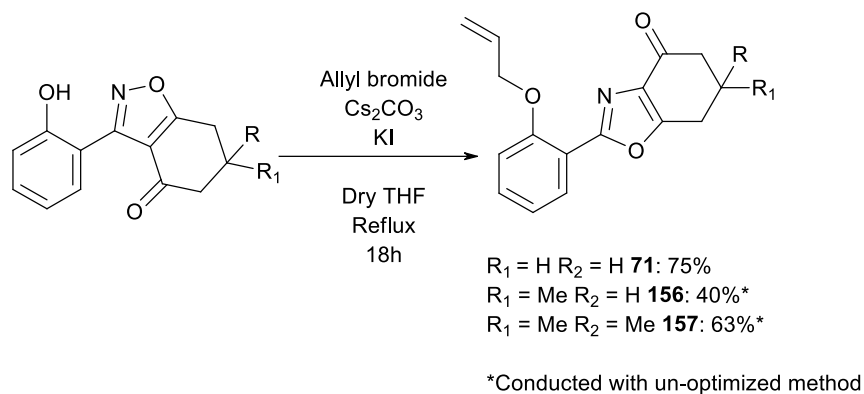
In terms of alkene J values, 6-10 and 12-18 Hz correspond to *cis*- and *trans*-disubstituted alkenes respectively, and as such, this is strong evidence for the presence of a *cis* configuration.¹⁰⁸

It is also interesting to note that RCM went ahead despite the presence of an amine; we believe this is due to the fact that nitrogen lone pair less available in this system, as it is tied up in the enamine-ketone conjugation, a vinylogous amide.

The success of ring closing metathesis on this system supports our hypothesis that the isoxazole ring adds too much rigidity to the system and as such, ring closing metathesis cannot take place, however, once this rigidity is removed, metathesis is possible.

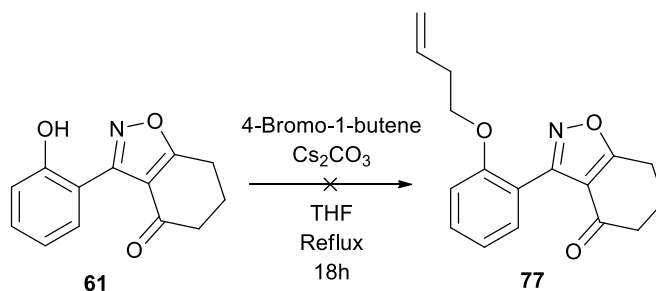
2.7 Benzisoxazole to Oxazole Rearrangement

Previously in this thesis it was noted that an interesting rearrangement had been observed (Scheme 76).



Scheme 76

This rearrangement was originally discovered when it was found that it was not possible to O-alkylate phenolic benzisoxazole **61** with an alkyl chain longer than allyl, *via* base mediated alkylation (Scheme 77).



Scheme 77

The ^1H NMR spectra indicated that neither desired but-3-enyl benzisoxazole **77** nor starting material were isolated, and a new, unknown compound was being formed.

As mentioned previously, the Mitsunobu based alkylation method had been developed to overcome the problem of O-alkylating with alkenyl halides. In an effort to compare O-allylation yields, the two methods were performed in tandem.

It was at this point it was noted that the ^1H NMR spectra for the two O-allyl compounds were significantly different (Figure 18).

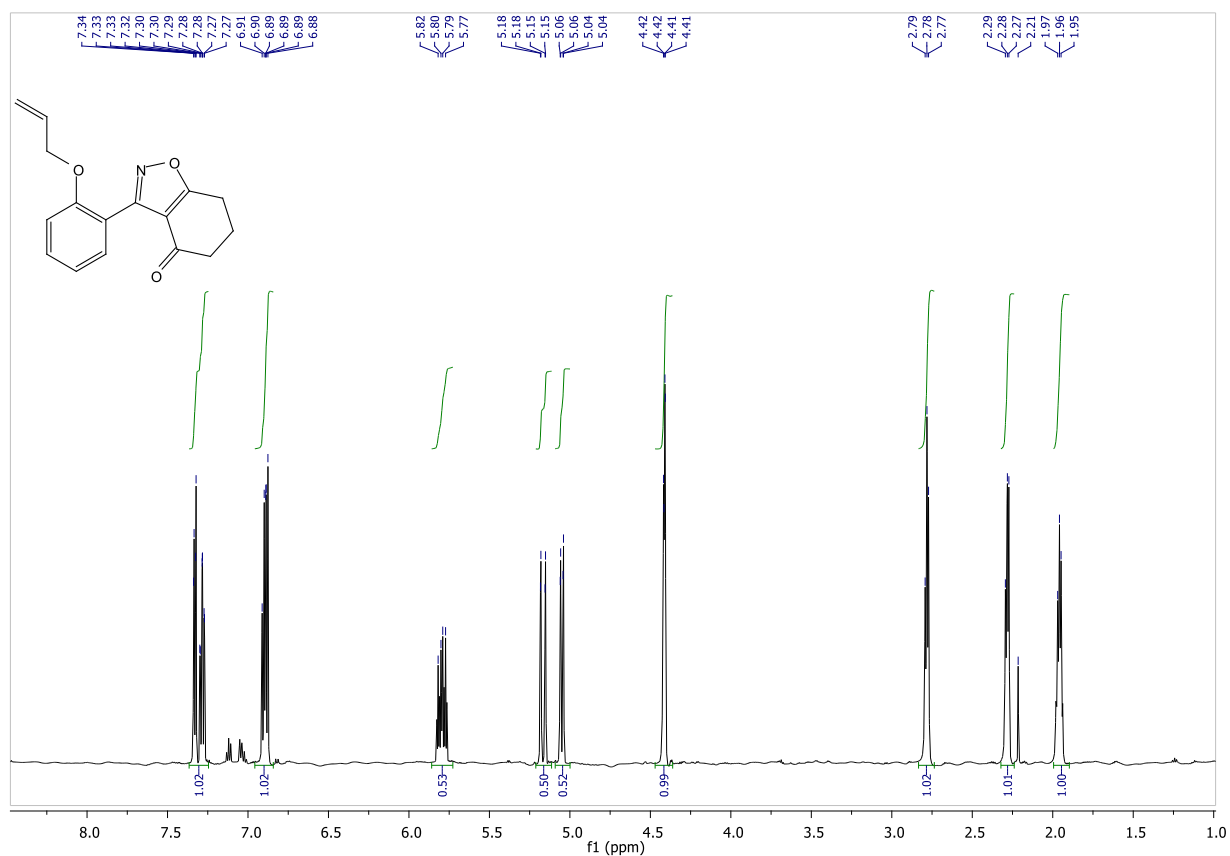
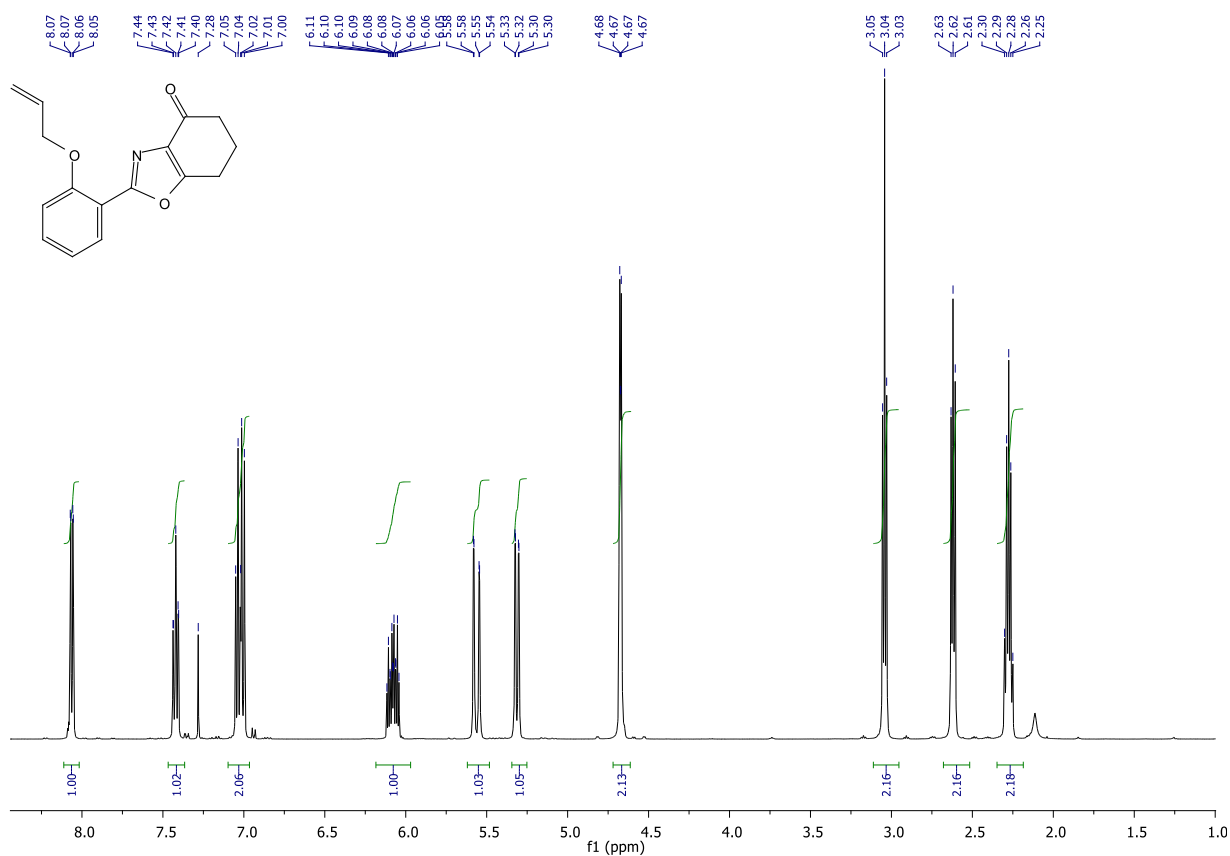
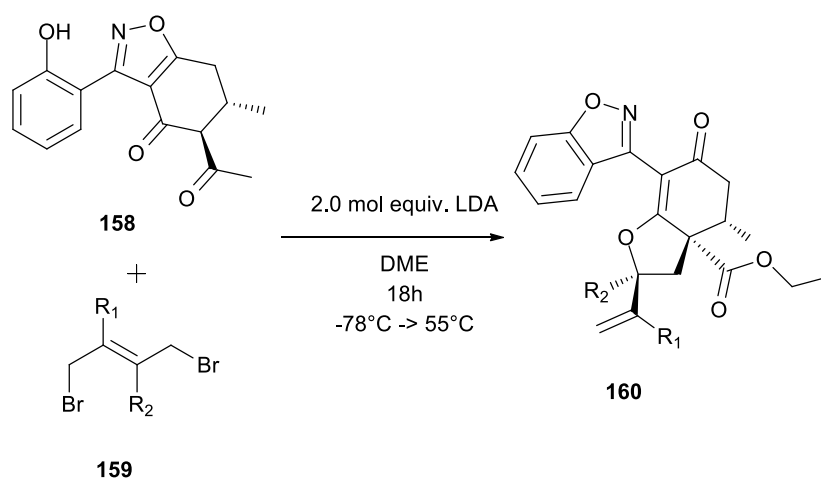


Figure 18. (top) O-allyl benzoxazole **71** and (bottom) O-allyl isoxazole **70**.

Although the differences may appear obvious in retrospect; both the spectra in figure **18**, could also be interpreted as corresponding to allyl benzisoxazole **70** if no evidence to the contrary was presented.

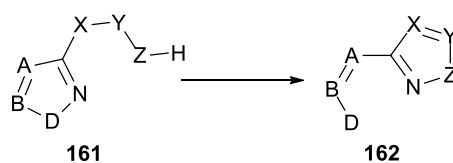
At this point it was known that two different compounds were being obtained from a process that, on paper, should have resulted in the same compound; due to this efforts were made to determine the absolute structure of both.

Searches into this area suggested a rearrangement with this class of compounds had been observed elsewhere, albeit under different conditions (Scheme 78).¹⁰⁹



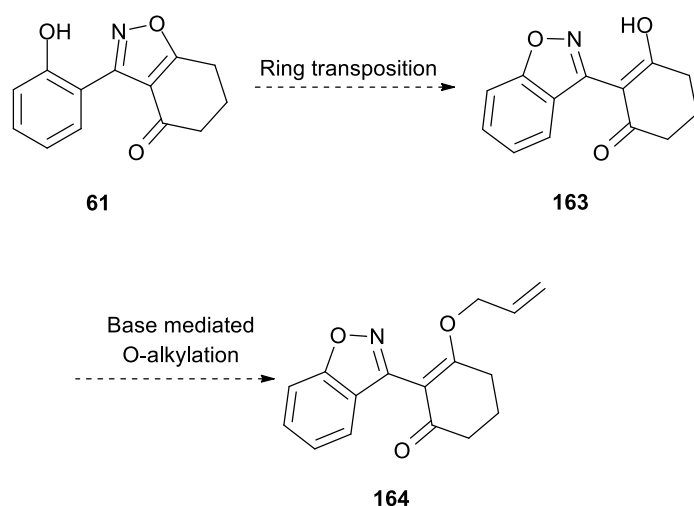
Scheme 78

The above reaction is an example of an example of a Boulton-Katritzky type rearrangement (Scheme 79).¹¹⁰



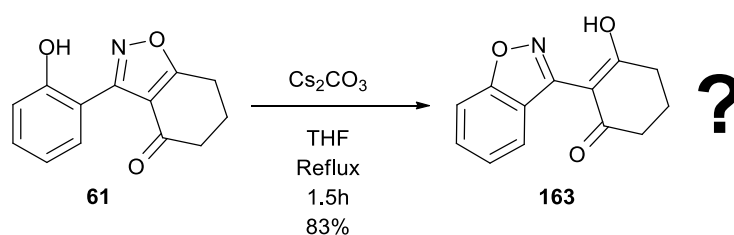
Scheme 79

As a result of this, it was initially proposed that the isoxazole ring was simply being transposed, and then base mediated alkylation of enol **163** was taking place (Scheme 80).



Scheme 80

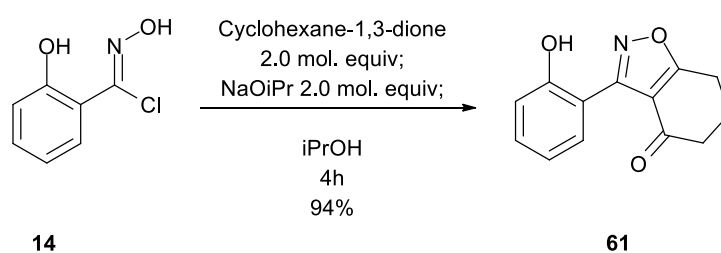
To help determine if this was indeed the case, phenolic benzisoxazole **61** was heated in the presence of base but no alkylating agent (Scheme 81).



Scheme 81

This reaction proved to be very successful, generating what was at that stage believed to be ring transposed benzisoxazole **163** in very good yields. The ^1H NMR spectrum of phenolic benzisoxazole **61** was compared against that of the presumed ring transposed product **163**, and they proved to be different.

However, as the isoxazole ring formation itself requires base, it was important to prove that phenolic benzisoxazole **61** was indeed being generated and not some, as yet, unknown product (Scheme 82).



Scheme 82

As mentioned earlier, it was possible to prove the exact constitution of phenolic benzisoxazole **61** via single crystal X-ray crystallography (Figure 19).

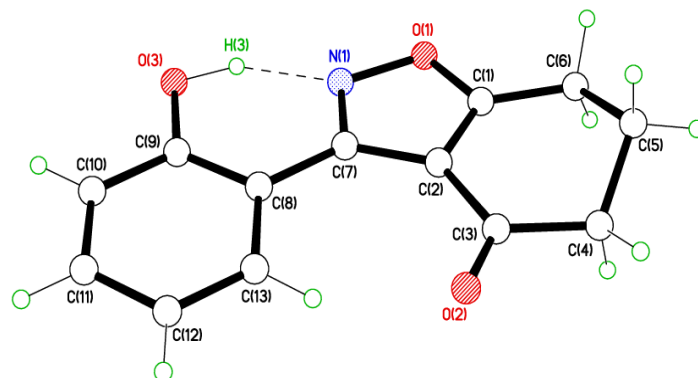
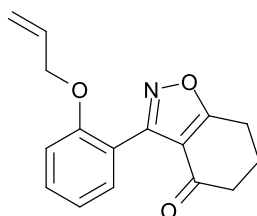


Figure 19. X-Ray crystal structure of 3-(2-Hydroxyphenyl)-6,7-dihydrobenzo[d]isoxazol-4(5H)-one **61**. This crystal structure was solved by Dr Mark Elsegood of Loughborough University.

We hypothesise that the formation of fused phenolic benzisoxazole **61** is successful for the following reasons: although two equivalents of base are used, the first is used to form nitrile oxide from the imidoyl chloride **14** which is believed to be the fastest process. While the second equivalent of isopropoxide could in principle deprotonate phenolic benzisoxazole **61**, the excess 1,3-cyclohexanedione is more acidic (pKa of approximately 14.8 vs 10.3 respectively) and therefore the second equivalent of dione acts as a buffer.^{111,112}

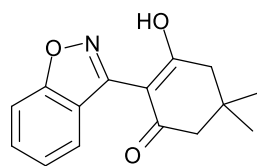
Following this, it was then necessary to prove that the Mitsunobu procedure had indeed formed allyl benzisoxazole **70**. This was achieved using a specialized type of ¹³C NMR spectroscopy: Incredible Natural Abundance Double Quantum Transfer Experiment (INADEQUATE). The INADEQUATE spectra successfully displayed the ¹³C-¹³C 1-bond couplings within allyl benzisoxazole **70**, therefore allowing the exact structure of the carbon skeleton to be determined. Using this in conjunction with other data that had been gathered, it was possible to prove that allyl benzisoxazole **70** had been successfully synthesised using the Mitsunobu method (Figure 20).



70

Figure 20

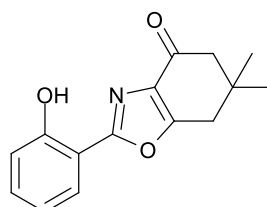
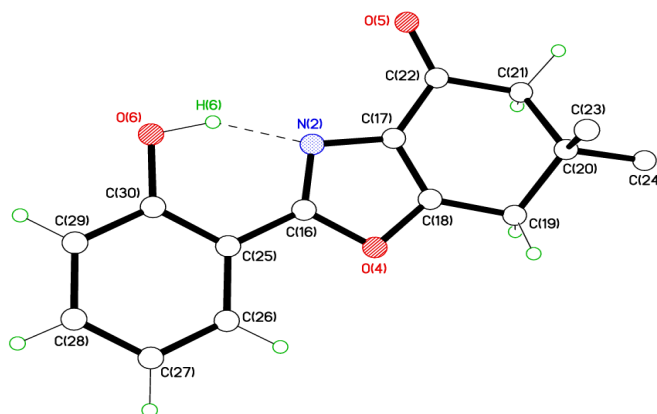
As these investigations had been taking place, attempts were made to grow crystals of what was believed to be ring transposed dimethyl benzisoxazole **164** (Figure 21).



165

Figure 21

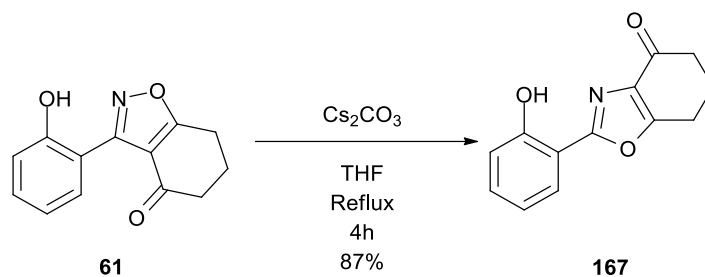
These attempts proved to be successful and it was possible to determine the exact structure by X-ray crystallography (Figure 22).



166

Figure 22. X-Ray crystal structure of 2-(2-Hydroxyphenyl)-6,6-dimethyl-6,7-dihydrobenzo[d]oxazol-4(5H)-one **166**. This crystal structure was solved by Dr Mark Elsegood of Loughborough University.

However, we were surprised to find that what was believed to be an isoxazole ring transposition was in fact benzisoxazole to benzoxazole rearrangement (Scheme 83).



Scheme 83

To help confirm if this was also the case in the allylation reaction, ^1H Nuclear Overhauser Effect Spectroscopy (NOESY) was performed on what was believed up to this point to be ring transposed allyl enol ether **168** (Figure 22).

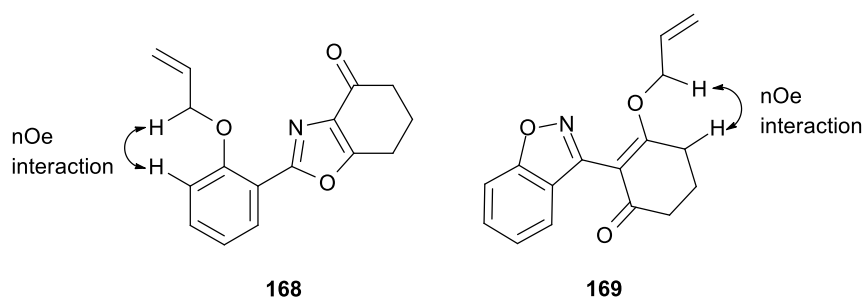
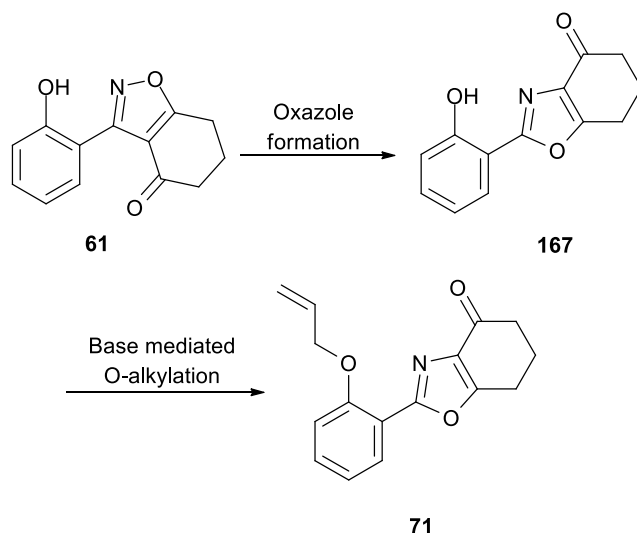


Figure 22

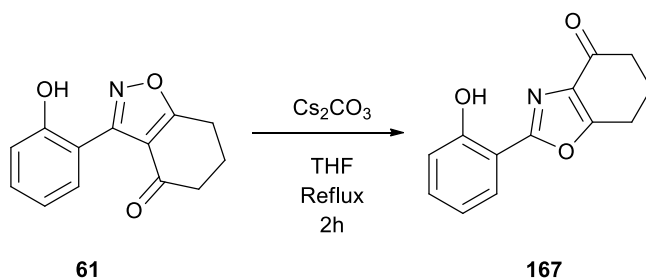
^1H NOESY spectroscopy is used to detect through space interactions between protons. As a result it should be possible to detect if the allyl chain was on either the aromatic or cyclohexanone ring by looking for NOESY interactions with the corresponding aromatic or aliphatic protons.

The ^1H NOESY spectra indicated there were interactions between the CH_2 of the allyl chain and the CH of the aromatic ring, which strongly suggests that oxazole formation under these conditions, followed O-alkylation (Scheme 84). No interaction of this CH with the cyclohexanedione moiety was observed, which would have been expected for allyl enol ether **169**.



Scheme 84

In an effort to gain additional information, the reaction for formation of benzoxazole **167** was carefully monitored by LC-MS to determine if any intermediates were forming (Scheme 85).



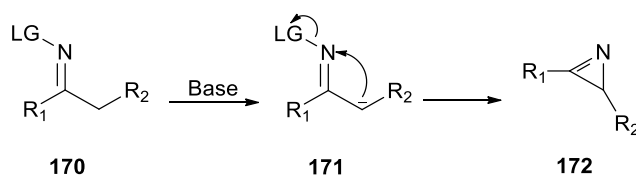
Scheme 85

This investigation indicated that a more polar intermediate with the same molecular weight ($[M+H] = 230$) as benzoxazole **61** was forming, before being converted to benzoxazole **167**.

An attempt was made to isolate and purify this intermediate by preparative reverse phase high performance liquid chromatography (HPLC). This attempt proved successful and it was possible to obtain a small quantity of the unknown intermediate. The ^1H and ^{13}C NMR spectra suggested the cyclohexanedione ring had become symmetrical and was demonstrating delocalisation. These were two key pieces of information.

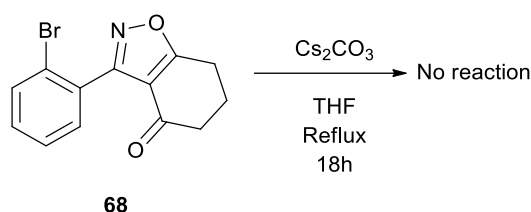
Literature indicates that it is possible to generate an oxazole from an azirine and that it is possible to form an azirine from an isoxazole under thermolysis conditions (200°C).^{113,114} If it is postulated that the observed oxazole formation is taking place *via* a similar route, then azirine formation is most likely occurring *via* another pathway, as our rearrangement takes place at 66°C .

Further research suggested that one possible route to azirines at lower temperatures is the Neber rearrangement (Scheme 86).¹¹⁵



Scheme 86

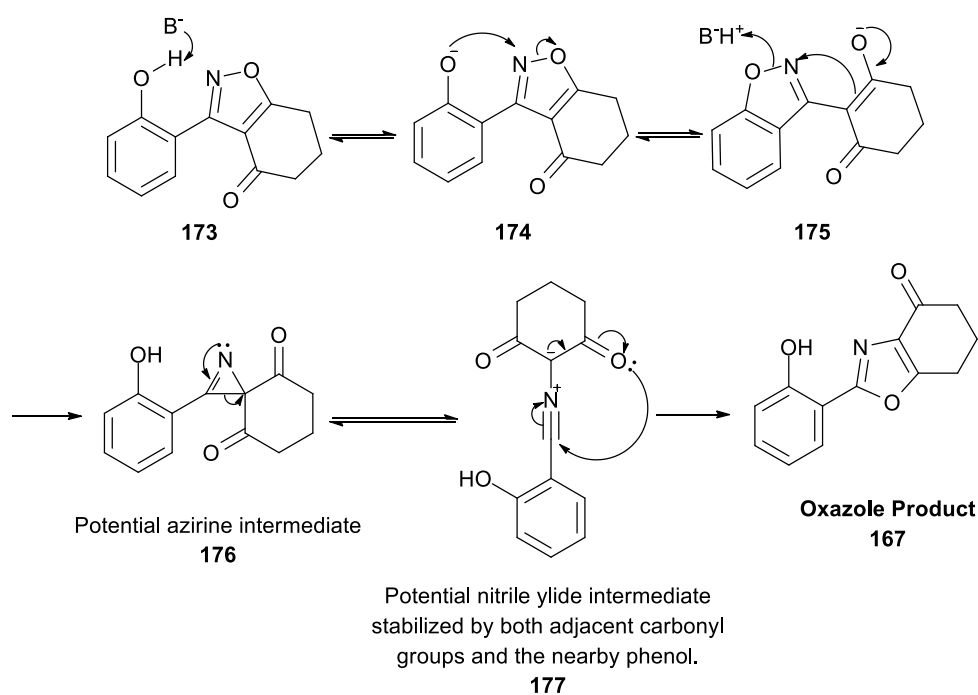
We conducted a control experiment to determine if the free phenol was essential to the transposition process (Scheme 87).



Scheme 87

This result suggests that the phenol is necessary for the rearrangement to take place and as such we can reason that it must be involved in a key step.

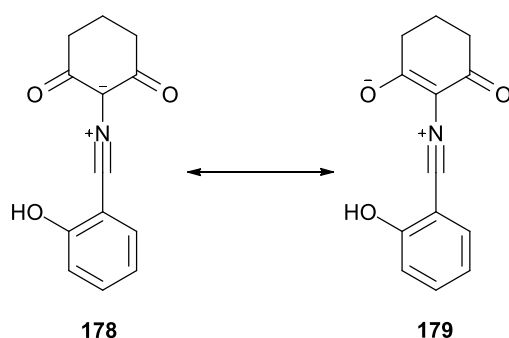
Based on the above pieces of information it is believed that two sequential rearrangement reactions are taking place; firstly a Boulton-Katritzky type reaction followed by a Neber rearrangement with a phenolate anion serving as the leaving group to form azirine **176** (Scheme 88). The azirine could be in equilibrium with a nitrile ylide intermediate that can ring close to an oxazole *via* an electrocyclic process.



Scheme 88

This mechanism meets the criteria of what is preceded in the literature, as well as helping us to understand why azirine formation is occurring at lower temperatures, and why the reaction only appears to take place with the free phenol.

While the NMR spectral data gathered correspond to either of the possible intermediates (azirine or nitrile ylide), infrared (IR) spectral data display a carbonyl shift at a much lower than expected adsorption band, 1595 cm^{-1} ; the expected ketone carbonyl shift is $1680\text{-}1750\text{ cm}^{-1}$.¹⁰⁸ This suggests that the C=O bond is much weaker than usual; this could be explained by the presence of an anionic carbon α to both of the ketones, as in intermediate **178**. An anionic carbon at this location would be delocalised to stabilize the negative charge (Scheme 89).



Scheme 89

This stabilization would result in a much weaker than normal carbonyl bond, which in turn would significantly lower the observed ketone carbonyl adsorption band in the spectrum. The fact that ylide **178** is doubly stabilized by both carbonyls would also increase the likelihood of being able to isolate it. In addition the positive end of the dipole is stabilised by the attached phenolic unit.

Unfortunately it was not possible to grow a single crystal of the intermediate isolated during the non-methyl benzisoxazole **61** to benzoxazole **167** rearrangement. A second sample of intermediate was isolated from the rearrangement of dimethyl benzisoxazole **62** to oxazole **166**. However attempts to grow a single crystal from this intermediate failed and it is believed that it collapsed under crystallization conditions as the structure obtained was that of dimethyl benzoxazole **166** (Figure 23).

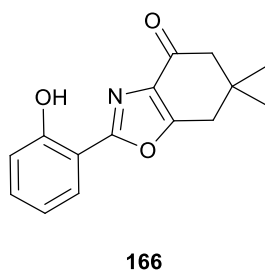
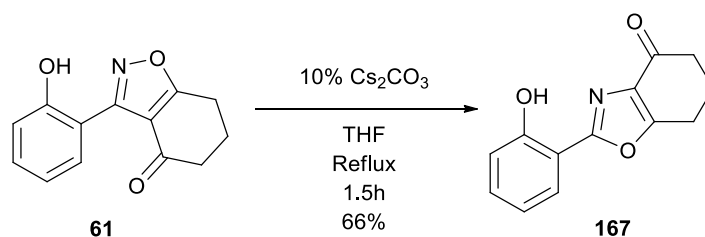


Figure 23

Another feature of this mechanism is that only catalytic amounts of base would be required for it to take place; this theory was put to the test (Scheme 90). Reducing the base to 10% level still resulted in ring transformation.



Scheme 90

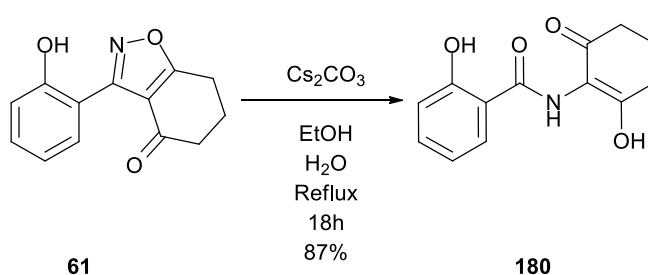
This success lends credence to our proposed mechanism. We then went on to determine if the rearrangement would occur under a range of basic conditions (Table 14).

| Base | Solvent | Yield (%) ^b |
|-------------------------------------|-----------------------|------------------------|
| Cs₂CO₃ | THF | 87 |
| K₂CO₃ | THF | 84 |
| Na₂CO₃ | THF | 5 |
| Et₃N | THF | 0 |
| DMAP | THF | 0 |
| DBU | THF | 83 |
| LDA | THF | 37 |
| Cs₂CO₃ | Toluene | 97 |
| NaOⁱPr | ⁱ PrOH | 85 |
| Cs₂CO₃ | EtOH-H ₂ O | 87 (for 7a) |
| none | H ₂ O | 8 |
| Cs₂CO₃ | H ₂ O | 91 (for 7a) |

Table 14. ^a Isoxazole **61** (2.18 mmol), Base (4.37 mmol), reaction time 4 h, solvent under reflux; ^b Isolated yields refers to oxazole **167** unless otherwise stated. All entries in this table were generated by Romain Marty, a summer project student.

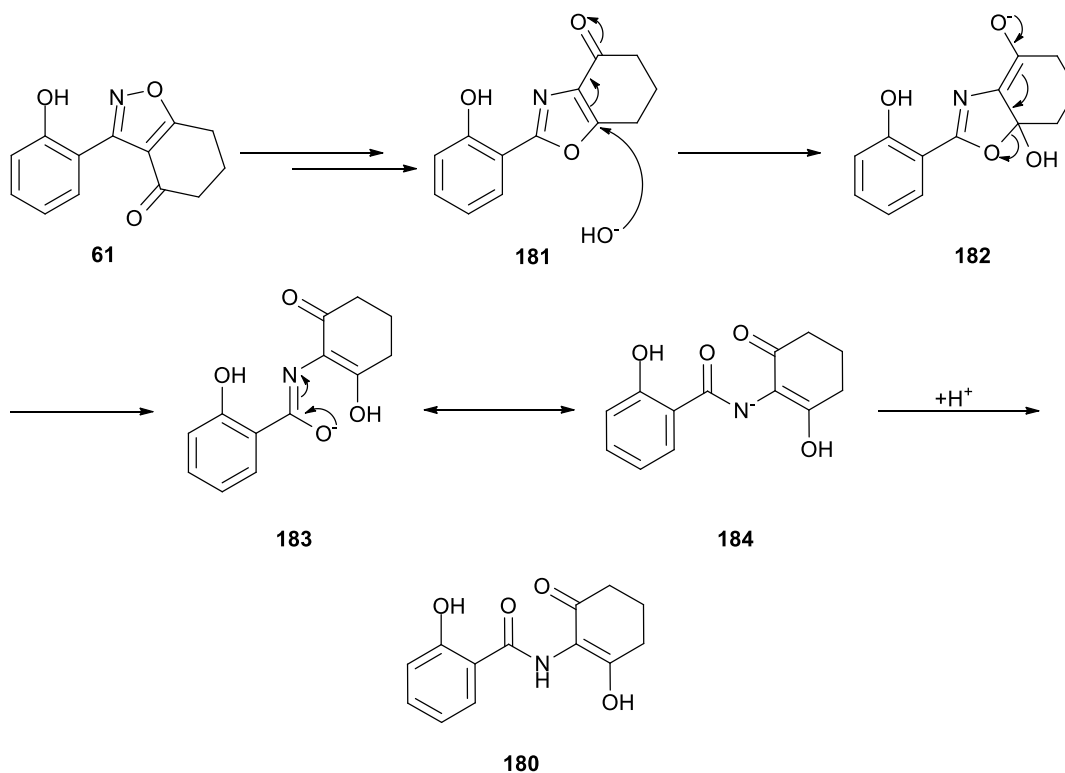
We found that the best yields are obtained using caesium and potassium carbonate; sodium carbonate provided a much lower yield, possibly due to its poor solubility in THF. We also found that the reaction does not appear to proceed with triethylamine (Et₃N) or (4-dimethylaminopyridine (DMAP), however, it will proceed with 1,8-diazabicycloundec-7-ene (DBU) and to a lesser extent with LDA.

We also observed that under nucleophilic conditions (i.e. Cs₂CO₃ in aqueous ethanol) amide **180** was obtained (Scheme 91).



Scheme 91

This is believed to a product of nucleophilic ring opening (Scheme 92).



Scheme 92

The basic aqueous medium attacks the oxazoles ring, presumably by attack at C-5, the ring then opens to yield amide anion **184**, which undergoes protonation to yield enol **180**. The structure of enol **180** was confirmed by crystallography (Figure 24).

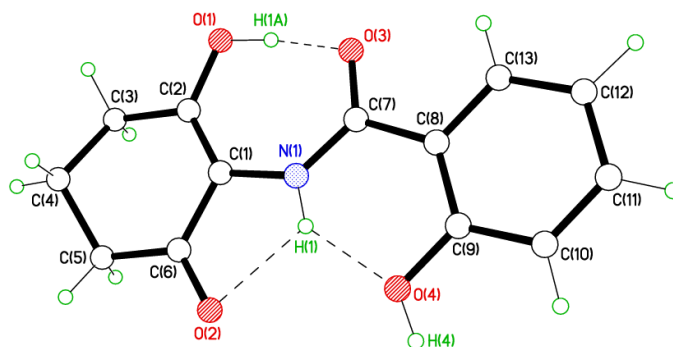
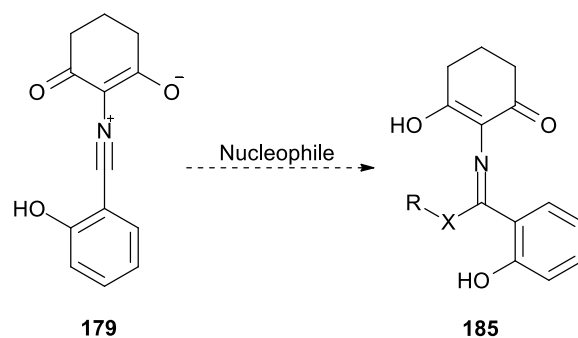


Figure 24. X-Ray crystal structure of 2-Hydroxy-N-(2-hydroxy-6-oxocyclohex-1-en-1-yl)benzamide **180**.

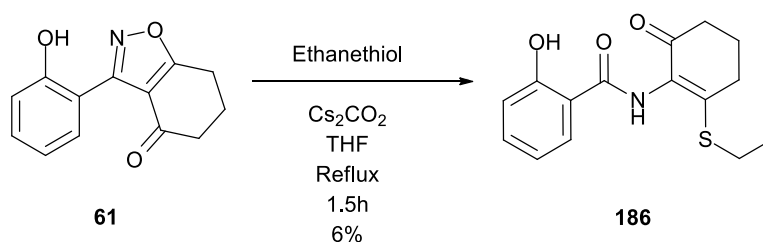
This crystal structure was solved by Dr Mark Elsegood of Loughborough University.

We hypothesised that it might be possible to trap the proposed nitrile ylide intermediate with an appropriate nucleophile (Scheme 93).



Scheme 93

This was attempted using ethanethiol (Scheme 94).



Scheme 94

Instead a thioimidate being formed, thio-ether **186** was isolated, again, presumed to be a product of ring opening. This result was confirmed *via* X-ray crystallography (Figure 25).

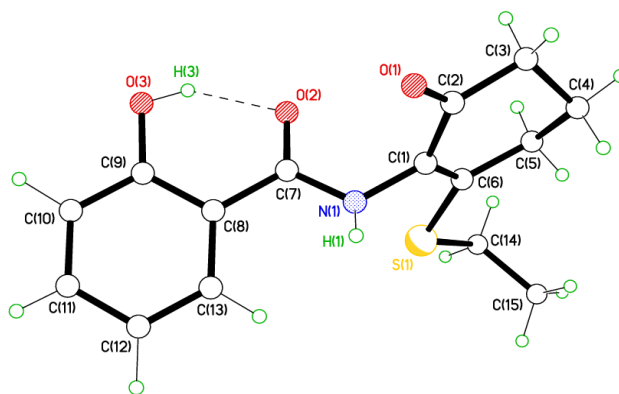


Figure 25. X-Ray crystal structure of N-(2-(ethylthio)-6-oxocyclohex-1-en-1-yl)-2-hydroxybenzamide **186**. This crystal structure was solved by Dr Mark Elsegood of Loughborough University.

There are some interesting differences between the two crystal structures. Enol **180** possess a network of hydrogen bonds linking the two rings together, whilst thioether **186** does not. We believe there to be two reasons for this, firstly the greater steric bulk of the thioether chain. Secondly and more importantly, sulfur is a poor hydrogen bond acceptor when compared to oxygen.¹⁰³

Thioether formation suggests the initiation of ring opening favours the carbon of the cyclohexanone ring (oxazole C-5) rather than at the carbon alpha to the phenol (oxazole C-2) (Figure 26).

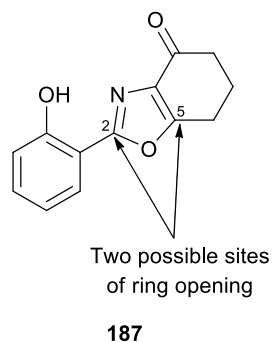


Figure 26

If this was not the case, a mixture of thioether **186** and thioimidate **188** would be observed (Figure 27).

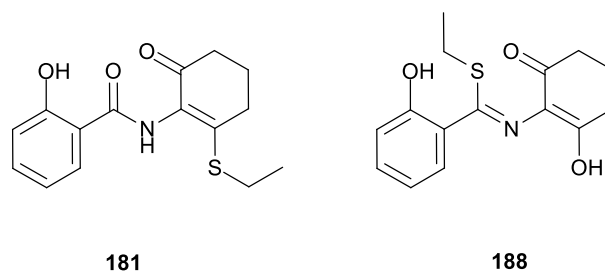
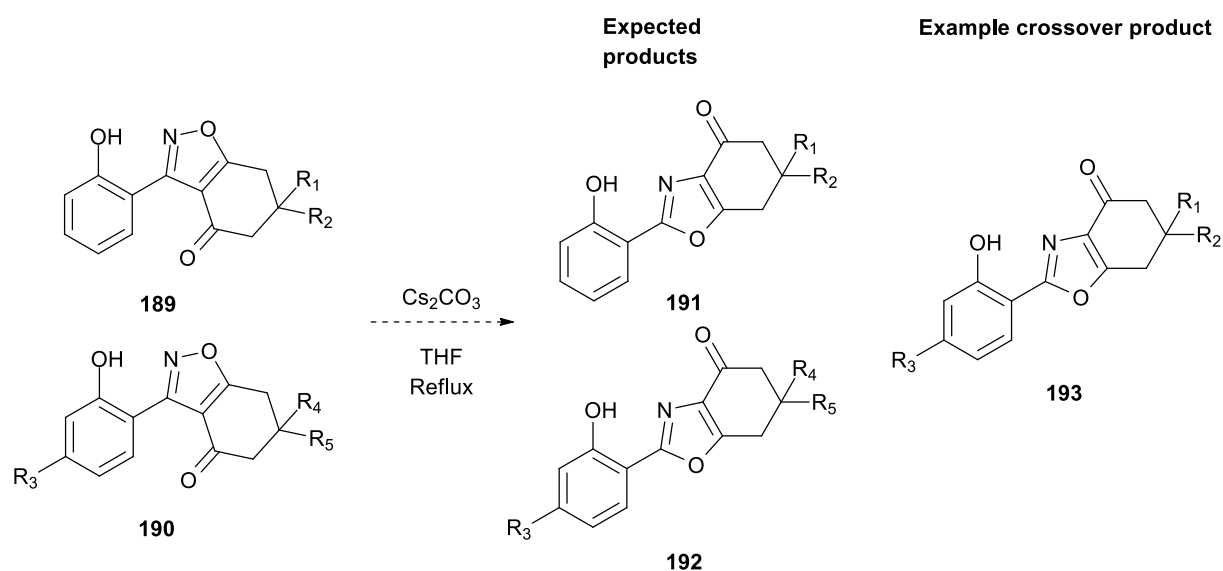


Figure 27

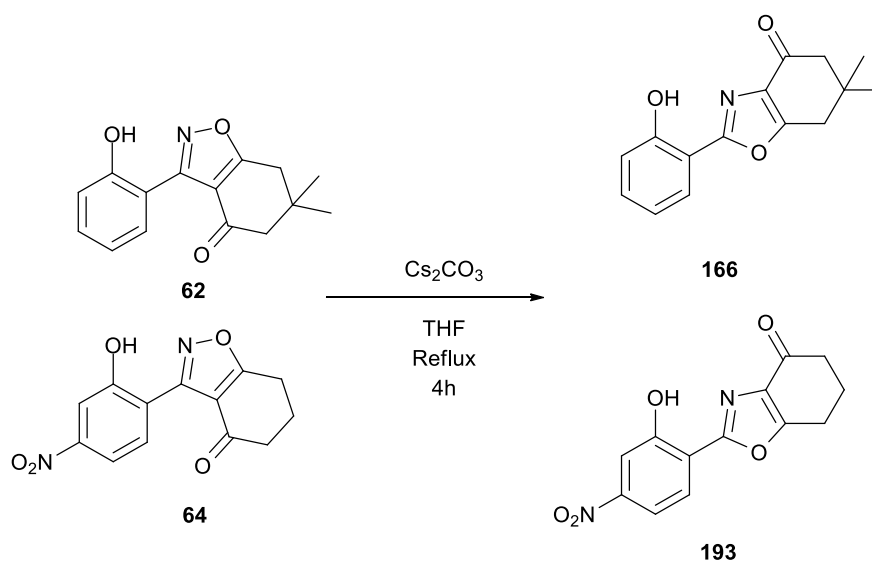
This is unexpected as one would expect the carbon atom attached to the aromatic ring to be reasonably electropositive as it is between two electronegative heteroatoms. However, the electron donating ability of the phenol ring, as well as the extended resonance of the anion that is formed on the cyclohexanone ring may explain this why ring opening is initiated at that position. No further attempts were made at trapping the unknown intermediate as we believed that similar results would be observed.

To discount the possibility of the oxazoles being formed by retro-1,3-dipolar cycloaddition from the isoxazoles and recombination *via* a different connectivity, a cross-over experiment was planned (Scheme 95). This required two isoxazoles with both their aromatic and cyclohexyl rings being different.



Scheme 95

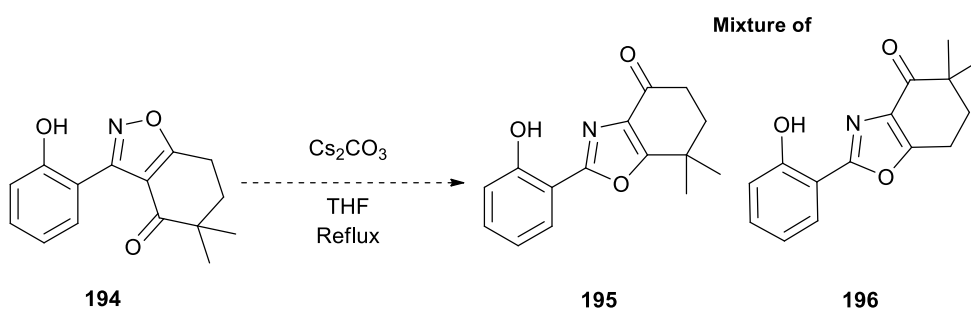
If our mechanism is correct, mixed oxazole **193** should not be observed. The cross-over experiment was attempted using di-methyl and nitro isoxazoles **62** and **64** (Scheme 96).



Scheme 96

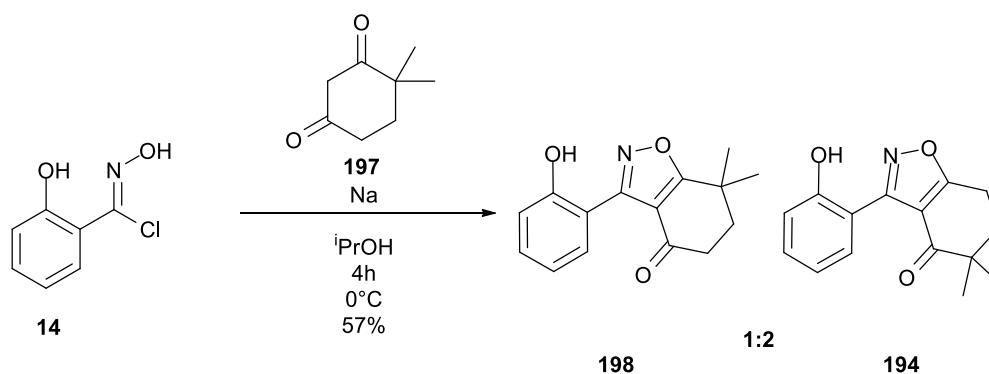
No evidence of any cross-over was observed. This result suggests that the molecule is not splitting in two during the rearrangement, and supports our proposed mechanism

We hypothesised that if a linear intermediate was being generated, then when a benzisoxazole asymmetrically substituted in the cyclohexane ring is subjected to rearrangement conditions a mixture should be obtained (Scheme 97).



Scheme 97

As a suitable asymmetric di-ketone was commercially available in 4,4-dimethylcyclohexane-1,3-dione **197**, we synthesised and isolated the resultant isoxazoles (Scheme 98). A separable 1:2 mixture of isoxazole cycloadducts was obtained.



Scheme 98

It was possible to grow a single crystal of the major product to confirm the identity of each fraction of the reaction (Figure 28).

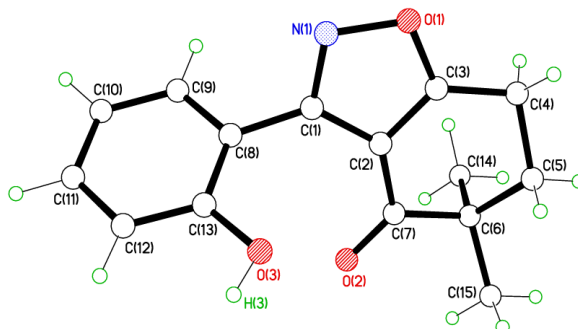
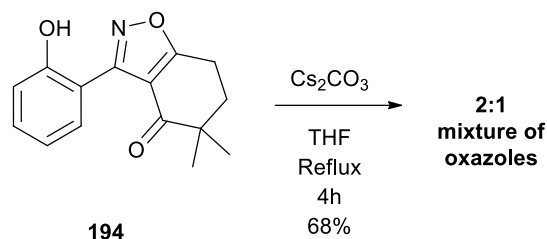


Figure 28. X-Ray crystal structure of 3-(2-Hydroxyphenyl)-5,5-dimethyl-6,7-dihydrobenzo[d]isoxazol-4(5H)-one **194**. This crystal structure was solved by Dr Mark Elsegood of Loughborough University.

This result is not unsurprising, as the major product is most likely slightly more favoured during the ring closure process as a result of steric factors.

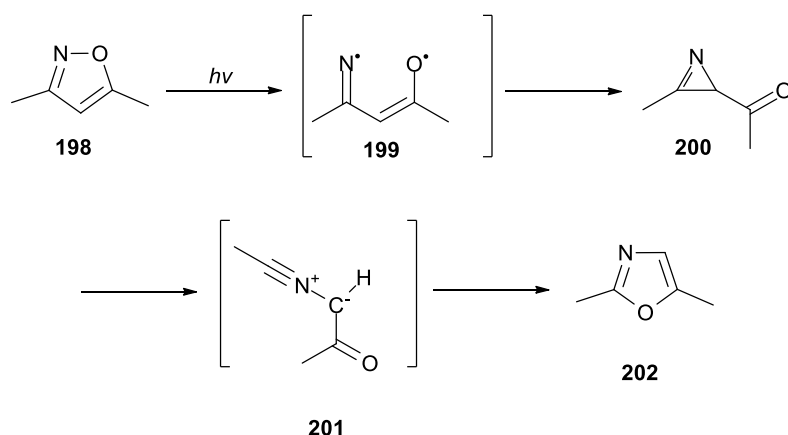
The major isomer was subjected to rearrangement conditions (Scheme 99).



Scheme 99

The rearrangement was successful, yielding a mixture of benzoxazoles. This result supports our hypothesis that a linear intermediate is formed, as a mixture of isomers is obtained. The ratio of isomers currently cannot be assigned, as it was not possible to separate the mixture.

Recently more evidence to support our mechanism has come to light in a paper published by Nunes *et al.*¹¹⁶ In this paper they state that they have been able to spectroscopically observe anti-nitrile ylide **201** which rotated and closed on upon higher energy irradiation during the photo-catalysed isoxazole to oxazole rearrangement illustrated below (Scheme 100).



Scheme 100

This group were able to isolate and observe both the azirine and nitrile ylide *via* infrared (IR) spectroscopy. The results published in this paper strongly support our proposed mechanism as the only difference is the method by which the azirine is formed.

To conclude we have demonstrated that this rearrangement takes place on a range electron rich/neutral and deficient aromatic benzisoxazoles (Figure 29).

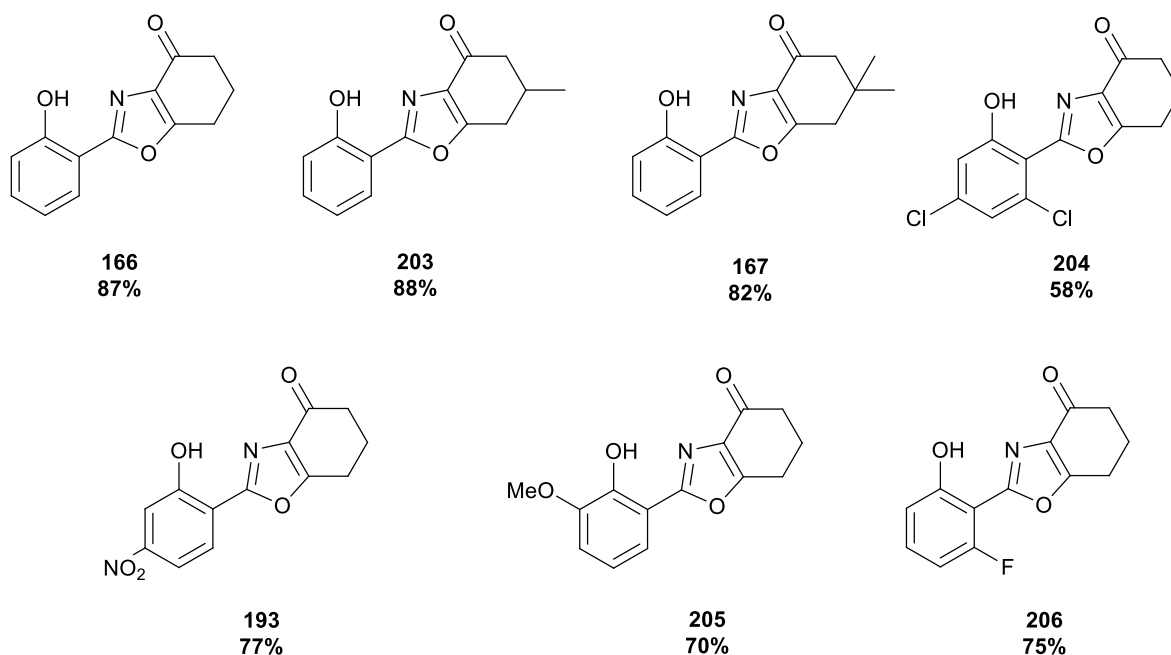


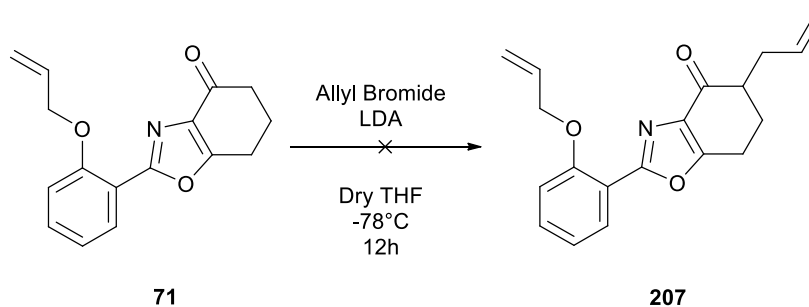
Figure 29

Benzoxazole Chemistry

As we did not identify the rearrangement straight away, some investigations were carried out unknowingly on allyl benzoxazole **72**, under the assumption that it was an isoxazole. These results could now be correctly interpreted as below.

Carbonyl Addition

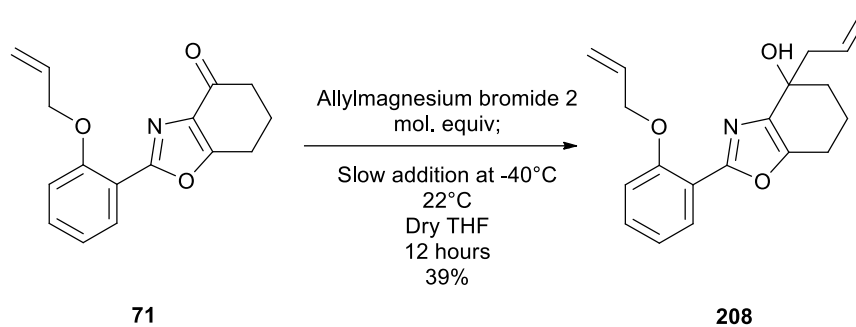
Allyl benzoxazole **71** is similar to allyl benzisoxazole **70** in that it seems relatively unreactive towards electrophiles after being subjected to LDA under standard conditions (Scheme 101).



Scheme 101

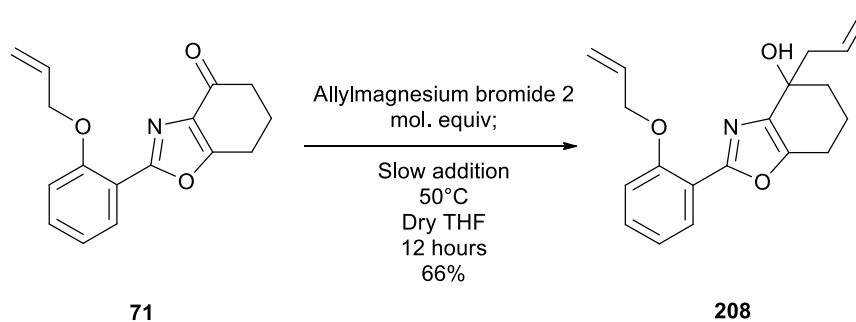
This reaction was not repeated with the new conditions illustrated previously in this thesis and as a result, enolate formation and C-alkylation may be possible.

However, when subject to an allyl Grignard reagent, benzoxazole **71** reacted readily (Scheme 102).



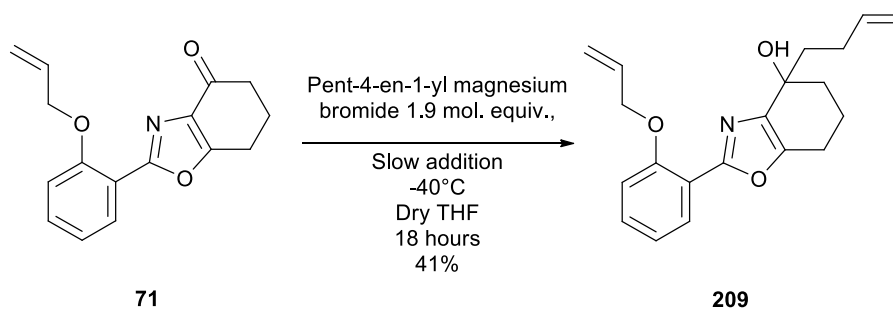
Scheme 102

Initial attempts at low temperature afforded only moderate yields of tertiary alcohol **208**. With some optimization it was possible to further increase the yield to 66% with warming to 50°C (Scheme 103).



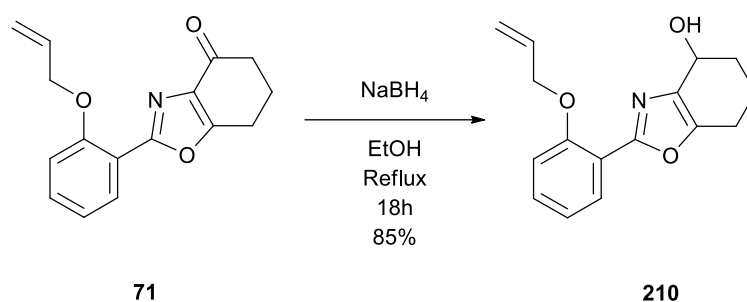
Scheme 103

it was also possible to introduce a longer alkyl chain using the same methodology to produce a pent-4-enyl adduct (Scheme 104).



Scheme 104

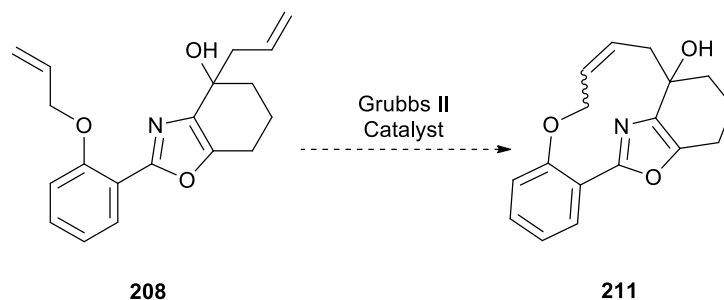
We also determined it was possible to reduce the cyclohexenone ring of the oxazole in a similar fashion to that of the isoxazole with sodium borohydride affording secondary alcohol **210** in good yield (Scheme 105).



Scheme 105

Ring Closing Metathesis

Some ring closing metathesis investigations were carried out on the above substrates. While they do not possess the same motif as the natural products, they still served as a suitable series of compounds for testing RCM conditions; as steric constraints should be reasonably similar between the two classes of compounds (Scheme 106).



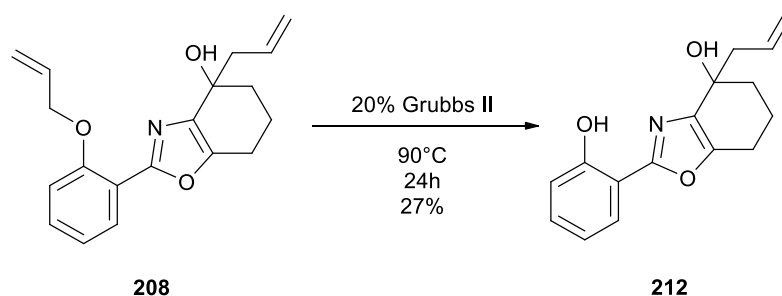
Scheme 106

Ring closing was tested on the diallyl material at a series of different temperatures (Table 15) and using Grubbs 2nd generation catalyst (Grubbs II).

| Solvent | Temperature | Duration | Outcome |
|-------------|-------------|----------|-------------------------------------|
| Dry DCM | 40°C | 5 Days | 80% of starting material recovered. |
| Dry Toluene | 60°C | 5 Days | 33% of starting material recovered. |
| Dry Toluene | 70°C | 3 Days | Unknown compound isolated |
| Dry Toluene | 80°C | 5 Days | Unknown compound isolated |
| Dry Toluene | 100°C | 3 Days | Unknown compound isolated |

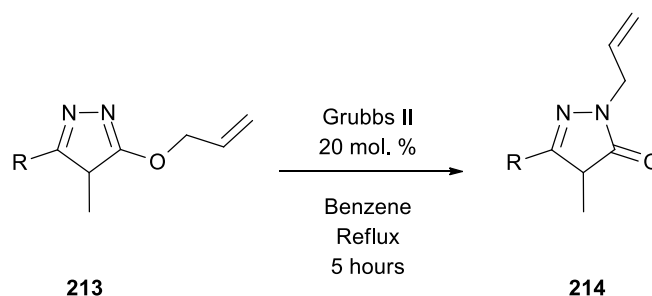
Table 15. All reactions were carried out on a 37mg (1.18 mM) scale with regards to starting oxazole **208** and 20% catalyst loading in 10mL of dry solvent. Unless otherwise stated, the remaining mass balance was unidentifiable baseline material.

None of the above attempts produced a ring closed substrate, however, there appeared to be signs that de-allylation may have taken place. To investigate this, the reaction was repeated on a larger (0.50g) scale to determine if this was the case (Scheme 107).



Scheme 107

The reaction was monitored by LC-MS until [M+H]⁺ for the starting material was no longer present. No [M+H]⁺ peak was observed for the ring closed product, however, a strong peak was observed at 271, which correlates to [M+H]⁺ for de-allylated benzoxazole **212**. This is also consistent with ¹H NMR spectra obtained from this reaction; these spectra lacked peaks that are indicative of the O-allyl functionality. Evidence that Grubbs II catalyst is capable of deallylating hetero atoms has been presented by other groups (Scheme 108).^{117,118}



Scheme 108

Synthetic Utility

We have also demonstrated that this rearrangement possesses synthetic utility. A class of pyrimidine containing fused benzoxazoles has been described in patents filed by Udea *et al.* (Figure 30).¹¹⁹

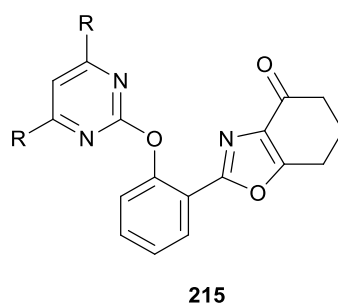
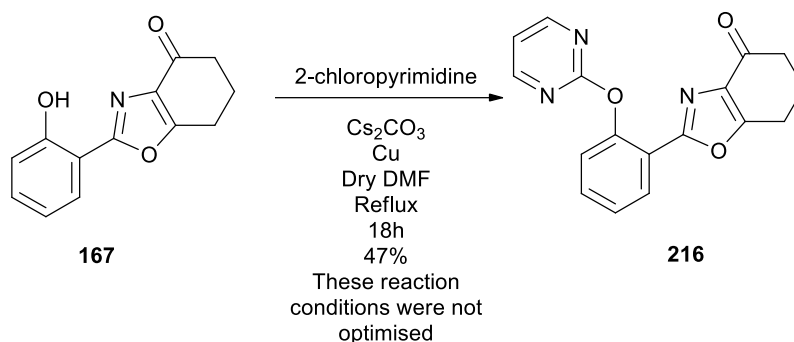


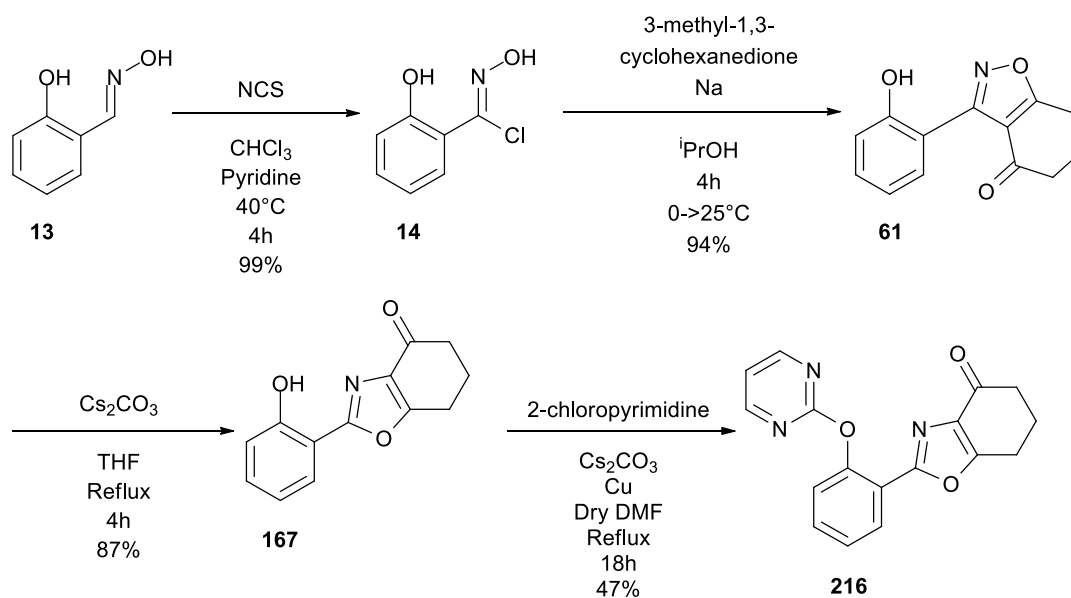
Figure 30

We have demonstrated that it is possible to access these structures in just one step from our rearranged benzoxazole *via* an Ullmann-type coupling (Scheme 109).¹²⁰



Scheme 109

With this success we have demonstrated that it is possible to access this class of herbicides in just four steps with an overall yield of 38%, with the potential for further optimisation available (Scheme 110).



38% over 4 steps

Scheme 110

2.8 Progress towards Coleophomone D

As mentioned, one of the objectives of this project has been the synthesis of coleophomone D **217**

(Figure 31)

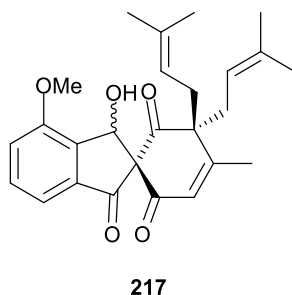


Figure 31

Earlier in this thesis it was illustrated how we have been able to successfully synthesise a potential precursor for coleophomone D from *o*-vanillin (Figure 32).

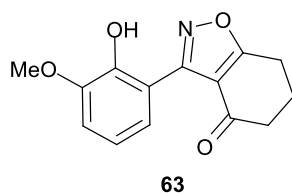
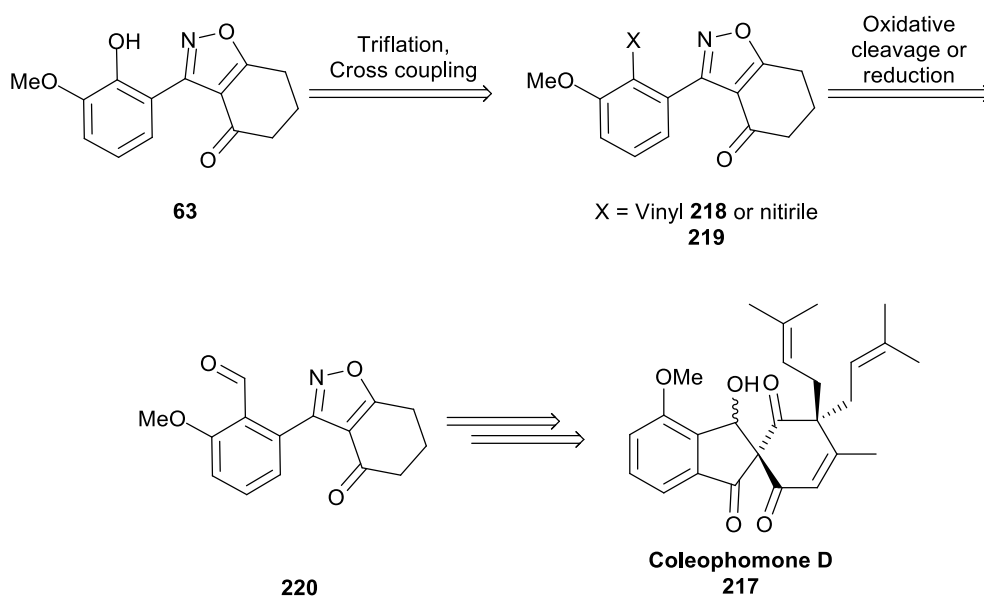


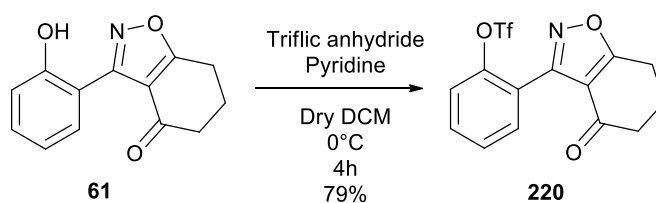
Figure 32

With this precursor in hand, the next step was to determine how we were going to install the aldehyde functionality present in the natural product. Previously we have had some success with metal mediated cross coupling chemistry on this class of compounds, and were hopeful we might apply it here (Scheme 111).



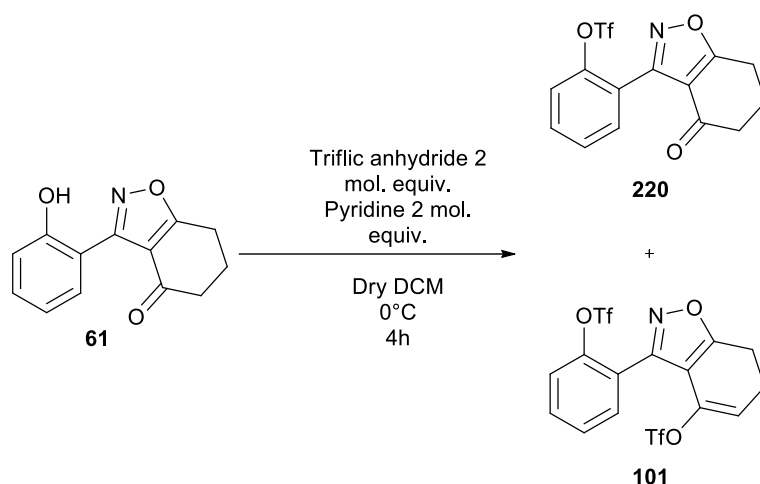
Scheme 111

So going forwards, our first step would be to convert the phenol **63** to the triflate precursor in order to activate it towards metal mediated cross coupling. Following this we would couple it with vinylboronic acid or potassium cyanide, then cleave the alkene or perform a low temperature diisobutylaluminium hydride (DIBAL) reduction of the nitrile to yield the desired aldehyde.¹²¹ As phenolic benzisoxazole **61** was readily available, we used it as a test compound (Scheme 112).



Scheme 112

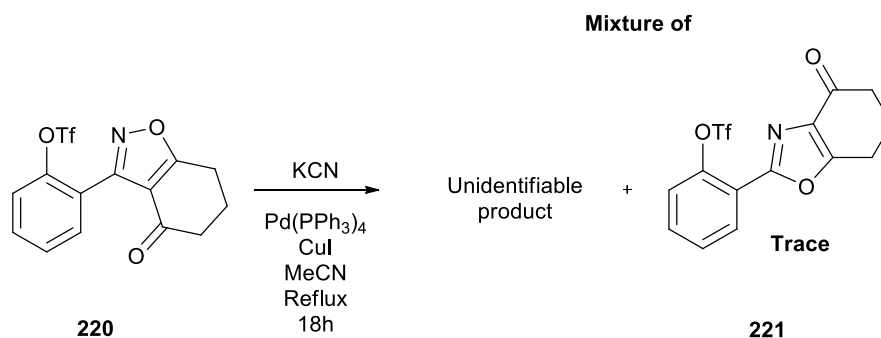
Triflation was very successful, however, it should be noted if multiple equivalents of base and anhydride are used, a mixture of mono- and *bis*-triflated benzisoxazoles **220** and **101** was observed (Scheme 113).



Scheme 113

This result is interesting because again, it suggests that not only is the carbon alpha to the carbonyl reasonably acidic, but the enolate oxygen at least, is reactive towards electrophiles.

With the successful formation of triflated benzoxazole **220**, the next stage was to attempt cyanation (Scheme 114).



Scheme 114

This result was very interesting, as we did not isolate any of the desired cross-coupling product, nor was starting material returned; what we did isolate was an amorphous unidentified product with dimeric features in the ¹H NMR spectra *i.e.* unexplained doubling of the integrals in the ¹H NMR spectra. Upon subjecting this product to crystallization procedures, small crystals of triflated benzoxazole **221** were obtained identified by X-ray structure determination (Figure 33).

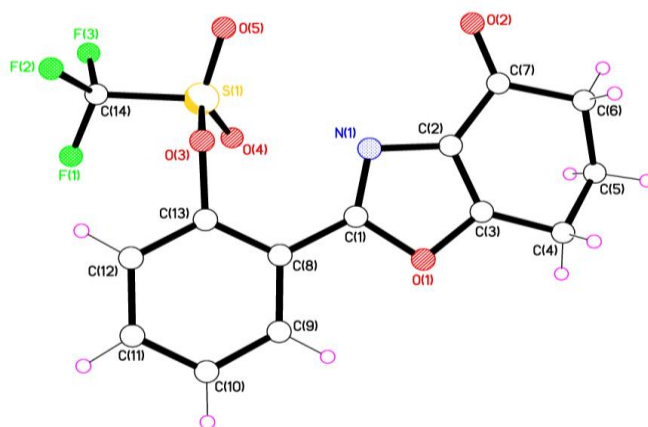
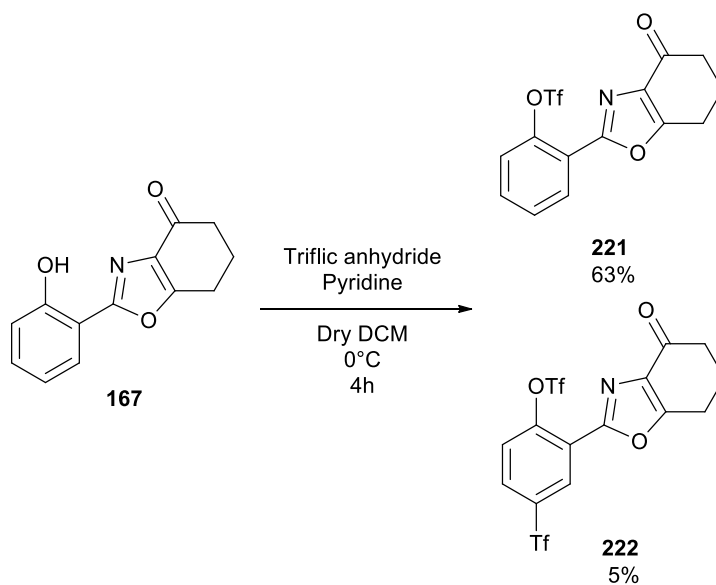


Figure 33. X-Ray crystal structure of 2-(4-Oxo-4,5,6,7-tetrahydrobenzo[d]oxazol-2-yl)phenyl trifluoromethanesulfonate **221**. This crystal structure was solved by Dr Mark Elsegood of Loughborough University.

In order to confirm this result, benzoxazole **167**, available from the rearrangement studies was triflated (Scheme 115).



Scheme 115

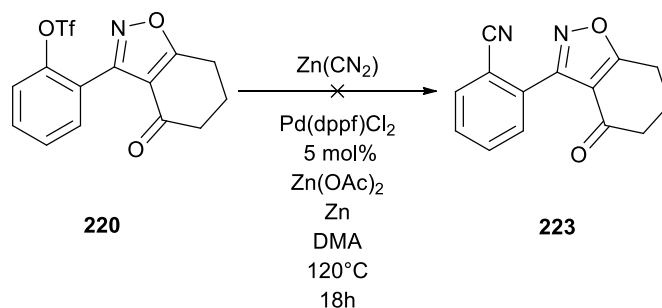
This yielded both the desired triflated benzoxazole **221** and a small amount of electrophilic addition product, *bis*-triflated benzoxazole **222**. Single crystal X-ray crystallography has confirmed that the triflated oxazoles obtained from both reactions are the same. However, the ^1H NMR spectra of the bulk material from the cyanation reaction does not match that of triflated benzoxazole **221**.

Initially we hypothesized that this triflated benzoxazole was a product of rearrangement during triflation, as this takes place under basic conditions. However, there is no evidence of this product in

the ^1H or ^{13}C NMR spectra of triflated benzisoxazole **220**. Another key fact is that the study of the rearrangement in various bases indicated that the rearrangement does not occur with (4-(4-dimethylamino)pyridine)pyridine (DMAP) in refluxing THF, so we can speculate that the same is true at 0°C with pyridine.

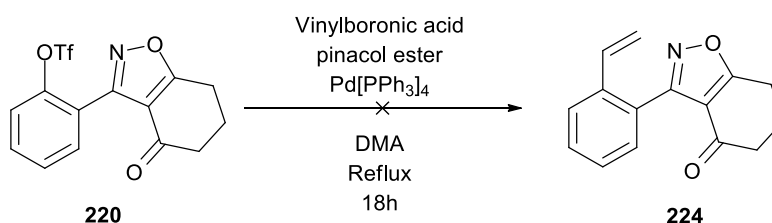
If these data are accurate, then it suggests that the rearrangement is either happening during the cyanation reaction or upon subjection of the amorphous product to crystallization conditions. Currently we are unable to explain how this could occur as it is inconsistent with our proposed mechanism of rearrangement.

Following this result, alternative cyanation conditions, suggested by our industrial collaborator, were attempted (Scheme 116).



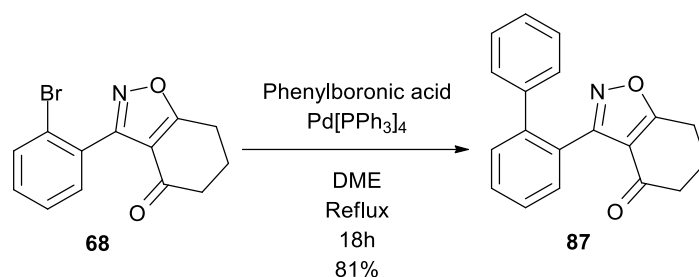
Scheme 116

This attempt failed, but unlike the previous attempt starting material was retained; there was no indication that any rearrangement had taken place. We also attempted to couple triflated benzisoxazole **220** with vinylboronic acid pinacol ester (Scheme 117). This attempt failed and again starting material was retained.



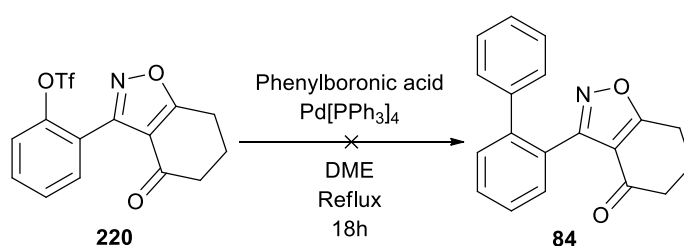
Scheme 117

As mentioned, previously, it has been possible to couple bromobenzisoxazole **68** with phenylboronic acid (Scheme 118).



Scheme 118

It should also be possible to carry out this reaction on triflated benzisoxazole **220** and this was attempted to help determine if the triflate group was incompatible with fused isoxazole functionality (Scheme 119).



Scheme 119

This reaction did not yield the desired product; however, it did yield an unknown compound, with spectral features similar to that displayed by the unknown compound isolated from the initial cylation attempts.

These results seem to indicate that there is a problem with our triflate functionality in the presence of palladium-tetrakis(triphenylphosphine).

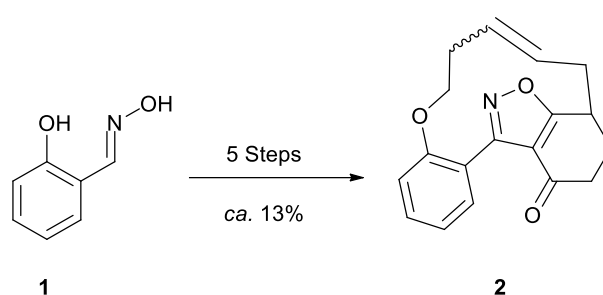
Due to time constraints we were not able to investigate these results any further and we are presently unable to interpret our experimental observations.

3.0 Conclusions and Future Research

This chapter of the thesis will discuss the overall conclusions drawn from each research area of this PhD, as well as any future avenues of investigation that are available.

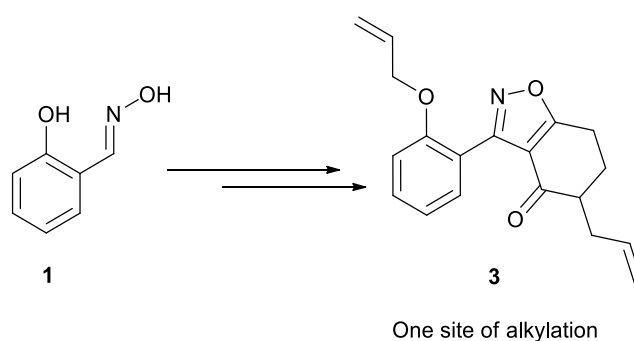
Coleophomones A, B and C

The main objective of this project was to generate macrocyclic structures relating to the coleophomone natural products *via* an isoxazole route. This aim has been achieved in three ways: firstly we have demonstrated that it is possible to synthesize 12-13 membered macrocycles with the isoxazole in place, from commercially available starting materials in 5 steps with an overall yield of approximately 13% (Scheme 1).



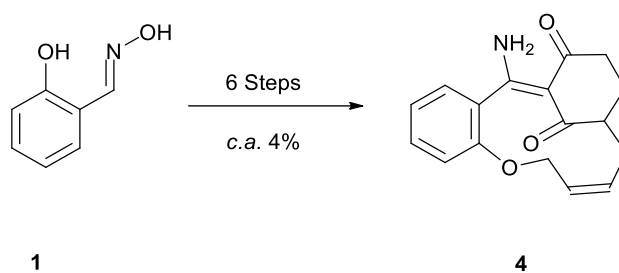
Scheme 1

Secondly we have made significant progress towards generating these macrocycles *via* a regiochemically pure route using hydrazone methodology (Scheme 2)



Scheme 2

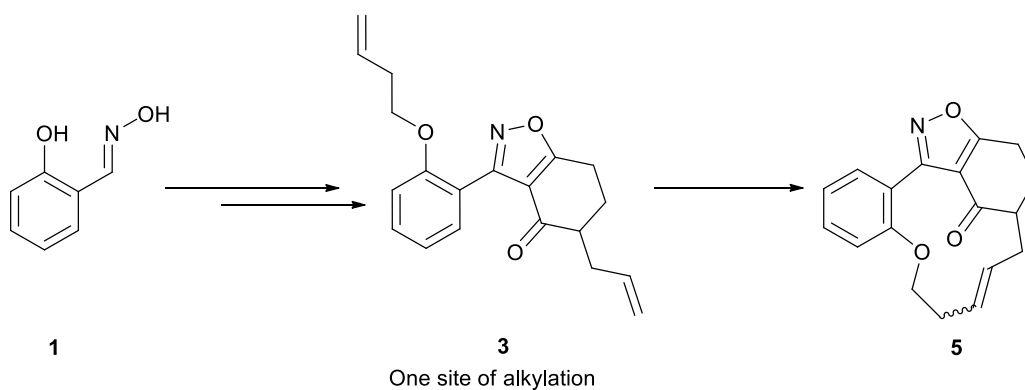
Finally we have demonstrated that if the isoxazole is cleaved then it is possible to generate the 11-membered macrocycle necessary for the natural products over 6 steps in approximately 4% yield (Scheme 3).



Scheme 3

This 11-membered ring is of special interest as it represents a scaffold towards the natural products themselves, and as such, we hope to publish its synthesis.

Many avenues remain open for the continuation of this project. The first is the optimization and continued study of hydrazone route towards regio-chemically pure macrocyclic structures in good yields (Scheme 4).



Scheme 4

Once this has been successfully undertaken then these structures could be further furnished with additional functionality in an effort to afford analogues that are closer to the natural products.

Coleophomone D

Reasonable progress has been made towards the total synthesis of coleophomone D. Efforts towards a core benzisoxazole skeleton for the total synthesis of coleophomone D have met with some problems (Figure 1).

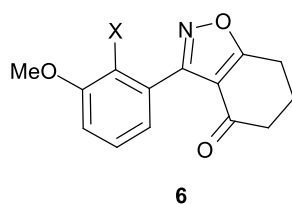
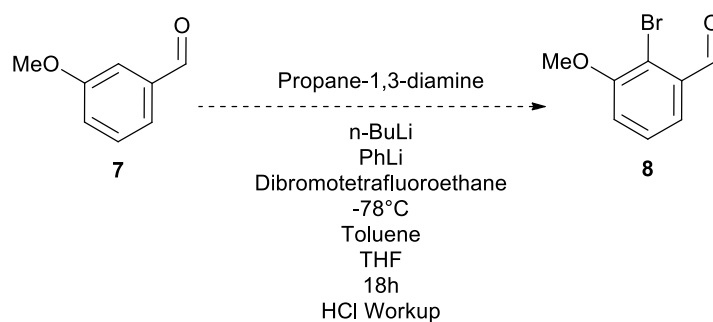


Figure 1

Initially it was believed that it would be possible to use *o*-vanillin as a starting point, then convert the phenol to a triflate and employ metal mediated cross coupling to introduce a route to the requisite aldehyde functionality. However, due to an as yet unknown reaction this has been unsuccessful and as such a new route towards this core structure would be essential for any future investigations.

A potential route for this would be *via* a Meyers type directed lithiation of *m*-anisaldehyde (Scheme 5).¹²²



Scheme 5

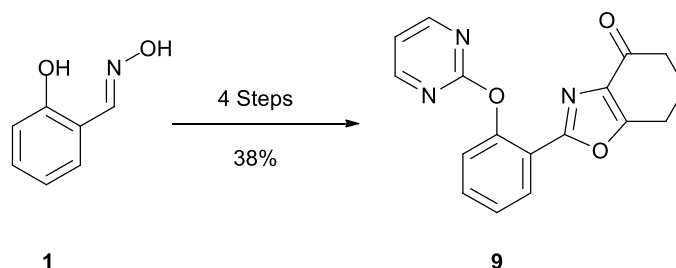
If this were to be successful, then the aldehyde can either be introduced *via* the originally planned metal mediated cross coupling; or the aldehyde could be formed directly *via* metal halogen exchanged followed by a quench with dimethyl formamide.

It should also be noted that allylation investigations carried out in efforts towards the synthesis of coleophomones A, B and C, also apply to D; once initial hurdles have been crossed, it should be possible to readily alkylate the core structure of coleophomone D.

If this were to be successful then established chemistry could be used to furnish the rest of the core structure with the desired functionality, yielding coleophomone D within a few steps.

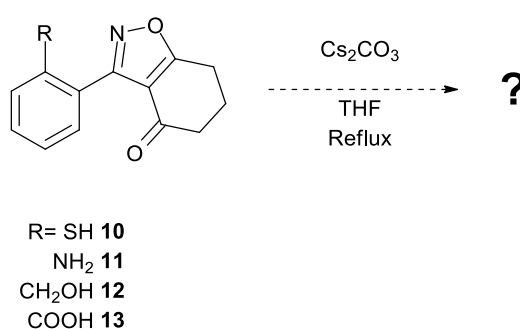
Benzisoxazole to Oxazole Rearrangement

This novel and unexpected rearrangement has proved to be an unexpected, but never the less very interesting diversion from the core aims of the PhD project. Initial investigations into probing the exact nature of this rearrangement have been carried out and accepted for publication in Chemical Communications. Finally, due to this rearrangement it has been possible to readily access a known, biologically active product in 4 steps with a total yield of 38% (Scheme 6).



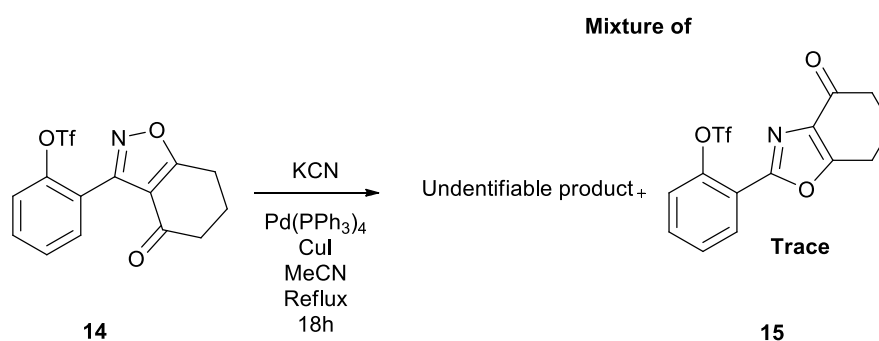
Scheme 6

Future investigations would aim to test the rearrangement with a broader range of examples (scheme 7).



Scheme 7

Another possible route of investigation would be to try and determine the nature of the unknown reaction that is taking place when we attempted to couple triflate **14** with potassium cyanide (Scheme 8).



Scheme 8

If these two routes proved to be successful they would could the basis for future publications in this area.

4.0 Experimental

Compound numbers in this chapter reference to compound numbers in Chapter 2.

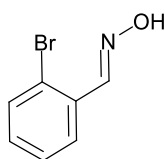
General

Commercially available reagents and solvents were used throughout without further purification, except tetrahydrofuran distilled (THF) (benzophenone/Na) and N-Chlorosuccinimide which was freshly purified by recrystallization from boiling toluene, in accordance to the literature procedure.¹²³ Light petroleum refers to the fraction with bp 40-60°C. Thin layer chromatography was carried out on Merck Kieselgel 60 GF254 aluminium foil backed plates. The plates were visualized under UV light. Flash column chromatography was carried out using Merck Kieselgel 60 H silica or Matrix silica 60, with the eluent specified. IR spectra were recorded using a Perkin Elmer FTIR Spectrometer (Paragon 100) as neat, or solutions using dichloromethane as solvent or using attenuated total reflectance for solids. ¹H, ¹⁹F, ¹⁵N and ¹³C NMR spectra were recorded using a Bruker 400 MHz NMR spectrometer (¹H 400, ¹⁹F 376, 100 MHz ¹³C frequencies respectively), Bruker 500 MHz NMR spectrometer (¹H 500, ¹⁵N 50, ¹³C 125 MHz frequencies respectively), a Bruker 600 MHz NMR spectrometer (¹H 600, ¹³C 150 MHz frequencies respectively) or a JEOL 400 MHz NMR machine (¹H 400, ¹⁹F 376, ¹³C 100 MHz frequencies respectively); chemical shifts are quoted in ppm and coupling constants, *J*, are quoted in Hz; d-Chloroform was used throughout unless otherwise stated. In the ¹³C spectra, signals corresponding to C, CH, CH₂ or CH₃ groups, as assigned from either DEPT or HSQC, are noted. Quaternary carbons were assigned using a combination of NMR techniques including COSY, HSQC and HMBC, unless otherwise stated. Spectra were calibrated to residual solvent peaks. High resolution mass spectra were recorded on a Thermofisher Exactive (Orbi) high resolution mass spectrometer. Melting points were recorded on a Stuart Scientific apparatus and are uncorrected. LCMS were recorded using an Agilent Technologies spectrometer, model G1956B, using a 50 x 2mm Gemini C18 3µm column running at 1.00 mL/minute with acetonitrile:formic acid (99.9:0.1 v/v) as eluent. Unless otherwise stated all air sensitive reactions were carried out under an atmosphere of nitrogen.

General Procedure for Oxime formation

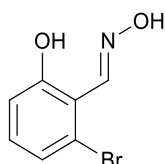
Sodium acetate (4 mMol) was added to a solution of hydroxylamine hydrochloride (2 mMol) and aromatic aldehyde (1 mMol) in ethanol (10 mL) and water (5 mL). The reaction mixture was heated to reflux for 30 minutes and then allowed to cool to room temperature. Following this the reaction mixture was stored in a refrigerator overnight, after which it was filtered to yield the desired oxime. If the oxime did not crystallise out, then the mixture was acidified, and washed with DCM(3 x 10 mL). The organic extracts were washed once with saturated sodium chloride solution (30 mL), dried over magnesium sulfate and concentrated under reduced pressure to yield the desired oxime.

2-Bromobenzaldehyde oxime **12** ¹²⁴



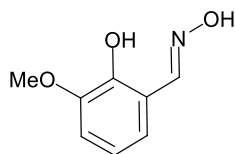
Colourless needles (83%), M.p. 98-100°C lit. 102°C¹²⁴; HRMS(EI+) C₇H₆BrNONa requires 221.9530 [M+Na] found 221.9523 -3.1538 ppm; ν_{\max} (ATR)/cm⁻¹ 945 (NO), 3248 (OH); δ_{H} (400MHz; CDCl₃) 7.22-7.26 (m, H, Ar CH), 7.23-7.34 (m, H, Ar CH) 7.58 (dd, J=1.20, 7.60 Hz, H, Ar CH), 7.81 (dd, J=1.60, 7.60 Hz, Ar CH), 8.37 (broad s, H, NOH), 8.55 (s, H, CH); δ_{C} (100MHz; CDCl₃) 123.9 (Ar C), 127.5 (Ar CH), 127.6 (Ar CH), 131.3 (Ar CH), 131.3 (Ar C), 133.2 (Ar C), 149.9 (C).

2-Bromo-6-hydroxybenzaldehyde oxime **45**



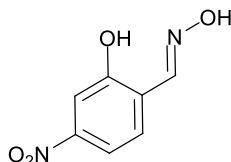
Beige solid (77%) M.p. 149-151°C; MS(EI+) C₇H₆NO₂⁷⁹BrNa requires 237.9480 [M+Na] found 237.9470 - 4.2026 ppm; ν_{\max} (ATR)/cm⁻¹ 974 (N-O), 3391 (OH); δ_{H} (400MHz; CDCl₃) 6.83 (dd, J=2.00 Hz, 8.40 Hz, H, Ar CH), 7.03 (d, J=2.00 Hz, H, Ar CH), 7.64 (d, J=8.40 Hz, H, Ar CH), 8.20 (broad s, H, OH), 10.25 (broad s, H, OH), 11.29 (s, H, CH); δ_{C} (100MHz; CDCl₃) 115.7 (Ar CH), 118.9 (Ar CH), 122.5 (C), 123.0 (C), 127.9 (Ar CH), 146.5 (C), 159.2 (C=NOH).

2-Hydroxy-3-methoxybenzaldehyde oxime 48¹²⁵



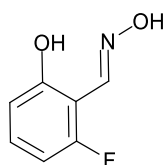
Beige solid (85%), M.p 122-124°C lit. 123°C; HRMS(EI+) $C_7H_6N_2O_4Na$ requires 190.0480 [M+Na] found 190.0475 -2.6309 ppm; ν_{max} (ATR)/ cm^{-1} 3367 (OH); δ_H (400MHz; $CDCl_3$) 3.90 (s, 3H, OCH_3), 6.82 (dd, $J=7.60, 2.00$ Hz, H, Ar CH), 6.86 (t, $J=7.60$, H, Ar CH), 6.91 (dd, $J=7.60, 2.00$, H, Ar CH), 8.23 (broad s, H, OH), 8.23 (s, H, CH), 9.94 (broad s, H, OH); δ_C (100MHz; $CDCl_3$) 56.2 (OCH_3), 113.3 (Ar CH), 116.7 (C), 119.6 (Ar CH), 122.3 (Ar CH), 146.9 (C), 148.2 (C), 152.7 (Ar CH).

2-Hydroxy-4-nitrobenzaldehyde oxime 51



Pale yellow solid (93%), decomposes 210-212°C; HRMS(EI+) $C_7H_6N_2O_4Na$ requires 205.0225 [M+Na] found 205.0218 -3.4143 ppm; ν_{max} (ATR)/ cm^{-1} 949 (NO), 1336 (NO), 1620 (C=N), 3290 (OH); δ_H (400MHz; d_6 -DMSO) 7.15 (d, $J=8.80$ Hz, H, Ar CH), 8.10 (dd, $J=8.80, 3.00$, H, Ar CH), 8.33 (s, H, CH), 8.41 (d, $J=3.00$ Hz, H, Ar CH), 11.70 (broad s, 2H, 2 x OH); δ_C (100MHz; d_6 -DMSO) 116.6 (Ar CH), 119.4 (Ar C), 122.2 (Ar CH), 125.6 (Ar CH), 139.6 (Ar C), 144.0 (Ar CH), 161.6 (C).

2-Fluoro-6-hydroxybenzaldehyde oxime 53



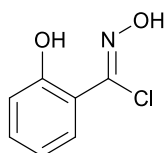
Brown solid (90%), M.p. 114-116°C; HRMS(EI+) C_7H_7FNO requires 156.0455 [M+H] found 156.0454 - 1.0700 ppm; ν_{max} (ATR)/ cm^{-1} 970 (NO), 1628 (C=N), 3374 (OH); δ_H (400MHz; d_6 -DMSO) 6.87 (td, $J=8.00, 4.80$ Hz, H, Ar CH), 7.19-7.25 (m, H, Ar CH), 7.32 (d, $J=6.80$ Hz, H, Ar CH), 8.38 (s, H, CH), 10.31 (broad s, H, OH) 11.58 (broad s, H, OH); δ_C (100MHz; d_6 -DMSO) 117.4 (d, $J=18.0$ Hz C-F, Ar CH), 120.2 (d, $J=7.00$ (C-F), Ar CH), 121.9 (d, $J=4.00$ C-F, Ar C), 124.0 (d, $J=3.00$ Hz C-F, Ar CH), 144.5 (d, $J=14.0$ Hz C-F, Ar C), 147.8 (d, $J=4.00$ Hz C-F, Ar CH), 151.5 (d, $J=239$ Hz, Ar C-F).

General Procedure for imidoyl chloride formation

Oxime (2 mMol) and freshly purified N-chlorosuccinimide (2.2 mMol) were dissolved in chloroform (20 ml), followed by addition of anhydrous pyridine (0.2 mMol). The reaction mixture was heated to 40°C and stirred for 18 hours under an atmosphere of nitrogen unless otherwise stated. The reaction mixture was allowed to cool to room temperature and the washed with water (2 x 20 mL) and with brine (20 mL). The organic extracts were then dried over sodium sulfate, filtered and concentrated under reduced pressure to yield the crude imidoyl chloride which was used with no further purification.

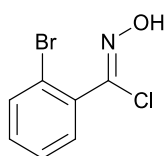
Note: This series of imidoyl chloride are not stable, even when stored under an atmosphere of nitrogen and should be used within 2 days.

2-Hydroxyphenylhydroximdoyl chloride **14**³⁰



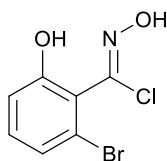
Orange solid 99%; ν_{\max} (ATR)/ cm^{-1} 651 (C-Cl), 941 (NO), 3293 (OH); δ_{H} (400MHz; CDCl_3) 6.96-7.02 (m, 2H, 2 x Ar CH), 7.33-7.37 (m, H, Ar CH), 7.81-7.83 (dd, $J=1.59, 8.00$ Hz, H, Ar CH), 8.40 (broad, H, NOH), 10.07 (s, H, Ar OH); δ_{C} (100MHz; CDCl_3) 115.7 (C) 117.1 (Ar CH), 119.8 (Ar CH), 129.4 (Ar CH), 132.3 (Ar CH) 156.4 (C), 171.4 (C). This compound was not of sufficient purity to obtain an accurate melting point and was unstable to mass spectrometry conditions. The spectra reported above are in agreement with the literature data.³⁰

2-Bromo-N-hydroxybenzimidoyl chloride **15**¹²⁶



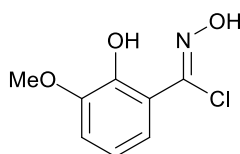
Yellow oil (94%); ν_{\max} (neat)/ cm^{-1} 757 (C-Cl), 937 (NO), 3338 (OH); δ_{H} (400MHz; CDCl_3) 7.26-7.30 (m, H, Ar CH), 7.33-7.35 (m, H, Ar CH), 7.42-7.44 (m, H, Ar CH), 7.60-7.62 (dd, $J=1.20, 8.00$ Hz, H, Ar CH), 9.40 (broad, H, NOH); δ_{C} (100MHz; CDCl_3) 122.2 (C), 127.5 (Ar CH), 131.2 (Ar CH), 131.6 (Ar CH), 133.5 (Ar CH), 135.6 (C), 172.0 (C). This compound was not of sufficient purity to obtain an accurate melting point and was unstable to mass spectrometry conditions. The data reported above is in good agreement with the literature data.¹²⁶

2-Bromo-N,6-dihydroxybenzimidoyl chloride 46



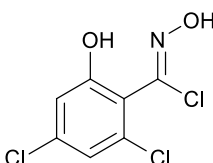
Beige solid (62%); δ_{H} (400MHz; CDCl_3) 6.85-6.87 (dd, $J=2.40, 8.40$ Hz, H, Ar CH), 7.10-7.11 (d, $J=2.40$ Hz, H, Ar CH), 7.33-7.57 (d, $J=8.40$ Hz, H, Ar CH), 11.50 (broad s, H, Ar OH), 12.31 (s, H, NOH). This compound was not of sufficient purity to obtain an accurate melting point and was unstable to mass spectrometry conditions.

N,2-Dihydroxy-3-methoxybenzimidoyl chloride 49



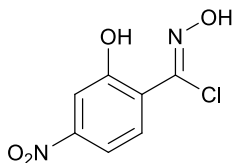
Reaction time: 3.5 days. Brown solid 83% m.p. 143-146°C; ν_{max} (DCM)/ cm^{-1} 3691 (OH); δ_{H} (400MHz; CDCl_3) 3.91 (s, 3H, OCH_3), 6.83-6.93 (m, 2H, 2 x Ar CH), 7.41 (d, $J=7.20$ Hz, H, Ar CH), 7.99 (broad s, H, NOH), 10.05 (broad, H, OH); δ_{C} (100MHz; CDCl_3) 56.2 (OCH_3), 114.1 (Ar CH), 116.1 (C), 119.3 (Ar CH), 121.0 (Ar CH), 142.2 (C), 146.5 (C), 158.2 (C). This compound was not of sufficient purity to obtain an accurate melting point and was unstable to mass spectrometry conditions.

2,4-Dichloro-N,6-dihydroxybenzimidoyl chloride 50



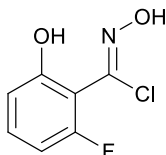
Brown solid (88%), δ_{H} (400MHz; d_6 -DMSO) 7.56 (d, $J=2.56$ Hz, H, Ar CH), 7.77 (d, $J=2.56$ Hz, H, Ar CH), 10.80 (broad s, H, OH), 12.96 (broad s, H, OH); δ_{C} (100MHz; d_6 -DMSO) 120.9 (C), 122.3 (C), 123.1 (C), 127.4 (Ar CH), 130.9 (Ar CH), 134.6 (C), 150.5 (C). This compound was not of sufficient purity to obtain an accurate melting point and was unstable to mass spectrometry conditions.

N,2-Dihydroxy-4-nitrobenzimidoyl chloride 52



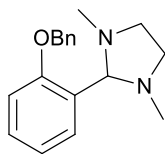
Yellow solid 96%; (400MHz; d_6 -DMSO) 7.18 (d, $J=8.00$ Hz, H, Ar CH), 8.24-8.30 (m, 2H, 2 x Ar CH), 11.72 (broad s, H, OH), 12.64 (broad s, H, OH); δ_c (100MHz; d_6 -DMSO) 117.6 (Ar CH), 120.9 (C), 126.5 (Ar CH), 127.7 (Ar CH), 132.7 (C), 139.7 (C), 162.2 (C). This compound was not of sufficient purity to obtain an accurate melting point and was unstable to mass spectrometry conditions.

2-Fluoro-N,6-dihydroxybenzimidoyl chloride 54



Brown solid 81%; ν_{max} (DCM)/ cm^{-1} 3691 (OH); δ_H (400MHz; $CDCl_3$) 6.76-6.79 (m, H, Ar CH), 7.08-7.15 (m, H, Ar CH), 7.19-7.24 (m, H, Ar CH). This compound was not of sufficient purity to obtain an accurate melting point and was unstable to mass spectrometry conditions. This compound decomposed rapidly and should be used immediately.

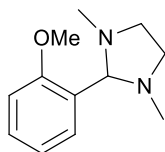
2-(2-(Benzyloxy)phenyl)-1,3-dimethylimidazolidine **25**



2-(Benzyloxy)benzaldehyde (3.00 g, 2.26 ml, 14.2 mMol) and *N,N'*-dimethylethylenediamine (1.48 g, 1.79 ml, 16.8 mMol) in ethanol (100 ml) was stirred at room temperature for 12 hours. Magnesium sulfate (4.50 g) was added, and the resulting mixture was stirred for a further 15 min. The reaction mixture was filtered and washed with diethyl ether and the solvent was removed under reduced pressure to yield the product 2-(2-(benzyloxy)phenyl)-1,3-dimethylimidazolidine **25** (2.90 g, 70 %) as a yellow solid.

M.p 84-86°C; MS(EI+) $C_{18}H_{23}ON_2$ requires 283.1810 [M+H] found 283.1800 -3.5313 ppm; ν_{max} (ATR)/ cm^{-1} 2946 (CH); δ_H (400MHz; $CDCl_3$) 2.21 (s, 6H, 2 x CH_3), 2.57-2.60 (m, 2H, 2 x CH), 3.35-3.37 (m, 2H, 2 x CH), 4.14 (s, H, NCHN), 5.08 (s, 2H, $ArOCH_2$), 6.94 (dd, $J=0.80, 8.40$ Hz, H, Ar CH), 7.03 (t, $J=7.60$ Hz, H, Ar CH), 7.22-7.25 (m, H, Ar CH), 7.32-7.45 (m, 5H, 5 x Ar CH), 7.72 (dd, $J=1.56, 7.60$ Hz, H, Ar CH); δ_C (100MHz; $CDCl_3$) 39.8 (2 x NCH_3), 53.5 (2 x NCH_2), 70.2 ($ArOCH_2$), 82.8 (NCHN), 111.8 (Ar CH), 121.5 (Ar CH), 127.2 (2 x Ar CH), 127.8 (Ar CH), 128.1 (Ar C), 128.5 (2 x Ar CH), 128.9 (Ar CH), 129.5 (Ar CH), 137.3 (Ar C), 158.0 (Ar CO).

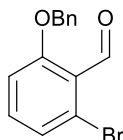
2-(2-Methoxyphenyl)-1,3-dimethylimidazolidine **28** ⁷⁷



2-Methoxybenzaldehyde (3.00 g, 22.0 mMol) and *N,N'*-dimethylethylenediamine (2.33 g, 26.4 mMol) in ethanol (100 ml) was stirred at room temperature overnight. Magnesium sulfate (4.50 g) was added, and the resulting mixture was stirred for a further 15 min. The reaction mixture was filtered and washed with diethyl ether and the solvent was removed under reduced pressure to yield the product 2-(2-methoxyphenyl)-1,3-dimethylimidazolidine **28** (3.28 g, 95%) as a yellow solid.

Mp: 46-48°C lit. 41-42°C⁷⁷; $C_{12}H_{18}ON_2Na$ requires 229.1317 [M+Na] found 229.1308 -3.9279; ν_{max} (ATR)/ cm^{-1} 2939 (CH); δ_H (400MHz; $CDCl_3$) 2.20 (s, 6H, 2 x CH_3), 2.59-2.63 (m, 2H, 2 x CH), 3.33-3.46 (m, 2H, 2 x CH), 3.82 (s, 3H, OCH_3), 4.06 (s, H, NCHN), 6.87-6.89 (s, 2H, OCH_2), 6.88 (dd, $J=0.80$, 8.40 Hz, H, Ar CH), 7.01 (dd, $J=0.80$, 8.00 Hz, H, Ar CH), 7.24-7.27 (m, H, Ar CH), 7.67 (dd, $J=2.00$, 7.60 Hz, H, Ar CH); δ_C (100MHz; $CDCl_3$) 39.7 (2 x NCH_3), 53.5 (2 x NCH_2), 55.5 ($ArOCH_3$), 82.8 (NCHN), 110.4 (Ar CH), 121.1 (Ar CH), 127.6 (Ar C), 128.9 (Ar CH), 129.3 (Ar CH), 158.9 (Ar CO). The 1H and ^{13}C data reported above are in good agreement with those reported in the literature.⁷⁷

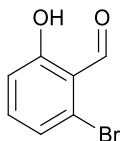
2-(Benzyloxy)-6-bromobenzaldehyde **26**¹²⁷



Benzyl alcohol (0.160 g, 0.160 ml, 1.65 mMol) was added to a suspension of sodium hydride (0.660 g 1.65 mMol) in anhydrous DMF (25 mL) and allowed to stir for 15 min. 2-Bromo-6-fluorobenzaldehyde **30** (0.300 g, 1.47 mMol) was added and the reaction mixture was left to stir under an atmosphere of nitrogen for 4 hours. Following this the reaction mixture was diluted with water (25 mL) and extracted with diethyl ether (3 x 25 mL). The combined organic extracts were then washed with water (2 x 25 mL) and brine (1 x 25 mL), dried over sodium sulfate and concentrated under reduced pressure. The crude product was purified by flash column chromatography using light petroleum:ethyl acetate (97.5:2.5 v/v) to yield 2-(benzyloxy)-6-bromobenzaldehyde **26** as a yellow solid (0.10 g, 23%).

Mp: 56-60°C lit. 54-56°C¹²⁸; MS(EI+) C₁₄H₁₁O₂⁷⁹BrNa; requires 312.9840 [M+Na] found 312.9830 - 3.1951 ppm; ν_{\max} (ATR)/cm⁻¹ 1688 (C=O), 2880 (CH); δ_{H} (400MHz; CDCl₃) 5.18 (s, 2H, OCH₂), 6.99 (dd, J=1.60, 8.00 Hz, H, Ar CH), 7.23-7.45 (m, 9H, 9 x Ar CH), 10.48 (s, H, CHO); δ_{C} (100MHz; CDCl₃) 70.9 (OCH₂), 115.5 (Ar C), 124.0 (Ar CH), 124.3(Ar CH), 126.9 (Ar CH), 127.1 (2 x Ar CH), 128.0 (Ar CH), 128.7 (2 x Ar CH), 161.2 (Ar CO), 190.1 (Ar CHO). The data reported above is in agreement with that reported in the literature.¹²⁸

2-Bromo-6-hydroxybenzaldehyde **44**¹²⁸



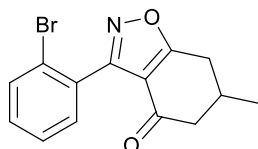
3-Bromophenol (5.50 g, 32.0 mmol) was added to a solution of sodium hydroxide (10.24 g, 256 mmol) in water (200 ml) and heated to 75°C. Chloroform (11.45 g, 7.70 mL, 96.0 mmol) was added drop wise over 45 minutes. The mixture was heated at 75°C until signs of chloroform reflux were no longer observed. The orange-brown suspension was then cooled to 0°C and acidified with 2M hydrochloric acid. The reaction mixture was then extracted with ethyl acetate (3 x 100 mL) and the combined organic extracts were washed with water (2 x 100 mL) and brine (1 x 100 mL), dried with sodium sulfate and concentrated under reduced pressure. The crude product was then purified by flash column chromatography using light petroleum:ethyl acetate (92.5:7.5 v/v) as eluent to yield 2-bromo-6-hydroxybenzaldehyde **44** as a brown solid (3.57 g, 56%).

M.p. 49-51°C lit. 50-52°C¹²⁹; ν_{\max} (ATR)/cm⁻¹ 1645 (C=O), 3081 (OH); MS(EI+) C₇H₅O₂⁷⁹BrNa; requires 222.9371 [M+Na] found 222.9360 -4.9341 ppm; δ_{H} (400MHz; CDCl₃) 6.92-6.95 (dd, J=2.40, 8.80 Hz, H, Ar CH), 7.11-7.12 (d, J=2.40 Hz, H, Ar CH), 7.74-7.77 (d, J=8.80 Hz, H, Ar CH), 10.03 (s, H, CHO), 11.10 (broad s, H, Ar OH); δ_{C} (100MHz; CDCl₃) 115.6 (Ar CH), 119.8 (Ar CH), 125.0 (Ar C), 127.8 (Ar C), 131.9 (Ar CH), 163.6 (Ar OH), 189.7 (Ar CHO). The data reported above is in agreement with that reported in the literature.¹²⁸

General Procedure for Benzisoxazole formation

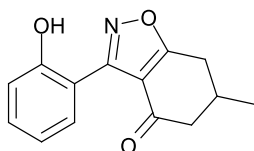
Sodium isopropoxide (2 mMol) was added to a solution of dione (2 mMol) in isopropyl alcohol (10 mL) at room temperature and left to stir for 10 minutes. Afterwards this solution was added very slowly to a solution of benzimidoyl chloride (1mMol) in isopropyl alcohol (10 mL) at 0°C and left to stir for 4 hours at room temperature under an atmosphere of nitrogen. Following this, the reaction mixture was concentrated under reduced pressure. The crude mixture was then dissolved in either ethyl acetate or dichloromethane (20 mL) and washed twice with water (20 mL) and once with saturated sodium chloride solution (20 mL), dried over magnesium sulfate and concentrated under reduced pressure to yield crude benzisoxazole. This was used without purification, recrystallized from a mixture of ethyl acetate and light petroleum or purified *via* column chromatography using light petroleum: ethyl acetate (1:1 v/v) as a eluent.

3-(2-Bromophenyl)-6-methyl-6,7-dihydrobenzo[d]isoxazol-4(5H)-one 4



Brown solid (28%) Mp 68-71°C; HRMS(EI+) $C_{14}H_{12}NO_2^{79}BrNa$; requires 327.9950 [M+Na], found 313.9782 -3.6586 ppm; ν_{max} (ATR)/ cm^{-1} 1682 (C=O), 2962 (C-H); δ_H (400MHz; $CDCl_3$) 1.14-1.16 (d, J=6.40 Hz, 3H, CH_3), 2.23-2.28 (m, 1H, CH), 2.49-2.54 (m, 2H, 2 x CH), 2.62-2.69 (dd, J=10.00, 17.60 Hz, 1H, CHH), 3.09-3.15 (dd, J=4.80, 17.60Hz, 1H, CH_2), 7.24-7.33 (m, 3H, 3 x Ar H), 7.59-7.61 (m, 1H, Ar H); δ_C (100MHz; $CDCl_3$) 28.4 (CH_3), 35.5 (CH), 37.0 (CH_2), 52.5 (CH_2), 114.4 (C), 123.4 (Ar C), 127.2 (Ar CH), 129.1 (Ar C), 131.2 (Ar CH), 131.3 (Ar CH), 133.0 (Ar CH), 159.2 (C), 180.5 (C), 190.0 (C).

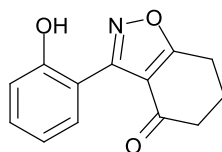
3-(2-Hydroxyphenyl)-6-methyl-6,7-dihydrobenzo[d]isoxazol-4(5H)-one 5



Pale yellow solid (83%) M.p. 121-122°C; HRMS(EI+) $C_{14}H_{13}NO_3Na$; requires 266.0793 [M+Na] found 266.0782, -4.1341 ppm; ν_{max} (ATR)/ cm^{-1} 1689 (C=O), 3078 (OH); δ_H (400MHz; $CDCl_3$) 1.24-1.26 (d, J=6.80 Hz, 3H, CH_3), 2.38-2.42 (m, H, CH), 2.45-2.59 (m, H, CH), 2.70-2.76 (m, 2H, CH_2), 3.20-3.26 (dd, J=5.12, 17.20Hz, H, CH), 6.99-7.08 (m, 2H, 2 x Ar CH), 7.35-7.41 (m, H, Ar CH), 8.62-8.65 (dd, J=2.00, 8.00 Hz, H, Ar CH), 9.49 (s, H, Ar OH); δ_C (100MHz; $CDCl_3$) 20.7 (CH_3), 29.9 (CH), 31.1 (CH_2), 47.4 (CH_2),

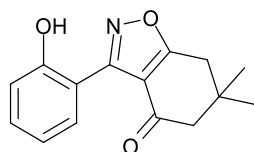
112.8 (C), 114.6 (C), 116.8 (Ar CH), 117.5 (Ar CH), 119.8 (Ar CH), 131.9 (Ar CH), 132.5 (Ar CH), 156.6 (C), 159.5 (C), 181.5 (C), 191.7 (C).

3-(2-Hydroxyphenyl)-6,7-dihydrobenzo[d]isoxazol-4(5H)-one 61³⁰



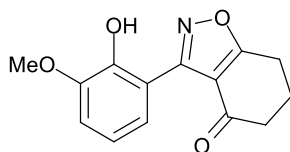
Pale yellow solid (94%), M.p. 108-110°C lit. 107-110°C³⁰; HRMS(EI+) C₁₃H₁₁NO₃Na; requires 252.0637 [M+Na] found 252.0623, -5.5541 ppm; ν_{\max} (ATR)/cm⁻¹ 1679 (C=O), 3136 (OH); δ_{H} (400MHz; CDCl₃) 2.28 (dt, J=6.40, 12.40 Hz, 2H, CH₂), 2.67 (t, J=6.40 Hz, 2H, OCCH₂), 3.10 (t, 2H, J=12.40 Hz, O=CCH₂), 7.01-7.08 (m, 2H, 2 x Ar CH), 7.36-7.41 (m, H, Ar CH,) 8.60 (dd, J=1.60, 8.00 Hz, H, Ar CH); δ_{C} (100MHz; CDCl₃) 21.6 (CH₂), 23.4 (CH₂), 39 (CH₂), 112.9 (C), 114.8 (C), 117.5 (Ar CH), 119.9 (Ar CH), 131.9 (Ar CH), 132.5 (Ar CH), 156.6 (C), 159.5 (C), 181.6 (C), 192.2 (C). The data reported above is in good agreement with the literature data.³⁰

3-(2-Hydroxyphenyl)-6,6-dimethyl-6,7-dihydrobenzo[d]isoxazol-4(5H)-one 62



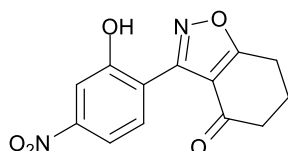
Clear crystals (78%) M.p. 111-113°C; HRMS(EI+) C₁₅H₁₅NO₃Na requires 280.0950 [M+Na]found 280.0946, -1.0711 ppm; ν_{\max} (ATR)/cm⁻¹ 1685 (C=O), 3103 (OH); δ_{H} (400MHz; CDCl₃) 1.25 (s, 6H, 2 x CH₃), 2.58 (s, 2H, OCCH₂), 2.98 (s, 2H, O=CCH₂), 7.04-7.12 (m, 2H, 2 x Ar CH), 7.39-7.43 (m, H, Ar CH,) 8.67-8.69 (dd, J=1.60, 8.00 Hz, H, Ar CH); δ_{C} (100MHz; CDCl₃) 28.1 (2 x CH₃), 34.8 (C), 36.9 (CH₂), 53.5 (CH₂), 112.8 (C), 113.8 (C), 117.5 (Ar CH), 119.8 (Ar CH), 131.9 (Ar CH), 132.5 (Ar CH), 156.7 (C), 159.5 (C), 181.1 (C), 191.5 (C).

3-(2-Hydroxy-3-methoxyphenyl)-6,7-dihydrobenzo[d]isoxazol-4(5H)-one 63



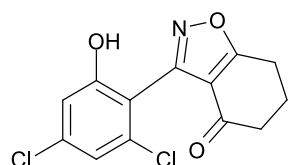
Beige solid (50%) M.p. 112-114°C; HRMS(EI+) $C_{14}H_{13}NO_4Na$ requires 282.0742 [M+Na] found 282.0732 -3.5452 ppm; ν_{max} (DCM)/ cm^{-1} 1692 (C=O), 3521 (OH); δ_H (400MHz; $CDCl_3$) 2.29-2.32 (m, 2H, CH_2), 2.66 (t, J=6.0 Hz, 2H, $OCCH_2$), 3.13 (t, J=6.4 Hz, 2H, $O=CCH_2$), 3.95 (s, 3H, OCH_3), 6.99-7.03 (m, 2H, 2 x Ar CH) 7.88 (d, J=6.00, H, Ar CH), 8.55 (broad s, H, Ar OH); δ_C (100MHz; $CDCl_3$) 21.7 (CH_2), 23.3 (CH_2), 38.7 (CH_2), 56.1 (OCH_3), 113.6 (C), 113.8 (Ar CH), 114.97 (C), 119.6 (Ar CH), 123.2 (Ar CH), 145.9 (C), 148.2 (C), 158.6 (C), 181.6 (C), 192.2 (C).

3-(2-Hydroxy-4-nitrophenyl)-6,7-dihydrobenzo[d]isoxazol-4(5H)-one 64



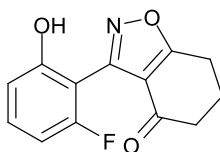
Pale yellow solid (23%) M.p. 159-161°C; HRMS(EI+) $C_{13}H_{11}N_2O_5$ requires 275.0668 [M+H], found 275.0659 -3.2719 pmm; ν_{max} (DCM)/ cm^{-1} 1342 (NO_2), 1691 (C=O), 3689 (OH); δ_H (400MHz; $CDCl_3$) 2.33-2.40 (m, 2H, CH_2), 2.77 (t, J=6.0 Hz, 2H, $OCCH_2$), 3.19 (t, J=6.4 Hz, 2H, $O=CCH_2$), 7.17 (d, J=8.80 Hz, H, Ar CH), 8.30 (dd, J=2.80, 8.80 Hz, H, Ar CH,) 10.01 (d, J=2.80 Hz, H, Ar CH), 10.50 (broad s, H, Ar OH); δ_C (100MHz; $CDCl_3$) 21.6 (CH_2) 23.3 (CH_2), 38.8 (CH_2), 112.6 (C), 113.5 (C), 118.1 (Ar CH), 127.8 (Ar CH), 128.9 (Ar CH), 139.8 (C), 158.7 (C), 162.1 (C), 182.1 (C), 192.8 (C).

3-(3,5-Dichloro-2-hydroxyphenyl)-6,7-dihydrobenzo[d]isoxazol-4(5H)-one 65



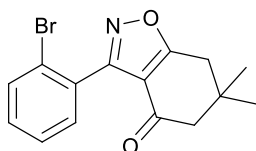
Brown solid (19%) decomposes 133-135°C; ν_{max} (DCM)/ cm^{-1} 1692 (C=O), 3690 (OH); δ_H (400MHz; d_6 -DMSO) 2.16-2.19 (m, 2H, CH_2), 2.47-2.52 (m, 2H, $OCCH_2$), 3.14 (t, J=6.00 Hz, 2H, $O=CCH_2$), 7.41 (d, J=2.40 Hz, H, Ar CH), 7.71 (d, J=2.40, Ar CH,) 10.08 (broad s, H, Ar OH); δ_C (100MHz; $CDCl_3$) 21.6 (CH_2), 23.4 (CH_2), 38.9 (CH_2), 114.7 (C), 115.8 (C), 123.1 (C), 124.6 (Ar CH), 130.0 (Ar CH), 132.4 (Ar CH), 151.4 (C), 158.3 (C), 182.1 (C), 192.4 (C). This compound did not ionize under the mass spectrometry conditions.

3-(2-Fluoro-6-hydroxyphenyl)-6,7-dihydrobenzo[d]isoxazol-4(5H)-one 66



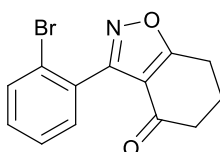
White crystals (47%) M.p. 133-135°C; HRMS(EI+) $C_{13}H_{11}NO_3F$ requires 248.0723 [M+H], found 248.0716 -2.8218 ppm; ν_{max} (DCM)/ cm^{-1} 1692 (C=O), 3690(OH); δ_H (400MHz; $CDCl_3$) 2.32 (quin, J=6.40 Hz, 2H, CH_2), 2.70 (t, J=6.40 Hz, 2H, $OCCH_2$), 3.15 (t, J=6.40 Hz, 2H, $O=CCH_2$), 6.85 (td, J= 8.40, 5.20 Hz, H, Ar CH), 7.21-7.26 (m, Ar CH,) 8.39 (dt, J=8.00, 1.6 Hz, H, Ar CH), 9.49 (broad s, H, Ar OH); δ_C (100MHz; $CDCl_3$) 21.6 (CH_2), 23.3 (CH_2), 38.9 (CH_2), 114.9 (C), 115.3 (d, J=3 Hz C-F, Ar C), 118.7 (d, J=18 Hz C-F, Ar CH), 119.6 (d, J=7 Hz C-F, Ar CH), 126.9 (d, J= 4Hz C-F, Ar CH), 145.2 (d, J=13 Hz C-F, Ar C), 152.1 (d, J=240 Hz C-F, Ar CF), 158.1 (d, J=3 Hz C-F, Ar C) 181.9 (C), 192.4 (C).

3-(2-Bromophenyl)-6,6-dimethyl-6,7-dihydrobenzo[d]isoxazol-4(5H)-one 67



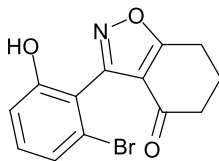
Orange solid (36%) Mp 177-179°C; HRMS(EI+) $C_{15}H_{14}NO_2^{79}BrNa$; requires 342.0105 [M+Na], found 313.9782 -2.9239 ppm; ν_{max} (ATR)/ cm^{-1} 1606 (C=O), 2956 (C-H); δ_H (400MHz; $CDCl_3$) 1.20 (s, 6H, 2 x CH_3), 2.43 (s, 2H, CH_2), 2.95 (s, 2H, CH_2), 7.34-7.42 (m, 3H, 3 x Ar-H), 7.68-7.70 (dd, J=0.80, 7.60 Hz, 1H, Ar H); δ_C (100MHz; $CDCl_3$) 28.4 (2x CH_3), 31.4 (C), 37.0 (CH_2), 52.5 ($O=CCH_2$) 114.4 (C), 123.4 (C), 127.2 (Ar CH), 129.1 (Ar C), 131.1 (Ar CH), 131.3 (Ar CH), 133.0 (Ar CH), 159.2 (C), 180.5 (C), 190.8(C).

3-(2-Bromophenyl)-6,7-dihydrobenzo[d]isoxazol-4(5H)-one 68³⁰



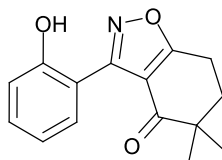
Brown solid (68%) Mp 78-82°C lit. 99°C³⁰; HRMS(EI+) $C_{13}H_{10}NO_2^{79}BrNa$; requires 313.9793 [M+Na], found 313.9782 -3.5034 ppm; ν_{max} (ATR)/ cm^{-1} 1684 (C=O), 2984 (C-H); δ_H (400MHz; $CDCl_3$) 2.29-2.31 (quintet, J=6.00 Hz, 2H, CH_2), 2.53-2.57 (m, 2H, $OCCH_2$), 3.08-3.12 (t, J=6.00 Hz, 2H, $O=CCH_2$), 7.32-7.41 (m, 3H, 3 x Ar-H), 7.67 (m, 1H, Ar H); δ_C (100MHz; $CDCl_3$) 20.8 (CH_3), 22.2 (CH_2), 23.1 (CH_2), 38.1 (CH_2), 115.3 (C), 123.3 (C), 129.1 (Ar C), 131.2 (Ar CH), 131.2 (Ar CH), 133.0 (Ar CH), 159.3 (C), 180.1 (C), 191.3(C). The 1H and ^{13}C spectra are in good agreement with literature data.³⁰

3-(2-Bromo-6-hydroxyphenyl)-6,7-dihydrobenzo[d]isoxazol-4(5H)-one 69



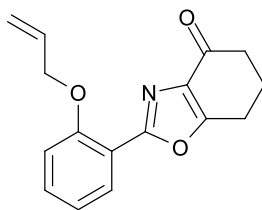
Orange solid (16%) sublimes 157°C; MS(EI+) found 329.9726 [M+Na], $C_{13}H_{10}NO_3^{79}BrNa$; requires 329.9736 [M+Na]; ν_{max} (ATR)/ cm^{-1} 1672 (C=O), 2957 (C-H) and 3216 (OH); δ_H (400MHz; d_6 -DMSO) 2.15-2.18 (m, 2H, CH_2), 2.45-2.50 (m, 2H, $OCCH_2$), 3.10-3.14 (m, 2H, $O=CCH_2$), 6.85-6.89 (dd, $J=2.40, 8.00$ Hz, 1H, Ar-H), 7.13 (d, $J=2.40$ Hz, 1H, Ar H), 7.26-7.29 (d, $J=8.00$ Hz, 1H, Ar H); δ_C (100MHz; d_6 -DMSO) 21.7 (CH_2), 22.6 (CH_2), 37.6 ($O=CCH_2$), 114.5 (C), 119.1 (Ar C), 119.3 (Ar CH), 122.9 (Ar CH), 132.2 (Ar CH), 158.6 (C), 159.5 (C), 181.9 (C), 191.6 (C).

3-(2-Hydroxyphenyl)-5,5-dimethyl-6,7-dihydrobenzo[d]isoxazol-4(5H)-one 194



Brown solid (57% as a mix of two isomers). Note the following data is for the above isomer only. 96-97°C; HRMS(EI+) $C_{15}H_{16}NO_3$ requires 258.1130 [M+H] found 258.1120 -3.8743 ppm; ν_{max} (DCM)/ cm^{-1} 1683 (C=O), 3275 (OH); δ_H (400MHz; $CDCl_3$) 1.27 (s, 6H, 2 x CH_3), 2.13 (t, $J=6.40$ Hz, 2H, CH_2), 3.12 (t, $J=6.40$ Hz, 2H, CH_2), 7.03-7.10 (m, 2H, 2 x Ar CH), 7.38-7.40 (m, 2H, Ar CH), 8.55 (dd, $J=8.00, 1.60$ Hz, H, Ar CH), 9.45 (broad s, H, OH); δ_C (100MHz; $CDCl_3$) 20.50 (CH_2), 24.2 (2 x CH_3), 35.1 (CH_2), 43.4 (C), 113.1 (C), 113.2 (C), 117.6 (Ar CH), 119.8 (Ar CH), 131.9 (Ar CH), 132.5 (Ar CH), 156.4 (C), 160.0 (C), 180.3 (C), 197.6 (C).

Optimised procedure for 2-(2-(prop-2-enyloxy)phenyl)-6,7-dihydrobenzo[d]isoxazol-4(5H)-one **71**



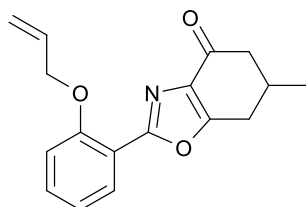
3-(2-Hydroxyphenyl)-6,7-dihydrobenzo[d]isoxazol-4(5H)-one **61** (5.00 mMol), 3-bromoprop-1-ene (5.50 mMol) and freshly purified potassium iodide (1 mMol) were dissolved in dry THF (50 ml). To this, caesium carbonate (5.50 mMol) was added and the solution was heated to reflux for 18 hours. Following this, the reaction mixture was cooled to room temperature and quenched with 1M aqueous hydrochloric acid (25 mL). The reaction mixture was then extracted with DCM (3 x 25 mL) and the combined organic extracts were washed with 1M sodium hydroxide (2 x 75 mL) and brine (1 x 75 mL). This was then dried over magnesium sulfate, filtered and evaporated to dryness under reduced pressure to yield 2-(2-(Allyloxy)phenyl)-6,7-dihydrobenzo[d]isoxazol-4(5H)-one **71** as a white solid (75%) which could be used without further purification.

M.p 132-133°C; C₁₅H₁₅NO₃Na; HRMS(EI+) requires 292.0950 [M+Na] found 292.0938 -4.1083 ppm; ν_{\max} (ATR)/cm⁻¹ 1681 (C=O); δ_{H} (400MHz; CDCl₃) 2.26-2.34 (m, 2H, CH₂) 2.64 (t, J=7.20 Hz, 2H, CH₂), 3.06 (t, J=6.40 Hz, 2H, CH₂), 4.67-4.69 (m, 2H, OCH₂) 5.03-5.34 (dd, J=10.40, 1.60 Hz, H, *cis-gem.* CH₂), 5.54-5.60 (dd, J=17.20, 1.60 Hz, H, *trans-gem.* CH₂), 6.04-6.13 (m, H, alkene CH), 6.94-7.11 (m, H, Ar CH), 7.38-7.45 (m, H, Ar CH), 7.83 (dd, J=8.00, 1.60 Hz, H, Ar CH), 8.08 (dd, J=7.60, 1.60 Hz, H, Ar CH); δ_{C} (100MHz; CDCl₃) 22.4 (2 x CH₂), 38.0 (CH₂), 69.4 (OCH₂), 113.4 (Ar CH), 116.1 (C), 117.2 (*gem.* CH₂), 121.0 (Ar CH), 131.2 (Ar CH), 132.4 (Ar CH), 132.7 (alkene CH), 134.9 (C), 156.8 (C), 160.8(C), 163.0 (C), 191.7 (C=O).

Un-optimised general procedure for one pot isoxazole to O-allyl benzoxazole transformation

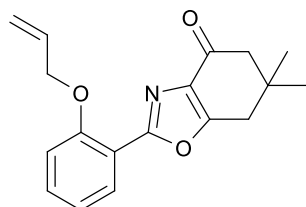
Hydroxyphenyl benzisoxazole (1.00 mMol) and 3-bromoprop-1-ene (1.10 mMol) were dissolved in dry THF (50 ml). To this, potassium carbonate (1.10 mMol) was added and the solution was heated to reflux for 18 hours. Following this, the reaction mixture was cooled to room temperature and quenched with 1M aqueous hydrochloric acid (25 mL). The reaction mixture was then extracted with DCM (3 x 25 mL) and the combined organic extracts were washed with 1M sodium hydroxide (2 x 75 mL) and brine (1 x 75 mL). This was then dried over magnesium sulfate, filtered and evaporated to dryness under reduced pressure to yield the desired O-allyl benzoxazole which could be used without further purification.

2-(2-(Prop-2-enyloxy)phenyl)-6-methyl-6,7-dihydrobenzo[d]oxazol-4(5H)-one 156



White solid (40%), m.p. 109-111°C; HRMS $C_{17}H_{17}O_3NNa$ requires 306.1106 [M+Na] found 306.1095 - 3.5935 ppm; ν_{max} (ATR)/ cm^{-1} 1679 (C=O); δ_H (400MHz; $CDCl_3$) 1.24 (d, J=6.40 Hz, 3H, CH_3), 2.41 (dd, J=16.00, 11.20 Hz, H, CH), 2.55-2.77 (m, 3H, 3 x CH), 3.12 (dd, J=16.80, 4.40 Hz, 1 H, CH), 4.68 (d, J=4.80 Hz, 2H, OCH_2), 5.33 (dd, J=10.10, 1.60Hz, 2H, *cis-gem.* CH_2), 5.58 (dd, J=17.20, 1.60 Hz, H, *trans-gem.* CH_2), 6.05-6.14 (m, H, alkene CH), 7.01-7.07 (m, 2H, 2 x Ar CH), 7.41-7.46 (m, H, Ar CH), 8.07 (dd, J=8.00, 2.00 Hz, H, Ar CH); δ_C (100MHz; $CDCl_3$) 21.1 (CH_3), 30.3 (CH_2), 30.8 (CH), 46.3 (CH_2), 69.3 (OCH_2), 113.3 (Ar CH), 116.0 (C), 117.2 (CH), 120.9 (Ar CH), 131.1 (Ar CH), 132.4 (Ar CH), 132.7 (Alkene CH), 134.7 (C), 156.8 (C), 161.4 (C), 163.7 (C), 191.3 (C=O).

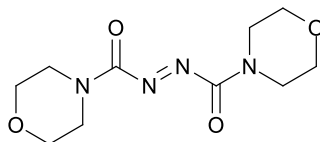
2-(2-(Prop-2-enyloxy)phenyl)-6,6-dimethyl-6,7-dihydrobenzo[d]oxazol-4(5H)-one 157



White solid (63%), M.p. 64-66°C; ν_{max} (ATR)/ cm^{-1} 1694 (C=O); HRMS $C_{18}H_{20}O_3NNa$ requires 298.1443 [M+H] found 298.1438 -1.6770 ppm; δ_H (400MHz; $CDCl_3$) 1.16 (s, 6H, 2 x CH_3), 2.45 (s, 2H, CH_2), 2.86 (s, 2H, CH_2), 4.60-4.68 (m, 2H, OCH_2), 5.27 (dd, J=10.80, 1.60 Hz, H, *gem.* CH_2), 5.54 (dd, J=15.60 Hz, 1.60 Hz, H, *gem.* CH_2), 6.00-6.07 (m, H, alkene CH), 6.95-7.01 (m, 2H, 2 x Ar CH), 7.35-7.39 (m, H, Ar CH),

8.04 (dd, $J=8.00, 2.00$ Hz, H, Ar CH); δ_c (100MHz; CDCl₃) 29.2 (2 x CH₃), 36.0 (C), 36.7 (CH₂), 52.8 (CH₂), 69.4 (CH₂), 113.8 (Ar CH), 116.4 (C), 117.5 (*gem.* CH₂), 121.4 (Ar CH), 131.5 (Ar CH), 132.9 (Ar CH), 133.2 (alkene CH), 134.4 (C), 157.2 (C), 161.6 (C), 163.7 (C).

Dimorpholine azodicarboxamide **81**¹²⁹



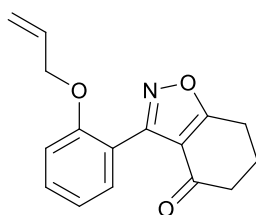
Morpholine (50.25 g, 575 mMol) was slowly added to a solution of diethyl azodicarboxylate **74** (50.00 g, 287 mMol) in diethylether (1 L) at 0°C; this mixture was then stirred under an atmosphere of nitrogen for 4 hours. The reaction mixture was then filtered under suction to yield diazene-1,2-diylbis(morpholinomethanone) **81** (48.49 g, 66%) as an orange solid which was used without further purification.

M.p. 138-140°C lit. 140-141°C⁸⁹; HRMS(EI+) C₁₀H₁₆O₄N₄Na requires 279.1069 [M+Na] found 279.1060 - 3.2246 ppm; ν_{\max} (DCM)/cm⁻¹ 1439 (N=N), 1706 (C=O); δ_{H} (400MHz; CDCl₃) 3.60-3.62 (m, H, CH), 3.71-3.77 (m, 2H, 2 x CH), 3.81-3.84 (m, H, CH); δ_{C} (100MHz; CDCl₃) 42.5 (CH₂), 44.1 (CH₂), 65.1 (CH₂), 65.2 (CH₂), 159.3 (C). The data above is in good agreement with literature data.^{89,130}

General Procedure for Benzisoxazole O-alkylation

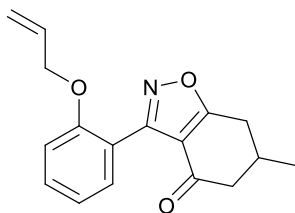
DMDC (54.5 mMol) was added to a solution of phenolic benzisoxazole (21.8 mMol), prop-2-en-1-ol (54.5 mMol) and triphenylphosphine (54.5 mMol) in dry THF (360 mL) at 0°C. This mixture was then allowed to stir overnight while slowly warming to room temperature. Following that, the mixture was cooled to 0°C and filtered through a prepacked ISOLUTE SCX-2 column with two column lengths of THF. The filtrate was then dried over magnesium sulfate and concentrated under reduced pressure. The crude product was then purified *via* flash column chromatography using light petroleum:ethyl acetate (1:1 v/v) as an eluent to yield the desired O-alkyl benzisoxazole.

3-(2-(Prop-2-enyloxy)phenyl)-6,7-dihydrobenzo[d]isoxazol-4(5H)-one 70



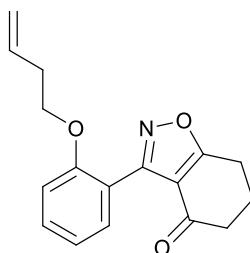
Orange gel (99%); HRMS(EI+) $C_{16}H_{16}O_3N$ requires 270.1130 [M+H] found 270.1122 -2.9617 ppm; ν_{max} (ATR)/ cm^{-1} 1687 (C=O); δ_H (600 MHz, $CDCl_3$) 1.96 (dd, $J = 12.90, 6.30$ Hz, 2H, CH_2), 2.24-2.32 (m, 2H, $CH_2, OCCH_2$), 2.78 (t, $J = 6.30$ Hz, 2H, $O=CCH_2$), 4.41 (dd, $J = 5.00, 1.30$ Hz, 2H, OCH_2), 5.05 (dd, $J = 10.60, 1.50$ Hz, H, *cis-gem* CH_2), 5.17 (dd, $J = 17.20, 1.70$ Hz, H, *trans-gem.* CH_2), 5.71-5.85 (m, H, alkene CH), 6.85-6.95 (m, 2H, 2 x Ar CH), 7.26-7.31 (m, H, Ar CH), 7.33 (dd, $J = 7.50, 1.70$ Hz, H, Ar CH); δ_C (150 MHz, $CDCl_3$) 22.0 (CH_2), 23.0 (CH_2), 38.1 (CH_2), 69.0 (OCH_2), 112.5 (Ar CH), 115.5 (C), 116.7 (*gem.* CH_2), 117.4 (C), 120.4 (Ar CH), 130.3 (Ar CH), 131.5 (Ar CH), 133.2 (Alkene CH), 157.0 (C), 157.3 (C), 180.8 (Isoxazole CO), 191 (C=O).

3-(2-(Prop-2-enyloxy)phenyl)-6-methyl-6,7-dihydrobenzo[d]isoxazol-4(5H)-one 84



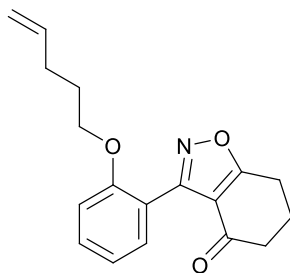
Yellow gel (83%); HRMS(EI+) $C_{17}H_{18}O_3N$ requires 284.1287 [M+H] found 284.1275 -4.2234 ppm; ν_{max} (ATR)/ cm^{-1} 1689 (C=O); δ_H (400 MHz, $CDCl_3$) 1.12 (d, $J=6.40$ Hz, 3H, CH_3), 2.21 (dd, $J=15.60, 5.20$ Hz, H, CH), 2.41-2.50 (m, 2H, 2 x CH), 2.60 (dd, $J=17.20, 9.60$, H, CH), 3.07 (dd, $J=4.80, 17.20$ Hz, H, CH), 4.50 (dd, $J=4.80, 0.80$ Hz, 2H, OCH_2), 5.14 (dd, $J=10.40, 1.60$ Hz, H, *cis-gem.* CH_2), 5.24 (dd, $J=17.20, 1.60$ Hz, H, *trans-gem.* CH_2), 5.83-5.92 (m, H, alkene CH), 6.95-7.01 (m, 2H, 2 x Ar CH), 7.36-7.41 (m, 2H, 2 x Ar CH); δ_C (100 MHz, $CDCl_3$) 20.7 (CH_3), 30.4 (CH), 30.9 (CH_2), 46.7 (CH_2), 69.1 (OCH_2), 112.4 (Ar CH), 115.4 (C), 116.9 (*gem.* CH_2), 117.2 (C), 120.5 (Ar CH), 130.4 (Ar CH), 131.6 (Ar CH), 133.2 (Alkene CH), 157.0 (C), 157.4 (C), 180.5 (Isoxazole CO), 191.0 (C=O).

3-(2-(But-3-en-1-yloxy)phenyl)-6,7-dihydrobenzo[d]isoxazol-4(5H)-one 77



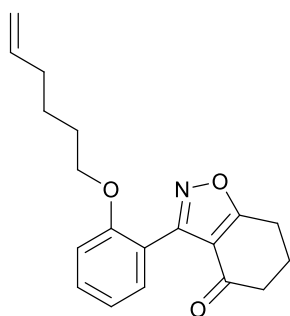
Beige solid (83%) M.p. 79-81°C; HRMS(EI+) $C_{17}H_{18}O_3N$ requires 284.1287 [M+H] found 284.1277 - 3.5195 ppm; ν_{max} (ATR)/ cm^{-1} 1685 (C=O); δ_H (400 MHz, $CDCl_3$) 2.23 (quintet, $J=6.40$ Hz, 2H, CH_2), 2.40 (quartet, 6.80 Hz, 2H, CH_2), 2.54 (t, $J=6.40$, 2H, CH_2), 3.09 (t, $J=6.40$, 2H, CH_2), 4.04 (t, $J=6.80$ Hz, CH_2), 5.01-5.10 (m, 2H, *gem.* CH_2), 5.73-5.83 (m, H, alkene CH), 6.99 (d, $J=8.80$ Hz, H, Ar CH), 7.04 (dd, $J=7.60, 1.20$ Hz, 1 H, Ar CH), 7.41-7.48 (m, 2H, 2 x Ar CH); δ_C (100 MHz, $CDCl_3$) 22.3 (CH_2), 23.3 (CH_2), 33.6 (CH_2), 38.4 (CH_2), 67.4 (OCH_2), 111.8 (Ar CH), 115.8 (C), 116.8 (*Gem.* CH_2), 117.0 (C), 120.4 (Ar CH), 130.5 (Ar CH), 131.6 (Ar CH), 134.6 (Alkene CH), 157.3 (C), 157.7 (C), 180.4 (Isoxazole CO), 191.3 (C=O).

3-(2-(Pent-4-en-1-yloxy)phenyl)-6,7-dihydrobenzo[d]isoxazol-4(5H)-one 82



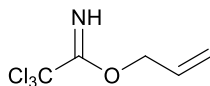
Beige solid (74%) M.p. 57-58°C; HRMS(EI+) $C_{18}H_{19}O_3NNa$ requires 320.1263 [M+Na] found 320.1253 - 3.1238 ppm; ν_{max} (ATR)/ cm^{-1} 1691 (C=O); δ_H (500 MHz, $CDCl_3$) 1.63 – 1.74 (m, 2H, CH_2), 1.97-2.07 (m, 2H, CH_2), 2.09-2.17 (m, 2H, CH_2), 2.39-2.46 (m, 2H, CCH_2), 2.94 (t, $J=6.30$ Hz, 2H, CH_2), 3.94 (t, $J=6.40$ Hz, OCH_2), 4.82-5.05 (m, 2H, *gem.* CH_2), 5.75 (m, H, alkene CH), 6.93-6.97 (m, 2H, 2 x Ar CH), 7.36-7.39 (m, 2H, 2 x Ar CH); δ_C (125 MHz, $CDCl_3$) 22.2 (CH_2), 23.1 (CH_2), 28.3 (CH_2), 30.0 (CH_2), 38.2 (CH_2), 67.3 (OCH_2), 111.8 (Ar CH), 115.0 (*gem.* CH_2), 115.7 (C), 117.1 (C), 120.1 (Ar CH), 130.3 (Ar CH), 131.5 (Ar CH), 137.8 (Alkene CH), 157.4 (C), 157.6 (C), 180.1 (Isoxazole CO), 191.3 (C=O).

3-(2-(Hex-5-en-1-yloxy)phenyl)-6,7-dihydrobenzo[d]isoxazol-4(5H)-one 83



Brown gel (94%); HRMS(EI+) $C_{19}H_{22}O_3N$ requires 312.1560 [M+H] found 312.1598 12.1734 ppm; ν_{max} (ATR)/ cm^{-1} 1689 (C=O); δ_H (400 MHz, $CDCl_3$) 1.37-1.48 (m, 2H, CH_2), 1.62 (quintet, $J=6.40$ Hz, 2H, CH_2), 1.99-2.09 (m, 2H, CH_2), 2.47 (t, $J=5.60$ Hz, 2H, CH_2), 3.00-3.02 (m, 2H, CH_2), 3.96 (t, $J=6.40$, 2H, OCH_2), 4.92-5.01 (m, 2H, *gem.* CH_2), 5.72-5.79 (m, H, alkene CH), 6.95-7.00 (m, 2H, 2 x Ar CH), 7.37-7.43 (m, 2H, 2 x Ar CH); δ_C (100 MHz, $CDCl_3$) 22.2 (CH_2), 23.2 (CH_2), 25.2 (CH_2), 28.3 (CH_2), 33.4 (CH_2), 38.2 (CH_2), 68.6 (OCH_2), 111.7 (Ar CH), 114.7 (*Gem.* CH_2), 115.7 (C), 116.9 (C), 120.1 (Ar CH), 130.3 (Ar CH), 131.6 (Ar CH), 138.5 (Alkene CH), 157.4 (C), 157.6 (C), 180.5 (Isoxazole CO), 191.4 (C=O).

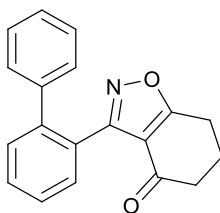
3-(2,2,2-Trichloro-1-iminoethoxy)prop-1-ene **86**⁹⁰



2,2,2-Trichloroacetonitrile **82** (9.82 g, 68.2 mMol) was added to a solution of 1,8-diazabicyclo[5.4.0]undec-7-ene (10.5 g, 68.2 mMol) in dichloromethane (100 ml) and cooled to 0°C. To this prop-2-en-1-ol (2.00 g, 2.34 ml, 34.5 mMol) was slowly added; following this the reaction mixture was stirred at 0°C for 1 hour. The insoluble material was then filtered off and the reaction mixture concentrated under reduced pressure. The crude product was purified by flash chromatography using light petroleum:ethyl acetate (95:5 v/v) as eluent to yield 3-(2,2,2-trichloro-1-iminoethoxy)prop-1-ene **83** as a clear oil (12.6 g, 80%). This compound slowly decomposed over time.

δ_{H} (400MHz; CDCl_3) 4.81-4.83 (m, 2H, CH_2), 5.32 (dd, $J=1.20, 10.40$ Hz, H, *cis-gem.* CH_2), 5.84 (dd, $J=1.20, 17.20$ Hz, H, *trans-gem.* CH_2), 5.99-6.10 (m, H, alkene CH), 8.34 (broad s, H, NH); δ_{C} (100MHz; CDCl_3) 69.4 (OCH_2), 91.4 (CCl_3), 118.5 (*gem.* CH_2), 131.4 (Alkene CH), 162.4 (C=N). The data above is in good agreement with literature data.⁹⁰

3-([1,1'-Biphenyl]-2-yl)-6,7-dihydrobenzo[d]isoxazol-4(5H)-one **87**



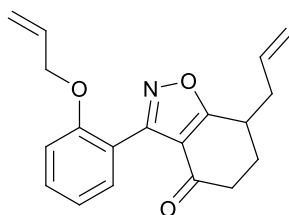
Tetrakis(triphenylphosphine)palladium (0.120 g, 0.103 mMol) and 3-(2-bromophenyl)-6,7-dihydrobenzo[d]isoxazol-4(5H)-one **4** (0.300 g, 1.03 mMol) were added to degassed dimethoxyethane (DME) (10 mL) and the solution was purged with nitrogen for 10 minutes. Two separated solutions of phenylboronic acid (0.180 g, 1.55 mMol) in ethanol (10 mL) and aqueous sodium carbonate (1.04 mL, 2.06 mMol) were degassed with nitrogen and added to the reaction mixture sequentially. The reaction mixture was then heated at reflux for 18 hours; following this the reaction was diluted with water (50 mL) and the mixture was extracted with ethyl acetate (3 x 50 mL), dried over magnesium sulfate, filtered and concentrated under reduced pressure. The crude product was purified using column chromatography with light petroleum:ethyl acetate (15:75 v/v) eluent to yield 3-([1,1'-biphenyl]-2-yl)-6,7-dihydrobenzo[d]isoxazol-4(5H)-one **84** (0.241 g, 81%) as a yellow solid.

MS(EI+) $C_{19}H_{16}NO_2$; requires 290.1181 [M+H], found 290.1179 -0.6894 ppm; ν_{max} (ATR)/ cm^{-1} 1684 (C=O); δ_H (400MHz; $CDCl_3$) 2.26-2.32 (m, 2H, CH_2), 2.55-2.58 (m, 2H, CH_2), 3.11 (t, J=6.33 Hz, 2H, CH_2), 7.24 (m, H, Ar CH), 7.34-7.63 (m, 5H, 5 x Ar CH), 7.71 (d, J=7.60 Hz, H, Ar CH), 8.27-8.27 (m, H, Ar CH).

General procedure for preparation of O-alkyl-C-allyl benzisoxazoles alpha to the isoxazole

O-Alkyl benzisoxazole (1 mMol) was dissolved in anhydrous THF (10 mL) and cooled to -78°C under an atmosphere of nitrogen. Following this, lithium bis(trimethylsilyl)amide (1.01 mMol) was slowly added to ensure the temperature remained below -70°C. This mixture was kept at -78°C for 1 hour before being warmed to 0°C. After an hour at this temperature a solution of 3-bromoprop-1-ene (1.00 mMol) and freshly purified potassium iodide (1.00 mmol) in dry THF (10 mL) at 0°C was slowly added and the reaction mixture was allowed to warm to room temperature overnight. Saturated ammonium chloride solution (10 mL) was then added to the solution and it was allowed to stir for 30 minutes under an open atmosphere. The mixture was then diluted with DCM (30 mL) and water (10mL), the organic layer was separated and washed with water (10mL) and saturated sodium chloride solution (10mL). The organic layer was dried over magnesium sulfate and concentrated under reduced pressure. The crude product was purified *via* flash column chromatography using light petrol:ethyl acetate:dichloromethane (5:1:4 v/v/v) as eluent to yield a mixture of C-allylated-O-alkyl benzisoxazoles.

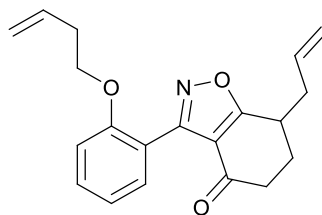
7- Prop-2-enyl-3-(2-(prop-2-enyloxy)phenyl)-6,7-dihydrobenzo[d]isoxazol-4(5H)-one 88



Yellow oil (56%); MS(EI+) $C_{19}H_{20}NO_3$; requires 310.1443 [M+H] found 310.1435 -2.5794 ppm; ν_{max} (ATR)/ cm^{-1} 1688 (C=O); δ_H (500 MHz, $CDCl_3$) 1.80-1.89 (m, H,CH), 2.05-2.09 (m, H, CH), 2.13-2.22 (m, H, CH), 2.33-2.36 (m, H, CH), 2.50-2.54 (m, H, CH), 2.86-3.00 (m, 2H, CH_2), 4.35-4.47 (m, 2H, OCH_2), 4.91-5.00 (m, 2H, *gem.* CH_2), 5.06 (dd, H, $J=10.60, 1.40$ Hz, *cis-gem.* CH_2), 5.16 (dd, H, $J=17.10, 1.20$ Hz, *trans-gem.* CH_2), 5.60-5.71 (m, H, alkene CH), 5.79 (m, H, alkene), 6.82-6.95 (m, 2H, 2 x Ar CH), 7.28-7.32 (2H, m, 2 x Ar CH); δ_C (125 MHz, $CDCl_3$) 21.3 (CH_2), 26.0 (CH_2), 32.2 (CH_2), 45.5 (CH) 68.1 (OCH_2), 111.3 (Ar CH), 114.4 (C), 115.9 (*gem.* CH_2), 116.1 (*gem.* CH_2), 116.20 (C), 119.5 (Ar CH), 129.4 (Ar CH), 130.5 (Ar CH), 132.2 (Alkene CH), 134.8 (Alkene CH), 156 (C), 157 (C), 179 (Isioxazole CO), 191 (C=O).

Both the high resolution mass and NMR spectra indicated the presence of other multiply allylated materials.

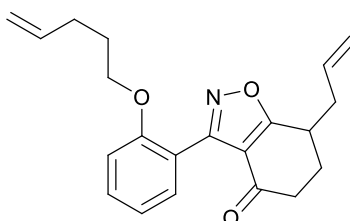
7- Prop-2-enyl-3-(2-(but-3-en-1-yloxy)phenyl)-6,7-dihydrobenzo[d]isoxazol-4(5H)-one 90



Yellow oil (28%); MS(EI+) $C_{20}H_{22}NO_3$; requires 324.1560 [M+H] found 324.1593 10.1802 ppm; ν_{max} (ATR)/ cm^{-1} 1688 (C=O); δ_H (400 MHz, $CDCl_3$) 1.90-1.96 (m, H,CH), 2.08-2.47 (m, 5H, 5 x CH), 2.62-2.69 (m, 1 H, CH), 2.91-3.10 (m, 2H, CH_2), 3.97-4.03 (m, 2H, OCH_2), 4.96-5.10 (m, 4H, 2 x *gem.* CH_2), 5.68-5.79 (m, 2H, 2 x alkene CH), 6.94-7.00 (m, 2H, 2 x Ar CH), 7.36-7.42 (m, 2 x Ar CH); δ_C (100 MHz, $CDCl_3$) 22.5 (CH_2), 27.2 (CH_2), 33.2 (CH_2), 33.6 (CH_2), 46.7 (CH), 67.4 (OCH_2), 111.9 (Ar CH), 115.5 (*Gem.* CH_2), 116.8 (C), 117.2 (*Gem.* CH_2), 117.3 (C), 120.3 (Ar CH), 130.4 (Ar CH), 131.6 (Ar CH), 134.5 (Alkene CH), 135.9 (Alkene CH), 157.3 (C), 157.9 (C), 180.0 (Isoxazole CO), 192.4 (C=O).

Both the high resolution mass and NMR spectra indicated the presence of other multiply allylated materials.

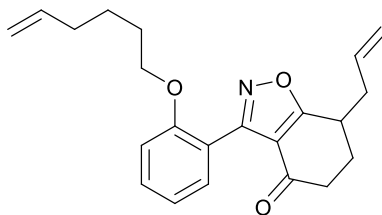
7- Prop-2-enyl-3-(2-(pent-4-en-1-yloxy)phenyl)-6,7-dihydrobenzo[d]isoxazol-4(5H)-one 91



Yellow oil (42%); MS(EI+) $C_{21}H_{23}NO_3Na$; requires 360.1576 [M+Na] found 360.1571 -1.3883 ppm; ν_{max} (ATR)/ cm^{-1} 1688 (C=O); δ_H (400 MHz, $CDCl_3$) 1.65-1.75 (m, 2H, CH_2), 1.94-2.34 (m, 5H, 5 x CH), 2.42-2.70 (m, 3H, 3 x CH), 3.00-3.15 (m, 2H, CH_2), 3.93-4.01 (m, 2H, OCH_2), 4.92-5.22 (m, 4H, 2 x *gem.* CH_2), 5.68-5.80 (m, 2H, 2 x Alkene CH), 7.00-7.03 (m, 2H, 2 x Ar CH), 7.34-7.45 (m, 2 H, 2 x Ar CH); δ_C (100 MHz, $CDCl_3$) 22.5 (CH_2), 27.1 (CH_2), 28.3 (CH_2), 30.1 (CH_2), 39.2 (CH_2), 46.7 (CH), 67.4 (OCH_2), 111.8 (Ar CH), 115.1 (C), 117.3 (*gem.* CH_2), 118.6 (*gem.* CH_2), 120.2 (Ar CH), 130.4 (Ar CH), 131.6 (Ar CH), 133.6 (Alkene CH), 135.9 (C), 137.8 (Alkene CH), 157.4 (2 x C), 179.9 (Isoxazole CO), 192.4 (C=O).

Both the high resolution mass and NMR spectra indicated the presence of other multiply allylated materials.

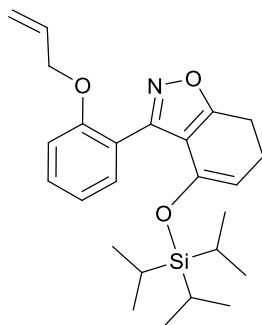
7- Prop-2-enyl-3-(2-(hex-5-en-1-yloxy)phenyl)-6,7-dihydrobenzo[d]isoxazol-4(5H)-one 92



Yellow oil (24%); MS(EI+) $C_{22}H_{25}NO_3Na$; requires 374.1732 [M+Na] found 374.1728 -1.0690 ppm; ν_{max} (ATR)/ cm^{-1} 1688 (C=O); δ_H (400 MHz, $CDCl_3$) 1.36-1.45 (m, 2H, CH_2), 1.57-1.68 (m, 2H, CH_2), 1.87-2.37 (m, 5H, 5 x CH), 2.45-2.52 (m, H, CH), 2.68-2.73 (m, H, CH), 3.02-3.13 (m, H, CH_2), 3.94-4.02 (m, 2H, OCH_2), 4.89-5.14 (m, 4H, 2 x *gem.* CH_2), 5.73-5.84 (m, 2H, 2 x alkene CH), 6.90-7.08 (m, 2H, 2 x Ar CH), 7.38-7.55 (m, 2H, 2 x Ar CH); δ_C (100 MHz, $CDCl_3$) 22.5 (CH_2), 24.8 (CH_2), 27.1 (CH_2), 28.6 (CH_2), 33.2 (CH_2), 33.4 (CH_2), 46.6 (CH), 67.8 (OCH_2), 117.3 (Ar CH), 114.7 (*gem.* CH_2), 115.5 (C), 116.9 (C), 117.2 (*gem.* CH_2), 120.2 (Ar CH), 130.2 (Ar CH), 131.5 (Ar CH), 135.9 (alkene CH), 138.5 (alkene CH), 157.4 (C), 157.8 (C), 179.9 (isoxazole CO), 192.4 (C=O).

Both the high resolution mass and NMR spectra indicated the presence of other multiply allylated materials.

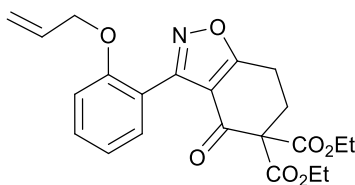
3-(2-(Prop-2-enyloxy)phenyl)-4-((triisopropylsilyl)oxy)-6,7-dihydrobenzo[d]isoxazole **95**



A solution of 3-(2-(prop-2-enyloxy)phenyl)-6,7-dihydrobenzo[d]isoxazol-4(5H)-one **70** (1.00 g, 3.72 mMol) in anhydrous THF (50 mL), was prepared and cooled to -78°C under an atmosphere of nitrogen. Following this, lithium bis(trimethylsilyl)amide (4.08 mL, 4.08 mMol) was slowly added, this addition was tapered to ensure the temperature remained under -70°C . After an hour at this temperature triisopropyl triflate (1.14 g, 3.72 mMol) was added and the reaction mixture was allowed to warm to room temperature overnight. Following this saturated ammonium chloride solution (10 mL) was added to the solution and it was allowed to stir for 30 minutes under an open atmosphere. The mixture was then diluted with DCM (25 mL) and water (25mL), the organic layer was separated and washed with water (25mL) and saturated sodium chloride solution (25mL). The organic layer was dried over magnesium sulfate and concentrated under reduced pressure. The crude product was then purified *via* flash column chromatography using isohexane:ethyl acetate (1:1 v/v) as eluent to yield 3-(2-(prop-2-enyloxy)phenyl)-4-((triisopropylsilyl)oxy)-6,7-dihydrobenzo[d]isoxazole **95** (1.17g, 74%) as a brown oil. Compound slowly decomposes in air.

HRMS(EI+) $\text{C}_{25}\text{H}_{36}\text{O}_3\text{NSi}$ requires 426.2464 [M+H] found 426.2460 -0.9384 ppm; ν_{max} (DCM)/ cm^{-1} 1596 (Si-O); δ_{H} (500 MHz, CDCl_3) 0.67 (m, 2H, 6 x CH_3 , 3 x CH), 2.43 (td, $J=8.70$, 4.50 Hz, 2H, CH_2), 2.76 (t, $J=8.70$ Hz, 2H, CH_2), 4.62 (t, $J=4.50$ Hz, H, alkene CH), 5.05 (dd, $J=10.70$, 1.30 Hz, H, *cis-gem.* CH_2), 5.21 (dd, $J=17.30$, 1.30 Hz, H, *trans-gem.* CH_2), 5.84 (m, H, alkene CH), 6.80 (d, $J=8.30$ Hz, H, Ar CH), 6.87 (t, $J=7.40$ Hz, H, Ar CH), 7.20-7.26 (m, H, Ar CH), 7.30 (dd, $J=7.40$, 1.40 Hz, 2H).

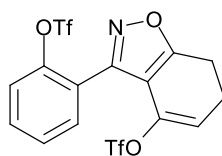
Diethyl 3-(2-(prop-2-enyloxy)phenyl)-4-oxo-6,7-dihydrobenzo[d]isoxazole-5,5(4H)-dicarboxylate **98**



A solution of 3-(2-(prop-2-enyloxy)phenyl)-6,7-dihydrobenzo[d]isoxazol-4(5H)-one **70** (0.250 g, 0.93 mMol) in anhydrous THF (20 mL), was prepared and cooled to -78°C under an atmosphere of nitrogen. Following this, lithium bis(trimethylsilyl)amide (0.93 mL, 0.93 mMol) was slowly added, this addition was tapered to ensure the temperature remained under -70°C . After an hour at this temperature ethyl chloroformate (0.101 g, 0.93 mMol) was added and the reaction mixture was allowed to warm to room temperature overnight. Following this saturated ammonium chloride solution (10 mL) was added to the solution and it was allowed to stir for 30 minutes under an open atmosphere. The mixture was then diluted with DCM (20 mL) and water (20 mL), the organic layer was then separated and washed with water (20 mL) and saturated sodium chloride solution (20 mL). The organic layer was dried over magnesium sulfate and concentrated under reduced pressure. The crude product was then purified *via* flash column chromatography using light petroleum:ethyl acetate (1:1 v/v) as eluent to yield diethyl 3-(2-(prop-2-enyloxy)phenyl)-4-oxo-6,7-dihydrobenzo[d]isoxazole-5,5(4H)-dicarboxylate **98** (73 mg, 20%) as a clear oil.

MS(EI+) $\text{C}_{22}\text{H}_{23}\text{NO}_7\text{Na}$ requires 436.1372 [M+Na] found 436.1366 -1.3757 ppm; ν_{max} (ATR)/ cm^{-1} 1687 (C=O); δ_{H} (400 MHz, CDCl_3) 1.24 (t, $J=7.20$, 6H, 2 x CH_3), 2.84 (t, $J=6.00$, 2H, CH_2), 3.07 (t, $J=6.00$ Hz, 2H, CH_2), 4.17-4.30 (m, 4H, 2 x CH_2), 4.57 (d, $J=5.20$ Hz, 2H, OCH_2), 5.18 (dd, $J=10.40$, 1.20 Hz, H, *cis-gem.* CH_2), 5.28 (dd, $J=17.60$, 1.20 Hz, H, *trans-gem.* CH_2), 5.90-5.99 (m, H, alkene CH), 6.96-7.00 (m, 2H, 2 x Ar CH), 7.37-7.41 (m, 2H, 2 x Ar CH); δ_{C} (100 MHz, CDCl_3) 14.0 (2 x CH_3), 20.1 (CH_2), 29.6 (CH_2), 62.6 (2 x CH_2), 67.1 (C), 69.7 (OCH_2), 112.7 (Ar CH), 114.9 (C), 116.6 (C), 117.2 (*gem.* CH_2), 120.6 (Ar CH), 130.8 (Ar CH), 131.8 (Ar CH), 133.5 (alkene CH), 157.3 (C), 158.2 (C), 167.0 (C), 179 (C), 182.8 (C).

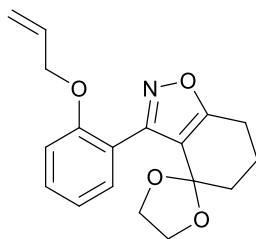
2-(4-(((Trifluoromethyl)sulfonyl)oxy)-6,7-dihydrobenzo[d]isoxazol-3-yl)phenyl trifluoromethanesulfonate **101**



Triflic anhydride (1.47 mL, 8.73 mMol) was added drop wise to a solution of 3-(2-hydroxyphenyl)-6,7-dihydrobenzo[d]isoxazol-4(5H)-one **61** (1.00g, 4.37 mMol) and pyridine (0.70 mL, 8.73 mMol) in dichloromethane (50 mL) at 0°C. After 18 hours the reaction mixture was quenched with saturated ammonium chloride (25 mL) and separated. The organic layer was washed with 1M sodium hydroxide solution (2 x 25 mL) and saturated sodium chloride solution (50 mL). The organic layer was then dried over sodium sulfate, filtered and concentrated under reduced pressure. The crude product was then purified *via* flash column chromatography using light petroleum:ethyl acetate (1:1 v/v) as eluent to yield 2-(4-(((trifluoromethyl)sulfonyl)oxy)-6,7-dihydrobenzo[d]isoxazol-3-yl)phenyl trifluoromethanesulfonate **101** as a brown gel (0.93g , 43%).

MS(EI+) C₁₅H₁₀NO₇F₆S₂ requires 493.9803 [M+H] found 493.9807 1.0122 ppm; ν_{\max} (ATR)/cm⁻¹ 1134 (S=O), 1423 (SO); δ_{H} (400 MHz, CDCl₃) 2.78-2.83 (m, 2H, CH₂), 3.09 (t, J=9.20, 2H, CH₂), 5.78 (t, J=4.40 Hz, H, alkene CH), 7.46-7.81 (m, 4H, 4 x Ar CH); δ_{C} (100 MHz, CDCl₃) 20.8 (CH₂), 23.2 (CH₂), 109.6 (C), 113.1 (Alkene CH), 121.8 (C), 121.9 (Ar CH), 128.7 (Ar CH), 132.2 (Ar CH), 132.4 (Ar CH), 139.9 (C), 147.3 (C), 152.5 (C), 172.3 (C), CF₃ quaternary carbon atoms could not be detected in time allocated for this experiment; δ_{F} (376 Mhz, CDCl₃) 88.13 (CF₃), 88.35 (CF₃).

3-(2-(Prop-2-enyloxy)phenyl)-6,7-dihydro-5H-spiro[benzo[d]isoxazole-4,2'-[1,3]dioxolane] 107

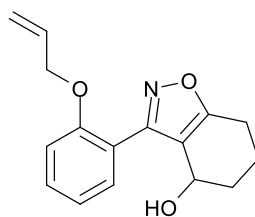


3-(2-(Allyloxy)phenyl)-6,7-dihydrobenzo[d]isoxazol-4(5H)-one **70** (1.00 g, 3.72 mMol) was added to a solution of ethylene glycol (0.46 g, 7.43 mMol) and *para*-toluenesulfonic acid (0.035 g, 0.186 mMol) in dry toluene (40 mL) and heated under Dean-Stark conditions for 18 hours. The reaction mixture was allowed to cool to room temperature, after which it was diluted with water (40 mL) and extracted. The organic extracts were then washed with water (40 mL) and saturated sodium chloride solution (40 mL) before being dried over magnesium sulfate and concentrated under reduced pressure to yield 3-(2-(prop-2-enyloxy)phenyl)-6,7-dihydro-5H-spiro[benzo[d]isoxazole-4,2'-[1,3]dioxolane] **107** (1.02 g, 88%) as a yellow oil.

MS(EI+) $C_{18}H_{19}NO_4Na$ requires 336.1212 [M+H] found 336.1206 -1.7851 ppm; δ_H (500 MHz, $CDCl_3$) 1.70-1.78 (m, 2H, CH_2), 1.85-1.96 (m, 2H, CH_2), 2.64 (t, $J=6.30$ Hz, 2H, CH_2), 3.20 (t, $J=6.50$ Hz, 2H, 2 x *eq.* CH), 3.61 (t, $J=6.50$ Hz, 2H, 2 x *ax.* CH), 4.45 (d, $J=4.90$ Hz, 2H, OCH_2), 5.06 (dd, $J=10.60, 1.10$ Hz, H, *cis-gem.* CH_2), 5.21 (dd, $J=17.30, 1.10$ Hz, H, *trans-gem.* CH_2), 5.85 (m, H, alkene CH), 6.86 (m, 2H, 2 x Ar CH), 7.20-7.27 (m, 2H, Ar CH); δ_C (125 MHz, $CDCl_3$) 19.6 (CH_2), 21.6 (CH_2), 34.1 (CH_2), 63.9 (2 x OCH_2), 68.4 (OCH_2), 104.8 (C), 111.8 (Ar CH), 114.6 (C), 115.9 (*gem.* CH_2), 118.3 (C), 119.1 (Ar CH), 129.4 (Ar CH), 130.4 (Ar CH), 132.3 (alkene CH), 155.6 (Ar C), 156.8 (C), 170.0 (isoxazole CO).

Both the mass and NMR spectra indicated the presence of starting 3-(2-(Prop-2-enyloxy)phenyl)-6,7-dihydrobenzo[d]isoxazol-4(5H)-one following multiple purification attempts.

3-(2-(Prop-2-enyloxy)phenyl)-4,5,6,7-tetrahydrobenzo[d]isoxazol-4-ol **108**



Sodium borohydride method

3-(2-(Prop-2-enyloxy)phenyl)-6,7-dihydrobenzo[d]isoxazol-4(5H)-one **70** (0.294g, 1.09 mMol) was dissolved in ethanol (20 mL). Sodium borohydride (0.041g, 1.09 mMol) was added and the mixture was heated at reflux for 18 hours. The reaction mixture was then quenched with water (10 mL) and washed three times with dichloromethane (3 x 10 mL). The combined organic extracts were then washed with saturated sodium chloride solution (30 mL), dried over magnesium sulfate, filtered and concentrated under reduced pressure to yield 3-(2-(prop-2-enyloxy)phenyl)-4,5,6,7-tetrahydrobenzo[d]isoxazol-4-ol **108** as a cream solid (0.271g. 92%).

Lithium aluminium hydride method

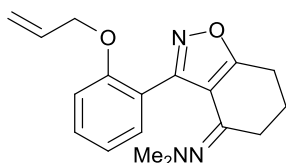
3-(2-(Prop-2-enyloxy)phenyl)-6,7-dihydrobenzo[d]isoxazol-4(5H)-one **70** (0.203g, 0.755 mMol) was dissolved in dry diethyl ether (10 mL) and cooled to 0°C. Lithium aluminium hydride (0.029g, 0.755 mMol) was carefully added and the solution was allowed to warm to room temperature. After six hours the reaction mixture was diluted with diethyl ether (20 mL), quenched with water (10%) in THF and washed with 1M sodium hydroxide (1M), water (2 x 10mL) and saturated sodium chloride solution (10 mL). The organic layer was then dried over magnesium sulfate, filtered and concentrated under reduced pressure to yield 3-(2-(prop-2-enyloxy)phenyl)-4,5,6,7-tetrahydrobenzo[d]isoxazol-4-ol **108** as a cream solid (0.156g. 76%).

MS(EI+) C₁₆H₁₈NO₃ requires 272.1286 [M+H] found 272.1281 -1.8374 ppm; ν_{\max} (ATR)/cm⁻¹ 3334 (OH); δ_{H} (400 MHz, CDCl₃) 1.59-1.65 (m, H, CH), 1.78-1.88 (m, 2H, 2 x CH), 2.03-2.13 (m, H, CH), 2.55-2.63 (m, H, CH), 2.76-2.81 (m, H, CH), 3.09 (broad s, H, OH), 4.49-4.58 (m, 2H, OCH₂), 4.64 (s, H, CH), 5.23 (d, J=10.40 Hz, H, *cis-gem.* CH₂), 5.31 (d, J=16.80 Hz, H, *trans-gem.* CH₂), 5.88-5.98 (m, H, alkene CH), 6.94-7.02 (m, 2H, 2 x Ar CH), 7.34-7.42 (m, 2H, 2 x Ar CH); δ_{C} (100 MHz, CDCl₃) 17.5 (CH₂), 22.9 (CH₂), 31.1 (CH₂), 61.2 (CH), 70.2 (OCH₂), 113.3 (Ar CH), 116.3 (C), 119.0 (C), 119.2 (*gem.* CH₂), 121.8 (Ar CH), 131.3 (CH), 131.7 (CH), 132.2 (CH), 155.8 (C), 159.1 (C), 169.7 (C).

General procedure for hydrazone formation

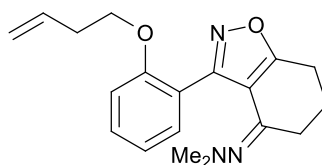
O-Alkyl benzisoxazole (1 mMol), N,N-dimethylhydrazine (10 mMol) and trifluoroacetic acid were dissolved in toluene (25 mL) and heated under Dean-Stark conditions for six hours. Following this the reaction mixture was allowed to cool to room temperature, upon which it was washed with water (2 x 25 mL) and brine (25 mL), dried over magnesium sulfate, filtered and concentrated under reduced pressure. The crude product was purified *via* column chromatography using light petroleum:ethyl acetate (4:6 v/v) as a solvent.

3-(2-(Prop-2-enyloxy)phenyl)-4-(2,2-dimethylhydrazono)-4,5,6,7-tetrahydrobenzo[d]isoxazole 110



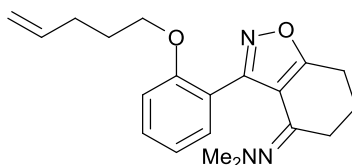
Orange gel (68%); MS(EI+) $C_{18}H_{22}N_3O_2$ requires 312.1712 [M+H] found 312.1701 -3.5237 ppm; ν_{max} (ATR)/ cm^{-1} 1628 (C=N); δ_H (400 MHz, $CDCl_3$) 2.02-2.05 (m, 2H, CH_2), 2.30 (s, 6H, 2 x CH_3), 2.65-2.68 (m, 2H, CH_2), 2.89 (t, J=6.00, 2H, CH_2), 4.50-4.52 (m, 2H, OCH_2), 5.13-5.16 (m, H, *gem.* CH_2), 5.22-5.27 (m, H, *gem.* CH_2), 5.88-5.92 (m, H, alkene CH), 6.88 (d, J=8.00, H, Ar CH), 6.96-7.00 (m, H, Ar CH), 7.35-7.40 (m, 2H, 2 x Ar CH); δ_C (100 MHz, $CDCl_3$) 22.1 (CH_2), 23.3 (CH_2), 25.9 (CH_2), 47.3 (2 x CH_3), 68.5 (OCH_2), 111.3 (Ar CH), 113.7 (C), 116.3 (*gem.* CH_2), 119.3 (C), 120.0 (Ar CH), 130.5 (2 x Ar CH), 133.3 (alkene CH), 158.9 (C), 157.1 (C), 157.9 (C), 172.1 (C).

3-(2-(But-3-en-1-yloxy)phenyl)-4-(2,2-dimethylhydrazono)-4,5,6,7-tetrahydrobenzo[d]isoxazole 111



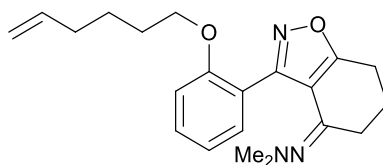
Orange gel (74%); MS(EI+) $C_{19}H_{23}N_3O_2Na$ requires 348.1688 [M+Na] found 348.1675 -3.7338 ppm; ν_{max} (ATR)/ cm^{-1} 1631 (C=N); δ_H (400 MHz, $CDCl_3$) 2.02-2.06 (m, 2H, CH_2), 2.30 (s, 6H, 2 x CH_3), 2.37-2.42 (m, 2H, CH_2), 2.66-2.69 (m, 2H, CH_2), 2.89 (t, J=6.80 Hz, 2H, CH_2), 3.97 (t, J=6.80 Hz, 2H, OCH_2), 4.98-5.06 (m, 2H, *gem.* CH_2), 5.69-5.83 (m, H, alkene CH), 6.87 (d, J=8.40 Hz, H, Ar CH), 6.95-6.99 (m, H, Ar CH), 7.35-7.43 (m, 2H, 2 x Ar CH); δ_C (100 MHz, $CDCl_3$) 22.2 (CH_2), 23.0 (CH_2), 33.8 (CH_2), 47.3 (2 x CH_3), 67.2 (OCH_3), 111.0 (Ar CH), 113.8 (C), 116.7 (*gem.* CH_2), 119.3 (C), 119.8 (Ar CH), 130.3 (Ar CH), 130.5 (Ar CH), 134.5 (alkene CH), 154.8 (C), 157.4 (C), 157.9 (C), 171.9 (C).

4-(2,2-Dimethylhydrazono)-3-(2-(pent-4-en-1-yloxy)phenyl)-4,5,6,7-tetrahydrobenzo[d]isoxazole 112



Orange gel (60%); MS(EI+) $C_{20}H_{26}N_3O_2$ requires 340.2025 [M+H] found 340.2014 -3.2334 ppm; ν_{max} (ATR)/ cm^{-1} 1633 (C=N); δ_H (400 MHz, $CDCl_3$) 1.73 (quintet, $J=7.20$ Hz, 2H, CH_2), 2.01-2.09 (m, 4H, 2 x CH_2), 2.29 (s, 6H, 2 x CH_3), 2.64-2.67 (m, 2H, CH_2), 2.88 (t, $J=6.40$ Hz, 2H, CH_2), 3.93 (t, $J=6.40$, 2H, OCH_2), 4.91-4.99 (m, 2H, *gem.* CH_2), 5.70-5.83 (m, H, alkene CH), 6.86 (d, $J=8.40$ Hz, H, Ar CH), 6.93-6.970 (m, H, Ar CH), 7.34-7.37 (m, 2H, Ar CH); δ_C (100 MHz, $CDCl_3$) 24.5 (CH_2), 25.3 (CH_2), 28.2 (CH_2), 30.8 (CH_2), 32.5 (CH_2), 49.6 (2 x CH_3), 69.5 (OCH_2), 113.3 (Ar CH), 116.1 (C), 117.2 (*gem.* CH_2), 121.6 (C), 122.0 (Ar CH), 132.6 (Ar CH), 132.8 (Ar CH), 140.3 (alkene CH), 157.0 (C), 159.9 (C), 160.3 (C), 174.2 (C).

4-(2,2-Dimethylhydrazono)-3-(2-(hex-5-en-1-yloxy)phenyl)-4,5,6,7-tetrahydrobenzo[d]isoxazole 113

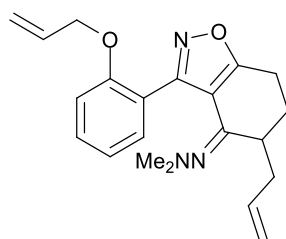


Orange gel (69%); MS(EI+) $C_{21}H_{28}N_3O_2$ requires 354.2182 [M+H] found 354.2168 -3.9524 ppm; ν_{max} (ATR)/ cm^{-1} 1631 (C=N); δ_H (400 MHz, $CDCl_3$) 1.39-1.43 (m, 2H, CH_2), 1.63-1.67 (m, 2H, CH_2), 2.00-2.05 (m, 4H, 2 x CH_2), 2.30 (s, 6H, 2 x CH_3), 2.64-2.67 (m, 2H, CH_2), 2.89 (t, $J=6.40$ Hz, 2H, CH_2), 3.93 (t, $J=6.40$ Hz, 2H, OCH_2), 4.92-5.00 (m, 2H, *gem.* CH_2), 5.70-5.81 (m, H, alkene CH), 6.86 (d, $J=8.80$ Hz, H, Ar CH), 6.94-6.98 (m, H, Ar CH), 7.35-7.39 (m, 2H, 2 x Ar CH); δ_C (100 MHz, $CDCl_3$) 22.2 (CH_2), 23.0 (CH_2), 25.3 (CH_2), 25.9 (CH_2), 28.7 (CH_2), 33.5 (CH_2), 47.3 (2 x CH_3), 67.9 (OCH_2), 110.9 (Ar CH), 113.8 (C), 114.6 (*gem.* CH_2), 119.2 (C), 119.6 (Ar CH), 130.2 (Ar CH), 130.5 (Ar CH), 138.6 (alkene CH), 154.7 (C), 157.6 (C), 158.0 (C), 171.9 (C).

General procedure for preparation of O-alkyl-C-prop-2-enyloxy benzisoxazole hydrazones

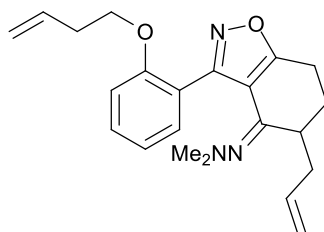
O-Alkyl isoxazole hydrazone (1 mMol) was dissolved in anhydrous THF (10 mL) and cooled to -78°C under an atmosphere of nitrogen. Following this, freshly prepared LDA (1.01 mMol) was slowly added to ensure the temperature remained below -70°C . After fifteen minutes a solution of 3-bromoprop-1-ene (1 mMol) and freshly purified potassium iodide (1 mMol) in anhydrous THF at -78°C was added dropwise *via* cannula. After two hours the reaction was warmed to 0°C and then allowed to warm to room temperature over an hour. After saturated ammonium chloride solution (10 mL) was added to the solution and it was allowed to stir for 30 minutes under an open atmosphere. The mixture was then diluted with DCM (30 mL) and water (10 mL), the organic layer was separated and washed with water (10 mL) and saturated sodium chloride solution (10 mL). The organic layer was dried over magnesium sulfate and concentrated under reduced pressure. The crude product was purified *via* flash column chromatography using light petrol:ethyl acetate:dichloromethane (5:1:4 v/v/v) as eluent to yield the desired C-allyl-O-alkyl benzisoxazole hydrazone.

5-prop-2-enyl-3-(2-(prop-2-enyloxy)phenyl)-4-(2,2-dimethylhydrazono)-4,5,6,7-tetrahydrobenzo[d]isoxazole 114



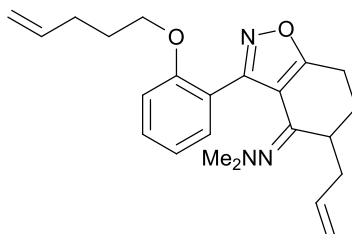
Orange gel (34%); MS(EI+) $\text{C}_{21}\text{H}_{26}\text{N}_3\text{O}_2$ requires 352.2025 [M+H] found 352.2012 -3.6911 ppm; ν_{max} (ATR)/ cm^{-1} 1629 (C=N); δ_{H} (400 MHz, CDCl_3) 1.65-1.74 (m, H, CH), 2.01-2.09 (m, H, CH), 2.22 (s, 6H, 2 x CH_3), 2.28-2.38 (m, 2H, 2 x CH), 2.65-2.72 (m, H, CH), 2.84-2.91 (m, H, CH), 3.00-3.07 (m, H, CH), 4.41-4.43 (m, 2H, OCH_2), 5.04-5.22 (m, 4H, 2x *gem.* CH_2), 5.70-5.88 (m, 2H, 2 x alkene CH), 6.80 (d, $J=8.00$ Hz, H, Ar CH), 6.89-6.93 (m, H, Ar CH), 7.28-7.38 (m, 2H, 2 x Ar CH); δ_{C} (100 MHz, CDCl_3) 24.0 (CH_2), 26.7 (CH_2), 33.2 (CH), 35.0 (CH_2), 46.3 (2 x CH_3), 67.4 (OCH_2), 110.3 (Ar CH), 112.5 (C), 115.1 (*gem.* CH_2), 116.8 (*gem.* CH_2), 118.3 (C), 119.0 (Ar CH), 129.5 (2 x Ar CH), 132.2 (alkene CH), 133.9 (alkene CH), 153.8 (C), 156.0 (C), 156.9 (C), 173.0 (C).

5-Prop-2-enyl-3-(2-(but-3-en-1-yloxy)phenyl)-4-(2,2-dimethylhydrazono)-4,5,6,7-tetrahydrobenzo[d]isoxazole 115



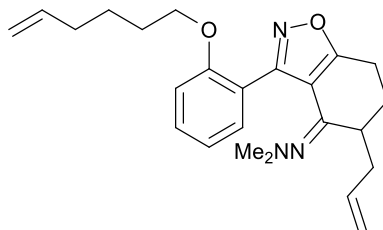
Orange gel (45%); MS(EI+) $C_{22}H_{28}N_3O_2$ requires 366.2182 [M+H] found 366.2167 -4.0959 ppm; ν_{max} (ATR)/ cm^{-1} 1629 (C=N); δ_H (400 MHz, $CDCl_3$) 1.73-1.81 (m, H, CH), 2.08-2.14 (m, H, CH), 2.29 (s, 6H, 2 x CH_3), 2.36-2.49 (m, 4H, 4 x CH), 2.72-2.78 (m, H, CH), 2.93-3.02 (m, H, CH), 3.07-3.14 (m, H, CH), 3.96 (t, $J=6.80$ Hz, 2H, OCH_2), 4.97-5.05 (m, 2H, *gem.* CH_2), 5.11-5.18 (m, 2H, *gem.* CH_2), 5.70-5.92 (m, 2H, 2 x alkene CH), 6.86 (d, $J=8.40$ Hz, H, Ar CH), 6.94-6.98 (m, H, Ar CH), 7.34-7.41 (m, 2H, 2 x Ar CH); δ_C (100 MHz, $CDCl_3$) 25.0 (CH_2), 27.7 (CH_2), 33.8 (CH_2), 34.2 (CH), 36.1 (CH_2), 47.3 (2 x CH_3), 67.1 (OCH_2), 111.0 (Ar CH), 113.6 (C), 116.7 (*gem.* CH_2), 117.8 (*gem.* CH_2), 119.3 (C), 119.8 (Ar CH), 130.3 (Ar CH), 130.5 (Ar CH), 134.6 (alkene CH), 134.9 (alkene CH), 154.8 (C), 157.4 (C), 158.0 (C), 173.8 (C).

5-Prop-2-enyl-4-(2,2-dimethylhydrazono)-3-(2-(pent-4-en-1-yloxy)phenyl)-4,5,6,7-tetrahydrobenzo[d]isoxazole 116



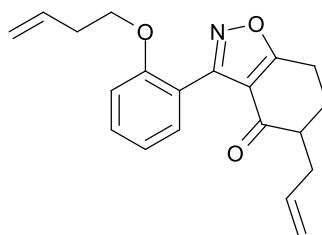
Orange gel (49%); MS(EI+) $C_{23}H_{30}N_3O_2$ requires 380.2338 [M+H] found 380.2329 -2.3670 ppm; ν_{max} (ATR)/ cm^{-1} 1630 (C=N); δ_H (400 MHz, $CDCl_3$) 1.70-1.83 (m, 3H, 3 x CH), 2.05-2.12 (m, 3H, 3 x CH), 2.31 (s, 6H, 2 x CH_3), 2.38-2.53 (m, 2H, 2 x CH), 2.74-2.80 (m, H, CH), 2.93-2.99 (m, H, CH), 3.07-3.15 (m, H, CH), 3.94 (t, $J=6.40$ Hz, 2H, OCH_2), 4.93-5.03 (m, 2H, *gem.* CH_2), 5.13-5.20 (m, 2H, *gem.* CH_2), 5.72-5.94 (m, 2H, 2 x alkene CH), 6.88 (d, $J=8.40$ Hz, H, Ar CH), 6.96-7.04 (m, H, Ar CH), 7.36-7.46 (m, 2H, 2 x Ar CH); δ_C (100 MHz, $CDCl_3$) 23.9 (CH_2), 26.6 (CH_2), 27.5 (CH_2), 29.1 (CH_2), 33.2 (CH), 35.0 (CH_2), 46.3 (2 x CH_3), 66.1 (OCH_2), 110.0 (Ar CH), 112.6 (C), 113.9 (*gem.* CH_2), 116.8 (*gem.* CH_2), 118.2 (C), 118.7 (Ar CH), 129.2 (Ar CH), 129.4 (Ar CH), 133.8 (alkene CH), 137.0 (alkene CH), 153.7 (C), 156.5 (C), 157.0 (C), 172.8 (C).

5-Prop-2-enyl-4-(2,2-dimethylhydrazono)-3-(2-(hex-5-en-1-yloxy)phenyl)-4,5,6,7-tetrahydrobenzo[d]isoxazole 117



Orange gel (63%); MS(EI+) $C_{24}H_{32}N_3O_2$ requires 394.2495 [M+H] found 394.2481 -3.5511 ppm; ν_{max} (ATR)/ cm^{-1} 1633 (C=N); δ_H (400 MHz, $CDCl_3$) 1.24-1.32 (m, 2H, 2 x CH), 1.48-1.67 (m, 3H, 3 x CH), 1.87-2.00 (m, 3H, 3 x CH), 2.16 (s, 6H, 2 x CH_3), 2.23-2.33 (m, 2H, 2 x CH), 2.58-2.64 (m, H, CH), 2.80-2.86 (m, H, CH), 2.93-2.99 (m, H, CH), 3.80 (t, J=6.40 Hz, 2H, OCH_2), 4.79-5.08 (m, 4H, 2 x *gem.* CH_2), 5.56-5.79 (m, 2H, 2 x alkene CH), 6.73 (d, J=8.00 Hz, H, Ar CH), 6.82 (t, J=7.20 Hz, H, Ar CH), 7.19-7.29 (m, 2H, 2 x Ar CH); δ_C (100 MHz, $CDCl_3$) 23.9 (CH_2), 24.3 (CH_2), 26.7 (CH_2), 27.7 (CH_2), 32.5 (CH_2), 33.1 (CH), 35.0 (CH_2), 46.2 (2 x CH_3), 66.6 (OCH_2), 109.8 (Ar CH), 112.6 (C), 113.6 (*gem.* CH_2), 116.7 (*gem.* CH_2), 118.3 (C), 118.5 (Ar CH), 129.1 (Ar CH), 129.4 (Ar CH), 133.8 (alkene CH), 137.5 (alkene CH), 153.6 (C), 156.6 (C), 157.0 (C), 172.7 (C).

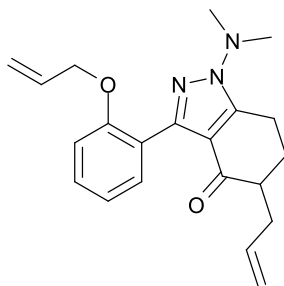
5-Prop-2-enyl-3-(2-(but-3-en-1-yloxy)phenyl)-6,7-dihydrobenzo[d]isoxazol-4(5H)-one **90'**



A solution of 5-prop-2-enyl-3-(2-(but-3-en-1-yloxy)phenyl)-4-(2,2-dimethylhydrazono)-4,5,6,7-tetrahydrobenzo[d]isoxazole **108** (0.369g, 1.01 mMol) and iodomethane (3.58g, 25.2 mMol) in THF (25 mL) was refluxed for two days. After this 2M hydrochloric acid (10 mL) was added and the solution was left to stir for another six hours. Following this the reaction mixture was extracted with dichloromethane (3 x 10 mL). The combined organic extracts were washed with water (15 mL) and brine (15 mL), dried over magnesium sulfate, filtered and concentrated under reduced pressure. The crude product was purified *via* preparative thin layer chromatography using light petroleum:ethyl acetate (1:1 v/v) to yield 5-prop-2-enyl-3-(2-(but-3-en-1-yloxy)phenyl)-6,7-dihydrobenzo[d]isoxazol-4(5H)-one **86** as a yellow oil (24 mg, 7%).

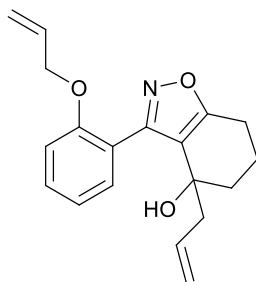
HRMS(EI+) $C_{20}H_{21}O_3NNa$ requires 346.1419 [M+Na] found 346.1410 -2.6001 ppm; ν_{max} (ATR)/ cm^{-1} 1689 (C=O); δ_H (400MHz; $CDCl_3$) 1.96-2.04 (m, H, CH), 2.35-2.42 (m, 3H, CH, CH_2), 2.45-2.54 (m, 2H, 2 x CH), 2.58-2.56 (m, H, CH), 2.82-2.92 (m, H, CH), 3.23-3.34 (m, H, CH), 4.04 (t, J-6.80 Hz, 2H, OCH_2), 5.00-5.09 (m, 2H, *gem.* CH_2), 5.13-5.27 (m, 2H, *gem.* CH_2), 5.70-5.96 (m 2H, 2 x alkene CH), 6.98-7.06 (m, 2H, 2 x Ar CH), 7.45-7.51 (m, 2H, 2 x Ar CH); δ_C (100MHz; $CDCl_3$) 27.7 (CH_2), 33.6 (CH_2), 34.6 (CH), 35.6 (CH_2), 37.6 (CH_2), 67.3 (OCH_2), 111.8 (Ar CH), 115.3 (C), 116.7 (*gem.* CH_2), 117.0 (Ar C), 118.5 (*gem.* CH_2), 120.4 (Ar CH), 130.4 (Ar CH), 131.1 (Ar CH), 134.1 (alkene CH), 134.6 (alkene CH), 157.3 (C), 157.7 (C), 182.1 (isoxazole CO), 191.3 (C=O).

5-Prop-2-enyl-3-(2-(prop-2-enyl)phenyl)-1-(dimethylamino)-6,7-dihydro-H-indazol-4(5H)-one 129



Brown crystal (by-product); MS(EI+) $C_{21}H_{26}N_3O_2$ requires 352.2025 [M+H] found 352.2012 -3.6911 ppm; ν_{max} (ATR)/ cm^{-1} 1666 (C=O); δ_H (400 MHz, $CDCl_3$) 1.84-1.94 (m, H, CH), 2.10-2.25 (m, 2H, 2 x CH), 2.36-2.43 (m, H, CH), 2.63-2.69 (m, H, CH), 2.72-2.82 (m, H, CH), 2.90 (s, 6H, 2 x CH_3), 2.94-3.06 (m, H, CH), 4.52 (m, 2H, OCH_2), 5.01-5.08 (m, 2H, *gem.* CH_2), 5.13 (dd, $J=10.80, 1.60$ Hz, H, *cis-gem.* CH_2), 5.26 (dd, $J=17.20, 1.60$ Hz, H, *trans-gem.* CH_2), 5.75-5.97 (m, 2H, 2 x alkene CH), 6.92-6.90 (m, 2H, 2 x Ar CH), 7.28-7.33 (m, H, Ar CH), 7.39 (dd, $J=7.20, 1.60$ Hz, H, Ar CH); δ_C (100 MHz, $CDCl_3$) 20.3 (CH_2), 27.9 (CH_2), 33.7 (CH_2), 46.1 (2 x CH_3), 47.0 (CH), 69.4 (OCH_2), 112.7 (Ar CH), 114.6 (C), 116.4 (*gem.* CH_2), 116.6 (*gem.* CH_2), 120.6 (Ar CH), 122.7 (C), 129.9 (Ar CH), 131.0 (Ar CH), 133.9 (alkene CH), 136.9 (alkene CH), 146.1 (C), 147.2 (C), 157.1 (C), 192.9 (C=O).

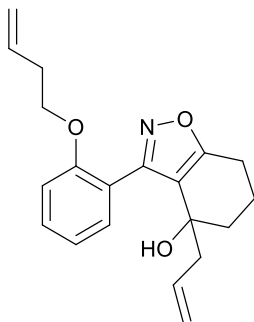
4-Prop-2-enyl-3-(2-(prop-2-enyloxy)phenyl)-4,5,6,7-tetrahydrobenzo[d]isoxazol-4-ol **130**



A solution of 3-(2-(prop-2-enyloxy)phenyl)-6,7-dihydrobenzo[d]isoxazol-4(5H)-one **70** (0.250 g, 0.930 mMol) in anhydrous THF (10 mL) was prepared and cooled to 0°C under an atmosphere of nitrogen. Following this, prop-2-enyl magnesium bromide (1.02 mL, 1.02 mMol) was slowly added over an hour and then left to warm to room temperature over 30 minutes. Saturated ammonium chloride solution (2 mL) was then added to the solution and it was allowed to stir for 30 minutes under an open atmosphere. The mixture was then diluted with DCM (10 mL) and water (10mL), the organic layer was separated and washed with water (10mL) and saturated sodium chloride solution (10mL). The organic layer was dried over magnesium sulfate and concentrated under reduced pressure. The crude product was purified *via* flash column chromatography using isohexane:ethyl acetate (1:1 v/v) as eluent to yield 4-prop-2-enyl-3-(2-(prop-2-enyloxy)phenyl)-4,5,6,7-tetrahydrobenzo[d]isoxazol-4-ol **130** (0.109g, 38%) as a yellow oil.

ν_{\max} (ATR)/ cm^{-1} 3529 (OH); MS(EI+) $\text{C}_{19}\text{H}_{22}\text{NO}_3$ requires 312.1560 [M+H] found 312.1593 10.5716 ppm; δ_{H} (500 MHz, CDCl_3) 1.54-1.64 (m, H, CH), 1.79-1.87 (m, H, CH), 1.88-1.98 (m, H, CH), 2.11-2.21 (m, 2H, 2 x CH), 2.26 (dd, $J=13.90, 7.40$ Hz, H, CH), 2.60 (ddd, $J=17.50, 11.70, 6.00$ Hz, H, CH), 2.82 (m, H, CH), 3.82 (s, H, OH), 4.55-4.67 (m, 2H, OCH_2), 4.77 (dd, $J=17.10, 1.10$ Hz, H, *trans-gem.* CH_2), 4.88 (dd, $J=10.20, 1.10$ Hz, H, *cis-gem.* CH_2), 5.31 (dd, $J=10.40, 0.9$ Hz, H, *cis-gem.* CH_2), 5.37 (dd, $J=17.20, 0.90$ Hz, H, *trans-gem.* CH_2), 5.40-5.49 (m, H, alkene CH), 5.93-6.01 (m, H, alkene CH), 7.05 (dd, $J=8.30$ Hz, H, Ar CH), 7.10 (t, $J=7.50$ Hz, H, Ar CH), 7.41 (dd, $J=7.50, 1.50$ Hz, H, Ar CH), 7.42-7.47 (m, H, Ar CH). δ_{C} (125 MHz, CDCl_3) 18.4 (CH_2), 23.1 (CH_2), 34.7 (CH_2), 45.4 (CH_2), 68.5 (COH), 70.8 (OCH_2), 113.6 (Ar CH) 117.2 (C), 118.0 (*gem.* CH_2), 119.9 (*gem.* CH_2), 120.5 (C), 122.2 (Ar CH), 131.3 (Ar CH), 131.6 (Ar CH), 131.7 (alkene CH), 133.6 (alkene CH), 155.3 (Ar C), 158.1 (C), 170.1 (C).

4-Prop-2-enyl-3-(2-(but-3-en-1-yloxy)phenyl)-4,5,6,7-tetrahydrobenzo[d]isoxazol-4-ol **131**



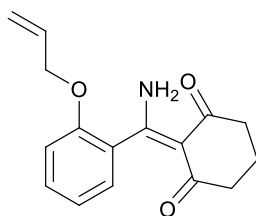
A solution of 3-(2-(but-3-en-1-yloxy)phenyl)-6,7-dihydrobenzo[d]isoxazol-4(5H)-one **77** (0.250 g, 0.880 mMol) in anhydrous THF (10 mL) was prepared and cooled to 0°C under an atmosphere of nitrogen. Following this, prop-2-enyl magnesium bromide (1.66 mL, 1.66 mMol) was slowly added over an hour and left to warm to room temperature over 10 minutes. Saturated ammonium chloride solution (2 mL) was then added to the solution and it was allowed to stir for 30 minutes under an open atmosphere. The mixture was then diluted with DCM (10 mL) and water (10mL), the organic layer was separated and washed with water (10mL) and saturated sodium chloride solution (10mL). The organic layer was dried over magnesium sulfate and concentrated under reduced pressure. The crude product was purified *via* flash column chromatography using isohexane:ethyl acetate (1:1 v/v) as eluent to yield 4-prop-2-enyl-3-(2-(but-3-en-1-yloxy)phenyl)-4,5,6,7-tetrahydrobenzo[d]isoxazol-4-ol **131** (0.199g, 70%) as a yellow oil.

MS(EI+) $C_{20}H_{23}NO_2Na$ requires 348.1576, $[M+Na]$ found 348.1567 -2.5850 ppm; δ_H (500 MHz, $CDCl_3$) 1.56-1.65 (m, H, CH), 1.77-1.86 (m, H, CH), 1.88-1.99 (m, H, CH), 2.14 (dd, $J=14.00$, 7.30 Hz, 2H, 2 x CH), 2.24 (dd, $J=14.00$, 7.30 Hz, H, CH), 2.39-2.50 (m, 2H, CH_2), 2.59 (m, H, CH), 2.86 (m, H, CH), 3.91 (s, H, OH), 3.97 (dt, $J=9.40$, 7.00 Hz, H, OCH_2), 4.22 (dt, $J=9.40$, 7.00 Hz, H, OCH_2), 4.77 (dd, $J=17.10$, 1.30 Hz, H, *trans-gem.* CH_2), 4.88 (dd, $J=9.60$, 1.30 Hz, H, *cis-gem.* CH_2), 5.01-5.11 (m, 2H, *gem.* CH_2), 5.45 (m, H, alkene CH), 5.64-5.77 (m, H, alkene CH), 7.02-7.14 (m, 2H, 2 x Ar CH), 7.39 (dd, $J=7.50$, 1.60 Hz, H, Ar CH), 7.44 (td, $J=8.30$, 1.60 Hz, H, Ar CH); δ_C (125 MHz, $CDCl_3$) 18.5 (CH_2), 23.1 (CH_2), 33.3 (CH_2), 34.7 (CH_2), 45.5 (CH_2), 68.5 (COH), 69.67 (OCH_2), 114.2 (Ar CH), 117.2 (C), 117.8 (*gem.* CH_2), 117.9 (*gem.* CH_2), 120.7 (C), 122.3 (Ar CH), 131.3 (Ar CH), 131.4 (Ar CH), 133.1 (alkene CH), 133.6 (alkene CH), 155.6 (C), 158.0 (C), 170.0 (C).

General procedure for isoxazole ring cleavage

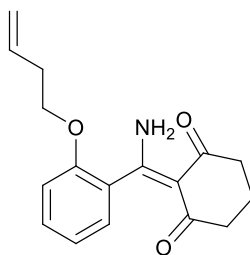
Isoxazole (1.00 mMol) was added to a solution of molybdenum hexacarbonyl (1.00 mMol) in acetonitrile (8 mL) and water (2 mL). This mixture was then heated to reflux for 1 hour. Following this 2M hydrochloric acid (1mL) was added and the mixture was stirred for 30 minutes, before being filtered through a pad of celite. After the mixture was diluted with DCM (10 mL) and extracted. The extracted organic layers were then washed with water (10 mL) and saturated sodium chloride solution (10 mL) before being dried over magnesium sulfate and concentrated under reduced pressure. The crude product was then purified *via* flash column chromatography using light petroleum:ethyl acetate (1:1 v/v) as eluent to yield the desired enamino ketone.

2-((2-(Prop-2-enyloxy)phenyl)(amino)methylene)cyclohexane-1,3-dione 135



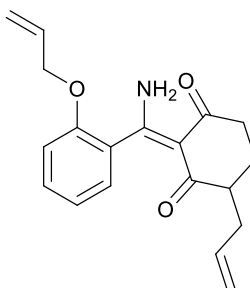
White crystals (85%) M.p. 168-170; HRMS(EI+) $C_{16}H_{17}NO_3Na$ requires 294.1106 [M+Na] found 294.1099 -2.3801 ppm; ν_{max} (ATR)/ cm^{-1} 1623 (C=O), 3185 (NH); δ_H (400 MHz, $CDCl_3$) 1.95 (quintet, $J=6.00$ Hz, 2H, CH_2), 2.49 (t, $J=6.00$ Hz, 4H, 2 x CH_2), 4.52-4.54 (m, 2H, OCH_2), 5.24 (dd, $J=10.80, 1.60$ Hz, H, *cis-gem.* CH_2), 5.36 (dd, $J=17.20, 1.60$ Hz, H, *trans-gem.* CH_2), 6.20 (broad s, H, NH), 6.91 (d, $J=8.40$ Hz, H, Ar CH), 7.01-7.05 (m, H, Ar CH), 7.15 (dd, $J=7.20$ Hz, 1.60 Hz, H, Ar CH), 7.37-7.41 (m, H, Ar CH), 12.01 (broad s, H, NH); δ_C (100MHz; $CDCl_3$) 18.2 (CH_2), 37.9 (2 x CH_2), 68.2 (OCH_2), 108.7 (C), 111.3 (Ar CH), 116.2 (*gem.* CH_2), 119.9 (Ar CH), 126.3 (Ar CH), 127.0 (C), 129.7 (Ar CH), 131.9 (alkene CH), 153.6 (C), 168.4 (C), 197.3 (broad s, 2 x C=O).

2-(Amino(2-(but-3-en-1-yloxy)phenyl)methylene)cyclohexane-1,3-dione 136



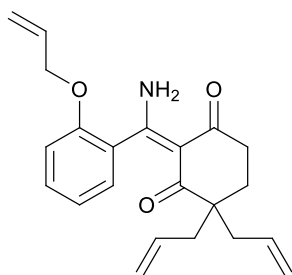
Yellow crystals (88%) M.p. 152-153; HRMS(EI+) $C_{17}H_{20}NO_3Na$ requires 286.1443 [M+Na] found 286.1435 -2.7958 ppm; δ_H (500 MHz, $CDCl_3$) 1.87-1.98 (m, 2H, CH_2), 2.41-2.46 (m, 6H, 3 x CH_2), 3.99 (t, J=6.60 Hz, 2H, CH_2), 5.01-5.15 (m, 2H, *gem.* CH_2), 5.73-5.85 (m, H, alkene CH), 6.31 (broad s, H, NH), 6.89 (d, J=8.30 Hz, H, Ar CH), 6.97 (t, J=7.40 Hz, H, Ar CH), 7.08 (d, J=7.40 Hz, H, Ar CH), 7.31-7.39 (m, H, Ar CH), 12.03 (bs, H, NH); δ_C (125 MHz, $CDCl_3$) 19.3 (CH_2), 33.6 (CH_2), 38.9 (CH_2), 67.6 (O CH_2), 109.5 (C), 112.0 (Ar CH), 117.1 (*gem.* CH_2), 120.7 (Ar CH), 127.4 (Ar CH), 127.9 (C), 130.7 (Ar CH), 134.4 (alkene CH), 154.9 (C), 169.8 (C), 198 (broad s 2 x C=O).

4-Prop-2-enyl-2-((2-(prop-2-enyloxy)phenyl)(amino)methylene)cyclohexane-1,3-dione 139



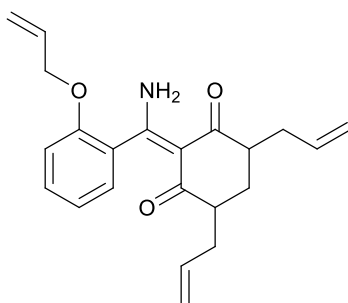
Yellow crystals (28%) M.p. 87-89; HRMS(EI+) $C_{19}H_{22}NO_3$ requires 312.1600 [M+H] found 312.1589 - 3.5238 ppm; ν_{max} (ATR)/ cm^{-1} 1630 (C=O); δ_H (500 MHz, $CDCl_3$) 1.65-1.72 (m, H, CH), 1.95-2.04 (m, H, CH), 2.06-2.22 (m, H, CH), 2.43-2.64 (m, 4H, 4 x CH), 4.49 (d, J=4.10 Hz, 2H, O CH_2), 5.01-5.06 (m, 2H, *gem.* CH_2), 5.22 (dd, J=10.60, 1.30, H, *cis-gem.* CH_2), 5.33 (dd, J=17.30, 1.30 Hz, *trans-gem.* CH_2), 5.73-5.81 (m, H, alkene CH), 5.84-6.02 (m, H, alkene CH), 6.25 (bs, H, NH), 6.89 (d, J=8.30 Hz, H, Ar CH), 6.99 (t, J=7.40 Hz, H, Ar CH), 7.10 (d, J=7.40 Hz, H, Ar CH), 7.31-7.39 (m, H, Ar CH), 12.04 (broad s, H, NH); δ_C (125 MHz, $CDCl_3$) 23.7 (CH_2), 34.7 (CH_2), 37.4 (CH_2), 46.4 (CH), 69.1 (O CH_2), 109.2 (C), 112.3 (Ar CH), 116.5 (*gem.* CH_2), 117.2 (*gem.* CH_2), 120.9 (Ar CH), 127.4 (Ar CH), 128.2 (C), 130.7 (Ar CH), 133.0 (alkene CH), 136.7 (alkene CH), 154.6 (C), 169.6 (C); the remaining quaternary carbons could not be detected under the experimental conditions.

4,4-Diprop-2-enyl -2-((2-(prop-2-enyloxy)phenyl)(amino)methylene)cyclohexane-1,3-dione 140



Yellow crystals (4%) M.p. 91-93; HRMS(EI+) $C_{22}H_{26}NO_3$ requires 352.1913 [M+H] found 352.1900 - 3.6912 ppm; ν_{max} (ATR)/ cm^{-1} 1631 (C=O); δ_H (400 MHz, $CDCl_3$) 1.79 (t, $J=6.80$ Hz, 2H, CH_2), 2.12-2.17 (m, 2H, 2 x CH), 2.37-2.45 (m, 4H, 4 x CH), 4.46-4.48 (m, 2H, OCH_2), 5.00-5.04 (m, 4H, 2 x *gem.* CH_2), 5.19 (dd, $J=10.80, 1.60$ Hz, H, *cis-gem.* CH_2), 5.31 (dd, $J=17.20, 1.60$ Hz, H, *trans-gem.* CH_2), 5.65-5.75 (m, 2H, 2 x alkene CH), 5.88-5.97 (m, H, alkene CH), 6.58 (broad s, H, NH), 6.86 (d, $J=8.40$ Hz, H, Ar CH), 6.97 (t, $J=7.60$ Hz, H, Ar CH), 7.05 (dd, $J=7.60, 1.60$ Hz, H, Ar CH), 7.31-7.36 (m, H, Ar CH), 12.01 (broad s, H, NH); δ_C (100 MHz, $CDCl_3$) 25.6 (CH_2), 33.3 (CH_2), 39.6 (CH_2), 46.2 (C), 68.0 (OCH_2), 107.8 (C), 111.2 (Ar CH), 116.2 (*gem.* CH_2), 116.8 (2 x *gem.* CH_2), 119.8 (Ar CH), 126.4 (Ar CH), 127.3 (C), 129.5 (Ar CH), 131.9 (alkene CH), 133.5 (2 x alkene CH), 153.4 (C), 169.2 (C), 197.2 (broad s C=O), 199.3 (broad s C=O).

4,6-Diprop-2-enyl-2-((2-(prop-2-enyloxy)phenyl)(amino)methylene)cyclohexane-1,3-dione 141

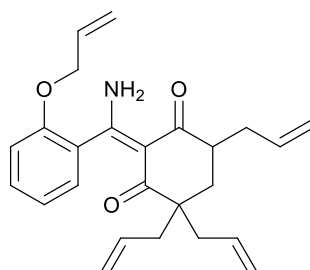


Yellow crystals (28%); HRMS(EI+) $C_{22}H_{26}NO_3$ requires 352.1913 [M+H] found 352.1906 -1.9876 ppm; ν_{max} (ATR)/ cm^{-1} 1629 (C=O); δ_H (400 MHz, $CDCl_3$) 1.33-1.43 (m, H, CH), 1.83 (t, $J=6.40$ Hz, H, CH), 2.00-2.04 (m, H, CH), 2.12-2.21 (m, 2H, 2 x CH), 2.41-2.69 (m, 4H, 4 x CH), 4.48-4.49 (m, 2H, OCH_2), 5.00-5.07 (m, 4H, 2 x *gem.* CH_2), 5.21-5.34 (m, 2H, *gem.* CH_2), 5.66-5.82 (m, 2H, 2 x alkene CH), 5.88-5.98 (m, H, alkene CH), 6.12 (broad s, $\frac{1}{2}H$, NH), 6.39 (broad s, $\frac{1}{2}H$, NH), 6.88 (d, $J=8.40$ Hz, H, Ar CH), 6.98 (t, $J=7.20$ Hz, H, Ar CH), 7.05-7.11 (m, H, Ar CH), 7.26-7.36 (m, H, Ar CH), 12.03 (broad s, H, NH); δ_C (100 MHz, $CDCl_3$) 25.6 (CH_2), 28.8 (CH_2), 33.3 (CH_2), 33.8 (CH_2), 39.6 (CH_2), 45.4 (2 x CH), 68.0 (OCH_2), 68.4 (OCH_2), 107.8 (C), 108.2 (C), 111.3 (Ar CH), 112.5 (Ar CH), 115.5 (*gem.* CH_2), 115.9 (*gem.* CH_2), 116.6 (*gem.* CH_2), 117.0 (*gem.* CH_2), 118.6 (Ar CH), 119.9 (Ar CH), 124.7 (C), 126.1 (Ar CH), 126.4 (Ar CH),

127.2 (C), 128.7 (C), 129.1 (Ar CH), 129.7 (Ar CH), 131.5 (Ar CH), 131.9 (Ar CH), 133.0 (CH), 133.2 (CH), 135.6 (2 x alkene CH), 152.2 (C), 153.4 (C), 158.7 (C), 168.5 (C), 197.8 (broad C=O).

^1H and ^{13}C spectra indicated the presence of a mixture of diastereomers.

4,4,6-Triprop-2-enyl -2-((2-(prop-2-enyl)phenyl)(amino)methylene)cyclohexane-1,3-dione 142

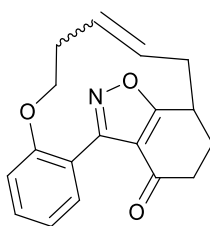


Brown gel (3%); HRMS(EI+) $\text{C}_{25}\text{H}_{30}\text{NO}_3$ requires 392.2226 [M+H] found 392.2221 -1.2748 ppm; ν_{max} (ATR)/ cm^{-1} 1633 (C=O); δ_{H} (400 MHz, CDCl_3) 1.63-1.77 (m, 2H CH_2), 2.03-2.11 (m, 2H, 2 x CH), 2.27-2.41 (m, 2H, 2 x CH), 2.56-2.58 (m, 2H, 2 x CH), 2.69-2.72 (m, H, CH), 4.50 (d, $J=4.80$ Hz, 2H, OCH_2), 4.99-5.09 (m, 6H, 3 x *gem.* CH_2), 5.22 (dd, $J=10.80, 2.80$ Hz, H, *cis-gem.* CH_2), 5.33 (dd, $J=15.60, 2.80$ Hz, H, *trans-gem.* CH_2), 5.62-5.83 (m, 3H, 3 x alkene CH), 5.88-5.99 (m, H, alkene CH), 6.12 (broad s, H, NH), 6.89 (d, $J=8.40$, H, Ar CH), 6.96-7.01 (m, H, Ar CH), 7.10 (dd, $J=7.20, 1.60$ Hz, Ar CH), 7.33-7.38 (m, H, Ar CH), 12.10 (broad s, H, NH); δ_{C} (100 MHz, CDCl_3) 31.3 (CH_2), 33.8 (CH_2), 40.5 (CH_2), 40.8 (CH) 46.8 (C), 68.0 (OCH_2), 111.3 (Ar CH), 116.2 (*gem.* CH_2), 116.5 (*gem.* CH_2), 116.6 (*gem.* CH_2), 117.1 (*gem.* CH_2), 119.9 (Ar CH), 126.4 (Ar CH), 127.5 (C), 129.6 (Ar CH), 131.9 (alkene CH), 132.9 (alkene CH), 134.0 (alkene CH), 135.7 (alkene CH), 153.4 (C), 168.7 (C); the remaining quaternary carbons could not be detected under the experimental conditions.

General procedure for ring closing metathesis

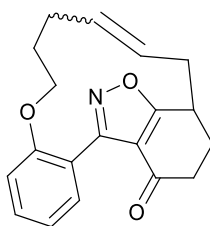
Diene (1.00 mMol) was dissolved in dry degassed dichloromethane. This Grubbs 2nd generation catalyst (0.10 mMol) was added in one portion and the mixture was stirred at reflux for 18 hours. The reaction was then allowed to cool to room temperature and evaporated to dryness under reduced pressure. The crude product was then purified *via* flash column chromatography using light petroleum:ethyl acetate:dichloromethane (5:1:4 v/v/v) as eluent (unless otherwise stated) to yield the purified macrocyclic compound.

5,6-Dihydro-3,5-ethanobenzo[2,3][1]oxacyclododecino[4,5-c]isoxazol-4(9H)-one 148



Dark green solid (60%); ν_{\max} (ATR)/ cm^{-1} 1683 (C=O); δ_{H} (400 MHz, CDCl_3) 3.93-4.03 (m, 2H, OCH_2), 6.93-6.99 (m, presumed multiple aromatic H), 7.25-7.42 (m, presumed to be multiple aromatic H); the remainder of the ^1H NMR suggests a complex mixture of diastereomers with peaks that may be consistent with the macrocyclic structure proposed. ^{13}C NMR spectra displayed a complex mixture of diastereomers with peaks that may be consistent with the macrocyclic structure proposed.

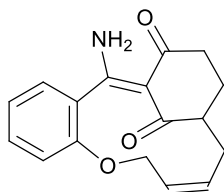
5,6-Dihydro-3,5-ethanobenzo[2,3][1]oxacyclotridecino[4,5-c]isoxazol-4(9H)-one 149



Beige solid (47%) not of sufficient purity for melting point analysis; HRMS(EI+) $\text{C}_{19}\text{H}_{20}\text{NO}_3$ requires 310.1443 [M+H] found 310.1431 -3.8692 ppm; ν_{\max} (ATR)/ cm^{-1} 1681 (C=O); δ_{H} (400 MHz, CDCl_3) 3.87-4.16 (m, 2CH, OCH_2), 6.91-7.01 (m, presumed multiple aromatic H), 7.25-7.41 (m, presumed to be multiple aromatic H); the remainder of the ^1H NMR suggests a complex mixture of diastereomers with peaks that may be consistent with the macrocyclic structure proposed. ^{13}C NMR spectra displayed a complex mixture of diastereomers with peaks that may be consistent with the macrocyclic structure proposed.

(3Z,10E)-11-Amino-5,6,7,8-tetrahydro-6,10-methanobenzo[b][1]oxacyclotridecine-9,16(2H)-dione

154

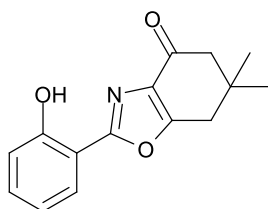


Column eluent: ethyl acetate; purple gel (30%); HRMS(EI+) $C_{17}H_{17}NO_3Na$ requires 306.1106 [M+Na] found 306.1093 -4.2468 ppm; δ_H (400 MHz, $CDCl_3$) 1.90-2.06 (m, 2H, CH_2), 2.39-2.54 (m, 3H, 3 x CH), 2.60 (dt, 16.40, 4.80 Hz, H, CH), 2.83-2.92 9 (m, H, CH), 4.21-4.25 (m, H, OCH), 4.60 (dd, J=10.40, 6.40 Hz, H, OCH), 5.95-6.12 (m, 3H, NH, 2 x alkene CH), 6.93 (d, J=8.40 Hz, H, Ar CH), 7.09 (t, J=7.60 Hz, H, Ar CH), 7.32 (dd, J=7.60, 2.00 Hz, H, Ar CH), 7.41-7.46 (m, H, Ar CH); δ_C (100 MHz, $CDCl_3$) 23.0 (CH_2), 29.3 (broad, CH_2), 37.0 (CH_2), 47.2 (CH), 62.5 (broad OCH_2), 110.7 (C), 113.4 (Ar CH), 121.7 (Ar CH), 124.9 (alkene CH), 127.7 (C), 128.0 (Ar CH), 131.7 (Ar CH), 137.7 (alkene CH), 154.4 (C), 166.5 (C), 198.5 (C=O), 199.0 (C=O).

General procedure for Benzisoxazole to Benzoxazole rearrangement

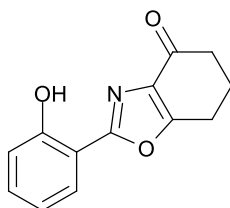
Benzisoxazole (4.37 mMol) and caesium carbonate (4.37 mMol) were dissolved in dry THF (30 mL), and the reaction mixture was heated under reflux for the stated period of time. 2M hydrochloric acid solution (10 mL) and dichloromethane (25 mL) or ethyl acetate (25 mL) were added to the reaction mixture after it had cooled to room temperature. The mixture was then separated and the organic layer was washed with water (25 mL) and saturated sodium chloride solution (25 mL), dried over magnesium sulfate and concentrated under reduced pressure to yield crude benzoxazole which used without purification, or purified *via* column chromatography using light petroleum:ethyl acetate (1:1 v/v) as a solvent.

2-(2-Hydroxyphenyl)-6,6-dimethyl-6,7-dihydrobenzo[d]oxazol-4(5H)-one 166



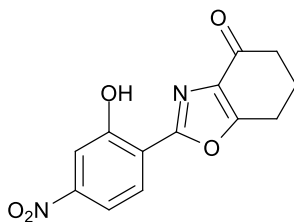
Beige solid (82%), m.p. 125-127°C, HRMS(EI+) $C_{15}H_{16}O_3N$ requires 258.1130 [M+H] found 258.1125 - 1.9371 ppm; ν_{max} (DCM)/ cm^{-1} 1694 (C=O), 3410 (OH); δ_H (400MHz; $CDCl_3$) 1.08 (s, 6H, 2 x CH_3), 2.41 (s, 2H, $OCCH_2$), 2.83 (s, 2H, $O=CCH_2$) 6.85 (t, J=8.00 Hz H, Ar CH), 6.97 (t, J=8.00 Hz, H, Ar CH), 7.29 (t, J=8.00 Hz H, Ar CH), 7.69 (d, J= 8.00Hz, H, Ar CH) 10.54 (broad s, H, OH); δ_C (100MHz; $CDCl_3$) 27.6 (2x CH_3), 34.5 (C) 34.9 (CH_2), 51.2 (CH_2) 109 (C), 116.4 (Ar CH), 118.5 (Ar CH), 125.3 (Ar CH), 131.9 (C), 132.1 (Ar CH), 156.5 (C), 160.6 (C,) 161.2 (C), 189.2 (C=O).

2-(2-Hydroxyphenyl)-6,7-dihydrobenzo[d]oxazol-4(5H)-one 167



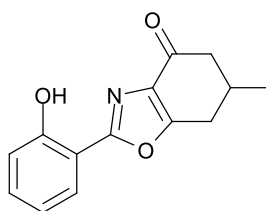
Beige solid (87%), decomposes 202-204°C, HRMS(EI+) $C_{13}H_{12}O_3N$ requires 230.0817 [M+H] found 230.0809 -3.4770 ppm; ν_{max} (DCM)/ cm^{-1} 1694 (C=O), 3408 (OH); δ_H (400MHz; $CDCl_3$) 2.20-2.27 (m, 2H, CH_2), 2.57 (t, J=5.60 Hz, 2H, $OCCH_2$), 3.00 (t, 2H, J=6.00 Hz, $O=CCH_2$), 6.86-6.90 (m, H, Ar CH), 7.10 (dd, J=0.80, 8.40Hz, H, Ar CH), 7.30-7.34 (m, H, Ar CH), 7.74 (dd, J=1.60, 8.00Hz, H, Ar CH) 10.58 (broad s, H, OH); δ_C (100MHz; $CDCl_3$) 22.2 (2x CH_2), 37.9 (CH_2), 110 (C), 117.6 (Ar CH), 119.5 (Ar CH), 126.3 (Ar CH), 133.2 (Ar CH), 133.7 (Ar C), 157.7 (C), 161.2 (C,) 163.0 (C), 190.7 (C=O).

2-(2-Hydroxy-4-nitrophenyl)-6,7-dihydrobenzo[d]oxazol-4(5H)-one 193



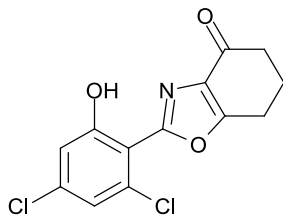
Yellow solid (77%) M.p. 184-186°C; HRMS(EI+) $C_{13}H_{11}N_2O_5$ requires 275.0668 [M+H] found 275.0659 - 3.2719 ppm; ν_{max} (DCM)/ cm^{-1} 1344 (NO₂) 1698 (C=O), 3584 (OH); δ_H (400MHz; CDCl₃) 2.35 (quin, J=6.40 Hz, 2H, CH₂), 2.69 (t, J=6.40 Hz, 2H, OCCH₂), 3.14 (t, J=6.4 Hz, 2H, O=CCH₂), 7.19 (d, J=9.20 Hz, H, Ar CH), 8.28 (dd, J= 9.20, 2.80 Hz, H, Ar CH), 8.78 (d, J=2.80 Hz, H, Ar CH), 11.50 (broad s, H, Ar OH); δ_C (100MHz; CDCl₃) 21.1 (CH₂), 21.2 (CH₂), 36.9 (CH₂), 109.2 (C), 117.4 (Ar CH), 121.8 (Ar CH), 127.3 (Ar CH), 132.7 (C), 139.4 (C), 158.4 (C), 161.3 (C), 162.6 (C), 189.3 (C).

2-(2-Hydroxyphenyl)-6-methyl-6,7-dihydrobenzo[d]oxazol-4(5H)-one 203



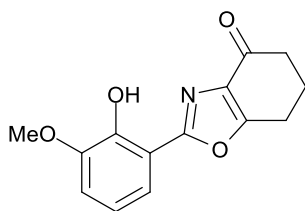
Beige solid (88%), M.p. 154-156°C, HRMS(EI+) $C_{14}H_{14}O_3N$ requires 244.0974 [M+H] found 244.0968 - 2.4580 ppm; ν_{max} (ATR)/ cm^{-1} 1680 (C=O), 3187 (OH); δ_H (400MHz; CDCl₃) 1.20 (d, J=6.40 Hz, 3H, CH₃), 2.32 (dd, J=16.00, 11.20 Hz, H, CH), 2.49-2.70 (m, 3H, 3 x CH), 3.07 (dd, J=17.20, 4.80 Hz H, CH), 6.87 (dd, J=8.00 Hz, H, Ar CH), 7.00 (d, 8.40 Hz, H, Ar CH), 7.30-7.34 (m, H, Ar CH), 7.69 (dd, J= 1.6, 8.00 Hz, H, Ar CH), 10.59 (broad s, H, OH); δ_C (100MHz; CDCl₃) 21.1 (CH₃), 29.9 (CH₂), 30.6 (CH), 46.4 (CH₂) 109.9 (C), 117.3 (Ar CH), 119.5 (Ar CH), 126.3 (Ar CH), 133.1 (Ar CH), 133.2 (Ar C), 157.4 (C), 161.2 (C), 162.8 (C), 190.3 (C=O).

2-(3,5-Dichloro-2-hydroxyphenyl)-6,7-dihydrobenzo[d]oxazol-4(5H)-one 204



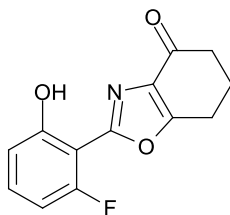
Brown solid (58%) Decomposes 165-167°C; HRMS(EI+) $C_{13}H_{10}NO_3^{35}Cl_2$ requires 298.0038 [M+H] found 298.0027 -3.6912 ppm; ν_{max} (DCM)/ cm^{-1} 1698 (C=O), 3691 (OH); δ_H (400MHz; $CDCl_3$) 2.32-2.35 (m, 2H, CH_2), 2.66 (t, J=6.40 Hz, 2H, $OCCH_2$), 3.11 (t, J=6.00 Hz, 2H, $O=CCH_2$), 7.46 (d, J=2.40 Hz, H, Ar CH), 7.70 (d, J= 2.40 Hz, H, Ar CH), 11.20 (broad s, H, Ar OH); δ_C (100MHz; $CDCl_3$) 22.1 (CH_2), 22.2 (CH_2), 37.9 (CH_2), 111.7 (C), 123.4 (C), 124.2 (Ar CH), 124.3 (C), 132.9 (Ar CH), 133.7 (C), 152.2 (C), 159.5 (C), 163.6 (C), 190.4 (C).

2-(2-Hydroxy-3-methoxyphenyl)-6,7-dihydrobenzo[d]oxazol-4(5H)-one 205



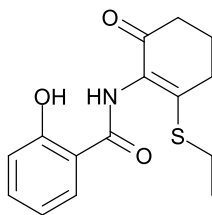
White solid (70%) M.p. 114-115°C; HRMS(EI+) $C_{14}H_{13}NO_4Na$ requires 282.0742 [M+Na] found 282.0731 -3.8997 ppm; ν_{max} (DCM)/ cm^{-1} 1693 (C=O), 3580 (OH); δ_H (400MHz; $CDCl_3$) 2.30 (quin, J=6.40 Hz, 2H, CH_2), 2.63 (t, J=6.40 Hz, 2H, $OCCH_2$), 3.06 (t, J=6.4 Hz, 2H, $O=CCH_2$), 3.92 (s, 3H, OCH_3), 6.89 (t, J=8.00, H, Ar CH), 6.98 (d, J=8.00, H, Ar CH), 7.41 (d, J=8.00 Hz, H, Ar CH), 10.79 (broad s, H, Ar OH); δ_C (100MHz; $CDCl_3$) 21.1 (CH_2), 21.2 (CH_2), 36.9 (CH_2), 55.4 (OCH_3), 109.2 (C), 113.7 (Ar CH), 116.8 (Ar CH), 118.3 (Ar CH), 132.6 (C), 146.8 (C), 147.6 (C), 160.2 (C), 161.9 (C), 189.6 (C).

2-(2-Fluoro-6-hydroxyphenyl)-6,7-dihydrobenzo[d]oxazol-4(5H)-one 206



White solid (75%), m.p. 200-202°C, HRMS(EI+) $C_{13}H_{11}O_3NF$ requires 248.07230 [M+H] found 248.0714 - 3.6280 ppm; ν_{max} (DCM)/ cm^{-1} 1684 (C=O), 3396 (OH); δ_H (400MHz; $CDCl_3$) 2.23-2.36 (m, 2H, CH_2), 2.67 (t, $J=7.20$ Hz, 2H, $OCCH_2$), 3.11 (t, $J=6.40$ Hz, 2H, $O=CCH_2$), 6.90 (td, $J=8.00, 4.80$ Hz, H, Ar CH), 7.18-7.23 (m, H, Ar CH), 7.29 (dt, $J=8.00, 1.20$ Hz, Ar CH), 10.54 (broad s, H, OH); δ_C (100MHz; $CDCl_3$) 21.1 (CH_2), 21.2 (CH_2) 36.9 (CH_2) 111.3 (d, $J=4$ Hz C-F, C), 118.1 (d, $J=2$ Hz C-F, Ar CH) 118.3 (d, $J=13$ Hz C-F, Ar CH), 120.3 (d, $J=3$ Hz C-F, Ar CH), 145.2 (d $J=13$ Hz C-F, C), 150.6 (d, $J=244$ Hz C-F, Ar CF), 159.4 (d, $J=4$ Hz C-F, C), 162.1 (C), 189.5 (C). The remaining quaternary carbon could not be distinguished from the noise in the time allocated for this experiment.

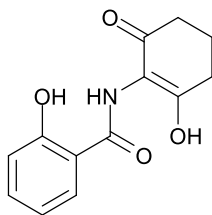
N-(2-(Ethylthio)-6-oxocyclohex-1-en-1-yl)-2-hydroxybenzamide **186**



3-(2-Hydroxyphenyl)-6,7-dihydrobenzo[d]isoxazol-4(5H)-one **61** (2.18 mMol, 0.500g), thioethane (2.18 mMol, 0.135g) and caesium carbonate (2.18 mMol, 0.720g) were dissolved in dry THF (10 mL), and the reaction mixture was heated under reflux for 4 hours. 2M Hydrochloric acid (10 mL) and dichloromethane (10 mL) were added to the reaction mixture after it had cooled to room temperature. The mixture was then separated and the organic layer was washed with water (10 mL) and saturated sodium chloride solution (10 mL), dried over magnesium sulfate and concentrated under reduced pressure to yield N-(2-(ethylthio)-6-oxocyclohex-1-en-1-yl)-2-hydroxybenzamide **175** as clear crystals (6%) decomposes 159-161°C.

HRMS(EI+) $C_{15}H_{17}O_3NSNa$ requires 314.0827 [M+Na] found 314.0819 -2.5471 ppm; ν_{max} (ATR)/ cm^{-1} 1628 (C=O), 3327 (OH); δ_H (400MHz; $CDCl_3$) 1.31 (t, J=7.20 Hz, 3H, CH_3), 2.14 (quintet, J=6.40 Hz, 2H, CH_2), 2.55 (t, J=6.40 Hz, 2H, O=C CH_2), 2.82 (t, J= 6.40 Hz, 2H, O=C CH_2), 2.90 (q, J=7.20 Hz, 2H, SCH $_2$), 6.84-6.89 (m, H, Ar CH), 6.95 (dd, J=8.40, 1.20 Hz, H, Ar CH), 7.38-7.40 (m, H, Ar CH), 7.59 (dd, J= 8.00, 1.60 Hz, H, Ar CH), 8.06 (broad s, H, NH), 11.85 (broad s, H, Ar OH); δ_C (100MHz; $CDCl_3$) 14.3 (CH_3), 22.0 (CH_2), 25.4 (CH_2), 29.5 (CH_2), 36.3 (CH_2), 114.1 (C), 118.5 (Ar CH), 118.9 (Ar CH), 126.3 (1 x Ar CH, 1 x C), 134.7 (Ar CH), 159.0 (C), 161.7 (C), 168.0 (C), 191.2 (C).

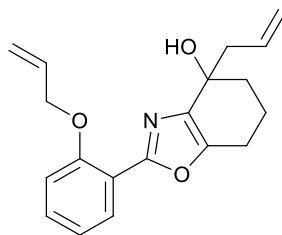
2-Hydroxy-N-(2-hydroxy-6-oxocyclohex-1-en-1-yl)benzamide **180**



3-(2-Hydroxyphenyl)-6,7-dihydrobenzo[d]isoxazol-4(5H)-one **61** (2.18 mMol, 0.500g) and caesium carbonate (4.36 mMol, 1.42g) were dissolved in ethanol (30 mL), and the reaction mixture was heated under reflux for the 4 hours. 1M Hydrochloric acid (20 mL) and dichloromethane (50 mL) was added to the reaction mixture after it had cooled to room temperature. The mixture was then separated and the organic layer was washed with water (50 mL) and saturated sodium chloride solution (50 mL), dried over magnesium sulfate and concentrated under reduced pressure to yield 2-hydroxy-N-(2-hydroxy-6-oxocyclohex-1-en-1-yl)benzamide **180** as a beige solid (91%).

M.p. 172-174°C; HRMS(EI+) $C_{13}H_{13}NO_4Na$ requires 270.0742 [M+Na] found 270.0729 -4.8135 ppm; ν_{max} (ATR)/ cm^{-1} 3177 (OH); δ_H (400MHz; $CDCl_3$) 2.06 (quin, $J=6.40$ Hz, 2H, CH_2), 2.56 (t, $J=6.40$ Hz, 2H, $OCCH_2$), 2.68 (t, $J=6.40$ Hz, 2H, $O=CCH_2$), 6.98 (t, $J=7.60$ Hz, Ar CH), 7.05 (d, $J=8.40$ Hz, H, Ar CH), 7.46-7.50 (m, H, Ar CH), 7.67 (d, $J=8.40$ Hz, H, Ar CH), 9.48 (broad s, H, OH), 10.93 (broad s, H, Ar OH), 12.88 (broad s, H, NH); δ_C (100MHz; $CDCl_3$) 20.3 (CH_2), 30.2(CH), 35.0 (CH_2), 113.4 (C), 113.7 (C), 118.9 (Ar CH), 119.8 (Ar CH), 127.1 (Ar CH), 135.2 (Ar CH), 160.8 (C), 165.9 (C), 167.4 (C), 192.9 (C).

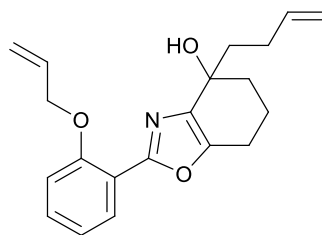
4-Prop-2-enyl-2-(2-(prop-2-enyloxy)phenyl)-4,5,6,7-tetrahydrobenzo[d]oxazol-4-ol **208**



1M Prop-2-enyl magnesium bromide solution in diethyl ether (12.12 mL, 12.12 mMol) was slowly added to a solution of 2-(2-hydroxyphenyl)-6,7-dihydrobenzo[d]oxazol-4(5H)-one **71** (1.63 g, 6.06 mMol) in dry THF (100 mL) at -50°C over an hour; after which the reaction mixture was left to warm to room temperature over 18 hours. The reaction was then quenched with aqueous hydrochloric acid (2M, 20 mL) and diluted with dichloromethane (100 mL). The reaction mixture was then washed with water (2 x 100 mL) and aqueous sodium chloride solution (1 x 100 mL) and dried over magnesium sulfate, filtered and concentrated under reduced pressure. The crude product was purified by flash column chromatography using isohexane:ethyl acetate (1:1 v/v) as eluent to yield 4-prop-2-enyl-2-(2-(prop-2-enyloxy)phenyl)-4,5,6,7-tetrahydrobenzo[d]oxazol-4-ol **208** (1.18g, 63%) as a yellow oil.

ν_{max} (ATR)/ cm^{-1} 3423 (OH); δ_{H} (400MHz; CDCl_3) 1.73-1.90 (m, 3H, 3 x CH), 1.95-2.06 (m, H, CH), 2.26 (s, H, OH), 2.53-2.61 (m, 2H, 2 x CH), 2.65-2.77 (m, 2H, 2 x CH), 4.53 (m, 2H, OCH_2), 5.06-5.14 (m, 2H, *gem.* CH_2), 5.22 (dd, $J=10.40$, Hz, *cis-gem.* CH_2), 5.53 (dd, $J=17.60$, 1.60 Hz, *trans-gem.* CH_2), 5.84-5.93 (m, H, alkene CH), 5.95-6.01 (m, H, alkene CH), 6.91-6.97 (m, 2H, 2 x Ar CH), 7.28-7.32 (m, H, Ar CH), 7.84 (dd, $J=7.60$, 1.60 Hz, H, Ar CH); δ_{C} (100MHz; CDCl_3) 19.3 (CH_2), 22.0 (CH_2), 35.4 (CH_2), 45.1 (CH_2), 69.3 (COH), 69.4 (OCH_2), 113.5 (Ar CH), 117.0 (2 x *gem.* CH_2), 117.7 (C), 118.8 (Ar CH), 130.5 (Ar CH), 131.2 (Ar CH), 132.9 (alkene CH), 133.9 (alkene CH), 138.5 (C), 148.0 (C), 156.4 (C), 159.0 (C).

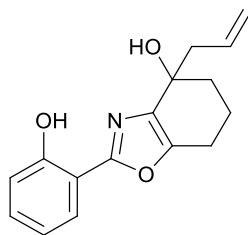
2-(2-(Prop-2-enyloxy)phenyl)-4-(but-3-en-1-yl)-4,5,6,7-tetrahydrobenzo[d]oxazol-4-ol 209



5-Bromo-1-pentene (1.00 g, 0.79 mL, 6.70 mMol) was added to magnesium turnings (0.179 g, 7.40 mMol) in dry THF (50 mL) and heated to reflux for one hour. This solution was then allowed to cool to room temperature before being slowly added to a solution of 3-(2-prop-2-enylphenyl)-6,7-dihydro-5H-1,2-benzoxazol-4-one **71** (0.90 g, 3.55 mMol) in dry THF (50 mL) at -40°C over an hour. The reaction mixture was allowed to warm to room temperature over 18 hours before being quenched with hydrochloric acid (2M, 10 mL) and diluted with dichloromethane (50 mL). The reaction mixture was then washed with water (2 x 50 mL) and aqueous sodium chloride solution (1 x 50 mL) and dried over magnesium sulfate, filtered and concentrated under reduced pressure. The crude product was purified by flash column chromatography using isohexane:ethyl acetate (1:1 v/v) as eluent to yield 3-(2-allyloxyphenyl)-4-pent-4-enyl-6,7-dihydro-5H-1,2-benzoxazol-4-ol **209** (0.46g, 41%) as a yellow oil.

δ_{H} (500MHz; CDCl_3) 1.43-1.48 (m, H, CH), 1.59-1.64 (m, H, CH), 1.76 (m, H, CH), 1.84-1.93 (m, 3H, 3 x CH), 1.99-2.11 (m, 4H, 4 x CH), 2.56-2.69 (m, 2H, 2 x CH), 2.93 (broad s, H, OH), 4.58-4.64 (m, 2H, OCH_2) 4.93 (dd, $J=10.00$, H, *cis-gem.* CH_2), 5.01 (dd, $J=18.50$, 1.50 Hz, H, *trans-gem.* CH_2), 5.28 (dd, $J=10.50$, 1.50 Hz, H, *cis-gem.* CH_2), 5.58 (dd, $J=17.50$, 1.50 H, *trans-gem.* CH_2), 5.77-5.86 (m, H, alkene CH), 6.02-6.10 (m, H, alkene CH), 6.95-7.02 (m, 2H, 2 x Ar CH), 7.32-7.40 (m, H, Ar CH), 7.88 (dd, $J=8.00$, 1.5, H, Ar CH); δ_{C} (125MHz; CDCl_3) 19.4 (CH_2), 22.0 (CH_2), 23.2 (CH_2), 34.2 (CH_2), 35.2 (CH_2), 37.0 (CH_2), 69.4 (COH), 69.8 (OCH_2), 113.5 (Ar CH), 114.4 (*gem.* CH_2), 117.0 (*gem.* CH_2), 117.6 (C), 120.9 (Ar CH), 130.4 (Ar CH), 131.2 (Ar CH), 132.8 (alkene CH), 138.9 (alkene CH), 139.0 (C), 147.7 (C), 156.4 (C), 158.7 (C).

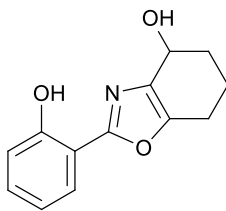
4- Prop-2-enyl-2-(2-hydroxyphenyl)-4,5,6,7-tetrahydrobenzo[d]oxazol-4-ol **212**



Grubbs II catalyst (0.273 g, 0.32 mMol) was added to a solution of 4-allyl-3-(2-allyloxyphenyl)-6,7-dihydro-5H-1,2-benzoxazol-4-ol **158** (0.50g, 1.60 mMol) in anhydrous toluene (80 mL). The reaction mixture was then heated to 90°C for 18 hours. Following this the residue was allowed to cool to room temperature before being concentrated under reduced pressure. The mixture was then purified by flash column chromatography using isohexane:ethyl acetate (1:1 v/v) as eluent to yield 4-prop-2-enyl-3-(2-hydroxyphenyl)-6,7-dihydro-5H-1,2-benzoxazol-4-ol **201** (0.12 g, 26%) as a dark green oil.

LCMS rt: 1.72 minutes; MS(ESI+) $C_{16}H_{18}NO_3$ requires 272.13 [M+H] found 272.15 73.49 ppm; δ_H (400MHz; $CDCl_3$) The aliphatic region of the spectra displays a complex mixture; 5.16-5.22 (m, 2H, *gem.* CH_2), 5.84-5.95 (m, H, alkene H), 6.88-6.96 (m, H, Ar CH), 7.04 (d, $J=7.60$ Hz, H, Ar CH) 7.30-7.35 (m, H, Ar CH), 7.78 (dd, $J=8.00, 2.00$ Hz, H, Ar CH), 11.13 (broad s, H, OH).

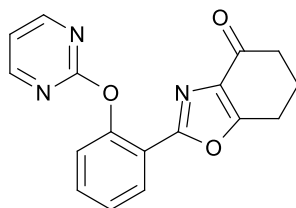
2-(2-Hydroxyphenyl)-4,5,6,7-tetrahydrobenzo[d]oxazol-4-ol 210



2-(2-Hydroxyphenyl)-6,7-dihydrobenzo[d]oxazol-4(5H)-one **167** (0.500g, 2.18 mMol) was dissolved in ethanol (20 mL). Sodium borohydride (0.082g, 2.18 mMol) was added and the mixture was heated at reflux for 18 hours. The reaction mixture was then quenched with water (15 mL) and washed three times with dichloromethane (3 x 15 mL). The combined organic extracts were then washed with saturated sodium chloride solution (30 mL), dried over magnesium sulfate, filtered and concentrated under reduced pressure to yield 2-(2-Hydroxyphenyl)-4,5,6,7-tetrahydrobenzo[d]oxazol-4-ol **108** as a cream solid (0.453g, 90%).

M.p. 142-143°C; HRMS(EI+) $C_{13}H_{13}O_3NNa$ requires 254.0793 [M+Na] found 254.0788 -1.9679 ppm; ν_{max} (ATR)/ cm^{-1} 3264 (OH); δ_H (400MHz; $CDCl_3$) 1.90-2.20 (m, 3H, 3 x CH), 2.30 (broad s, H, OH), 2.65-2.72 (m, H, CH), 2.77-2.84 (m, H, CH), 4.88 (t, J=4.00 Hz, 2H, OCH_2), 6.93-6.97 (m, H, Ar CH), 7.07 (dd, J=8.40, 1.20 Hz, H, Ar CH), 7.33-7.34 (m, H, Ar CH), 7.80 (dd, J=7.60, 1.20 Hz, H, Ar CH), 11.13 (broad s, H, OH); δ_C (100MHz; $CDCl_3$) 18.7 (CH_2), 21.7 (CH_2), 31.7 (CH_2), 63.1 (CH), 111.3 (C), 117.1 (Ar CH), 119.4 (Ar CH), 125.7 (Ar CH), 132.0 (Ar CH), 135.1 (C), 147.8 (C), 156.9 (C), 160.2 (C),

2-(2-(Pyrimidin-2-yloxy)phenyl)-6,7-dihydrobenzo[d]oxazol-4(5H)-one **216**



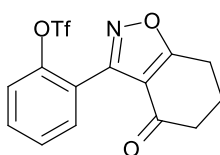
2-(2-Hydroxyphenyl)-6,7-dihydrobenzo[d]oxazol-4(5H)-one **167** (2.18 mMol, 0.500g), 2-chloropyrimidine (6.54 mMol, 0.750g), copper powder (2.18 mMol, 0.140g) and caesium carbonate (2.18 mMol, 0.720g) were dissolved in dry DMF (25 mL), and the reaction mixture was heated under reflux for 18 hours. Dichloromethane (50 mL) was added to the reaction mixture after it had cooled to room temperature. The mixture was then separated and the organic layer was washed with water (2 x 25mL) and saturated sodium chloride solution (25 mL), dried over magnesium sulfate and concentrated under reduced pressure. The crude residue was purified *via* flash column chromatography (light petroleum:ethyl acetate, (1:1 v/v) to yield 2-(2-(pyrimidin-2-yloxy)phenyl)-6,7-dihydrobenzo[d]oxazol-4(5H)-one **216** as intense yellow solid (47%).

M.p. 178-180°C; HRMS(EI+) $C_{17}H_{13}O_3N_3Na$ requires 330.0855 [M+Na] found 330.0846 -2.7265 ppm; ν_{max} (DCM)/ cm^{-1} 1692 (C=O); δ_H (400MHz; $CDCl_3$) 2.17 (quintet, J=6.40 Hz, 2H, CH_2), 2.55 (t, J=6.40 Hz, 2H, O=C CH_2), 2.80 (t, J= 6.40 Hz, 2H, O=C CH_2), 7.04 (t, J=4.80 Hz, H, Ar CH), 7.31 (dd, J=8.40, 1.20 Hz, H, Ar CH), 7.38-7.42 (m, H, Ar CH), 7.56-7.60 (m, H, Ar CH), 8.30 (dd, J=8.00, 1.60 Hz, H, Ar CH), 8.55 (d, J=4.80 H, Ar CH), 11.85 (broad s, H, Ar OH); δ_C (100MHz; $CDCl_3$) 22.1 (CH_2), 22.2 (CH_2), 37.9 (CH_2), 116.1 (Ar CH), 120.0 (C), 124.0 (Ar CH), 126.2 (Ar CH), 130.5 (Ar CH), 132.5 (Ar CH, C), 134.8 (C), 159.3 (C), 159.7 (C), 164.0 (2 x Ar CH), 165.6 (C), 191.4 (C).

General procedure for phenol *mono*-triflation

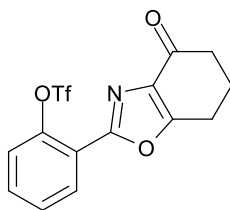
Triflic anhydride (1.47 mL, 4.37 mMol) was added dropwise to a solution of the phenol (4.37 mMol) and pyridine (0.70 mL, 4.37 mMol) in dichloromethane (50 mL) at 0°C. After 4 hours the reaction mixture was quenched with saturated ammonium chloride (25 mL) and separated. The organic layer was washed with 1M sodium hydroxide solution (2 x 25 mL) and saturated sodium chloride solution (50 mL). The organic layer was then dried over sodium sulfate, filtered and concentrated under reduced pressure. The crude product was purified *via* flash column chromatography using isohexane:ethyl acetate (1:1 v/v) as eluent to yield the desired phenol.

2-(4-Oxo-4,5,6,7-tetrahydrobenzo[d]isoxazol-3-yl)phenyl trifluoromethanesulfonate 220



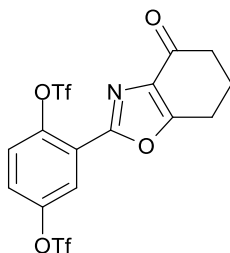
Brown gel (79%); MS(EI+) $C_{14}H_{10}NO_5F_3SNa$ requires 384.0130 [M+Na] found 384.0121 -2.3437 ppm; ν_{max} (ATR)/ cm^{-1} 1136 (S=O), 1691 (C=O); δ_H (400 MHz, $CDCl_3$) 2.27 (quintet, $J=6.40$ Hz, 2H, CH_2), 2.56 (t, $J=6.40$ Hz, 2H, CH_2), 3.10 (t, $J=6.40$ Hz, 2H, CH_2), 7.45 (dd, $J=8.40, 0.80$ Hz, H, Ar CH), 7.48-7.52 (m, H, Ar CH), 7.60-7.62 (m, H, Ar CH), 7.70 (dd, $J=7.60, 2.00$ Hz, H, Ar CH); δ_C (100 MHz, $CDCl_3$) 22.1 (CH_2), 23.22 (CH_2), 38.1 (CH_2), 114.8 (C), 118.5 (quartet, $J=319$ Hz, CF_3), 121.8 (Ar CH), 121.9 (C), 128.3 (Ar CH), 132.0 (Ar CH), 132.1 (Ar CH), 147.3 (C), 155.2 (C), 181.7 (isoxazole C), 191.5 (C=O); δ_F (376 Mhz, $CDCl_3$) 88.03 (CF_3).

2-(4-Oxo-4,5,6,7-tetrahydrobenzo[d]oxazol-2-yl)phenyl trifluoromethanesulfonate 221



White crystals (63%), M.p. 114-116°C; MS(EI+) $C_{14}H_{10}NO_5F_3SNa$ requires 384.0130 [M+Na] found 384.0115 1.5625 ppm; ν_{max} (ATR)/ cm^{-1} 1140 (S=O), 1688 (C=O); δ_H (400 MHz, $CDCl_3$) 2.31 (quintet, $J=6.00$ Hz, 2H, CH_2), 2.66 (t, $J=6.00$ Hz, 2H, CH_2), 3.09 (t, $J=6.00$ Hz, 2H, CH_2), 7.41 (d, $J=8.00$ Hz, H, Ar CH), 7.50-7.54 (m, H, Ar CH), 7.57-7.62 (m, H, Ar CH), 8.33 (dd, $J=8.00, 2.00$ Hz, H, Ar CH); δ_C (100 MHz, $CDCl_3$) 22.2 (2 x CH_2), 38.0 (CH_2), 118.6 (q, $J=319$ Hz, CF_3), 120.4 (C), 122.9 (Ar CH), 128.9 (Ar CH), 131.3 (Ar CH), 132.7 (Ar CH), 135.1 (C), 146.5 (C), 157.6 (C), 164.8 (C), 191.5 (C=O); δ_F (376 Mhz, $CDCl_3$) 88.65 (CF_3).

2-(4-Oxo-4,5,6,7-tetrahydrobenzo[d]oxazol-2-yl)-1,4-phenylene bis(trifluoromethanesulfonate) 222



Clear oil (5%); δ_{H} (400MHz; CDCl_3) 2.32 (quintet, $J=6.00$ Hz, 2H, CH_2), 2.68 (t, $J=6.00$ Hz, 2H, CH_2), 3.09 (t, $J=6.00$ Hz, 2H, CH_2), 7.35 (d, $J=9.20$ Hz, H, Ar CH), 7.53 (dd, $J=9.20, 2.80$ Hz, H, Ar CH), 8.38 (d, $J=2.80$ Hz, H, Ar CH); δ_{C} (100MHz; CDCl_3) 22.2 (2 x CH_2), 37.9 (CH_2), 117.0 (C), 121.8 (C), 124.3 (Ar CH), 130.9 (Ar CH), 132.5 (Ar CH), 134.9 (C), 135.3 (C), 144.7 (C), 156.5 (C), 165.0 (C), 191.2 (C=O). The remaining quaternary carbon could not be distinguished from the noise in the time allocated for this experiment.

5.0 References

1. Kamigaichi, T.; Nakashima, M.; Tani, H. Japanese patent JP 11158109 A2 , **1999** [CAN 131:72775 AN 1999: 378444]
2. Kamigakinai, T.; Nakashima, M.; Tani, H. Japanese patent JP 10101666 A2, **1998** [CAN 129:589 AN 1998:236773]
3. K. C. Nicolaou, T. Montagnon, G. Vassilikogiannakis, and C. J. N. Mathison, *J. Am. Chem. Soc.*, 2005, **127**, 8872.
4. K. Wilson, *Tetrahedron Lett.*, 2000, **41**, 8705.
5. N. Orlachs, M. E. G. Aarsman, J. Verheul, C. J. Arnusch, N. I. Martin, M. Hervé, W. Vollmer, B. de Kruijff, E. Breukink and T. Blaauwen, *ChemBioChem*, 2011, **12**, 1124.
6. H. Urata, A. Kinoshita, K. S. Misono, F. M. Bumpus, and A. Husain, *J. Biol. Chem.*, 1990, **265**, 22348.
7. D. B. Matchar, D. C. McCrory, L. A. Orlando, M. R. Patel, U. D. Patel, M. B. Patwardhan, B. Powers, G. P. Samsa and R. N. Gray, *Ann. Intern. Med.*, 2008, **148**, 16.
8. W. H. Yuen, Ph. D. Thesis, Loughborough University, 2007.
9. J. W. Bode and K. Suzuki, *Tetrahedron Lett.*, 2003, **44**, 3559.
10. L. Claisen and O. Lowman, *Chem. Ber.*, 1888, **21**, 1149.
11. A. Hantzsch, *Liebigs Ann.*, 1888, **249**, 1.
12. A. Quilico, R. Fusco and V. Rosnati, *Gazz. Chim. Ital.*, 1946, **76**, 30.
13. R. Fusco and S. Zumin, *Gazz. Chim. Ital.*, 1946, **76**, 223.
14. N. K. Kochetkov and E. D. Khomutova, *Zh. Obs. Khim.*, 1959, **29**, 535.
15. C. Kashima, *Heterocycles*, 1979, **12**, 1343
16. C. Kashima, Y. Yamamoto and Y. Tsuda, *Heterocycles*, 1977, **6**, 805.
17. A. El-Anani, P. E. Jones and A. R. Katritzky, *J. Chem. Soc. B Phys. Org.*, 1971, 2363.
18. R. C. F. Jones, C. E. Dawson and M. J. O'Mahony, *Synlett*, 1999, **Sup 1**, 873.
19. S. Hoz and J. L. Wolk, *Tetrahedron Lett.*, 1990, **31**, 4085.

20. F. E. Ward and R. T. Buckler, *J. Org. Chem.*, 1980, **45**, 4608.
21. R. Beugelmans and C. Morin, *J. Org. Chem.*, 1977, **42**, 1356.
22. A. Barco, S. Benetti, G. P. Pollini, P. G. Baraldi, M. Guarneri, D. Simoni, and C. Gandolfi, *J. Org. Chem.*, 1981, **46**, 4518.
23. R. Saxena, V. Singh and S. Batra, *Tetrahedron*, 2004, **60**, 10311.
24. M. Nitta and T. Kobayashi, *J. Chem Soc., Perkin. Trans.*, 1985, 1401.
25. N. R. Natale, *Tetrahedron Lett.*, 1982, **23**, 5009.
26. W. R. Dunstan and T. S. Dymond, *J. Chem. Soc. Trans.*, 1891, **59**, 410.
27. P. Grünanger and P. Vita-Finzi, *Isoxazole, The Chemistry of Heterocyclic Compounds*, John Wiley & Sons, Inc, Hoboken, NJ, USA., 1991, vol. 49.
28. T. L. Gilchrist, *Heterocyclic Chemistry 3rd Ed*, Addison Wesley Longman Ltd, 1997 Upper Saddle River, NJ, USA.
29. B. Das, H. Holla, G. Mahender, K. Venkateswarlu, and B. P. Bandgar, *Synthesis (Stuttg.)*, 2005, 1572.
30. J. W. Bode, Y. Hachisu, T. Matsuura, and K. Suzuki, *Org. Lett.*, 2003, **5**, 391.
31. G. S. Skinner, *J. Am. Chem. Soc.*, 1924, **46**, 731.
32. E. Inokuchi, A. Yamada, K. Hozumi, K. Tomita, S. Oishi, H. Ohno, M. Nomizu, and N. Fujii, *Org. Biomol. Chem.*, 2011, 3421.
33. A. Werner and H. Buss, *Chem. Ber.*, 1894, **27**, 2193.
34. T. Mukaiyama and T. Hoshino, *J. Am. Chem. Soc.*, 1960, **82**, 5339.
35. N. Maugein, *Tetrahedron Lett.*, 1997, **38**, 1547.
36. D. P. Curran and C. J. Fenk, *J. Am. Chem. Soc.*, 1985, **107**, 6023.
37. A. Dondoni, G. Barbaro, A. Battaglia and P. Giorgianni, *J. Org. Chem.*, 1972, **37**, 3196.

38. B. A. Mendelsohn, S. Lee, S. Kim, F. Teyssier, V. S. Aulakh and M. A. Ciufolini, *Org. Lett.*, 2009, **11**, 1539.
39. S. Bhosale, S. Kurhade, S. Vyas, V. P. Palle, and D. Bhuniya, *Tetrahedron*, 2010, **66**, 9582.
40. G. Just and K. Dahl, *Tetrahedron*, 1968, **24**, 5251.
41. J. N. Kim and E. K. Ryu, *Synth. Commun.*, 1990, **20**, 1373.
42. P. Muller, *Pure Appl. Chem.*, 1994, **66**, 1077.
43. R. Huisgen, *Angew. Chem. Int. Ed.*, 1963, **2**, 633.
44. N. Dubau-Assibat, A. Baceiredo and G. Bertrand, *J. Org. Chem.*, 1995, **60**, 3904.
45. Q. Zhang, J. Sun, F. Zhang and B. Yu, *Eur. J. Org. Chem.*, 2010, **2010**, 3579.
46. R. N. Butler, A. G. Coyne, P. McArdle, L. M. Sibley and L. A. Burke, *Tetrahedron Lett.*, 2007, **48**, 6684.
47. R. Huisgen, *J. Org. Chem.*, 1968, **33**, 2291.
48. Firestone, R A, *J. Org. Chem.*, 1968, **33**, 2285.
49. K. N. Houk, R. A. Firestone, L. L. Munchausen, P. H. Mueller, B. H. Arison, and L. A. Garcia, *J. Am. Chem. Soc.*, 1985, **107**, 7227.
50. R. Sustmann, *Tetrahedron Lett.*, 1971, **12**, 2717.
51. D. H. Ess and K. N. Houk, *J. Am. Chem. Soc.*, 2008, **130**, 10187.
52. S. Fukuzawa and H. Oki, *Org. Lett.*, 2008, **10**, 1747.
53. T. Saito, S. Nishihara, Y. Kataoka, Y. Nakanishi, Y. Kitagawa, T. Kawakami, S. Yamanaka, M. Okumura and K. Yamaguchi, *J. Phys. Chem. A*, 2010, **114**, 12116.
54. D. H. Ess, G. O. Jones and K. N. Houk, *Org. Lett.*, 2008, **10**, 1633.
55. S. J. Meek, R. V O'Brien, J. Llaveria, R. R. Schrock and A. H. Hoveyda, *Nature*, 2011, **471**, 461.
56. K. Ziegler, E. Holzkamp, H. Breil and H. Martin, *Angew. Chem.*, 1955, **67**, 426.

57. G. Natta, G. Dall'Asta and G. Mazzanti, *Angew. Chem. Int. Ed.*, 1964, **3**, 723.
58. N. Calderon, E. A. Ofstead, J. P. Ward, W. A. Judy and K. W. Scott, *J. Am. Chem. Soc.*, 1968, **90**, 4133.
59. T. J. Katz and J. McGinnis, *J. Am. Chem. Soc.*, 1975, **97**, 1592.
60. P. Jean-Louis Hérisson and Y. Chauvin, *Die Makromol. Chemie*, 1971, **141**, 161.
61. R. H. Grubbs, D. D. Carr, C. Hoppin and P. L. Burk, *J. Am. Chem. Soc.*, 2002, **9**, 3478.
62. F. N. Tebbe, G. W. Parshall and G. S. Reddy, *J. Am. Chem. Soc.*, 1978, **100**, 3611.
63. L. R. Gilliom and R. H. Grubbs, *J. Am. Chem. Soc.*, 1986, **108**, 733.
64. G. C. Fu and R. H. Grubbs, *J. Am. Chem. Soc.*, 1992, **114**, 5426.
65. T. M. Trnka and R. H. Grubbs, *Acc. Chem. Res.*, 2001, **34**, 18.
66. B. M. Novak and R. H. Grubbs, *J. Am. Chem. Soc.*, 1988, **110**, 7542.
67. E. L. Dias, S. T. Nguyen and R. H. Grubbs, *J. Am. Chem. Soc.*, 1997, **119**, 3887.
68. S. T. Nguyen, R. H. Grubbs and J. W. Ziller, *J. Am. Chem. Soc.*, 1993, **115**, 9858.
69. S. T. Nguyen, L. K. Johnson, R. H. Grubbs and J. W. Ziller, *J. Am. Chem. Soc.*, 1992, **114**, 3974.
70. P. Schwab, R. H. Grubbs and J. W. Ziller, *J. Am. Chem. Soc.*, 1996, **118**, 100.
71. T. Weskamp, W. C. Schattenmann, M. Spiegler and W. A. Herrmann, *Angew. Chem. Int. Ed.*, 1998, **37**, 2490.
72. R. R. Schrock and A. H. Hoveyda, *Angew. Chem. Int. Ed.*, 2003, **42**, 4592.
73. S. J. Malcolmson, S. J. Meek, E. S. Sattely, R. R. Schrock and A. H. Hoveyda, *Nature*, 2008, **456**, 933.
74. A. H. Hoveyda and A. R. Zhugralin, *Nature*, 2007, **450**, 243.
75. M. S. Sanford, J. A. Love and R. H. Grubbs, *J. Am. Chem. Soc.*, 2001, **123**, 6543.

76. W. P. D. Goldring, S. Bouazzaoui and J. F. Malone, *Tetrahedron Lett.*, 2011, **52**, 960.
77. A. Couture, E. Deniau, P. Grandclaoudon and C. Hoarau, *J. Org. Chem.*, 1998, **63**, 3128.
78. J. G. Colson, P. T. Lansbury and F. D. Saeva, *J. Am. Chem. Soc.*, 1967, **89**, 4987.
79. N. V. Moskalev and G. W. Gribble, *Tetrahedron Lett.*, 2002, vol. 43.
80. E. W. Warnhoff, *J. Chem. Soc., Chem. Comm.*, 1976, 517.
81. W. P. D. Goldring, S. Bouazzaoui and J. F. Malone, *Tetrahedron Lett.*, 2011, **52**, 960.
82. K. Reimer and F. Tiemann, *Chem. Ber.*, 1876, **9**, 824.
83. J. C. Lee, J. Y. Yuk and S. H. Cho, *Synth. Comm.*, 1995, **25**, 1367–1370.
84. G. Dijkstra, W. H. Kruizinga and R. M. Kellogg, *J. Org. Chem.*, 1987, **52**, 4230–4234.
85. O. Mitsunobu, M. Yamada, O. Y. O. Mitsunobu and O. Chemistry, *Bull. Chem. Soc. Jpn.*, 1967, **40**, 2380.
86. D. M. T. Chan, K. L. Monaco, R. Li, D. Bonne, C. G. Clark and P. Y. S. Lam, *Tetrahedron Lett.*, 2003, vol. 44.
87. M. Kiankarimi, R. Lowe, J. R. Mccarthy and J. P. Whitten, *Tetrahedron Lett.*, 1999, **40**, 4497.
88. E. Valeur and D. Roche, *Tetrahedron Lett.*, 2008, **49**, 4182.
89. H. Bock and J. Kroner, *Chem. Ber.*, 1966, **99**, 2039–2051.
90. H.-P. Wessel, T. Iversen and D. R. Bundle, *J. Chem. Soc, Perkin Trans 1*, 1985, 2247.
91. A. Suzuki, *J. Organomet. Chem.*, 1999, **576**, 147.
92. J. Clayden, N. Greeves and S. Warren, *Organic Chemistry, 2nd Edition*, Oxford University Press, 2012.
93. B. L. Lucht and D. B. Collum, *J. Am. Chem. Soc.*, 1994, **116**, 6009.
94. P. Ballinger and F. A. Long, *J. Am. Chem. Soc.*, 1960, **1050**, 3.

95. Y.R. Luo, *Comprehensive Handbook of Chemical Bond Energies*, CRC Press, Boca Raton, Florida, USA, 2007.
96. P. W. Atkins, *The Elements of Physical Chemistry, 3rd Ed.*, Oxford University Press, Oxford, UK, 2000.
97. I. Kuwajima, E. Nakamura, and M. Shimizu, *J. Am. Chem. Soc.*, 1982, **104**, 1025.
98. F. G. Bordwell and J. A. Harrelson Jr, *Can. J. Chem.*, 1990, **68**, 1714.
99. F. G. Bordwell and H. E. Fried, *J. Org. Chem.*, 1991, **56**, 4218.
100. E. J. Corey and D. Enders, *Tetrahedron Lett.*, 1976, **17**, 3.
101. H. Lindlar, *Helv. Chim. Acta*, 1952, **35**, 446.
102. M. Nitta and T. Kobayashi, *J. Chem. Soc., Chem. Commun.*, 1982, 877.
103. G. R. Desiraju and T. Steiner, *The Weak Hydrogen Bond: In Structural Chemistry and Biology*, Oxford University Press, Oxford, UK, 2001.
104. M. R. Crampton and I. A. Robotham, *J. Chem. Res.*, 1997, 22.
105. V. V. Zverev, T. N. Pylaeva, L. V. Ermolaeva, N. A. Filippova and Y. P. Kitaev, *Bull. Acad. Sci. USSR Div. Chem. Sci.*, 1977, **26**, 1865.
106. G. O. Wilson, K. A. Porter, H. Weissman, S. R. White, N. R. Sottos and J. S. Moore, *Adv. Synth. Catal.*, 2009, **351**, 1817.
107. P. Compain, *Adv. Synth. Catal.*, 2007, **349**, 1829.
108. D. H. Williams and I. Fleming, *Spectroscopic Methods in Organic Chemistry, 6th edition*, McGraw-Hill Higher Education, New York, USA, 2007.
109. J. W. Bode, H. Uesuka and K. Suzuki, *Org. Lett.*, 2003, **5**, 395.
110. A. J. Boulton and A. R. Katritzky, *Rev. Chim.*, 1962, **7**, 691.
111. E. M. Arnett and J. A. Harrelson, *J. Am. Chem. Soc.*, 1987, **109**, 809.
112. F. G. Bordwell, *Acc. Chem. Res.*, 1988, **21**, 456–463.

113. I. J. Turchi and M. J. S. Dewar, *Chem. Rev.*, 1974, **75**, 389.
114. K. K. Zhigulev and M. A. Panina, *Khimiya Geterotsiklicheskikh Soedin.*, 1974, **4**, 457.
115. P. W. Neber and A. V. Friedolsheim, *Liebigs Ann.*, 1926, **449**, 109.
116. C. M. Nunes, I. Reva and R. Fausto, *J. Org. Chem.*, 2013, **78**, 10657.
117. B. Alcaide, P. Almendros and J. M. Alonso, *Chem. Eur. J.*, 2003, **9**, 5793.
118. Á. Gyömöre, Z. Kovács, T. Nagy, V. Kudar, A. Szabó, and A. Csámpai, *Tetrahedron*, 2008, **64**, 10837.
119. T. A. Ueda, Y. Miyazawa, Y. Hara, M. Koguchi, A. Takahashi, T. Kawana, US Patent, US 6268310 B1 20010731, 2001.
120. F. Ullmann and J. Bielecki, *Berichte der Dtsch. Chem. Gesellschaft*, 1901, **34**, 2174.
121. B. A. Anderson, E. C. Bell, F. O. Ginah, N. K. Harn, L. M. Pagh, and J. P. Wepsiec, *J. Org. Chem.*, 1998, **63**, 8224.
122. A. Meyers, T. D. Nelson, H. Moorlag, D. J. Rawson, and A. Meier, *Tetrahedron*, 2004, **60**, 4459.
123. J. Einhorn, C. Einhorn, F. Ratajczak, and J.-L. Pierre, *J. Org. Chem.*, 1996, **61**, 7452.
124. N. Cosson, *J. Chem. Soc. Trans.*, 1925, **127**, 2427.
125. F. Noelting, *Ann. Chim.*, 1910, **8**, 476.
126. A. V. Dubrovskiy and R. C. Larock, *Org. Lett.*, 2010, **12**, 1180.
127. J. S. Wzorek, T. F. Kn, I. Sapountzis and D. A. Evans, *Org. Lett.* 2012, **12**, 5840.
128. M. Rawat, V. Prutyay, and W. D. Wulff, *J. Am. Chem. Soc.*, 2006, **128**, 11044.
129. M. E. Lanning and S. Fletcher, *Tetrahedron Lett.*, 2013, **54**, 4624.

Appendix i – Crystal Structures

All crystal structure data described herein was collected and solved by Dr Mark Elsegood of Loughborough University. Full data sets available on request to M.R.J.Elsegood@lboro.ac.uk or R.C.F.Jones@lboro.ac.uk.

X-Ray crystal structure of **3-(2-Hydroxyphenyl)-6,7-dihydrobenzo[d]isoxazol-4(5H)-one 61**

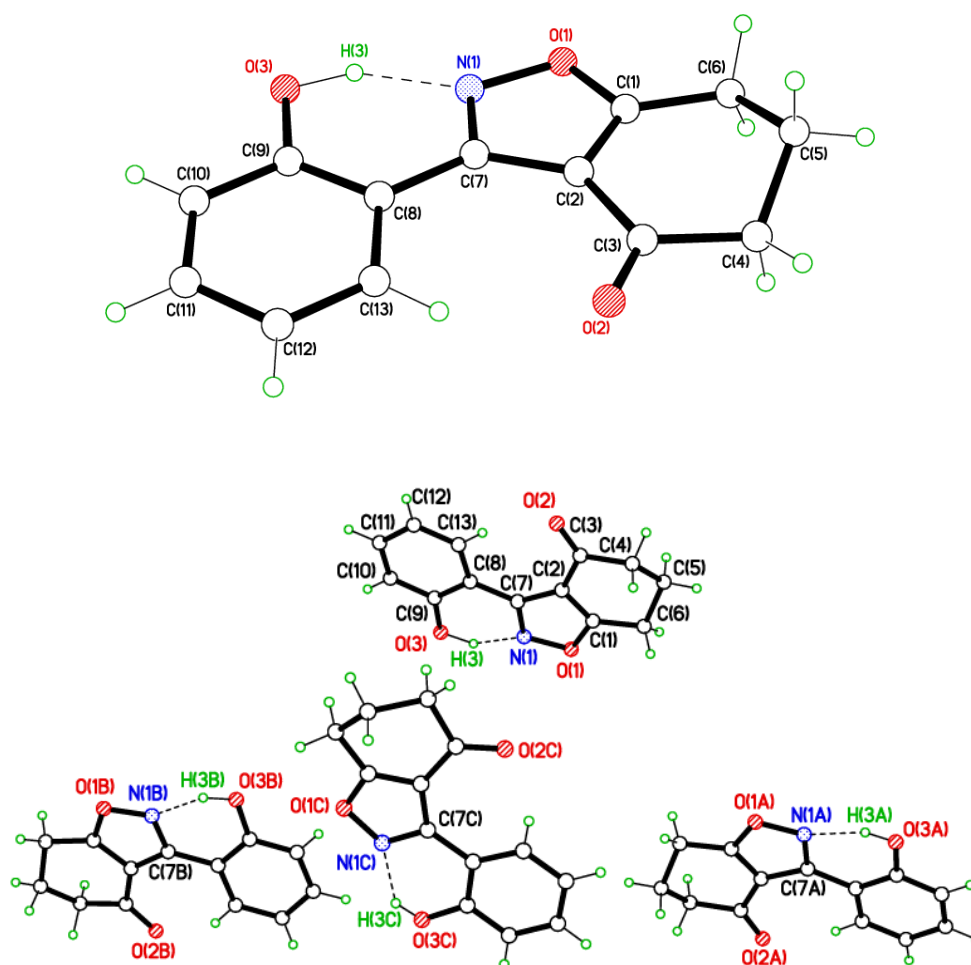
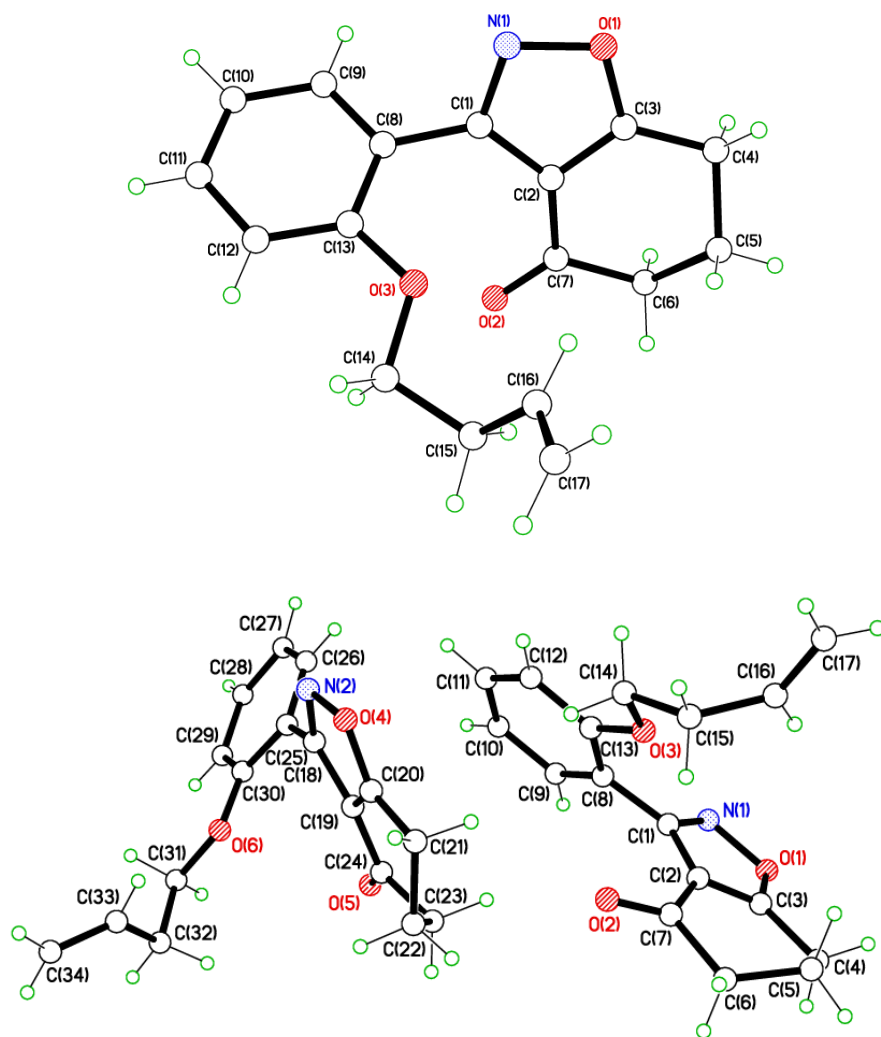


Table 1. Crystal data and structure refinement for **61**.

| | |
|-----------------------|---|
| Identification code | RCFJ39 |
| Chemical formula | C ₁₃ H ₁₁ NO ₃ |
| Formula weight | 229.23 |
| Temperature | 150(2) K |
| Radiation, wavelength | MoK α , 0.71073 Å |

| | | |
|--------------------------------------|---|---------|
| Crystal system, space group | orthorhombic, Pca2 ₁ | |
| Unit cell parameters | a = 15.024(3) Å | a = 90° |
| | b = 21.464(4) Å | b = 90° |
| | c = 13.309(3) Å | g = 90° |
| Cell volume | 4291.8(15) Å ³ | |
| Z | 16 | |
| Calculated density | 1.419 g/cm ³ | |
| Absorption coefficient m | 0.102 mm ⁻¹ | |
| F(000) | 1920 | |
| Crystal colour and size | colourless, 0.87 × 0.25 × 0.10 mm ³ | |
| Reflections for cell refinement | 4726 (q range 2.25 to 25.31°) | |
| Data collection method | Bruker APEX 2 CCD diffractometer w rotation with narrow frames | |
| q range for data collection | 0.95 to 26.54° | |
| Index ranges | h -18 to 18, k -26 to 26, l -16 to 16 | |
| Completeness to q = 26.54° | 99.4 % | |
| Intensity decay | 0% | |
| Reflections collected | 36812 | |
| Independent reflections | 8811 (R _{int} = 0.0638) | |
| Reflections with F ² >2s | 5081 | |
| Absorption correction | semi-empirical from equivalents | |
| Min. and max. transmission | 0.917 and 0.999 | |
| Structure solution | direct methods | |
| Refinement method | Full-matrix least-squares on F ² | |
| Weighting parameters a, b | 0.0580, 2.9563 | |
| Data / restraints / parameters | 8811 / 1 / 625 | |
| Final R indices [F ² >2s] | R1 = 0.0564, wR2 = 0.1288 | |
| R indices (all data) | R1 = 0.1218, wR2 = 0.1684 | |
| Goodness-of-fit on F ² | 1.008 | |
| Largest and mean shift/su | 0.000 and 0.000 | |
| Largest diff. peak and hole | 0.403 and -0.290 e Å ⁻³ | |

X-Ray crystal structure of **3-(2-(but-3-en-1-yloxy)phenyl)-6,7-dihydrobenzo[d]isoxazol-4(5H)-one 77**



RCFJ 44

| | |
|--------------------------------|---|
| $C_{17}H_{17}NO_3$ | $D_x = 1.291 \text{ Mg m}^{-3}$ |
| $M_r = 283.31$ | Mo $K\alpha$ radiation, $\lambda = 0.71073 \text{ \AA}$ |
| Orthorhombic, $Pbca$ | Cell parameters from 11913 reflections |
| $a = 15.8407 (11) \text{ \AA}$ | $\theta = 2.5\text{--}28.3^\circ$ |
| $b = 13.7859 (9) \text{ \AA}$ | $\mu = 0.09 \text{ mm}^{-1}$ |
| $c = 26.6923 (18) \text{ \AA}$ | $T = 150 \text{ K}$ |
| $V = 5829.0 (7) \text{ \AA}^3$ | Tablet, colourless |
| $Z = 16$ | $0.75 \times 0.66 \times 0.10 \text{ mm}$ |
| $F(000) = 2400$ | |

Data collection

| | |
|--|--|
| Bruker APEX 2 CCD diffractometer | 6149 reflections with $I > 2\sigma(I)$ |
| Radiation source: fine-focus sealed tube | $R_{\text{int}} = 0.045$ |
| ω rotation with narrow frames scans | $\theta_{\text{max}} = 30.6^\circ$, $\theta_{\text{min}} = 1.5^\circ$ |
| Absorption correction: multi-scan SADABS v2009/1, Sheldrick, G.M., (2009) | $h = -22 \rightarrow 22$ |
| $T_{\text{min}} = 0.936$, $T_{\text{max}} = 0.991$ | $k = -19 \rightarrow 19$ |
| 65102 measured reflections | $l = -37 \rightarrow 37$ |
| 8885 independent reflections | |

Refinement

| | |
|---------------------------------|---|
| Refinement on F^2 | Primary atom site location: structure-invariant direct methods |
| Least-squares matrix: full | Secondary atom site location: difference Fourier map |
| $R[F^2 > 2\sigma(F^2)] = 0.047$ | Hydrogen site location: mixed |
| $wR(F^2) = 0.129$ | H atoms treated by a mixture of independent and constrained refinement |
| $S = 1.01$ | $w = 1/[\sigma^2(F_o^2) + (0.0587P)^2 + 1.7931P]$ where $P = (F_o^2 + 2F_c^2)/3$ |
| 8885 reflections | $(\Delta/\sigma)_{\max} < 0.001$ |
| 514 parameters | $\Delta_{\max} = 0.49 \text{ e } \text{\AA}^{-3}$ |
| 21 restraints | $\Delta_{\min} = -0.20 \text{ e } \text{\AA}^{-3}$ |

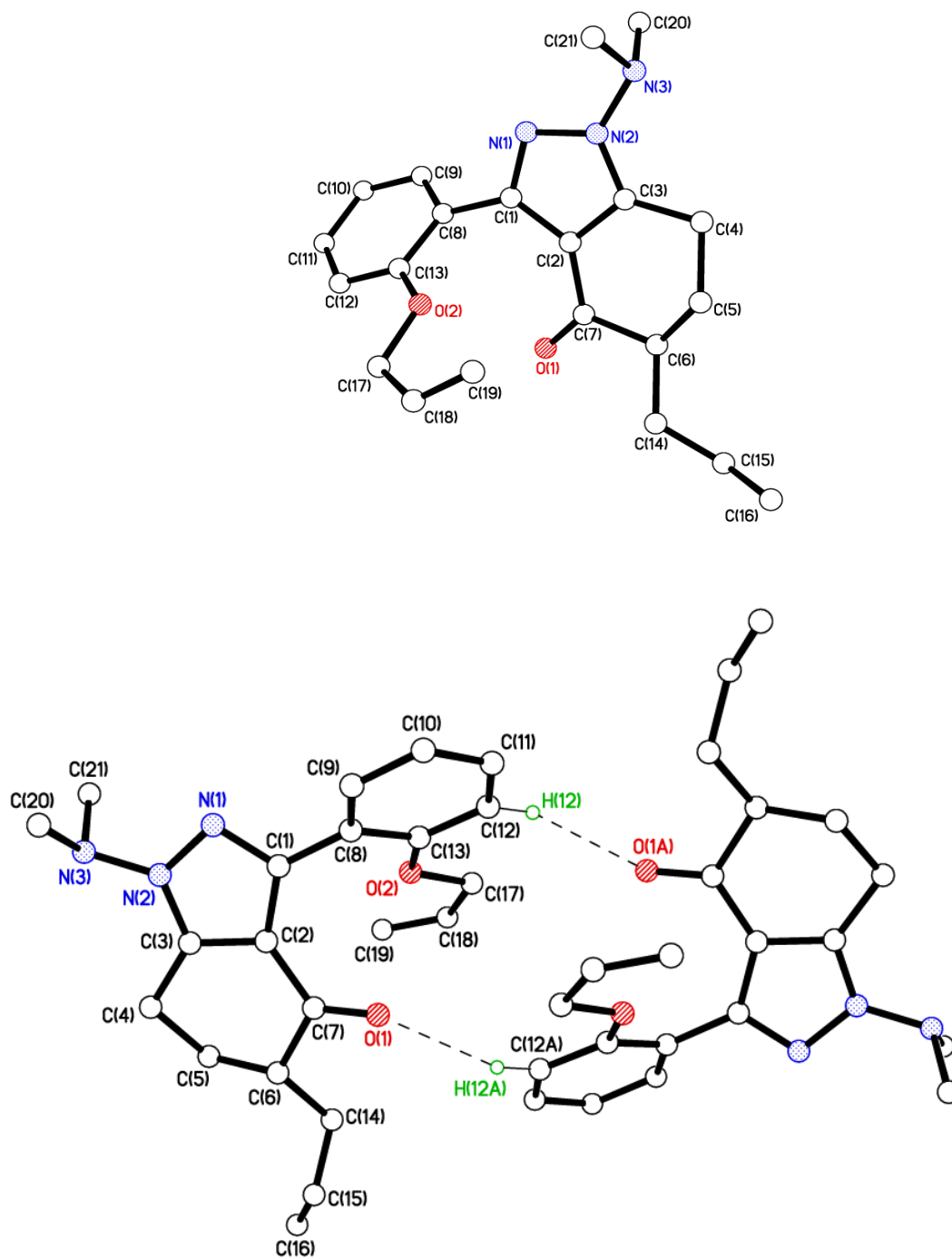
Computing details

Data collection: Bruker *APEX 2*; cell refinement: Bruker *S SAINT*; data reduction: Bruker *S SAINT*; program(s) used to solve structure: *SHELXS97* (Sheldrick, 2008); program(s) used to refine structure: *SHELXL2012* (Sheldrick, 2012); molecular graphics: Bruker *SHELXTL*; software used to prepare material

Special details

Geometry. All esds (except the esd in the dihedral angle between two l.s. planes) are estimated using the full covariance matrix. The cell esds are taken into account individually in the estimation of esds in distances, angles and torsion angles; correlations between esds in cell parameters are only used when they are defined by crystal symmetry. An approximate (isotropic) treatment of cell esds is used for estimating esds involving l.s. planes.

X-Ray crystal structure of **5-allyl-3-(2-(allyloxy)phenyl)-1-(dimethylamino)-6,7-dihydro-H-indazol-4(5H)-one 129**



RCJF 56

| | |
|-------------------------------|---|
| $C_{2H_{25}N_3O_2}$ | $Z = 2$ |
| $M_r = 351.44$ | $F(000) = 376$ |
| Triclinic, P^{-1} | $D_x = 1.201 \text{ Mg m}^{-3}$ |
| $a = 9.812 (4) \text{ \AA}$ | Mo $K\alpha$ radiation, $\lambda = 0.71073 \text{ \AA}$ |
| $b = 10.456 (4) \text{ \AA}$ | Cell parameters from 1987 reflections |
| $c = 10.951 (4) \text{ \AA}$ | $\theta = 2.4\text{--}23.8^\circ$ |
| $\alpha = 101.805 (5)^\circ$ | $\mu = 0.08 \text{ mm}^{-1}$ |
| $\beta = 112.996 (5)^\circ$ | $T = 150 \text{ K}$ |
| $\gamma = 99.966 (5)^\circ$ | Tablet, colourless |
| $V = 971.6 (7) \text{ \AA}^3$ | $0.61 \times 0.32 \times 0.09 \text{ mm}^3$ |

Data collection

| | |
|--|--|
| Bruker APEX 2 CCD diffractometer | 2577 reflections with $I > 2\sigma(I)$ |
| Radiation source: fine-focus sealed tube | $R_{\text{int}} = 0.046$ |
| ω rotation with narrow frames scans | $\theta_{\text{max}} = 26.5^\circ$, $\theta_{\text{min}} = 2.1^\circ$ |
| Absorption correction: multi-scan SADABS v2012/1, Sheldrick, G.M., (2012) | $h = -12 \rightarrow 12$ |
| $T_{\text{min}} = 0.954$, $T_{\text{max}} = 0.993$ | $k = -13 \rightarrow 13$ |
| 11195 measured reflections | $l = -13 \rightarrow 13$ |
| 3991 independent reflections | |

Refinement

| | |
|--|---|
| Refinement on F^2 | Hydrogen site location: mixed |
| Least-squares matrix: full | H atoms treated by a mixture of independent and constrained refinement |
| $R[F^2 > 2\sigma(F^2)] = 0.055$ | $w = 1/[\sigma^2(F_o^2) + (0.0626P)^2 + 0.3996P]$ where $P = (F_o^2 + 2F_c^2)/3$ |
| $wR(F^2) = 0.152$ | $(\Delta/\sigma)_{\max} < 0.001$ |
| $S = 1.03$ | $\Delta_{\max} = 0.51 \text{ e } \text{\AA}^{-3}$ |
| 3991 reflections | $\Delta_{\min} = -0.38 \text{ e } \text{\AA}^{-3}$ |
| 306 parameters | Extinction correction: <i>SHELXL</i> , $F_c^* = kFc[1 + 0.001xFc^2\lambda^3/\sin(2\theta)]^{-1/4}$ |
| 17 restraints | Extinction coefficient: 0.013 (3) |
| Primary atom site location: structure-invariant direct methods | |

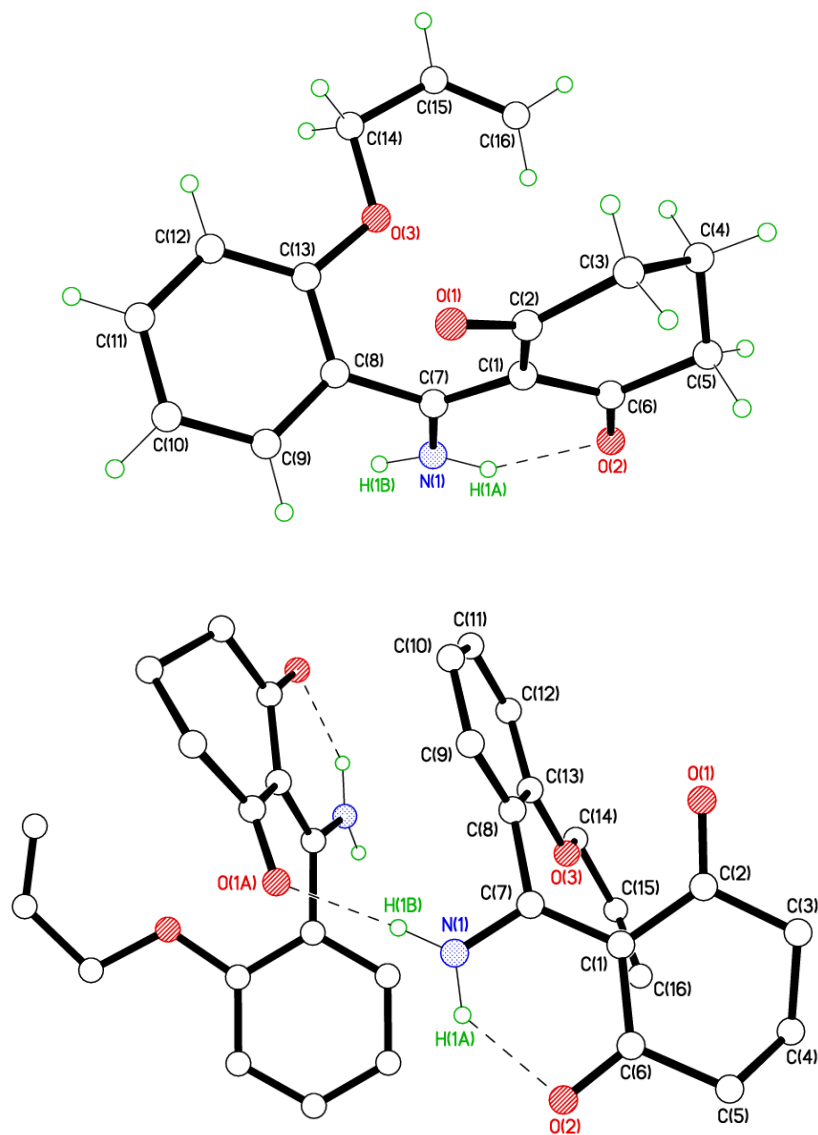
Computing details

Data collection: Bruker *APEX 2*; cell refinement: Bruker *SAINT*; data reduction: Bruker *SAINT*; program(s) used to solve structure: *SHELXS97* (Sheldrick, 2008); program(s) used to refine structure: *SHELXL2013* (Sheldrick, 2013); molecular graphics: Bruker *SHELXTL*; software used to prepare material for publication: Bruker *SHELXTL*.

Special details

Geometry. All esds (except the esd in the dihedral angle between two l.s. planes) are estimated using the full covariance matrix. The cell esds are taken into account individually in the estimation of esds in distances, angles and torsion angles; correlations between esds in cell parameters are only used when they are defined by crystal symmetry. An approximate (isotropic) treatment of cell esds is used for estimating esds involving l.s. planes.

X-Ray crystal structure of 2-((2-(allyloxy)phenyl)(amino)methylene)cyclohexane-1,3-dione 135



RCFJ 42

Crystal data

| | |
|--------------------------------|---|
| $C_{16}H_{17}NO_3$ | $F(000) = 576$ |
| $M_r = 271.30$ | $D_x = 1.321 \text{ Mg m}^{-3}$ |
| Monoclinic, $P2_1/c$ | Mo $K\alpha$ radiation, $\lambda = 0.71073 \text{ \AA}$ |
| $a = 10.7250 (17) \text{ \AA}$ | Cell parameters from 3054 reflections |
| $b = 8.1582 (13) \text{ \AA}$ | $\theta = 2.6\text{--}30.4^\circ$ |
| $c = 15.601 (3) \text{ \AA}$ | $\mu = 0.09 \text{ mm}^{-1}$ |
| $\beta = 91.636 (3)^\circ$ | $T = 150 \text{ K}$ |
| $V = 1364.5 (4) \text{ \AA}^3$ | Tablet, yellow |
| $Z = 4$ | $0.45 \times 0.29 \times 0.07 \text{ mm}$ |

Data collection

| | |
|---|--|
| Bruker APEX 2 CCD diffractometer | 4137 independent reflections |
| Radiation source: fine-focus sealed tube | 3017 reflections with $I > 2\sigma(I)$ |
| graphite | $R_{\text{int}} = 0.035$ |
| ω rotation with narrow frames scans | $\theta_{\text{max}} = 30.5^\circ$, $\theta_{\text{min}} = 1.9^\circ$ |
| Absorption correction: multi-scan <i>SADABS</i> v2009/1, Sheldrick, G.M., (2009) | $h = -15 \rightarrow 15$ |
| $T_{\text{min}} = 0.960$, $T_{\text{max}} = 0.994$ | $k = -11 \rightarrow 11$ |
| 15472 measured reflections | $l = -22 \rightarrow 21$ |

Refinement

| | |
|---------------------------------|---|
| Refinement on F^2 | Primary atom site location: structure-invariant direct methods |
| Least-squares matrix: full | Secondary atom site location: all non-H atoms found by direct methods |
| $R[F^2 > 2\sigma(F^2)] = 0.045$ | Hydrogen site location: difference Fourier map |
| $wR(F^2) = 0.125$ | All H-atom parameters refined |
| $S = 1.04$ | $w = 1/[\sigma^2(F_o^2) + (0.0672P)^2 + 0.1144P]$ where $P = (F_o^2 + 2F_c^2)/3$ |
| 4137 reflections | $(\Delta/\sigma)_{\max} < 0.001$ |
| 249 parameters | $\Delta_{\max} = 0.41 \text{ e } \text{\AA}^{-3}$ |
| 0 restraints | $\Delta_{\min} = -0.20 \text{ e } \text{\AA}^{-3}$ |

Computing details

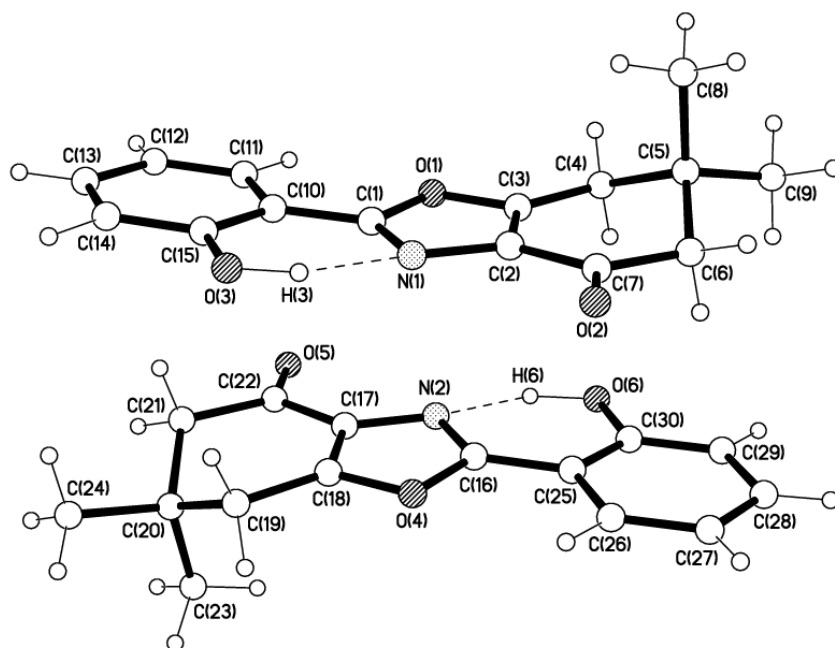
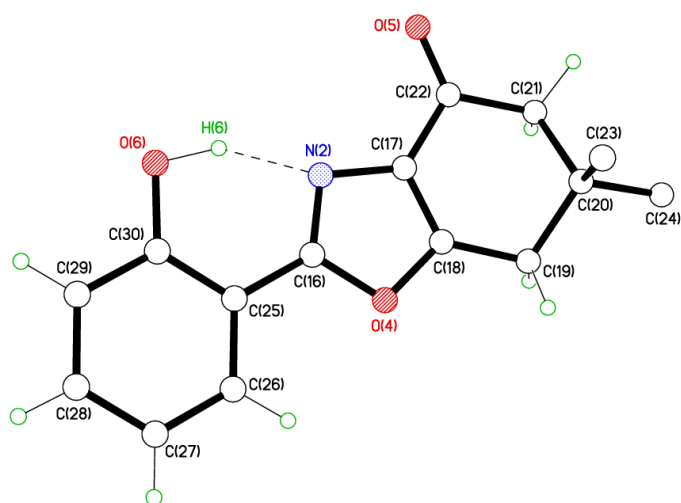
Data collection: Bruker *APEX 2*; cell refinement: Bruker *SAINT*; data reduction: Bruker *SAINT*; program(s) used to solve structure: *SHELXS97* (Sheldrick, 2008); program(s) used to refine structure: *SHELXL2012* (Sheldrick, 2012); molecular graphics: Bruker *SHELXTL*; software used to prepare material for publication: Bruker *SHELXTL*.

Special details

Geometry. All esds (except the esd in the dihedral angle between two l.s. planes) are estimated using the full covariance matrix. The cell esds are taken into account individually in the estimation of esds in distances, angles and torsion angles; correlations between esds in cell parameters are only used when they are defined by crystal symmetry. An approximate (isotropic) treatment of cell esds is used for estimating esds involving l.s. planes.

X-Ray crystal structure of 2-(2-hydroxyphenyl)-6,6-dimethyl-6,7-dihydrobenzo[d]oxazol-4(5H)-one

166



RCFJ46

Crystal data

| | |
|--------------------------------|---|
| $C_{15}H_{15}NO_3$ | $D_x = 1.305 \text{ Mg m}^{-3}$ |
| $M_r = 257.28$ | Mo $K\alpha$ radiation, $\lambda = 0.71073 \text{ \AA}$ |
| Orthorhombic, $Pna2_1$ | Cell parameters from 4807 reflections |
| $a = 12.9420 (14) \text{ \AA}$ | $\theta = 2.4\text{--}23.7^\circ$ |
| $b = 9.330 (1) \text{ \AA}$ | $\mu = 0.09 \text{ mm}^{-1}$ |
| $c = 21.682 (2) \text{ \AA}$ | $T = 150 \text{ K}$ |
| $V = 2618.1 (5) \text{ \AA}^3$ | Plate, colourless |
| $Z = 8$ | $0.48 \times 0.40 \times 0.04 \text{ mm}$ |
| $F(000) = 1088$ | |

Data collection

| | |
|--|--|
| Bruker APEX-II CCD diffractometer | $R_{\text{int}} = 0.037$ |
| Radiation source: fine-focus sealed tube | $\theta_{\text{max}} = 26.4^\circ$, $\theta_{\text{min}} = 1.9^\circ$ |
| ϕ and ω scans | $h = -16 \rightarrow 16$ |
| 20349 measured reflections | $k = -11 \rightarrow 11$ |
| 5338 independent reflections | $l = -27 \rightarrow 27$ |
| 4424 reflections with $I > 2\sigma(I)$ | |

Refinement

| | |
|--|---|
| Refinement on F^2 | Secondary atom site location: all non-H atoms found by direct methods |
| Least-squares matrix: full | Hydrogen site location: difference Fourier map |
| $R[F^2 > 2\sigma(F^2)] = 0.035$ | All H-atom parameters refined |
| $wR(F^2) = 0.084$ | $w = 1/[\sigma^2(F_o^2) + (0.0467P)^2 + 0.0138P]$ where $P = (F_o^2 + 2F_c^2)/3$ |
| $S = 1.04$ | $(\Delta/\sigma)_{\max} < 0.001$ |
| 5338 reflections | $\Delta_{\max} = 0.19 \text{ e } \text{\AA}^{-3}$ |
| 463 parameters | $\Delta_{\min} = -0.17 \text{ e } \text{\AA}^{-3}$ |
| 1 restraint | Absolute structure: Flack x determined using 1909 quotients $[(I+)-(I-)]/[(I+)+(I-)]$ (Parsons and Flack (2004), Acta Cryst. A60, s61). |
| Primary atom site location: structure-invariant direct methods | Flack parameter: 0.8 (5) |

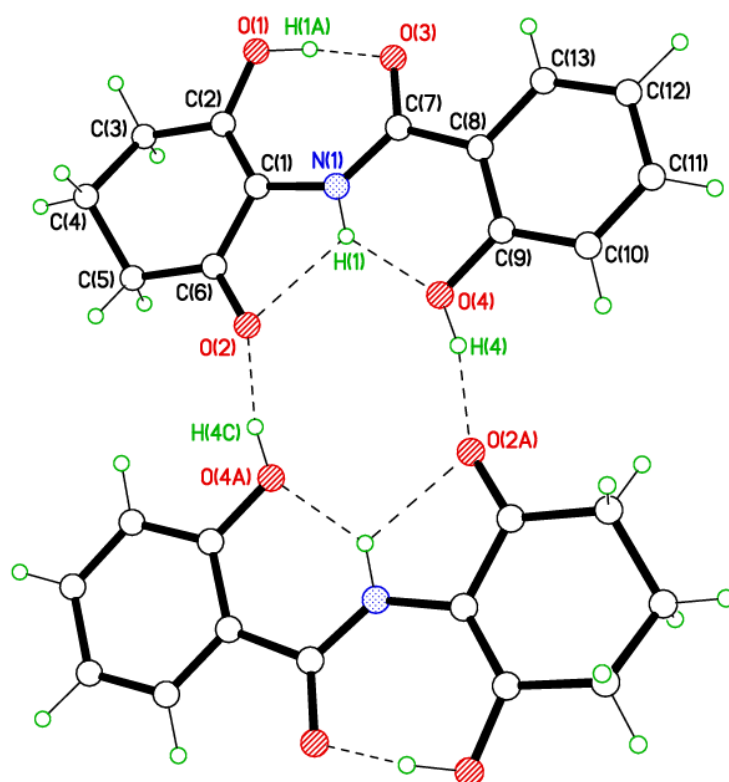
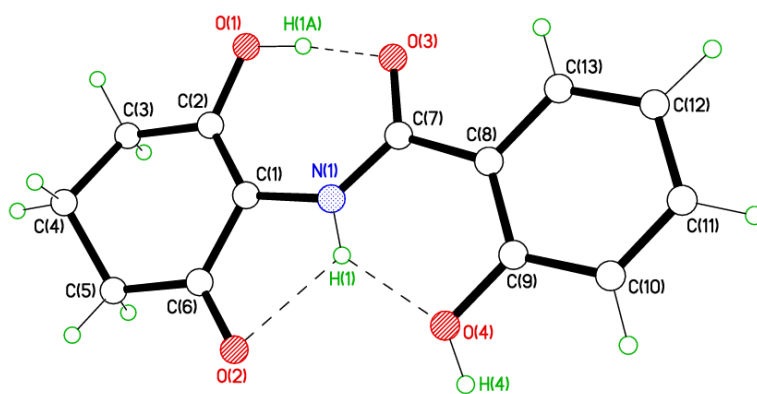
Computing details

Data collection: Bruker *APEX2*; cell refinement: Bruker *SAINT*; data reduction: Bruker *SAINT*; program(s) used to solve structure: *SHELXS97* (Sheldrick, 2008); program(s) used to refine structure: *SHELXL2012* (Sheldrick, 2012); molecular graphics: Bruker *SHELXTL*; software used to prepare material for publication: Bruker *SHELXTL*.

Special details

Geometry. All esds (except the esd in the dihedral angle between two l.s. planes) are estimated using the full covariance matrix. The cell esds are taken into account individually in the estimation of esds in distances, angles and torsion angles; correlations between esds in cell parameters are only used when they are defined by crystal symmetry. An approximate (isotropic) treatment of cell esds is used for estimating esds involving l.s. planes.

X-Ray crystal structure of **2-hydroxy-N-(2-hydroxy-6-oxocyclohex-1-en-1-yl)benzamide 180**



RCFJ43

Crystal data

| | |
|--------------------------------|---|
| $C_{13}H_{13}NO_4$ | $F(000) = 520$ |
| $M_r = 247.24$ | $D_x = 1.446 \text{ Mg m}^{-3}$ |
| Monoclinic, $P2_1/n$ | Mo $K\alpha$ radiation, $\lambda = 0.71073 \text{ \AA}$ |
| $a = 5.5001 (6) \text{ \AA}$ | Cell parameters from 6269 reflections |
| $b = 15.2463 (18) \text{ \AA}$ | $\theta = 2.7\text{--}30.6^\circ$ |
| $c = 13.6680 (16) \text{ \AA}$ | $\mu = 0.11 \text{ mm}^{-1}$ |
| $\beta = 97.7388 (18)^\circ$ | $T = 150 \text{ K}$ |
| $V = 1135.7 (2) \text{ \AA}^3$ | Block, colourless |
| $Z = 4$ | $1.02 \times 0.79 \times 0.38 \text{ mm}$ |

Data collection

| | |
|--|--|
| Bruker APEX 2 CCD diffractometer | 2970 reflections with $I > 2\sigma(I)$ |
| Radiation source: fine-focus sealed tube | $R_{\text{int}} = 0.026$ |
| ω rotation with narrow frames scans | $\theta_{\text{max}} = 30.6^\circ$, $\theta_{\text{min}} = 2.0^\circ$ |
| Absorption correction: multi-scan SADABS v2009/1, Sheldrick, G.M., (2009) | $h = -7 \rightarrow 7$ |
| $T_{\text{min}} = 0.898$, $T_{\text{max}} = 0.960$ | $k = -21 \rightarrow 21$ |
| 12997 measured reflections | $l = -19 \rightarrow 19$ |
| 3446 independent reflections | |

Refinement

| | |
|---------------------------------|--|
| Refinement on F^2 | Primary atom site location: structure-invariant direct methods |
| Least-squares matrix: full | Secondary atom site location: difference Fourier map |
| $R[F^2 > 2\sigma(F^2)] = 0.045$ | Hydrogen site location: mixed |
| $wR(F^2) = 0.131$ | H atoms treated by a mixture of independent and constrained refinement |
| $S = 1.05$ | $w = 1/[\sigma^2(F_o^2) + (0.080P)^2 + 0.2403P]$ where $P = (F_o^2 + 2F_c^2)/3$ |
| 3446 reflections | $(\Delta/\sigma)_{\max} < 0.001$ |
| 201 parameters | $\Delta_{\max} = 0.42 \text{ e } \text{\AA}^{-3}$ |
| 35 restraints | $\Delta_{\min} = -0.22 \text{ e } \text{\AA}^{-3}$ |

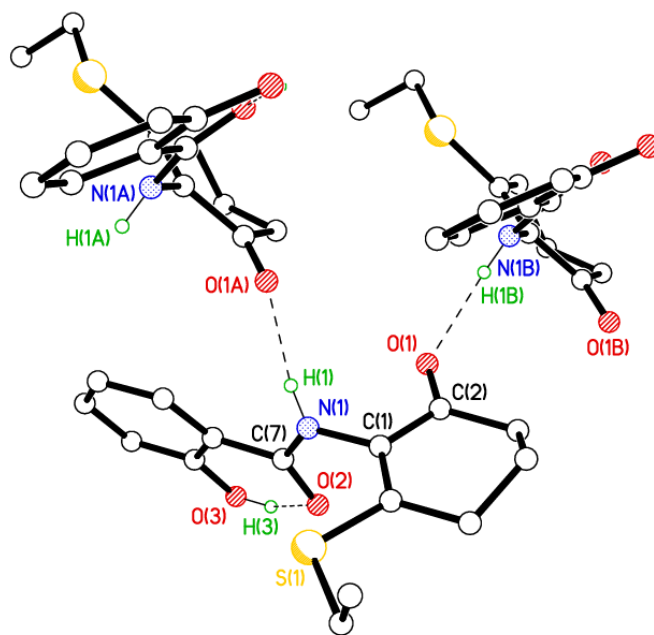
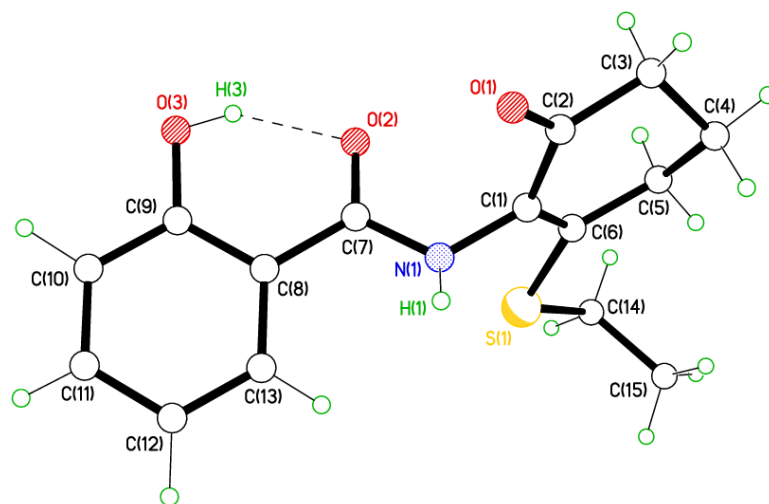
Computing details

Data collection: Bruker *APEX 2*; cell refinement: Bruker *S SAINT*; data reduction: Bruker *S SAINT*; program(s) used to solve structure: *SHELXS97* (Sheldrick, 2008); program(s) used to refine structure: *SHELXL2012* (Sheldrick, 2012); molecular graphics: Bruker *SHELXTL*; software used to prepare material for publication: Bruker *SHELXTL*.

Special details

Geometry. All esds (except the esd in the dihedral angle between two l.s. planes) are estimated using the full covariance matrix. The cell esds are taken into account individually in the estimation of esds in distances, angles and torsion angles; correlations between esds in cell parameters are only used when they are defined by crystal symmetry. An approximate (isotropic) treatment of cell esds is used for estimating esds involving l.s. planes.

X-Ray crystal structure of **N-(2-(ethylthio)-6-oxocyclohex-1-en-1-yl)-2-hydroxybenzamide 186**



RCFJ45

Crystal data

| | |
|----------------------------------|---|
| $C_{15}H_{17}NO_3S$ | $F(000) = 616$ |
| $M_r = 291.35$ | $D_x = 1.329 \text{ Mg m}^{-3}$ |
| Monoclinic, $P2_1/c$ | Mo $K\alpha$ radiation, $\lambda = 0.71073 \text{ \AA}$ |
| $a = 9.7309 (7) \text{ \AA}$ | Cell parameters from 6233 reflections |
| $b = 7.3003 (5) \text{ \AA}$ | $\theta = 2.9\text{--}30.4^\circ$ |
| $c = 20.4979 (14) \text{ \AA}$ | $\mu = 0.23 \text{ mm}^{-1}$ |
| $\beta = 91.268 (1)^\circ$ | $T = 150 \text{ K}$ |
| $V = 1455.78 (18) \text{ \AA}^3$ | Block, colourless |
| $Z = 4$ | $0.61 \times 0.23 \times 0.16 \text{ mm}$ |

Data collection

| | |
|---|--|
| Bruker APEX 2 CCD diffractometer | 3740 reflections with $I > 2\sigma(I)$ |
| Radiation source: fine-focus sealed tube | $R_{\text{int}} = 0.024$ |
| ω rotation with narrow frames scans | $\theta_{\text{max}} = 30.6^\circ$, $\theta_{\text{min}} = 2.0^\circ$ |
| Absorption correction: multi-scan <i>SADABS</i> v2009/1, Sheldrick, G.M., (2009) | $h = -13 \rightarrow 13$ |
| $T_{\text{min}} = 0.873$, $T_{\text{max}} = 0.964$ | $k = -10 \rightarrow 10$ |
| 16546 measured reflections | $l = -29 \rightarrow 29$ |
| 4425 independent reflections | |

Refinement

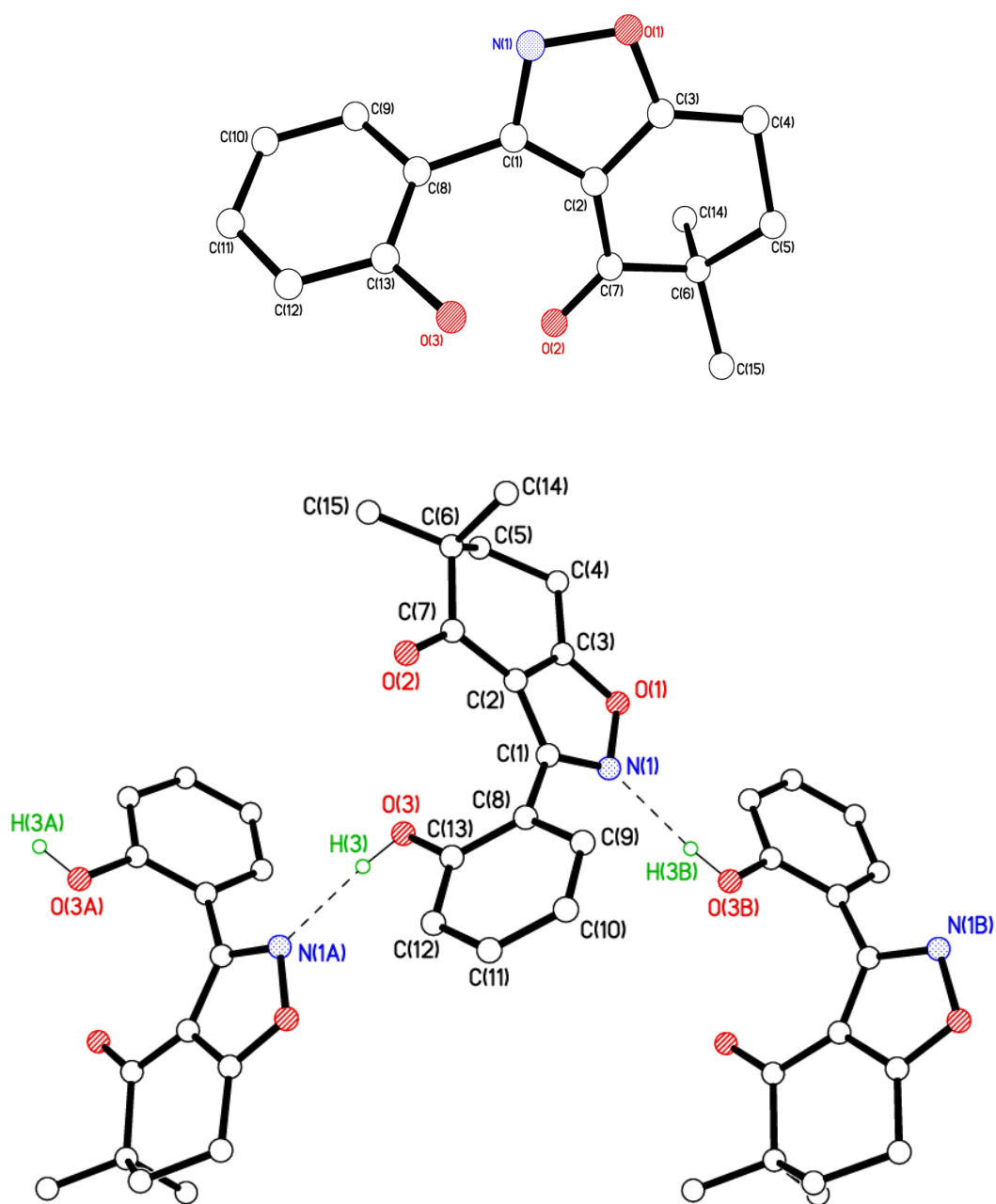
| | |
|---------------------------------|---|
| Refinement on F^2 | Primary atom site location: structure-invariant direct methods |
| Least-squares matrix: full | Secondary atom site location: all non-H atoms found by direct methods |
| $R[F^2 > 2\sigma(F^2)] = 0.042$ | Hydrogen site location: difference Fourier map |
| $wR(F^2) = 0.121$ | All H-atom parameters refined |
| $S = 1.06$ | $w = 1/[\sigma^2(F_o^2) + (0.078P)^2 + 0.188P]$ where $P = (F_o^2 + 2F_c^2)/3$ |
| 4425 reflections | $(\Delta/\sigma)_{\max} = 0.001$ |
| 249 parameters | $\Delta_{\max} = 0.75 \text{ e } \text{\AA}^{-3}$ |
| 0 restraints | $\Delta_{\min} = -0.24 \text{ e } \text{\AA}^{-3}$ |

Computing details

Data collection: Bruker *APEX 2*; cell refinement: Bruker *SAINT*; data reduction: Bruker *SAINT*; program(s) used to solve structure: *SHELXS97* (Sheldrick, 2008); program(s) used to refine structure: *SHELXL2012* (Sheldrick, 2012); molecular graphics: Bruker *SHELXTL*; software used to prepare material for publication: Bruker *SHELXTL*.

Special details

Geometry. All esds (except the esd in the dihedral angle between two l.s. planes) are estimated using the full covariance matrix. The cell esds are taken into account individually in the estimation of esds in distances, angles and torsion angles; correlations between esds in cell parameters are only used when they are defined by crystal symmetry. An approximate (isotropic) treatment of cell esds is used for estimating esds involving l.s. planes.



RCFJ55

Crystal data

| | |
|--------------------------------|---|
| $C_{15}H_{15}NO_3$ | $D_x = 1.370 \text{ Mg m}^{-3}$ |
| $M_r = 257.28$ | Mo $K\alpha$ radiation, $\lambda = 0.71073 \text{ \AA}$ |
| Orthorhombic, $Pbca$ | Cell parameters from 4851 reflections |
| $a = 11.1585 (12) \text{ \AA}$ | $\theta = 2.8\text{--}30.3^\circ$ |
| $b = 11.4154 (12) \text{ \AA}$ | $\mu = 0.10 \text{ mm}^{-1}$ |
| $c = 19.588 (2) \text{ \AA}$ | $T = 150 \text{ K}$ |
| $V = 2495.1 (5) \text{ \AA}^3$ | Tablet, colourless |
| $Z = 8$ | $0.58 \times 0.54 \times 0.16 \text{ mm}^3$ |
| $F(000) = 1088$ | |

Data collection

| | |
|---|--|
| Bruker APEX 2 CCD diffractometer | 3005 reflections with $I > 2\sigma(I)$ |
| Radiation source: fine-focus sealed tube | $R_{\text{int}} = 0.032$ |
| ω rotation with narrow frames scans | $\theta_{\text{max}} = 30.4^\circ$, $\theta_{\text{min}} = 2.1^\circ$ |
| Absorption correction: multi-scan <i>SADABS</i> v2012/1, Sheldrick, G.M., (2012) | $h = -15 \rightarrow 12$ |
| $T_{\text{min}} = 0.946$, $T_{\text{max}} = 0.985$ | $k = -16 \rightarrow 16$ |
| 18546 measured reflections | $l = -27 \rightarrow 27$ |
| 3766 independent reflections | |

Refinement

| | |
|---------------------------------|--|
| Refinement on F^2 | Primary atom site location: structure-invariant direct methods |
| Least-squares matrix: full | Hydrogen site location: difference Fourier map |
| $R[F^2 > 2\sigma(F^2)] = 0.043$ | All H-atom parameters refined |
| $wR(F^2) = 0.127$ | $w = 1/[\sigma^2(F_o^2) + (0.0729P)^2 + 0.574P]$ where $P = (F_o^2 + 2F_c^2)/3$ |
| $S = 1.03$ | $(\Delta/\sigma)_{\max} < 0.001$ |
| 3766 reflections | $\Delta_{\max} = 0.42 \text{ e } \text{\AA}^{-3}$ |
| 232 parameters | $\Delta_{\min} = -0.20 \text{ e } \text{\AA}^{-3}$ |
| 6 restraints | |

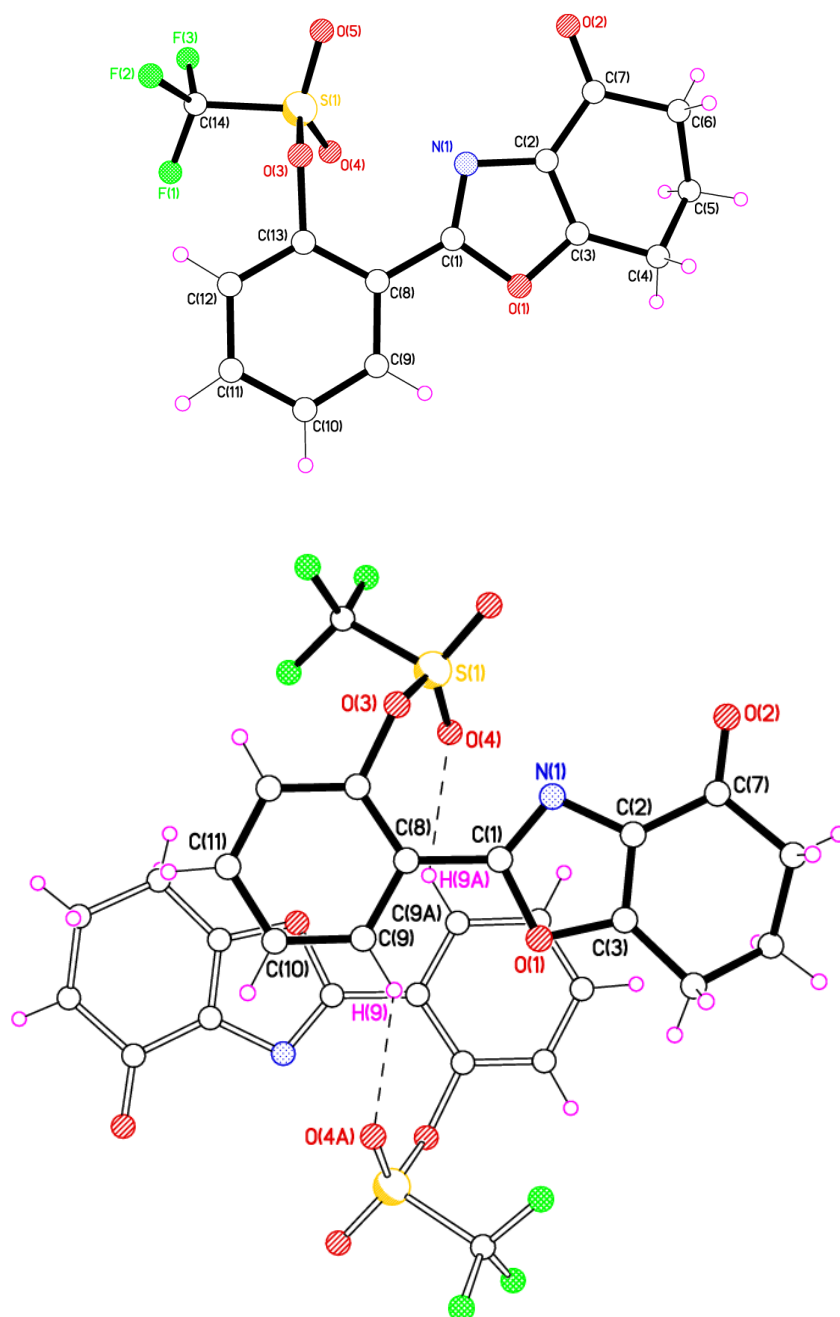
Computing details

Data collection: Bruker *APEX 2*; cell refinement: Bruker *SAINT*; data reduction: Bruker *SAINT*; program(s) used to solve structure: *SHELXS97* (Sheldrick, 2008); program(s) used to refine structure: *SHELXL2013* (Sheldrick, 2013); molecular graphics: Bruker *SHELXTL*; software used to prepare material for publication: Bruker *SHELXTL*.

Special details

Geometry. All esds (except the esd in the dihedral angle between two l.s. planes) are estimated using the full covariance matrix. The cell esds are taken into account individually in the estimation of esds in distances, angles and torsion angles; correlations between esds in cell parameters are only used when they are defined by crystal symmetry. An approximate (isotropic) treatment of cell esds is used for estimating esds involving l.s. planes.

X-Ray crystal structure of **2-(4-oxo-4,5,6,7-tetrahydrobenzo[d]oxazol-2-yl)phenyl trifluoromethanesulfonate 221**



RCFJ52

Crystal data

| | |
|--------------------------------|---|
| $C_{14}H_{10}F_3NO_5S$ | $F(000) = 1472$ |
| $M_r = 361.29$ | $D_x = 1.612 \text{ Mg m}^{-3}$ |
| Monoclinic, $C2/c$ | Mo $K\alpha$ radiation, $\lambda = 0.71073 \text{ \AA}$ |
| $a = 21.725 (4) \text{ \AA}$ | Cell parameters from 3754 reflections |
| $b = 11.1783 (19) \text{ \AA}$ | $\theta = 2.5\text{--}28.3^\circ$ |
| $c = 12.802 (2) \text{ \AA}$ | $\mu = 0.28 \text{ mm}^{-1}$ |
| $\beta = 106.781 (3)^\circ$ | $T = 150 \text{ K}$ |
| $V = 2976.6 (9) \text{ \AA}^3$ | Plate, colourless |
| $Z = 8$ | $0.61 \times 0.53 \times 0.07 \text{ mm}$ |

Data collection

| | |
|---|--|
| Bruker APEX 2 CCD diffractometer | 3202 reflections with $I > 2\sigma(I)$ |
| Radiation source: fine-focus sealed tube | $R_{\text{int}} = 0.037$ |
| ω rotation with narrow frames scans | $\theta_{\text{max}} = 29.6^\circ$, $\theta_{\text{min}} = 2.0^\circ$ |
| Absorption correction: multi-scan <i>SADABS</i> v2012/1, Sheldrick, G.M., (2012) | $h = -30 \rightarrow 30$ |
| $T_{\text{min}} = 0.849$, $T_{\text{max}} = 0.981$ | $k = -15 \rightarrow 15$ |
| 16267 measured reflections | $l = -17 \rightarrow 17$ |
| 4181 independent reflections | |

Refinement

| | |
|---------------------------------|---|
| Refinement on F^2 | Primary atom site location: structure-invariant direct methods |
| Least-squares matrix: full | Secondary atom site location: difference Fourier map |
| $R[F^2 > 2\sigma(F^2)] = 0.041$ | Hydrogen site location: difference Fourier map |
| $wR(F^2) = 0.106$ | All H-atom parameters refined |
| $S = 1.06$ | $w = 1/[\sigma^2(F_o^2) + (0.0449P)^2 + 2.0142P]$ where $P = (F_o^2 + 2F_c^2)/3$ |
| 4181 reflections | $(\Delta/\sigma)_{\max} < 0.001$ |
| 257 parameters | $\Delta_{\max} = 0.34 \text{ e } \text{\AA}^{-3}$ |
| 0 restraints | $\Delta_{\min} = -0.48 \text{ e } \text{\AA}^{-3}$ |

Computing details

Data collection: Bruker *APEX 2*; cell refinement: Bruker *SAINT*; data reduction: Bruker *SAINT*; program(s) used to solve structure: *SHELXS97* (Sheldrick, 2008); program(s) used to refine structure: *SHELXL2013* (Sheldrick, 2013); molecular graphics: Bruker *SHELXTL*; software used to prepare material for publication: Bruker *SHELXTL*.

Special details

Geometry. All esds (except the esd in the dihedral angle between two l.s. planes) are estimated using the full covariance matrix. The cell esds are taken into account individually in the estimation of esds in distances, angles and torsion angles; correlations between esds in cell parameters are only used when they are defined by crystal symmetry. An approximate (isotropic) treatment of cell esds is used for estimating esds involving l.s. planes.